Post-transcriptional Control of Cyclooxygenase-2

Thesis submitted for the degree of
Doctor of Medicine
At the University of Leicester

By

Stephen Justin Acton
MB BCH (Hons), N.U.I. (Galway)
University of Leicester

Date
28th February 2007

UMI Number: U490172

All rights reserved

INFORMATION TO ALL USERS
The quality of this reproduction is dependent upon the quality of the copy submitted.

In the unlikely event that the author did not send a complete manuscript
and there are missing pages, these will be noted. Also, if material had to be removed,
a note will indicate the deletion.

UMI U490172
Published by ProQuest LLC 2013. Copyright in the Dissertation held by the Author.
Microform Edition © ProQuest LLC.
All rights reserved. This work is protected against
unauthorized copying under Title 17, United States Code.

ProQuest LLC
789 East Eisenhower Parkway
P.O. Box 1346
Ann Arbor, MI 48106-1346

Acknowledgements

All work undertaken for this thesis was done in conjunction with Steve Cok, Washington University, St. Louis, USA. Special thanks to Aubrey Morrison, whose guidance, instruction and support made this work possible and an enjoyable experience.

To the staff and faculty of the Renal Division, Washington University, St. Louis for providing the environment and funding required for junior clinicians to pursue research training.

Also, I would like to thank Kevin Harris for his patience and assistance in editing this thesis and for facilitating my time in St. Louis.

Lastly, to my wife and family, whose support throughout this process was essential in bringing it to a conclusion.

Publications arising from this work

Manuscripts

Cok SJ, Acton SJ, Sexton AE, Morrison AR
Identification of RNA-binding proteins in RAW 264.7 cells that recognize a lipopolysaccharide-responsive element in the 3-untranslated region of the murine cyclooxygenase-2 mRNA.
J Biol Chem. 2004 Feb 27; 279(9): 8196-205.

Cok SJ, Acton SJ, Morrison AR
The proximal region of the 3'-untranslated region of cyclooxygenase-2 is recognized by a multimeric protein complex containing HuR, TIA-1, TIAR, and the heterogeneous nuclear ribonucleoprotein U.
J Biol Chem. 2003 Sep 19; 278(38): 36157-62.

Lui P, Zeng C, Acton S, Cok S, Sexton A, Morrison AR
Effects of p38MAPK isoforms on renal mesangial cell inducible nitric oxide synthase expression.
Am J Physiol Cell Physiol. 2004: 286(1): C145-152

Posters

Cok SJ, Acton SJ, Morrison AR
Multiple ARE binding proteins interact with the proximal region of the 3'UTR of Cyclooxygenase-2 Rat Mesangial Cells.
American Society of Nephrology, Philadelphia, October 2002.

Glossary of Terms

ARE – Adenosine-Uridine Rich Element
AUBP – Adenosine-Uridine Binding Protein
AUG – Adenosine-Uridine-Guanosine (translation initiation codon)
ATCC – American Type Tissue Collection
Cox – Cyclooxygenase
DEPC – Diethyl Pyrocarbonate
DMEM – Dulbecco's Modified Eagle's Medium
DMSO – Dimethyl Sulfoxide
DNA – Deoxyribonucleic Acid
DTT – Dithiothreitol
ECL – Enhanced Chemiluminescence
EDTA – Ethylenediaminetetraacetic Acid
EGTA – Ethylene Glycol-bis(β-aminoethyl)-N,N,N',N'-Tetraacetic Acid
ELAV – Embyronically Lethal and Abnormal Vision
GM-CSF – Granulocyte-Monocyte Colony Stimulating Factor
HEPES – N-2-hydroxyethylpiperazine-N'-2-ethanesulfonic acid
hnRNP – heterogenous Ribonucleoprotein
IL – Interleukin
KCl – Potassium Chloride
LPS – Lipopolysaccharide
MAPK – Mitogen Activated Protein Kinase
$MgCl_2$ – Magnesium Chloride
MK2 – MAPK activated Kinase 2
mRNA – messenger Ribonucleic Acid
mRNP – messenger Ribonucleoprotein
NaCl – Sodium Chloride
Na_3VO_4 – Sodium Orthovanadate
NP-40 – Nonidet P40
NSAID – Non-Steroidal Anti-inflammatory Drug
PAGE – Polyacrylamide Gel Electrophoresis
PBS – Phosphate Buffered Saline
PCR – Polymerase Chain Reaction
PG – Prostaglandin
Poly(A) – Polyadenosine
PVDF – Polyvinylidene Difluoride
RPMI – Roswell Park Memorial Institute
RRM – RNA Recognition Motif
SDS – Sodium Dodecyl Sulfate
TBS – Tris-Buffered Saline
TNF – Tissue Necrosis Factor
TTP – Tristetraprolin
uORF – Upstream Open Reading Frame
UTR – Untranslated Region

Contents

Figures

TABLES

Abstract

Cyclooxygenase-2 is an early response gene that is rapidly and transiently induced by a variety of extracellular ligands in many cell types, including macrophages and mesangial cells. The 3' untranslated region (UTR) of cox-2 mRNA plays a vital role in its post-transcriptional control by regulating mRNA stability and translation. The proximal 60-nucleotides of the 3' UTR contains highly conserved Adenosine-uridine Rich Elements (AREs) – AUUUA, which are known to regulate mRNA stability and translation.

Insertion of the 1 - 60 sequence was sufficient to cause a marked decrease (>65%) in expression of a luciferase reporter-gene, in a both rat mesangial and RAW 264.7 cells. Although, reporter-gene constructs proved unresponsive to stimulation with IL1β in the rat mesangial cells, a response was seen with LPS in the RAW 264.7 cells, which was dependent on the proximal 20 nucleotides of the 1 – 60 sequence.

Electromobility shift assays revealed that multiple RNA binding proteins, including HuR, TIA-1, TIAR, hnRNP U and AUF1, interacted with this region of the cyclooxygenase-2 3'UTR, with some noticeable differences occurring following removal of the LPS responsive sequence.

These studies provide further evidence of the role played by the 3' UTR in the post-transcriptional control of cyclooxygenase-2, as well as identifying several RNA binding proteins likely to be involved in this process.

Chapter 1

Cyclooxygenase Overview

Cyclooxygenase catalyses the conversion of arachidonic acid to PGH_2, the rate limiting step in the synthesis of prostaglandins, which are mediators of a diverse variety of pathophysiological processes[1,2]. To list some of these processes illustrates the importance of elucidating the mechanisms involved in the regulation of this enzyme. To date, prostaglandins have been shown to perform key roles in reproduction[3], inflammation and wound healing[4,5], T cell development[6], maintaining gastric mucosal integrity[7,8], platelet aggregation[9], neonatal renal development[10], salt and water homeostasis[11] and Ductus Arteriosus remodelling[12].

There is also increasing evidence that prostaglandins play a role in the pathogenesis of multiple carcinomas[13-19] and neurodegenerative diseases[20-23].

Not surprisingly, cyclooxygenase enzyme inhibition with aspirin and other NSAIDs is a widely used and effective therapy in many clinical settings, such as rheumatic and cardiovascular diseases[24]. However, use of these medications is associated with significant complications and side effects[25], which result in considerable morbidity and cost[26-28]. Well documented and relatively common side effects of cyclooxygenase inhibition include gastrointestinal ulceration[29,30], exacerbation of heart failure[31], hypertension[32] and asthma[33], as well as renal dysfunction[34,35].

It was hoped that the discovery of the second cyclooxygenase isoform (cox-2)[36-38] and the development of specific cox-2 inhibitors would ameliorate many of these problems[39,40]. Unfortunately, this has not proven to be the case[41-48] and recently two of these agents have been withdrawn due to unexpected side-effects[49]. There remains some optimism that these agents may prove useful adjuncts in the treatment of carcinogenesis[50-55] and neurodegenerative diseases[56-59]. Hence,

continued study into the regulation of cyclooxygenase isoforms may uncover new options for safer, targeted therapy for many common medical ailments and possibly allow progress in the treatment of specific malignancies and neurodegenerative diseases.

Cyclooxygenase and the Kidney

Both cyclooxygenase isoforms are constituitively expressed in the kidney. Cox-1 protein is predominantly found in the renal vasculature and collecting ducts, whereas cox-2 appears to be primarily expressed in the macula densa, the cortical thick ascending limb of Henle (cTALH) and the medullary interstitial cells[11,60-62]. The functional significance of cyclooxygenase's actions within the kidney are emphasised by the many adverse effects on renal function related to NSAIDs use. These include acute renal failure, sodium retention, hyperkalaemia and papillary necrosis[63]. Specific inhibitors of cox-2 produce a similar renal side-effect profile[64] suggesting that cox-2, rather than cox-1, is the primary isoform involved in the maintenance of renal function and normal sodium and potassium balance. This view is reinforced by the finding that Cox-2 interacts with many homeostatic systems within the kidney. Expression of Cox-2 within the renal cortex is directly inhibited by angiotensin II[65-67], indirectly inhibited by dopamine[68] and appears to be under the tonic inhibition of endogenous corticosteroids and mineralocorticoids[69,70]. While within the renal medulla, vasopressin stimulates its expression in interstitial cells[71].

Within the macula densa, renin release in response to salt restriction, diuretic use and ACE inhibition is controlled by cox-2 derived prostaglandins[66]. In these high renin states, cox-2 expression is increased within the macula densa and renin

expression can be inhibited with specific cox-2 inhibitors. Futhermore cox-2 null mice fail to increase renin production in response to salt restriction or ACE inhibition[72] while cox-1 null mice demonstrate a normal response under these conditions[73].

In addition to its effects on renin release, cox-2 appears to be involved in the control of renal haemodynamics and maintenance of GFR, particularly in the setting of physiological stress such as volume depletion and congestive heart failure. It cooperates with nitric oxide to fine-tune afferent arteriole tone in response to systemic pressure and tubuloglomerular feedback[74,75] and vasodilatory prostaglandins appear to maintain blood flow within the kidney and GFR in the presence of vasoconstrictors such as Angiotensin II. The "protective" effect of prostaglandins under these conditions is eliminated in the presence of Cox-2 inhibitors but not Cox-1 inhibitors[73]. Cox-2 inhibition results in decreased renal blood flow and urine flow in dogs on a low sodium diet but has no effect on these parameters when sodium intake is adequate[76]. A sustained fall in GFR and renal blood flow of over 30% occurs in dogs on a low sodium diet subjected to Cox-2 inhibition over an eight day period[77]. In agreement with animal studies, Cox-2 inhibition has little effect on renal function in healthy human subjects[78,79] but appears to play a role in maintaining renal function under salt depleted conditions[80,81].

Within the renal medulla, increased interstitial hydrostatic pressure results in sodium excretion, which is inhibited by non selective Cox inhibitors but not specific Cox-2 inhibition[82]. However, salt loading upregulates Cox-2 expression in the renal medulla[83] and it may play a role in controlling sodium excretion at this point, as, despite its effect on renin release, Cox-2 inhibition has been shown to impair sodium excretion in dogs and humans[79-81]. Cox-2 expression within medullary interstitial

cells is stimulated by the ambient tonicity[84] and its expression is critical to these cells' survival in a hypertonic environment[85]. This observation may have significant implications regarding the pathogenesis of NSAID induced papillary necrosis, as studies have suggested that the medullary interstitial cells are damaged early in this process[86] and papillary necrosis is more likely to occur in the setting of dehydration[87].

Cox-2 also plays a critical role in the late stages of renal development with Cox-2 null mice developing progressive renal dysplasia postnatally[88-90]. A similar abnormality can be induced by peri-natal treatment with specific Cox-2 inhibitors[91] but doesn't occur in Cox-1 null mice or with Cox-1 inhibition. Case studies documenting renal developmental abnormalities associated with maternal ingestion of non-selective and selective Cox-2 inhibitors support a similar role in renal development in humans[92-95].

In addition to its physiological and developmental roles in the kidney, Cox-2 has also been implicated in the pathogenesis of "hyperfiltration" injury, diabetic nephropathy and glomerulonephritis in animal models[96]. In rats, subtotal renal ablation results in upregulation of Cox-2 and visible expression within the glomerulus[97] and increased expression within the macula densa is evident in rat models of diabetic nephropathy[98,99]. Increased cyclooxygenase-2 expression has also been identified in passive Heymann nephritis[100] and Lupus nephritis in humans[101]. However, it is unclear in the setting of experimental glomerulonephritis whether Cox-2 derived prostaglandins are pro or anti-inflammatory[102,103].

Rather surprisingly, Cox-2 inhibitors have shown some promise in ameliorating progressive renal injury in animal models of subtotal renal ablation[97,104,105], diabetic nephropathy[106,107] and glomerulonephritis[100,108].

These multiple and somewhat conflicting roles of Cox-2 within the kidney emphasise the importance of determining how this enzyme is regulated before it can utilised as a viable therapeutic target. Before proceeding to describe what is currently known about the regulation of cyclooxygenase-2, it would be useful to briefly overview the post-transcriptional mechanisms involved in the control of gene expression.

Chapter 2

Post-Transcriptional Control of Gene Expression

Control of gene expression in mammalian cells extends beyond transcription, involves multiple steps in RNA processing and takes place in both the cytoplasm and the nucleus[109]. Messenger RNA undergoes a number of processes before it is eventually translated to produce its encoded protein. While our understanding of many of these processes is still in its infancy, it is already apparent that RNA processing is critically important in controlling the expression of many genes. These post-transcriptional "events" provide numerous regulatory points to fine-tune gene expression and can significantly alter the type, abundance, location and timing of protein expression within the cell[110,111].

In order to function properly, each mRNA must contain information that determines its nuclear export[112,113], subcellular localisation[114], stability and translation efficiency, as well as its protein coding sequence[115]. Much of this information is provided by specific RNA-binding proteins, many of which associate with messenger RNA during pre-mRNA processing in the nucleus[116-118], to produce large RiboNucleoProtein complexes[119]. These complexes are diverse, dynamic structures; the protein content of which is dictated by specific mRNA sequences as well as by the individual processes the pre-mRNA undergoes in the nucleus[120-124].

As transcription proceeds, the carboxy terminal domain of RNA polymerase II recruits the pre-mRNA processing machinery required to execute a number of finely regulated modifications[125-130], which alter the composition and function of the resultant messenger RNP complex[131,132]. The extent of pre-mRNA processing is illustrated by the fact that less than 5% of nascent phosphodiester bonds eventually end up as mature cytoplasmic mRNA[133,134].

The coding region of mRNA is flanked by two UnTranslated Regions, designated the 5′ and 3′UTRs[135] (Figure 1). At the upstream (5′) end, a cap structure is added and, in most cases, a poly(A) tract is added at the 3′ end[136-138]. Both of these modifications have been shown to enhance the stability and translational efficiency of mRNA[132,139-141]. Furthermore, many genes encode multiple alternative polyadenylation sites, allowing for alterations in the length of the 3′UTR of the mRNA[142]. While transcription continues, the splicing machinery removes intronic sequences to produce a contiguous protein coding sequence[143-145]. However, as many genes contain alternative splice sites, resulting in altered coding and non-coding sequences[146-148], multiple protein isoforms with varying functions can be produced from a single gene. To add to this increasing diversity, the RNA editing machinery[149-151] can alter multiple or individual nucleotides within the mRNA resulting in further changes to its protein coding sequence.

Following processing, mRNA must be actively transported to the cytoplasm before translation and protein expression can occur[112,152,153]. The preceding "processing history" of each mRNA is closely linked to its nuclear export[154-158], as well as its fate thereafter[119,131,159-161].

Translation of mRNA into protein occurs predominantly in the cytoplasm[134,162], with both ends of the molecule interacting to form a loop structure (Figure 1). The interaction of proximal and distal parts of the mRNA is intimately connected to the regulation of its translation[163,164] and degradation[165-167]. The balance between mRNA degradation and translation directly affects protein levels, as well as the temporal pattern of their expression[168,169], as the relative abundance of a given protein is related to its rate of translation versus its rate of degradation[170,171].

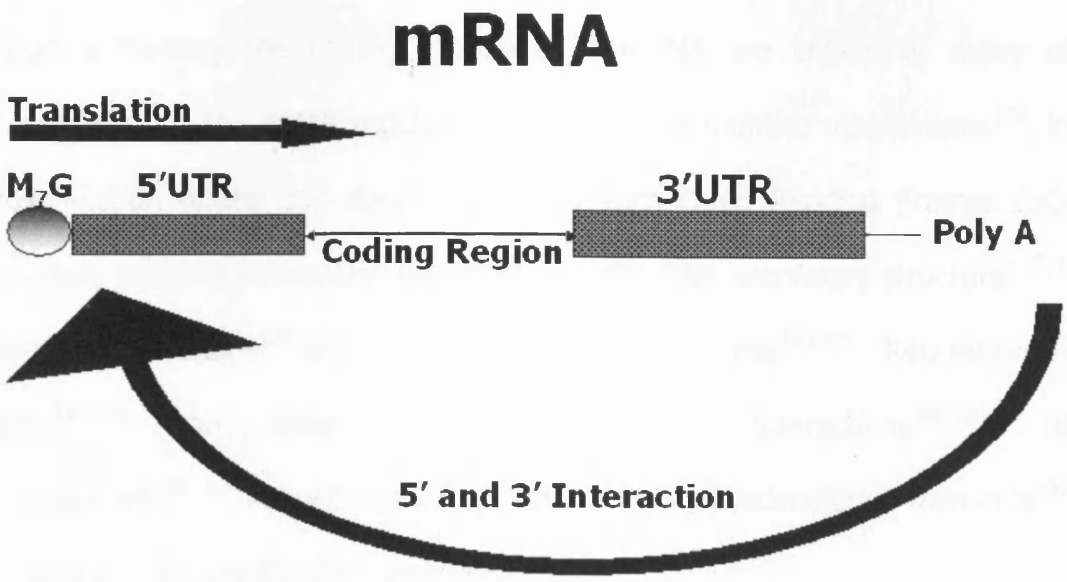

Figure 1: Mature Mammalian mRNA

The coding region is flanked by 5′ and 3′ untranslated regions (UTR).

A 7-methylguanosine cap structure and poly(A) tail are added co-transcriptionally. These modifications are of critical importance in maintaining efficient RNA processing, nuclear export, translation and mRNA stability, mainly via the interaction of specific RNA binding proteins.

Translation in mammalian cells is regulated in many ways[172,173] and the untranslated regions flanking the coding sequence of mRNA are critical to many of these processes[139]. The 5'UTR regulates translation via multiple mechanisms[174], including modification of the cap structure[175], upstream Open Reading Frames (uORFs)[176], multiple translation initiation sequences (AUG), RNA secondary structure[177,178], RNA-protein interactions[179] and Internal Ribosomal Entry Sites[180,181]. Regulation by the 3'-UTR[182-185] can occur through RNA-protein interactions[186,187], RNA-RNA interactions[188,189], as well as through cytoplasmic polyadenylation elements[190-193] and changes in the length of the poly-A tail[194-197].

Adenosine-Uridine Rich Elements

Many of previous mentioned mechanisms of regulation are dependent on cis-acting sequences within the untranslated regions, which govern the interaction of the mRNA with specific proteins and protein complexes[116,119,198-200]. One of these, the adenosine-uridine rich element (ARE) is found in the 3'-UTR of many early response genes, cytokines and growth factors[201,202]. The 3' untranslated region of cox-2 contains multiple copies of the regulatory sequence AUUUA, a class II ARE.

There are several classes of ARE with slightly different sequence characteristics, but they all share the ability to target their mRNAs for rapid deadenylation[203-205] and degradation[206-209]. However, in response to certain environmental stimuli, these sequences can stabilise their mRNA[210-212] and thereby enhance protein expression.

As well as their effects on degradation and stability, AREs have also been shown to regulate the translation[213] of multiple mRNAs including TNFα[214,215], and cyclooxygenase-2[216]. The alterations in mRNA stability and translation controlled by these sequences appear to be mediated by the association of specific trans-acting proteins called ARE-binding proteins (AUBP)[214,217-225].

AU-Binding Proteins

An increasing number of proteins have been identified that interact with ARE sequences[226-236] and affect stability, translation and subcellular localisation of their target mRNA[213,237,238]. AUF1, HuR, Tristetraprolin, TIA-1 and TIAR are among the most studied AUBPs, some of which have been shown to interact with the 3'UTR of cyclooxygenase-2[239-241]. Their mechanism of action remains unknown, but may involve recruitment of the exosome[242-247], alteration of RNA secondary structure[209,248] or recruitment of other proteins[231,246,249]. However, their role in posttranscriptional control of cox-2 has recently been disputed[250]. Aberrant activity of at least some of the known RNA binding proteins may be important in the pathogenesis of inflammatory[251-253], developmental[168,254-258] and neoplastic disease[240,259-267].

AUF1

Also known as heterogeneous ribonucleoprotein D, AUF1 consists of four alternatively spliced isoforms, designated p37, p40, p42 and p45[268-271]. All contain two RNA recognition motifs (RRM) and shuttle between the nucleus and the cytoplasm[272]. AUF1 has been shown to both stabilise[273,274] and destabilise[206,219,274-278] mRNA in a cell-type specific manner, plays an important role in the regulation of ARE-containing mRNA in development[257,279,280] and possibly in oncogenesis[260,281].

HuR

HuR is a ubiquitously expressed nucleocytoplasmic shuttling protein[282-284] and a member of the Hu / ELAV family of RNA binding proteins[285-287]. It is approximately 36Kda in size, contains three RRM and is predominantly nuclear in localisation. Many studies have shown that this protein is involved in ARE-dependent mRNA stabilisation[221,223-225,288-292] and that this process appears to be dependent on the translocation of HuR from the nucleus to the cytoplasm[293,294]. HuR may also ehance the translation of certain target mRNAs[295] and probably plays a role in the nuclear export of specific mRNAs[296]. Multiple protein ligands of HuR have been identified, which alter its function and/or its subcellular localisation[297-300]. HuR is involved in the regulation of cox-2[301] and up-regulation of this AUBP is associated with increased cyclooxygenase-2 expression in a colon cancer cell line[239].

TIA-1 and TIAR

TIA-1 and TIAR are closely related proteins that have three RRMs and shuttle between the nucleus and the cytoplasm[302,303]. Two isoforms of each protein have been identified[304,305] and post-translational modification has been documented for TIA-1[306]. They regulate the general translational arrest, which accompanies environmental stress, by recruiting most cytoplasmic mRNA to stress granules where they can't be translated[307-311]. They mediate the specific translational inhibition of TNFα[218,312] and are also involved in alternative splicing[305,313-316] and apoptosis[306,317,318]. Macrophages deficient in TIA-1 produce excessive TNFα resulting in lipopolysaccharide sensitivity[214]. TIA-1 appears to act as an "arthritis suppressor" gene and macrophages derived from TIA-1 (-/-) mice produce excessive cox-2 protein and develop arthritis[251]. Futhermore TIA-1 has recently been implicated in the translational inhibition of the cox-2 gene[241].

Tristetraprolin

Tristetraprolin (TTP) is the prototype of a family of CCCH zinc finger proteins[319,320], which specifically binds the ARE of TNFα and GM-CSF and destabilises their mRNAs[208,220,228,321]. In common with many AUBPs, TTP shuttles between the nucleus and the cytosol[322]. However, it is predominantly cytoplasmic in location and is readily induced[320,323], often by same stimulus that leads to expression of its target mRNA[324,325]. TTP knockout mice develop cachexia, arthritis and auto-immunity as a consequence of TNFα over-expression[252,253], as this AUBP is involved in feedback inhibition of TNFα controlled by p38 MAP kinase[326-329]. Cells derived from TTP knockout mice express excess cox-2, which is probably involved in the pathogenesis of their inflammatory state. Its phosphorylation by MK2, results in TTP complexing with 14-3-3 proteins, impairing its ability to destabilise TNFα mRNA[326,330,331]. It has recently been shown to bind to the cox-2 3'UTR and loss of this interaction results in excessive cox-2 expression in colon cancer cells[240,332].

Signal Transduction and Post-Transcriptional Regulation

Activation of the **MAP kinase** pathways, in particular p38[211,333-335], appears to be intimately linked to the regulated control of the RNA-protein interactions involved in these post-transcriptional processes. The exact downstream targets of these signal transduction systems are not known, but post-translational modifications of RNA-binding proteins may modify their affinities and/or their subcellular localisation, resulting in altered message expression[329,336,337].

From what's known, all of these post-transcriptional processes are under regulated control and have a significant effect on gene expression[338-345]. To date, most of this work has focused on genes involved in development, early response genes, cytokines and growth factors[346]. It can be appreciated that alterations in any or all of these post-transcriptional events could dramatically influence the level of protein expression and / or its location within the cell, ultimately leading to alterations in cell function. As our understanding of these processes increases, a growing number of genes are being identified which utilise post-transcriptional mechanisms[347-352] and they may well be a universal feature of gene expression. Already, abnormalities in post-transcriptional regulation have been shown to result in excessive immune cell activation and cellular transformation[259]. Hopefully, continued research in this area will shed light on the control of many physiological and developmental processes, as well as the pathogenesis of some common medical conditions[353-358] and may lead to the development of novel therapies[359,360].

Chapter 3

Cyclooxygenase Isoforms and their Regulation

Three isoforms of cyclooxygenase have been identified, designated cox-1, cox-2 and cox-3. The first two isoforms are products of different genes, share 60-65% amino acid sequence identity and are very similar in structure and catalytic mechanisms[361]. However, they vary significantly in tissue expression, regulation, and have unique physiological roles[5,362-364]. Cox-1 and cox-2 function within the cell as membrane associated homodimers[365]. Both enzymes are associated with the luminal surface of the endoplasmic reticulum and both surfaces of the nuclear envelope. However, cyclooxygenase-2 is more concentrated within the nuclear membrane suggesting that it may play a direct role in controlling nuclear function[366-368].

Briefly, cox-1 is the constitutively expressed isoform encoded by a 22 kilo-base gene on chromosome 9, which produces a 2.8 kilo-base mRNA[369]. The gene has a TATA-less promoter with multiple start sites for transcription. Relatively little is known about its regulation[370]. However, it is preferentially expressed at high levels in multiple cell types suggesting it is developmentally regulated. This enzyme is the sole source of prostaglandins involved in platelet aggregation[9], parturition[371,372] and intestinal crypt stem cell survival[373,374]. Cox-3 is an alternatively spliced form of cox-1 that retains intron 1[375,376]. It is expressed as a 5.2 kilo-base mRNA and is most abundant in the cerebral cortex and heart. The retained intron results in the insertion of a 30-34 amino acid sequence into the hydrophobic signal peptide. This isoform is selectively inhibited by paracetamol and some NSAIDs.

In contrast, cyclooxygenase-2 is an early response gene, encoded by a 7.5 kilo-base gene on chromosome 1[38,377,378]. Multiple polyadenylation sites are utilised resulting in the production of a number of different RNA species, with variable lengths of

3'UTR, which appear to be differentially regulated[379,380]. The largest includes a 3'-untranslated region of greater than 2000 bases.

This gene is rapidly and transiently induced by a variety of extracellular ligands in many cell types, including macrophages and mesangial cells, and its expression is inhibited by glucocorticoids[380-383]. Cox-2 expression is particularly responsive to multiple growth factors and cytokines consistent with its role in mitogenesis, inflammation and wound repair[384,385]. Constitutive, as well as inducible, expression also occurs in specialised cell types where its regulation is intimately linked to the specific physiological processes taking place[71,386-389].

The cox-2 protein's catalytic site is approximately 20% larger than that of cyclooxygenase-1, making selective pharmacological inhibition possible[362,390]. Prostaglandins produced by cox-2 are required in many physiological processes such as ovulation, implantation[3], neonatal renal development[10] and closure of the Ductus Arteriosus[12], as well as being involved in modulation of the immune response[391], maintaining gastro-intestinal integrity[8] and playing a significant role in carcinogenesis[384,385]. In fact overexpression of the cox-2 gene was shown to be sufficient to induce mammary tumours[392] and premalignant skin disease in murine models[393]. The exact mechanism by which cox-2 induces malignant transformation is not known, although in studies of colon cancer cell lines, it has been shown to be anti-apoptotic, promotes tumour-associated angiogenesis, increases epithelial cell spreading and migration leading enhanced metastatic potential[54,55].

Many signal transduction pathways have been shown to be involved in transcriptional activation of cox-2, including the NFκB, the cEBP and one or more of the MAP kinase

pathways[377,394-400]. As expected, the promoter region of the cox-2 gene contains multiple cis-regulatory elements involved in transcriptional regulation, including an overlapping E-box/CRE sequence, an NF-IL6/cEBP sequence and two NFκB sequences[377,401]. The signalling pathways and transcriptional activators involved vary, depending on the cell type and ligand studied.

In common with many early response genes, cox-2 expression is also controlled at the post-transcriptional level[212,216,402-404]. As in its transcriptional control, these processes vary substantially, depending on the stimulus and the cell type examined. Post-transcriptional control of cox-2 requires the 3'-UTR and involves activation of MAPKs[405,406]. The resultant changes in mRNA half-life and translational efficiency lead to a substantial and rapid increase in cox-2 protein expression and prostaglandin production.

The 3' untranslated region contains multiple cis-elements controlling mRNA stability and translation efficiency[216]. The proximal region of the 3'-UTR contains highly conserved Adenosine-uridine Rich Elements (Figure 2), which are required for p38 induced message stabilisation[212] and have been shown to bind a number of AU-binding proteins. Furthermore, dys-regulation of post-transcriptional control of cyclooxygenase-2 may be involved in the pathogenesis of some carcinomas[264], as altered expression/function of a number of AUBPs in colon cancer cell lines[239,241,332] has been shown to be associated with stabilisation and/or increased translation of cox-2 mRNA, resulting in increased protein expression. Increased cox-2 expression in these circumstances could enhance tumour growth and metastatic potential, related to the known effects of prostaglandins on angiogenesis, cell proliferation and migration[407]. In one of these articles[239], elevated levels of HuR were associated with

increased expression of VEGF and IL8, as well as cox-2, suggesting that the expression of multiple genes are affected by the dysfunction of a single AUBP or cis-acting element. It is tempting to speculate that even subtle mutations of an AUBP could lead to altered RNA binding, protein-protein interactions or subcellular localisation with resultant knock-on effects on multiple genes, including cox-2, leading to cellular dysfunction or transformation. The aetiology of cellular dysfunction could be readily apparent or may appear to be a polygenetic abnormality of obscure aetiology.

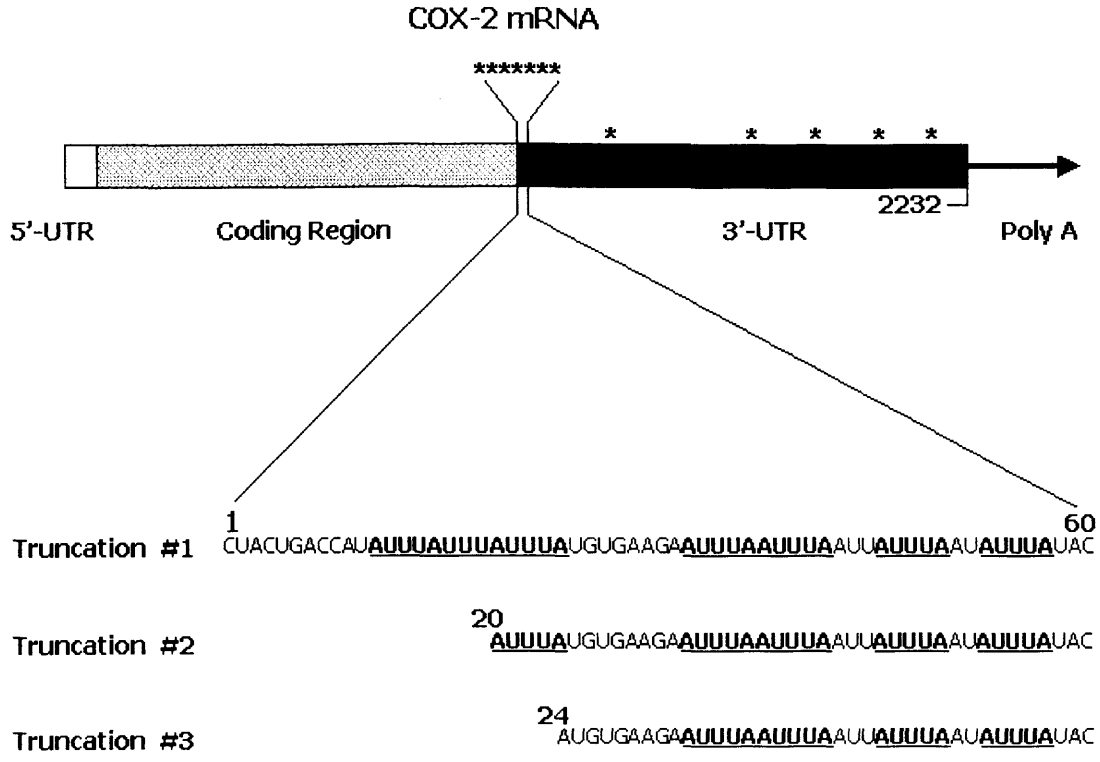

Figure 2: Basic structure of cox-2 mRNA

The basic structure of the Cox-2 mRNA is illustrated, showing the coding region flanked by the 5′ and 3′ untranslated regions. The 3′UTR contains multiple AUUUA (*) consensus sequences, seven of which are clustered within the proximal 60 nucleotides. The bottom half of the illustration shows the sequence of the proximal 60 nucleotide segment of the Cox-2 3′UTR used for construction of luciferase reporter genes and RNA probes. AUUUA elements are underlined and in bold and numbering begins with the first nucleotide of the 3′-UTR of COX-2. Removal of the first 19 and 23 nucleotides of this sequence disrupts and completely removes the proximal 3 overlapping AUUUAs respectively.

Chapter 4

Background to Current Investigations

Initial Studies in the Morrison lab using rat mesangial cells, showed rapid induction of cox-2 expression with IL1β stimulation, involving activation of both JNK and p38 MAPK signalling pathways[408-410]. The demonstration of increased mRNA half-life and altered protein interactions with the proximal 3'-UTR provided evidence of the involvement of post-transcriptional mechanisms in the control of cox-2 expression in these cells following IL1β stimulation[402].

Following on from this, hybrid reporter gene assays were used to identify multiple cis-acting elements within the 3'-UTR of cyclooxygenase-2[216]. The 2232 base 3'UTR of cox-2 was split into multiple smaller, more "user friendly", sections and subcloned downstream of the luciferase coding region of pGL3c. All subclones were under identical transcriptional control. Therefore, any observed differences in expression would be secondary to altered post-transcriptional regulation dependent on the subcloned 3'UTR sequence. The hybrid reporter genes were transiently expressed in immortalised mouse mesangial cells; steady state luciferase activity and mRNA were measured and compared to unaltered pGL3c. Although multiple regions of the cox-2 3'UTR were found to regulate luciferase expression by post-transcriptional mechanisms, the proximal 60 nucleotides sequence significantly decreased reporter gene expression, by changing mRNA half-life and translation. As previously mentioned, this region contains the highly conserved cox-2 ARE, required for p38 induced mRNA stabilisation[212], making it of particular interest. This 60 nucleotide sequence contains seven copies of the consensus AUUUA sequence, 3 of these are overlapping and located within the proximal 25 nucleotides and the remaining four are located in the distal half of the sequence (Figure 2).

While these studies illustrate the potential regions within the 2Kb 3'UTR, which regulate the post-transcriptional control of cox-2, they do not pinpoint the functional

cis-acting elements, nor do they identify the trans-acting factors involved or ascertain whether they are ligand responsive. Also, it is unclear whether all AUUUA pentamers within the proximal 60 nucleotides are required for post-transcriptional regulation. More precise identification of the sequences involved, in particular those that are ligand regulated, and identification of the RNA binding proteins that interact with them would bring us much closer to understanding the post-transcriptional regulation of cox-2 and its involvement in multiple pathophysiological processes.

In order to clarify the functional cis-acting elements within the proximal 60 nucleotide sequence, determine whether these were ligand responsive and interact with known RNA binding proteins, we developed the following lines of investigation.

We focused on the 1-60 region, as it contains the conserved cox-2 ARE and we already knew it had a significant post-transcriptional effect on reporter gene activity in mouse mesangial cells[216]. We created two further luciferase constructs, the 20 – 60 and 24 – 60 truncations, designed to disrupt/remove the proximal cluster of AUUUAs (Figure 2). We felt this would allow us to reveal whether the proximal three overlapping AUUUAs were functionally distinct from the remaining four AUUUAs. To test if these constructs were ligand-regulated, hybrid reporter genes were transiently transfected into rat mesangial cells and RAW 264.7 cells, a murine macrophage cell line. The results were analysed for changes in luciferase activity at baseline and following IL1β and LPS stimulation, which regulate the expression of cox-2 in rat mesangial[377,402,408-410] and RAW 264.7 cells[411,412] respectively, by both transcriptional and post-transcriptional mechanisms. The expression of cox-2 by macrophages and mesangial cells is known to be involved in both the mediation of the inflammatory response[413] and the development of glomerular inflammation and sclerosis[63].

Therefore, the study of its regulation in rat mesangial and RAW 264.7 cells may offer insights into the pathogenesis of inflammatory disease and glomerular injury.

Because the function of AREs is dependent on their interaction with RNA binding proteins, we constructed radiolabeled probes corresponding to the sequence of the 3'UTR used in the reporter gene studies (Figure 2). Electromobility shift assays and antibody supershift studies were performed to establish whether any of the better-known AUBPs associated with this region of the cox-2 gene and if this association was altered following disruption of the proximal 3 AUUUAs. Nuclear and cytosolic fractions of both cell lines, with and without ligand stimulation, were utilised to demonstrate any visible alteration in protein-mRNA interaction related to cellular location or ligand stimulation.

In summary, our investigations show that insertion of the 1 - 60 sequence was sufficient to cause a marked decrease (>65%) in expression of a luciferase reporter-gene, in both rat mesangial and RAW 264.7 cells. Truncation of this segment by removal of the first 20 nucleotides diminished the negative effect on luciferase activity, particularly in the RAW 264.7 cells. However, complete removal of the proximal 3 overlapping AUUUAs lead to an even greater decline in luciferase activity (≈89%) than seen with the 1 - 60 sequence. Although, luciferase reporter-gene constructs proved unresponsive to stimulation with IL1β in rat mesangial cells, a response was seen with LPS in RAW 264.7 cells, which was eliminated on removal of proximal 20 nucleotides of the 1 – 60 sequence. EMSA and supershift studies revealed that multiple known RNA binding proteins interacted with 1 – 60 sequence in both cell types examined. Those proteins identified included HuR, TIA-1, TIAR and AUF1. Even though some noticeable differences occurred following removal or

disruption of the proximal three AUUUAs, we were unable to detect any variation in complex formation related to subcellular location or ligand stimulation. We believe these results shed further light on the post-transcriptional regulation or cox-2 and identify additional avenues of investigation to help elucidate the mechanisms by which these sequences and proteins alter mRNA stability and translation.

We expect that as our understanding of the post-transcriptional machinery and its regulation improves, its involvement in a diverse variety of pathophysiological processes will become apparent and hopefully, allow the development of novel therapies for many common diseases.

Chapter 5

Materials and Methods

Materials

The following were used unless otherwise specified -

Human recombinant IL1β (Roche), Lipopolysaccharide (Sigma), SB203580 (Calbiochem), Rnase-free DNase (Qiagen), T4 Ligase (Promega), Xba1 (Promega), RNA STAT-60 (Tel-Test), T7 RNA polymerase-Plus (Ambion), Ribonuclease Inhibitor (Fischer), AMV reverse transcriptase (Fischer), Anti-Cox-2 (murine) polyclonal IgG (Cayman), Anti-Rabbit IgG-peroxidase linked (Amersham), ECL western blotting detection reagents (Amersham), Luciferase Assay System (Promega), Big Dye Version 3 premix (Applied Biosystems), Superfect transfection agent (Qiagen), Qiaex II gel extraction kit (Qiagen), QIAquick gel extraction kit (*Qiagen*)

Statistics

To allow for variation between multiple experiments, Luciferase activity was expressed as a percentage of control (Luciferase activity of pGL3c arbitrarily set at 100%). Fold increases in Luciferase activity following treatment with IL1β or LPS were calculated by dividing the Luciferase activity at each time point by the zero time point activity for each vector construct.

All data were expressed as mean ± standard error and comparison between each construct and pGL3c was performed using an un-paired Student's t-test. A value of $p<0.05$ was considered significant.

Cell Culture

Rat Mesangial Cells

Rat mesangial cells were prepared from male Sprague-Dawley[414] and grown in RPMI-1640 medium supplemented with 10% (v/v) heat-inactivated foetal bovine serum, 0.6% (v/v) insulin 100 U/ml, 100 U/ml penicillin, 100 μg/ml streptomycin, 250 μg/ml amphotericin B, and 15 mM HEPES (pH 7.4). All experiments were performed with cells passaged 4 to 12 times and, where indicated, mesangial cells were stimulated with IL-1β (100 U/ml) for the specified time.

RAW 264.7 Cells

RAW 264.7 cells, a murine macrophage cell line established from a tumor induced by Abelson murine leukaemia virus, were obtained from ATCC. Lipopolysaccharide induces Cox-2 expression in RAW 264.7 cells by both transcriptional and post-transcriptional mechanisms[412]. LPS acts via the TLR4 receptor[411], with downstream activation of NFκB and one or more of the MAPK pathways being involved in the transcriptional activation of the Cox-2 gene[397,411,412,415-419]. Although, it is well documented that post-transcriptional control is involved in IL1β induced Cox-2 expression in rat mesangial cells, most studies in RAW cells have focused on the transcriptional events and signalling pathways involved in LPS induced cox-2 expression. However, both these ligands signal through related receptors, with many similarities in intracellular signal transduction[420] and post-transcriptional control of LPS induced cox-2 has been documented in human macrophages[421]. Therefore, it

seems likely that post-transcriptional mechanisms will be active in LPS induced cox-2 expression in RAW 264.7 cells also.

RAW 264.7 cells were grown in DMEM supplemented with 10% (v/v) heat-inactivated foetal calf serum, 100 U/ml penicillin, 100 μg/ml streptomycin, and 15 mM HEPES (pH 7.4). Where indicated, RAW 264.7 cells where stimulated with LPS 10, 50, or 100ng/ml, Interferon γ 50-100 units/ml or TNFα 20-100ng/ml for the specified time. Where indicated, SB203580 (Calbiochem) dissolved in DMSO, at concentrations of 1 or 10μm/ml, was added 30mins before stimulation with LPS.

Cell Fractionation

All steps were performed on ice, using freshly prepared DEPC-treated buffers and an Rnase-free technique.

Rat mesangial cells were grown in T75 flasks to 70-80% confluency, and then stimulated with IL1β (100 U/ml) for the specified time. Cells were washed twice with 10mls of ice-cold, sterile phosphate buffered saline before 750μl of hypotonic buffer A - *10 mM HEPES pH 7.5, 10 mM KCl, 1 mM EDTA, 1 mM EGTA, 1 mM DTT, 1 mM* $MgCl_2$*, 5% glycerol, 0.1 mM* $NaVO_4$*, with protease inhibitors (1 μg/ml leupeptin, 2 μg/ml aprotinin, and 1 μg/ml pefabloc)* – was added. Cells were harvested by scraping, transferred into sterile microcentrifuge tubes and allowed to swell on ice for 15 min.

Cell membrane lysis was performed by adding 10% NP-40 (final concentration 0.25%) and nuclei were pelleted by centrifugation (10min x 1500g at 4°C). The cytosolic fraction was clarified from the supernatant by centrifugation (5min x 15,000g at 4°C).

The nuclei were resuspended gently by pipetting, washed two times in 250µl of buffer B - *10 mM HEPES pH 7.5, 10 mM KCl, 1 mM DTT and 1 mM $MgCl_2$* – and then isolated by centrifugation (10min x 1500g at 4°C). The final nuclear pellet was resuspended in 400µl of nuclear lysis buffer - *20 mM HEPES pH7.5, 0.4 M NaCl, 1 mM EDTA, 1 mM EGTA, 1 mM DTT, 1 mM $MgCl_2$, 25% glycerol with protease inhibitors*. Nuclear membrane lysis was achieved by incubating on ice for 15 min and vortexing every 2 to 3 min. The nuclear fraction was then clarified by centrifugation (5min x 15,000g at 4°C) and the supernatant saved.

The protein concentration was measured and all specimens were stored at -70°C until use. The purity of the cell fractions was assessed by western analysis using an antibody directed against the splicing factor U1 SnRNP 70 (Santa Cruz) as a marker of nuclear fractions and an antibody against GAPDH (Ambion) as a cytosolic protein marker.

RAW 264.7 cells were grown in T75 flasks to 70% confluency, and then stimulated with LPS (100ng/ml). Following this cells were harvested and fractionated using the same technique as described for the Rat mesangial cells. Again, the protein concentration was measured and all specimens were stored at -70°C until use.

Western Analysis

At the time of harvest, cells were washed with ice-cold phosphate buffered saline twice and lysed in 200-400µl of whole cell extract (WCE) buffer – *25 mM HEPES (pH 7.4), 0.3 M NaCl, 1.5 mM $MgCl_2$, 0.2 mM EDTA, 0.1% Triton X-100, 0.5 mM DTT, 20 mM β-glycerophosphate, 100 µM $NaVO_4$, 1 µg/ml leupeptin, 2 µg/ml aprotinin and 0.5mg/ml pefabloc*. Samples were clarified by centrifugation (10min x 15,000g) and the supernatant saved. Protein concentrations were measured and all samples saved at -70°C until use.

6X Laemmli sample buffer was added before heating. After boiling for 5 minutes, equal amounts of protein were run on 8% SDS-PAGE (40mA for four hours). Proteins were then transferred (20V for one hour) to polyvinylidene difluoride (PVDF) membranes (Immobilon BP; Millipore Corp., Bedford, MA). The membranes were saturated with 5 % fat-free dry milk in Tris-buffered saline (50 mM Tris-HCl, pH 8.0, 150 mM NaCl) with 0.05 % Tween 20 (TBS-T) for 1 hour at room temperature.

Blots were then incubated overnight with polyclonal anti-murine Cox-2 (Cayman) at 1:1000-dilution in TBS-T. After washing with TBS-T solution, blots were further incubated for 1 hour at room temperature with secondary antibody, anti-rabbit Ig antibody coupled to horseradish peroxidase (Amersham, Arlington Heights, IL) at 1:5000-dilution in TBS-T. Blots were then washed five times in TBS-T before visualization. The Enhanced ChemiLuminescence kit (ECL, Amersham) was used for detection. Blots were quantitated on a densitometer using Quantity One software from PDI. The densitometer was calibrated to an external standard.

Other antibodies used in western analysis were as follows:

Anti-GAPDH (Ambion) 1:4,000-dilution, secondary anti-mouse Ig 1:5000-dilution.

U1 snRNP 70 (Santa Cruz) 1:1,000-dilution, secondary anti-goat Ig 1:5000-dilution.

HuR (Santa Cruz) 1:1,000-dilution, secondary anti-mouse Ig 1:5000-dilution.

Plasmid Construction

Summary

pGL3c reporter-gene constructs were generated as follows. Specific regions of the 3'-UTR of COX-2 were amplified by PCR using primers terminating in Xba1 recognition sequences[216]. PCR products were ligated into TOPO TA cloning vector (Invitrogen), as per the manufacturer's instructions and subsequently excised with Xba1. DNA inserts were purified by agarose gel electrophoresis and extracted using a QIAquick gel extraction kit (*Qiagen*).

Following this, DNA inserts were ligated into the unique Xba1 site of the pGL3 control vector (Promega), located in the 3'-UTR of the firefly luciferase gene. 2μl of each ligation reaction was then electroporated into DH5α E. Coli and plated on selective media overnight. Plasmid DNA was isolated from multiple colonies, using a commercial miniprep kit (Promega), and resuspended in 50μl of water. 5μl of each miniprep was subjected to a restriction enzyme digest using Xba1 and separated by gel electrophoresis. Minipreps with appropriate size inserts were sequenced to confirm subcloning success and frozen stocks stored at -70°C for future use. When the correct sequence was confirmed, Maxipreps (Qiagen) of frozen stock samples were used to isolate larger quantities plasmid DNA, which was resuspended in nuclease-free water and stored at -20°C.

Primers

Specific regions of the 3'-UTR of cox-2 were amplified by PCR using primers terminating in Xba1 recognition sequences (in bold type). The following primers were used to amplify the 1-60, 20-60 and 24-60, 1-2232 and 62-2232 regions of the 3'UTR –

5'-Xba-1: 5'-(**TCTAGA**CTACTGACCATATTTATTTA)-3'

5'-Xba-20: 5'-(**TCTAG**ATTTATGTGAAGAATTTAATTTAA)-3'

5'-Xba-24: 5'-(**TATAG**ATGTGAAGAATTTAATTTAATTA)-3'

5'-Xba-62: 5'-(**TCTAGA**GAATTTTTTTTCATGTAAC)-3'

3'-Xba-60: 5'-(**TCTAGA**GTATAAATATTAAATAATTAAATTAAAT)-3'

3'-Xba-2232: 5'-(**TCTAGA**GGGCTGCAGGAA)-3'

Generation of the other luciferase reporter gene constructs used and their respective primer pairs was previously described[216]. The entire process is described in detail below.

Subcloning and DNA Isolation

TOPO TA Vector

The PCR reaction was performed as follows and 10μl of each PCR product was checked, using agarose gel (1.5%) electrophoresis, to confirm the presence of a single discrete band –

Taq polymerase 5 units, Buffer (10x) 2.5μl, $MgCl_2$ (10x) 2.5μl, dNTPs 1μl
Template DNA 40ng (Cox-2 in Bluescript®), Primers 1μL each (Conc 2μm)
H_2O to make up final volume of 25μl per reaction
PCR cycling conditions –
96°C x 2min,
96°C x 15sec, 50°C x 30sec, 72°C x 60sec - for 30 cycles
72°C x 7mins
4°C ∞

PCR products were ligated into TOPO TA cloning vector (Invitrogen), as per the manufacturer's instructions. Insertion of PCR product disrupts the LacZα gene resulting in the growth of white colonies in the presence of X-Gal. All TOPO TA clones were selected on Luria-Bertani (LB) agar plates (Index A), containing kanamycin 50μg/ml and coated with X-Gal 40μl (Concentration 40mg/ml). The procedure is briefly described as follows –

TOPO cloning reaction
H_2O 2μl, PCR product 2μl, pCR-TOPO vector 1μl
Mix gently and incubate reaction at room temperature for 5min

Chemical transformation
2μl of the TOPO cloning reaction was added to an aliquot of "One Shot Cells®" and mixed gently.
Incubate on ice for 30min, then heat shock at 42°C for 30sec,
Add 250μl SOC media and transfer to a 17x100mm polypropylene tube

Incubate at 37°C for 60min.

Plate 50µl and 200µl on selective media and incubate overnight

Analysis of Clones

5-10 white colonies were selected from each plate and cultured overnight in 3ml of selective LB media.

1ml was saved in 25% glycerol at -70°C, as frozen stock.

DNA was isolated using Wizard® Plus Miniprep (Promega) and eluted with 50µl nuclease-free water (stored at -20°C)

Restriction Enzyme Digest with Xba1 as follows

Miniprep DNA 10µl, Xba1 10 units, Buffer D 2µl

Add water to total volume of 20µl

Mix gently and incubate at 37°C for 60min

Agarose Gel (1.5%) Electrophoresis was used to confirm that an insert was present and "positive" clones were sequenced, using the T7 promoter sequence as a primer, 5'-(TAATACGACTCACTATAGGG)-3', as described below.

A larger quantity of each insert was produced using the frozen stock samples of sequence-confirmed clones, saved during the previous step, to perform Midipreps (Qiagen). DNA was eluted into 50µl of nuclease-free water (approximate concentration 2.5 - 4µg/µl) and another restriction enzyme digest using Xba1 was performed -

Midiprep DNA 10µl, Xba1 50units, Buffer D 5µl (10X)

Add H_2O to 50µl, mix gently and incubate 37°C x 60mins

All RED reactions were electrophoresed on a 1.5% agarose gel and inserts were extracted using a QIAquick gel extraction kit (Qiagen). The resultant DNA inserts, eluted in 100µl of TE buffer, were stored at -20°C until use.

TOPO® TA pCR®II

Downloaded from Invitrogen® website

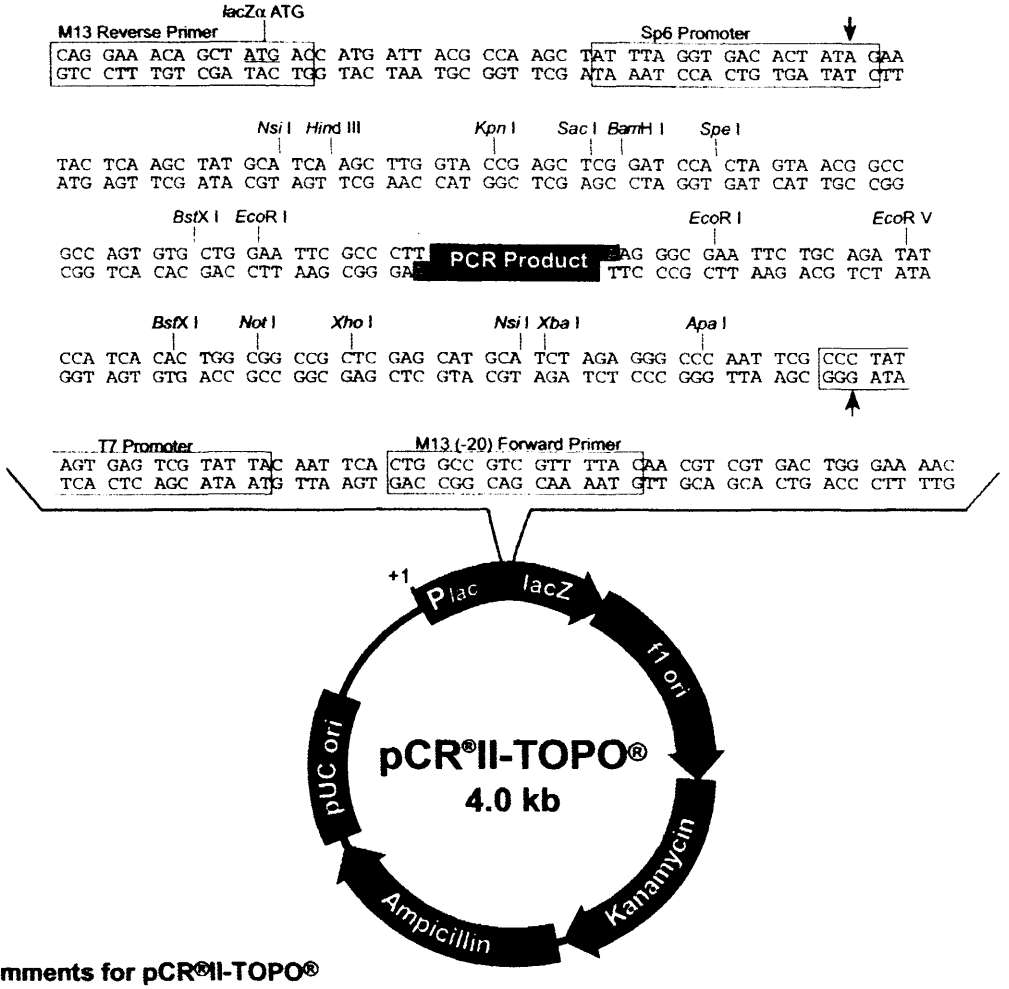

Comments for pCR®II-TOPO®
3973 nucleotides

LacZα gene: bases 1-589
M13 Reverse priming site: bases 205-221
Sp6 promoter: bases 239-256
Multiple Cloning Site: bases 269-383
T7 promoter: bases 406-425
M13 (-20) Forward priming site: bases 433-448
f1 origin: bases 590-1027
Kanamycin resistance ORF: bases 1361-2155
Ampicillin resistance ORF: bases 2173-3033
pUC origin: bases 3178-3851

pGL3c Vectors

30μg of pGL3c was subjected to a restriction enzyme digest with Xba1 -

Xba1 50units, Buffer D 5μl,

Add H_2O to 50μl, mix gently and incubate 37°C for 60mins

then treated with a phosphatase –

RED sample 50μl, Buffer 5μl (10X), Alkaline Phosphatase 1 unit

Following this, DNA inserts, isolated from the TOPO TA subclones, were ligated into the linearised pGL3c vector –

T4 Ligase 3 units, Buffer 2μl (10X), Insert DNA 8μl, pGL3c 3μl,

Add water to total volume of 20μl and incubate at 16°C for ≥ 2 hours

2μl of each ligation reaction was electroporated into 40μl DH5α E. Coli and plated on selective media overnight. All pGL3c constructs were selected using LB agar plates containing ampicillin 50μg/ml. Again, plasmid DNA was isolated from multiple colonies, using a commercial (Qiagen) miniprep kit and resuspended in 50μl of water.

Further analysis and identification of pGL3c constructs was the same as described for the TOPO TA clones, except that the following primer – 5'-AGAGATCGTGGATTACGTCG - 3' - was used for sequencing. Unfortunately, restriction enzyme digests of TOPO TA clones were "contaminated" with a ≈ 50-nucleotide segment of the vector itself, which could not be separated from the shorter sequences by agarose gel purification. Though, this prolonged the subcloning process, all clones were eventually isolated and single copy inserts, in the correct orientation confirmed by sequencing.

Frozen stocks of all confirmed clones were stored in 25% glycerol at -70°C. Subsequently, Maxipreps (Qiagen) kits were used to isolate plasmid DNA from frozen stock samples. DNA was eluted in 250μl of nuclease-free water and stored at -20°C until use. DNA concentration was measured using spectrophotometry (OD 260nm) and ranged from 0.8-2ug/ml in most cases.

pGL3c®

Downloaded from Promega® website

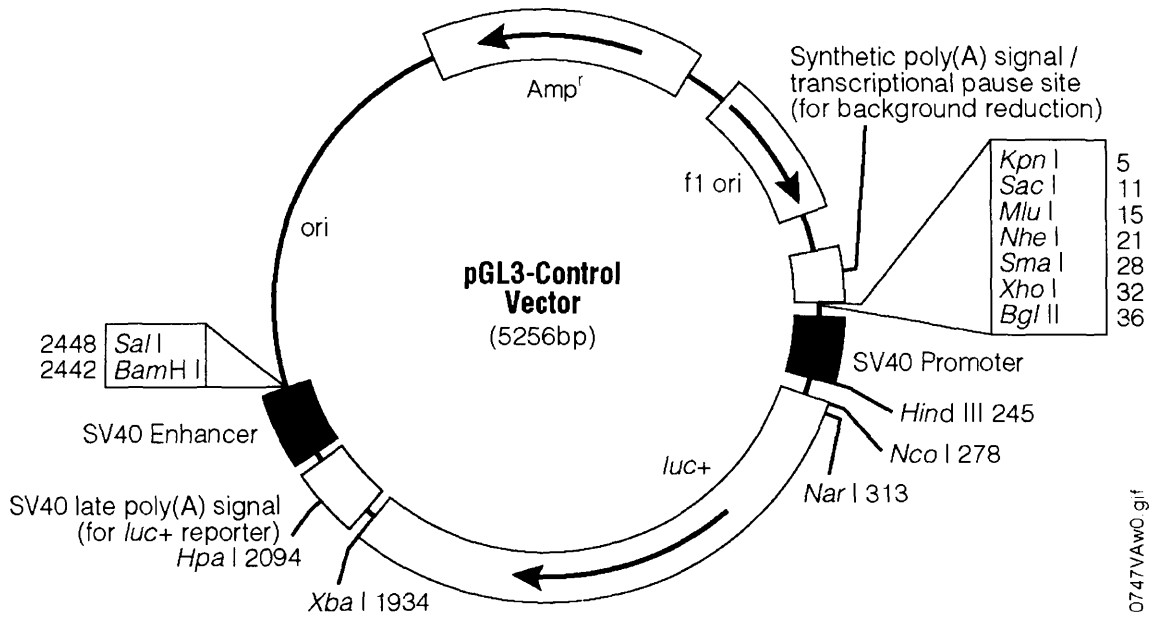

Base pairs	5256
Multiple cloning region	1-41
Promoter	48-250
Luciferase gene (luc+)	280-1929
GLprimer2 binding site	303-281
SV40 late poly (A) signal	1964-2185
Enhancer	2250-2441
RVprimer4 binding site	2518-2499
ColE1-derived plasmid replication origin	2756
Beta-lactamase gene (Ampr)	4378-3521
F1 origin	4511-4965
Upstream poly (A) signal	5096-5249
RVprimer3 binding site	5198-5217

pcDNA3 Vectors

RNA probes for electrophoretic mobility shift assays (EMSAs) were constructed by amplifying the same 3′-UTR sequences except that the primers encoded a HindIII recognition site a the 5′ end and a BamHI site at the 3′ end (in bold type).

The following primer sequences were used for amplification –

5′-Hind-III 1: 5′-(**AAGCTT**CTACTGACCATATTTATTTA)-3′

5′-Hind-III 20: 5′-(**AAGCTT**ATTTATGTGAAGAATTTAATTTAA)-3′

5′-Hind-III 24: 5′-(**AAGCTT**ATGTGAAGAATTTAATTTAATTA)-3′

3′-BamHI 60: 5′-(**GGATCC**GTATAAATATTAAATAATTAAATTAAAT)-3′ –

and the PCR cycling conditions used were as follows –

96°C x 2min,

96°C x 15sec, 45°C x 30sec, 72°C x 60sec - for 25 cycles

72°C x 5mins

4°C ∞

The PCR products were subcloned into the TOPO TA cloning vector (Invitrogen®), confirmed by sequencing and the inserts were gel purified, following a restriction enzyme digest using HindIII and BamHI.

The destination vector, pcDNA3 (Invitrogen®) was linearised using HindIII and BamHI, treated with a phosphatase and purified using a QIAquick gel extraction kit (Qiagen).

DNA inserts were ligated into linearised pcDNA3, electroporated into DH5α E. Coli and plated on selective media overnight. Again, plasmid DNA was isolated from

multiple colonies, using a commercial (Qiagen) miniprep kit and resuspended in 50µl of water. Further analysis and identification of pcDNA3 clones was the same as described for the pGL3c constructs.

Sequencing of pcDNA3 clones was performed using the T7 promoter [5′-(TAATACGACTCACTATAGGG)-3′] and SP6 promoter [5′-(ATTTAGGTGACACTATAG)-3′] sequences as primers.

Frozen stocks of all sequence-confirmed clones were stored at -70°C and Maxipreps (Qiagen) kits were used for isolation of plasmid DNA.

pcDNA3

Downloaded from Invitrogen® website

Comments for pcDNA3:
5446 nucleotides

CMV promoter: bases 209-863
T7 promoter: bases 864-882
Polylinker: bases 889-994
Sp6 promoter: bases 999-1016
BGH poly A: bases 1018-1249
SV40 promoter: bases 1790-2115
SV40 origin of replication: bases 1984-2069
Neomycin ORF: bases 2151-2945
SV40 poly A: bases 3000-3372
ColE1 origin: bases 3632-4305
Ampicillin ORF: bases 4450-5310

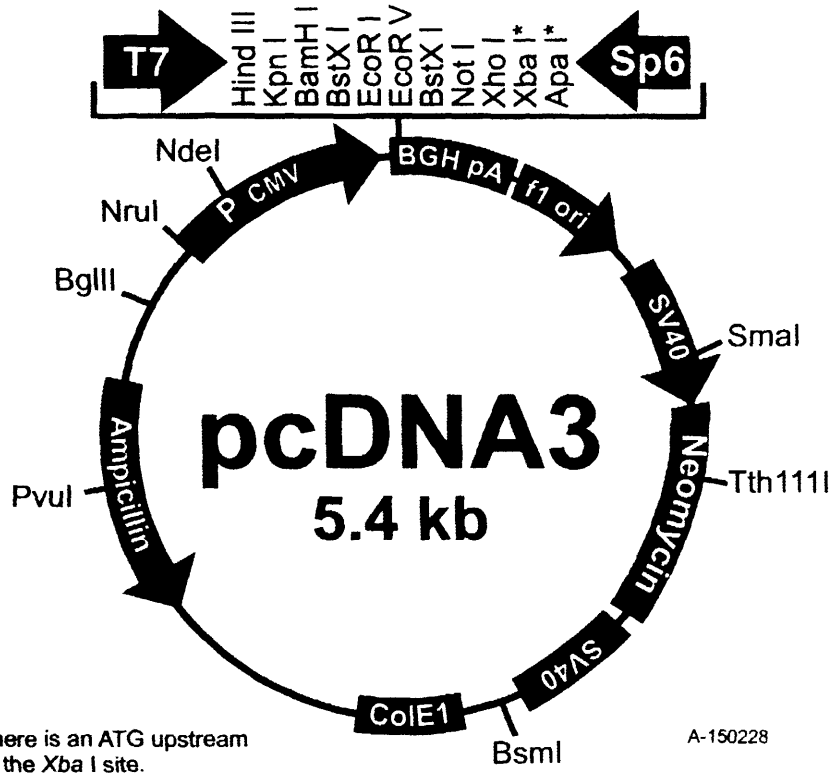

* There is an ATG upstream of the *Xba* I site.

Sequencing

All plasmid constructs had their sequences verified before use. The primers used for individual plasmids are described in the subcloning section above and sequencing reactions were made up as follows –

Miniprep DNA 0.5μg, Big Dye terminator 4μl, Primer 1μl
Add water to total volume of 12μl and mix gently

PCR cycling conditions –

94°C x 5min,
96°C x 10sec, 50°C x 5sec, 60°C x 4min - for 25 cycles
60°C x 4min
4°C ∞

Following PCR, samples were ethanol precipitated to remove unincorporated dyes, before being sent to the Protein and Nucleic Acid Chemistry Laboratory (PNACL) at Washington University for sequencing -

Transfer PCR reactions into 1.7ml microcentrifuge tubes
Add 20μl $MgCl_2$ (2mM) and 48μl isopropanol
Mix gently and incubate at room temperature for 15min
Centrifuge 15000g x 15min and discard supernatant

Resuspend in 100μl of ethanol 70%
Centrifuge 15000g x 15min
Discard supernatant and air-dry for 15min

Preparation of Electrocompetent E. Coli

DH5α E. Coli were grown in 3ml of Luria-Bertani medium overnight at 37°C and used to inoculate one litre of LB medium. Then cells were grown at 37°C, with vigorous

shaking, until an OD_{600nm} of 0.5-0.8 was reached. At this point, the culture was removed from the incubator and chilled on ice for 30 minutes.

All further steps were performed in a cold room at 4°C, with the cells kept on ice. Cells were precipitated by centrifugation (15min x 4000g x 4°) and the supernatant discarded. They were resuspended gently in one litre of chilled sterile water, precipitated as before and the supernatant was discarded. This wash-step was repeated once more with 0.5L of water. Cells were then resuspended in 20ml of sterile 10% glycerol, precipitated again and the supernatant discarded. Finally, they were resuspended in 2ml of 10% glycerol and then separated into 80μl aliquots before being frozen on dry ice and stored at -70°C.

Electroporation

All plasmids were electroporated into electrocompetent E. Coli (DH5α), which were thawed gently and kept on ice throughout the procedure. O.2cm cuvettes were sterilised using UV light for 10min and placed on ice. The Gene Pulser apparatus was set at 25μF and to 2.5 kV and the pulse controller to 200Ω.

0.5μl of miniprep DNA was added to 40μl of electrocompetent DH5α, mixed gently, incubated on ice for 30-60 seconds and transferred to 0.2cm cuvettes. The cuvette containing the mixture of cells and DNA was pulsed once and diluted immediately with 1ml of SOC medium. Then the cell suspension was transferred to a 17 x 100mm polypropylene tube and incubated at 37°C for one hour.

Following this 10μl was plated on selective LB agar and incubated overnight at 37°C. As a negative control DH5α were grown on selective LB agar without prior electroporation. Electroporation followed by growth on non-selective media was used as a positive control. A single colony was selected, a maxiprep (Qiagen) of plasmid DNA was completed according to the manufacturer's instructions and a frozen stock stored at -70°C in 25% glycerol. Each specimen's DNA concentration was measured using a spectrophotometer, diluted to a concentration of 1μg/μl and stored in water at -20°C for future use.

Following ligation reactions, the electroporation procedure was essentially the same, except for the following alterations. 2μl of miniprep DNA was added to 40μl of DH5α electrocompetent cells. After incubation in SOC, samples were pelleted and resuspended in 100μl of LB medium, all of which was plated on selective media.

Transient Transfection

Cells were transiently transfected using SuperFect Transfection Reagent (Qiagen) as per the manufacturer's protocol.

Rat mesangial cells were plated into 6 well plates, grown to 50 to 75% confluency and transfected with 2.5μg of reporter-gene plasmid DNA, using a 4:1 Superfect to DNA ratio. Plasmid DNA (2.5μg) was diluted with 75μl of serum free media. Then 10μl of superfect reagent was added and the mixture was incubated at room temperature for 5-10 minutes. During this time, cell monolayers were washed once with sterile phosphate buffered saline (1X). After incubation, the transfection

mixture was diluted with 0.5ml of serum-free media and layered onto the cells. Then 2ml of 10% FCS media was added per well. Following transfection, the media was changed after 2 hours and cells were incubated overnight in 10% FCS media to allow reporter-gene expression.

All cells were harvested on ice (see Luciferase assay below) and, where specified, following stimulation with IL1β (100 units/ml). 5μg of plasmid DNA was used for transfection of cell monolayers on 60mm plates. The transfection mixture was diluted in 1ml of serum-free media then layered on cells before adding 4ml of 10% FCS rat mesangial cell media.

RAW 264.7 cells were plated into 6 well plates or 60 mm dishes at 2×10^5 and 4×10^5 respectively, incubated overnight and transfected with 2 to 4μg of reporter-gene plasmid DNA at a 4:1 Superfect to DNA ratio. The procedure used being identical to that outlined above except for the amount of plasmid DNA used. Following transfection, the media was changed after 2 hours and cells were incubated overnight in 10% FCS media to allow reporter-gene expression. Again, all cells were harvested on ice (see Luciferase assay below) and, where specified, following stimulation with LPS (100ng/ml).

Luciferase Assay

Luciferase activity was determined using a Luciferase Assay System (Promega), following the manufacturer's protocol. All 6-well plates were placed on ice and each well was washed twice with 2ml of ice-cold phosphate buffered saline (1X). 100μl of reporter lysis buffer (Promega) was added per well. Cells were removed by scraping and transferred into 1.7ml microcentrifuge tubes. Then each sample was vortexed and the supernatant clarified by centrifugation for 60 seconds at 12,000g. The process for harvesting cell monolayers from 60mm cell culture dishes was the same, except that 4ml of PBS was used to wash each dish and cells were harvested in 250μl of reporter lysis buffer.

Luciferase activity was measured using a Lumat LB 9507 luminometer (E G & G Wallac). 100μl of luciferase assay reagent was injected into 20μl of supernatant and light output was measured over a 10 second period. Luciferase activity was expressed as relative light units (RLU) and normalised to whole cell protein content [216]. All samples were performed in duplicate and their normalised luciferase activity averaged and expressed as a percentage of activity measured in cells transfected with unaltered pGL3c.

Protein Assay

Protein concentration was measured using the BCA™ protein assay kit (Pierce). Samples (10-20μl) were tested in duplicate and the results averaged. Water was used as a "blank" and protein standards were made from a BSA stock solution, as

described in the index. 10μl of water and standard were added to designated wells in a 96-well plate. Then 10μl of the buffer used to isolate protein samples was added to all blanks and standards. Following this 20μl duplicates of sample protein were loaded onto the 96-well plate.

At this stage, working reagent was made up by adding copper sulphate 4% to the bicinchoninic solution (ratio - 200μl: 10ml) and mixing well. 180μl of working reagent was added to every well and the plate was mixed on a plate shaker for 30 seconds. The plate was covered and incubated at 37°C for 30 minutes and absorbance measured at 595nm using a microplate reader. A software package was used to correct for absorbance in the blank specimens, create a standard curve and calculate the average protein concentration of sample duplicates.

Quantitative RT-PCR

Luciferase mRNA from transiently transfected Rat Mesangial Cells was isolated as follows. Using an RNAse-free technique, RNA STAT-60 reagent (Tel-Test, Inc.) was used to isolate total RNA. Cells were grown to 50-75% confluency on 60mm plates, culture medium was aspirated and 500μl of RNA STAT-60 reagent was added. Cell monolayers were removed by scraping and transferred into sterile 1.7ml microcentrifuge tubes. 100μl of chloroform was added, the mixture shaken vigorously for 15 seconds and incubated at room temperature for 3 minutes. Samples were centrifuged (15min x 12000g at 4°C); the upper aqueous phase was transferred into a fresh microcentrifuge tube and saved. 250μl of isopropanol was

mixed with the aqueous phase and incubated at room temperature for 10 minutes. Samples were centrifuged (15min x 12000g at 4°C) and the supernatant discarded. In order to wash the RNA pellet, 500µl of ethanol (75%) was added and the samples vortexed. RNA was isolated by centrifugation (5min x 7500g at 4°C) and the pellet air-dried for 10 minutes. The RNA pellet was resuspended in 100µl of nuclease-free water.

Then total RNA was treated with Rnase-free DNase I (10 units, 37°C for 45 minutes) followed by repeat isolation of RNA using RNA-Stat reagent. DNase treatment was performed a total of three times to eliminate reporter-gene DNA, as well as genomic DNA. Following the three Dnase1 treatments and final RNA STAT isolation, RNA was resuspended in 50µl of nuclease-free water. The concentration was measured using spectrophotometry and samples stored at -70°C until use.

Total RNA (0.5µg) was reverse transcribed with AMV reverse transcriptase (Fischer), using random hexamer primers. Reactions were incubated for 15 minutes at room temperature, 30 minutes at 37°C, 30 minutes at 42°C and for 5 minutes at 95°C.

RNA 0.5µg
AMV RT 10 units
AMV RT Buffer (5x) 4µl
Ribonuclease Inhibitor (Fischer) 20 units
dNTP mix 2µl
$MgCl_2$ (25mM) 4µl
Primers (3µg/µl) 0.25µl
Water to total volume of 20µl

After first strand synthesis, the cDNA was quantified by TaqMan® real-time PCR. All standards and samples were done in triplicate and the results of three independent experiments averaged. The following concentrations of pGL3c vector were used as standards – *20fmol, 200fmol, 2pmol, 20pmol, 200pmol, 2nmol, and 20nmol.*

The sequence of luciferase amplification primers and Taqman® probe used were as follows – Forward primer - GCGCGGAGGAGTTGTGTT

Reverse primer - TCTGATTTTTCTTGCGTCGAGTT

Probe - 6-Fam-TGGACGAAGTACCGAAAGGTCTTACCGG

A mastermix of all reagents was made up and added to wells before the sample was added. A no template control was used in all cases and the original RNA samples were run alongside all RT reactions to confirm the success of DNase treatment in eliminating plasmid DNA. Standard Taqman® cycling conditions were used and each reaction contained –

Taqman® PCR mastermix 12.5µl
Probe (2µM) 2.5µl
Fwd primer (2µM) 2.5µl
Rev primer (2µM) 2.5µl
Sample 5µl

Luciferase mRNA was normalized to ribosomal RNA, measured using the TaqMan® Ribosomal RNA Control Reagents (Applied Biosystems). Relative amounts of luciferase cDNA were calculated by the comparative C_T method (Applied Biosystems user bulletin #2) and expressed as a percentage of luciferase cDNA measured in cells transfected with unaltered pGL3c.

Electromobility Shift Assay

RNA Probe Synthesis

Plasmids for RNA probes were synthesised (described above) and linearised with BamH1 in a restriction enzyme digest –

BamH1 5μl, Buffer E 5μl, Plasmid DNA 40μg
Add water to total volume of 50μl, mix gently and incubate at 37°C for 60min.

Linearised plasmid was purified by ethanol precipitation -

Total RED reaction
Add 0.1 vol Sodium Acetate (3M) and 2.5 vol Ethanol 100%
Incubate at -80°C for 30min
Centrifuge (15min x 15000g) and discard supernatant
Wash once with 150μl Ethanol 70%
Centrifuge (10min x 15000g) and discard supernatant
Resuspend in nuclease-free water and dilute to concentration of 1μg/μl

The TOPO® TA cloning vector, pCR-II®, was used as template for "sequence non-specific" probe. Linearised TOPO® TA was generated and isolated using the same protocol except that restriction enzyme digest was performed with EcoR1.

Labelled RNA probes were generated from linearised plasmid by in vitro transcription and unincorporated nucleotides removed using Sephadex G-25 mini Quick Spin RNA columns (Roche). Cold probes were synthesised by substituting ^{32}P-UTP with UTP 500μM.

In vitro transcription reaction -

T7 polymerase 100 units (Ambion)
Transcription Buffer 10x (Ambion)
Ribonuclease Inhibitor (Fischer) 20 units
DTT 10mM
ATP/CTP/GTP 500μM each
UTP 12.5μM
50μCi ^{32}P-UTP (3000 Ci/mmol, Perkin Elmer)
Water to total volume of 50μl
DNA 10μg (added last to start reaction)
Incubate at 37°C for 90min

The reaction was terminated with the addition of 1μl of RNAse-free DNAse1 and incubating at room temperature for 10 minutes. Labelled RNA probes were isolated, according to the manufacturer's instructions, using Sephadex G-25 mini Quick Spin RNA columns (Roche). Following this, radioactive nucleotide incorporation was calculated by dividing cpm of final product by cpm of input. Probes were stored at 4°C and used within 2 weeks.

Electromobility Shift Assay

Labelled RNA probes were incubated with cell fraction protein at 37°C for 30 minutes using the following binding reaction –

Binding buffer (10x) 2μl, Ribonuclease Inhibitor (Fischer) 0.5μl
Heparin (100 μg/μl) 1μl, Cell Fraction Protein 3-10μg
RNA Probe 1-2μl (2-3 x 10^5 CPM, 1-5pmol)
Add RNAse-free water to total volume of 20μl

After the 30-minute incubation period, 10 units of RNase T1 were added to EMSA samples and a further incubation was performed (30min x 37°C). 5μl of loading

buffer was added and samples were electrophoresed on non-denaturing 4% polyacrylamide gels at 250V for 150 minutes (until dye front just runs off). All gels were prerun for 60 minutes at 200V and visualised by autoradiography.

Antibody Supershift

The procedure was the same as that for electromobility shift assays, except that the following were added to the binding reaction –

0.2 μg affinity purified IgG raised against HuR, TIA-1, TIAR or TTP (Santa Cruz, polyclonal goat IgG)
1 μg affinity purified anti-AUF1 (Upstate Biotechnology, polyclonal goat IgG)
1 μl anti-hnRNP A1 and anti-hnRNP U (Generous gift of Gideon Dreyfuss)
1 μl normal goat serum (Sigma), as control

After 30-minutes incubation at 37°C, RNase T1 (10u) was added to the binding reactions and a further incubation was performed (30min x 37°C). After adding 5μl of loading buffer, samples were electrophoresed on non-denaturing polyacrylamide (4%) gels at 250V for 150 minutes. Again, all gels were prerun for 60 minutes at 200V and visualised by autoradiography.

Chapter 6

Rat mesangial cells results

Reporter Gene Transfections

The 3'UTR of cyclooxygenase-2 decreases the expression of the Luciferase reporter gene by post-transcriptional mechanisms

The first 60 nucleotides of the 3'-UTR of cox-2 mRNA contains multiple copies of the sequence AUUUA and has been reported to have a significant effect on post-transcriptional regulation of cox-2 expression[216]. These 60 nucleotides contain a major translational control element and caused a decrease in message stability when placed in a chimeric reporter gene expressed in an immortalized mouse mesangial cell system[216]. Four different chimeric-reporter gene constructs were used, containing the following regions of the cox-2 3' UTR – 1-60, 20-60, 24-60, as well as the full length 3' UTR. Unaltered pGL3c vector (Index B) was used as a control. Each construct contained the luciferase coding sequence under the control of an SV40 promoter and enhancer elements followed by its' 3'UTR and the SV40 late poly-A signal. Reporter gene constructs only differed in the region of the Cox-2 3'-UTR that was present. Therefore, any observed differences in reporter gene expression were likely to be secondary to post-transcriptional mechanisms, related to the different 3'-UTR sequences, as all constructs were under the same transcriptional control. Reporter gene constructs were transiently transfected into rat mesangial cells and incubated overnight. Samples were assayed for luciferase activity and steady state luciferase mRNA was quantified using RT-PCR. Luciferase activity and mRNA levels were expressed as a percentage of levels from rat mesangial cells transiently transfected with unaltered pGL3c. The results represent the average of n=3 identical experiments (Figure 3).

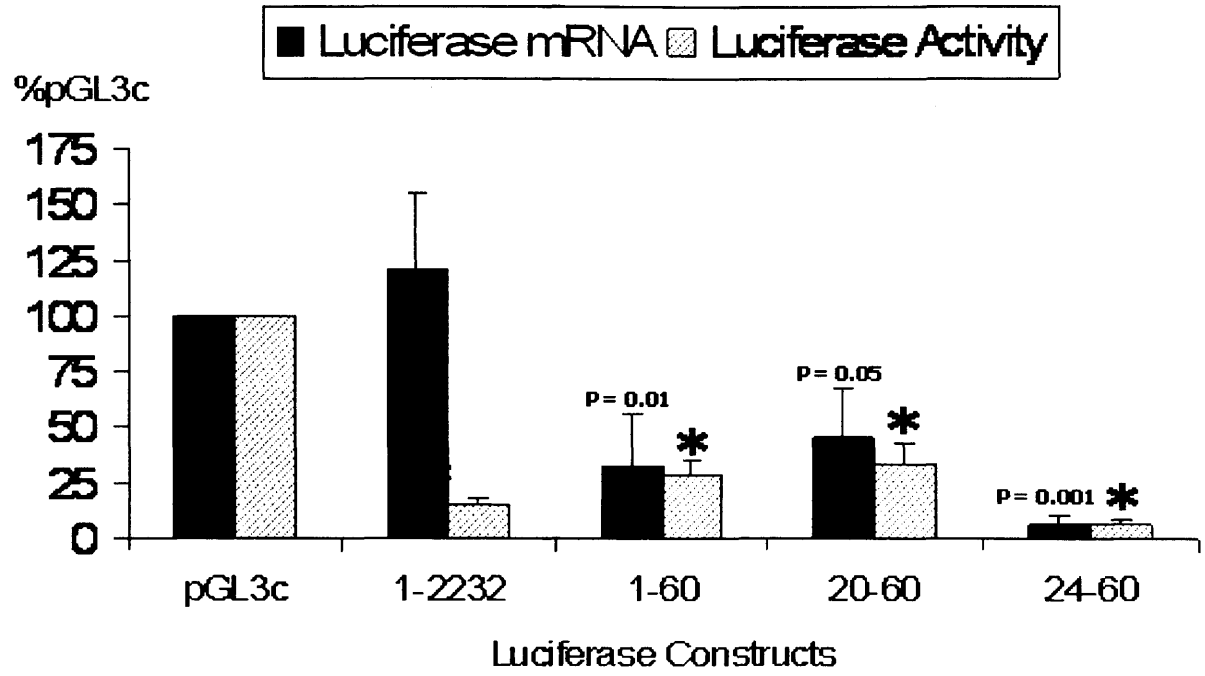

* Compared to pGL3c - P < 0.001

Other P values compared to 1-2232

Figure 3: Transient transfections in Rat Mesangial Cells

Result of transient transfections of pGL3c constructs into Rat Mesangial Cells. The graph represents the average of normalised luciferase activity and steady state luciferase mRNA levels expressed as a percentage of levels obtained using unaltered pGL3c (N ≥ 3 independent experiments).

Insertion of the full-length 3' UTR results in an 85% reduction in reporter gene activity, but no change in steady state mRNA. Insertion of the 1-60 region causes a 71% decrease in luciferase activity with a similar fall in mRNA levels. No appreciable additional change occurs following removal of the proximal 19 nucleotides of the 1-60 region. However, complete removal of the proximal 3 AUUUA sequences (24-60 truncation) did produce a further reduction in luciferase activity, 93% in total, as well as a fall in steady state mRNA.

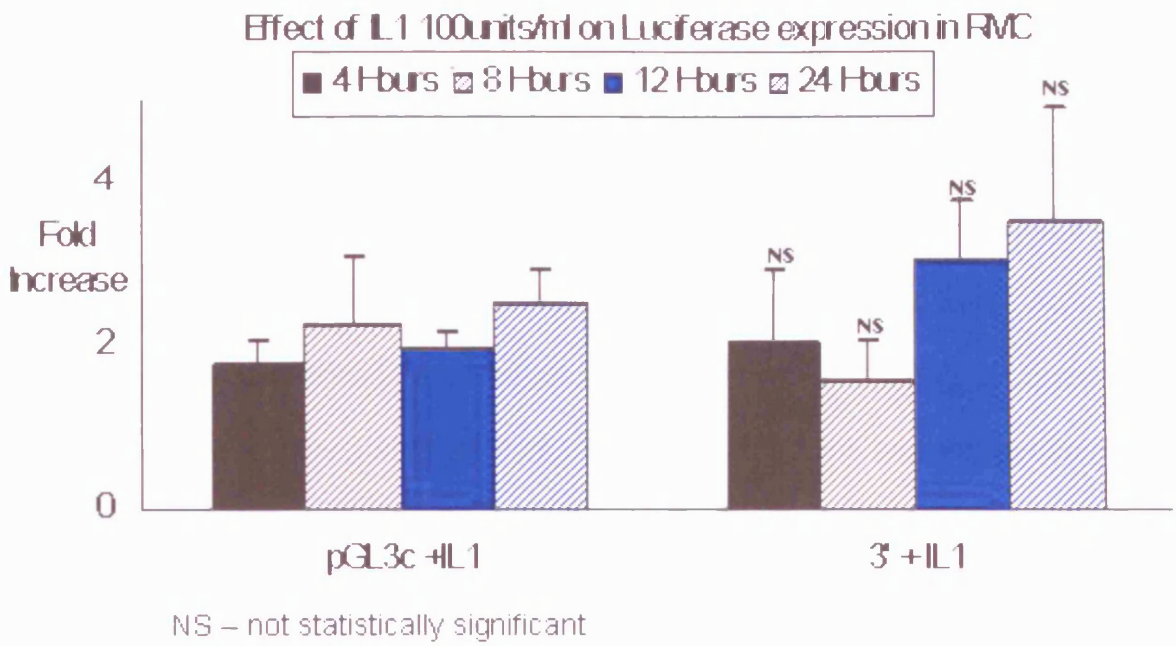

Figure 4: Lack of effect of IL1β on Luciferase activity

Rat mesangial cells were transiently transfected with pGL3c and the full-length 3'UTR construct and treated with IL1β (100 u/ml) over a 24-hour period. Cells were harvested at the above intervals and luciferase activity measured and averaged over three independent experiments. The fold change following IL1β stimulation was calculated by dividing the Luciferase activity at each time point for pGL3c and the 3'UTR by the baseline activity of pGL3c and the 3'UTR respectively. No significant change was seen in luciferase activity following IL1β treatment.

The addition of the full length 3′ UTR resulted in a significant reduction in reporter gene activity (85%) but no change in steady state mRNA levels. This suggests that the principal effect of the full length 3′ UTR involves inhibition of translation. However, insertion of the first 60 nucleotides of the 3′-UTR of COX-2 into the 3′-UTR of a luciferase reporter message resulted in a 71% decrease in luciferase activity and a similar decrease in steady state mRNA levels. This region contains 7 copies of the ARE consensus sequence AUUUA; 3 of these are overlapping and located within the proximal 25 nucleotides. The fall in steady state mRNA levels associated with insertion of 1-60 region is consistent with what's known about the effect of AREs on message stability. Disrupting the proximal overlapping AUUUA repeats by truncation of the first 19 nucleotides of the 1-60 region had no additional effect on luciferase reporter-gene activity or mRNA levels. Complete removal of the proximal 3 AUUUA sequences was achieved by further truncation to leave the 24-60 insert. This resulted in a further decrease in luciferase activity (93% overall) and mRNA levels. Despite repeated attempts, the insertion of the full length 3′UTR was insufficient to endow the luciferase reporter gene with IL1β responsiveness (Figure 4).

Overall, these results suggest that the 3′ UTR of Cox-2 decreased expression of our chimeric-reporter gene by post-transcriptional mechanisms. The conserved ARE sequence within the proximal 60 nucleotides results in decreased steady state mRNA levels, most likely due to decreased message stability. Furthermore, removal of the proximal 3 overlapping AUUUA sequences results in an additional fall in luciferase activity and mRNA levels (Figure 3). This suggests that the proximal 24 nucleotides of the 1-60 region contains a positive control element that modulates the effect of a negative control element in the distal part of 1-60 region.

Electromobility Shift Assay

1-60 region forms multiple RNA-protein complexes

To determine whether changes in luciferase activity following insertion of the 1-60 truncations of the Cox-2 3'UTR were associated with altered binding of proteins to this region of the message, EMSAs were performed using radiolabeled RNA probes corresponding to the proximal 60 nucleotides of the Cox-2 3'UTR (Figure 2) and protein fractions isolated from rat mesangial cells.

RNA-protein complexes of similar electromobility were seen with all three probes (Figure 5) suggesting that truncation of the 1-60 region had no visible effect on the type of the RNA-protein complexes formed. However, the intensity of complex formation was greatest with the 1 – 60 probe suggesting an improved ability to form stable complexes in the presence of the proximal 20 nucleotides. Similarly, nuclear fractions consistently formed greater "quantities" of RNA-protein complexes, despite using equal amounts of nuclear and cytosolic protein. This difference in intensity of complex formation between the nuclear and cytosolic fractions is presumably secondary to the greater concentration of RNA binding proteins within the nucleus. Stimulation of rat mesangial cells with IL1β had no effect on gel-shift pattern and lead to no discernible change in the intensity of the complex formation (Figure 5).

Figure 6 illustrates a cold competition study performed to determine whether RNA-protein complex formation was sequence specific. Nuclear protein fractions of rat mesangial cells were incubated with the 1 – 60 probe and resulted in the formation of 3 prominent RNA-protein complexes (C1 – 3). Increasing concentrations of "cold" probe effectively competed for all 3 complexes, but the addition of increasing amounts of a non-related RNA of similar size, derived from the TOPO TA cloning vector, had no effect on complex formation.

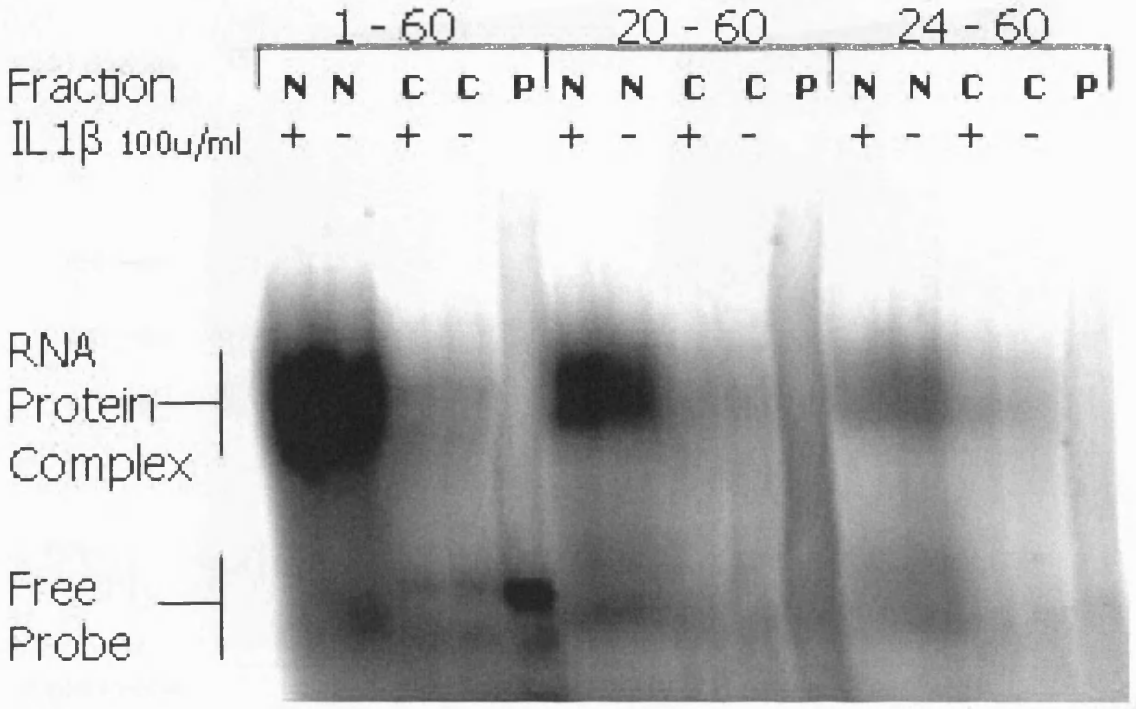

Figure 5: EMSA using Rat Mesangial Cell fractions

An electromobility shift assay was performed using nuclear (N) and cytosolic (C) fractions and RNA probes corresponding to the 1 – 60, 20 – 60 and the 24 – 60 regions of the Cox-2 3'UTR. Free probe (P) was used as a control. Where indicated, cells were treated with IL1β (100 units/ml) for 60mins.

RNA-protein complexes of similar electromobility can be seen with all three probes.

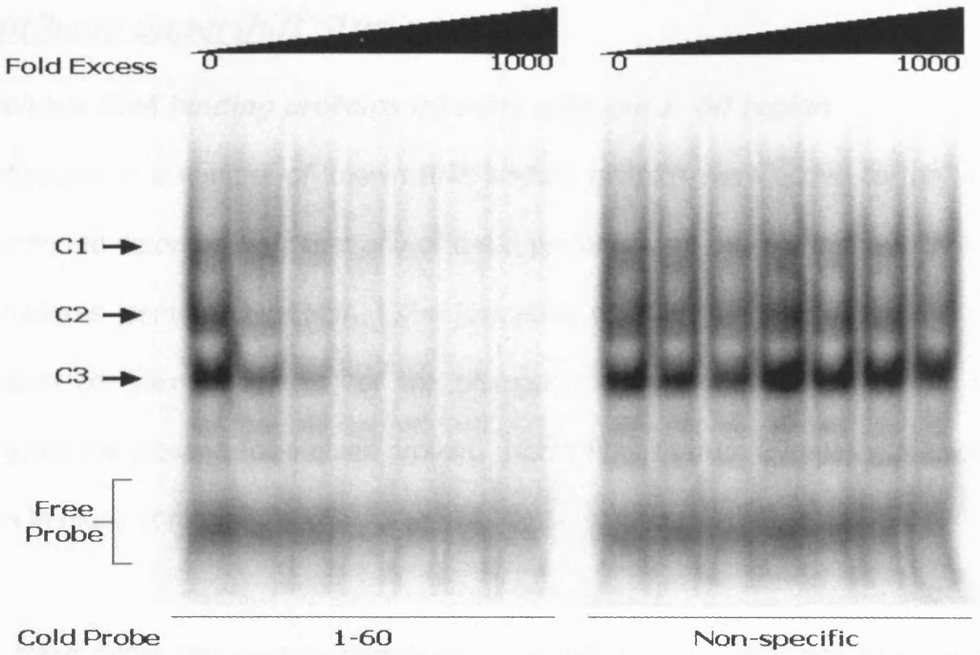

Figure 6: EMSA competition study

Electromobility shift assay using the nuclear fraction of rat mesangial cells incubated with the 1-60 probe (Lanes 1-7). Three prominent RNA-protein complexes were formed (C1, C2 and C3). Complex formation was sequence-specific, as the addition of increasing concentrations of "cold" 1-60 probe effectively competed for all 3 complexes and the addition of increasing amounts of a non-specific RNA probe (Lanes 8-14) had no effect on complex formation.

Antibody Supershift Studies

Multiple RNA binding proteins interact with the 1 -60 region

Antibodies to a number of known RNA-binding proteins were added to the binding reaction to determine whether any of these proteins were present in the RNA-protein complexes identified by EMSA. The formation of a higher molecular weight RNA-protein complex (supershift) or the disruption of one or more complexes would suggest the presence of a given protein. Normal goat serum (Sigma) was used as a non-immune control.

All three major RNA-protein complexes were still present when non-immune serum was included in the binding reaction (Figures 7 and 8). However, addition of anti-TIA-1, anti-TIAR, anti-HuR (Figure 7) and anti-hnRNP U (Figure 8) resulted in altered RNA-protein complex formation suggesting that all these proteins interact with the proximal 60 nucleotides of the Cox-2 3'UTR. Minor changes in RNA-protein complex formation were seen following the addition of antibodies directed against hnRNP A1 and tristetraprolin (Figure 8) raising the possibility that both these proteins may also interact with the RNA probes. Despite the fact that AUF1 has previously been shown to interact with the proximal region of the murine 3'UTR[212], no change was seen in complex formation on the addition of anti-AUF1 (Figure 7).

The addition of anti-TIA-1 and anti-TIAR antibodies produced a supershift (S1, figure 7), as well as a significant reduction in complex C2. The intensity of the supershift increased as the RNA probe was truncated suggesting that a more stable complex forms between these proteins and the shortened RNA probes. Also, the similarity between the supershift studies using these antibodies suggests that both proteins

are components of the same protein complexes.

Incubation with antibody directed against HuR resulted in both a supershift (S2, figure 7) and loss of the C3 complex. This supershift was most prominent with the 60-nucleotide probe and decreased in intensity as the probes were shortened. The loss of the C3 complex occurred with all of the RNA probes. This suggests that HuR binds to all three RNA probes, possibly in multiple different protein complexes.

In contrast, the supershift seen with anti-hnRNP U occurred only with the truncated RNA probes (S1, figure 8). No supershift was seen with either anti-hnRNP A1 or anti-TTP, though the intensity of complex formation (C1 and C2, figure 8) was diminished.

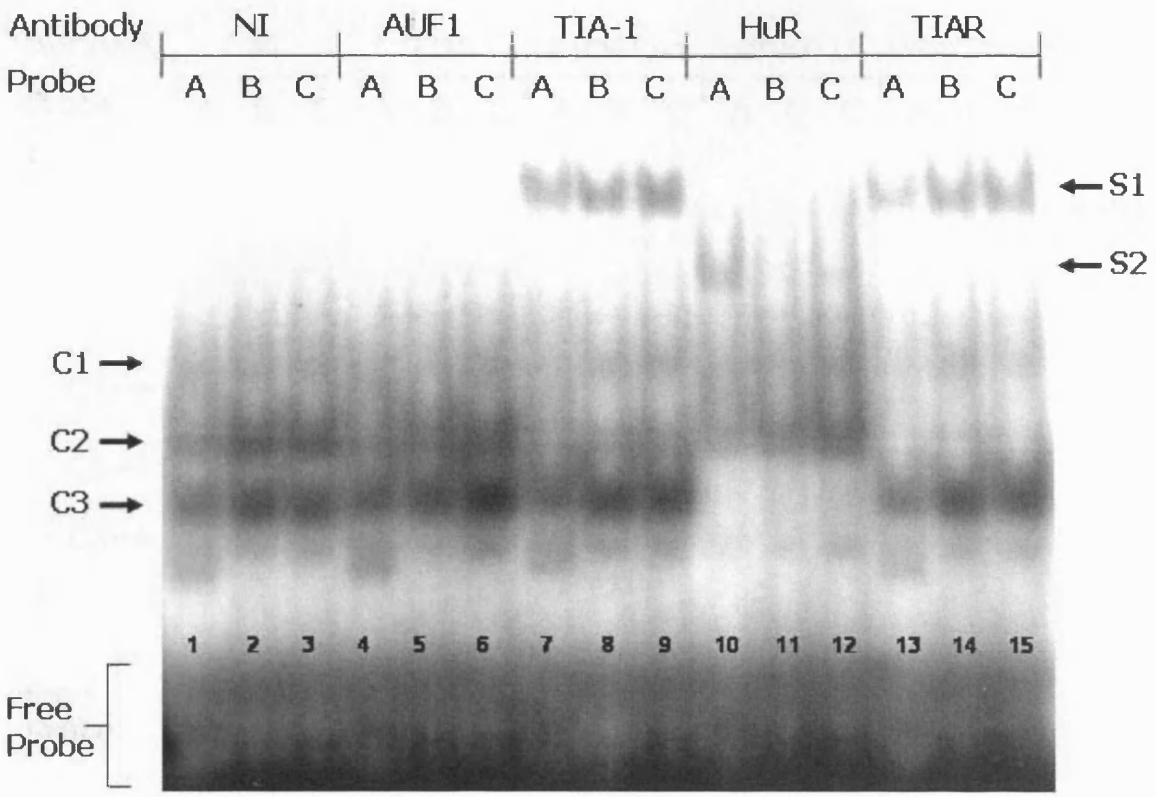

Figure 7: Antibody Supershift – AUF1, TIA-1, HuR, TIAR

Antibody supershift study, using the nuclear fraction of rat mesangial cells incubated with three labelled RNA probes – probe "A" (1-60), probe "B" (20-60) and probe "C" (24-60). Non-immune serum (Lanes 1-3) was used as a control and antibodies directed against the following known RNA-binding proteins were tested - AUF1 (Lanes 4-6), TIA-1 (Lanes 7-9), HuR (Lanes10-12), and TIAR (Lanes 13-15). Three major RNA-protein complexes were present when non-immune serum was included in the binding reaction (C1, C2 and C3). Prominent supershifts were seen with the addition of anti-TIA-1, anti-TIAR (S1) and anti-HuR (S2). These antibodies also resulted in decreased intensity of C2 (TIA-1 and TIAR) and complete loss of C3 (HuR). No significant change in RNA-protein complex formation occurred following the addition of anti-AUF1.

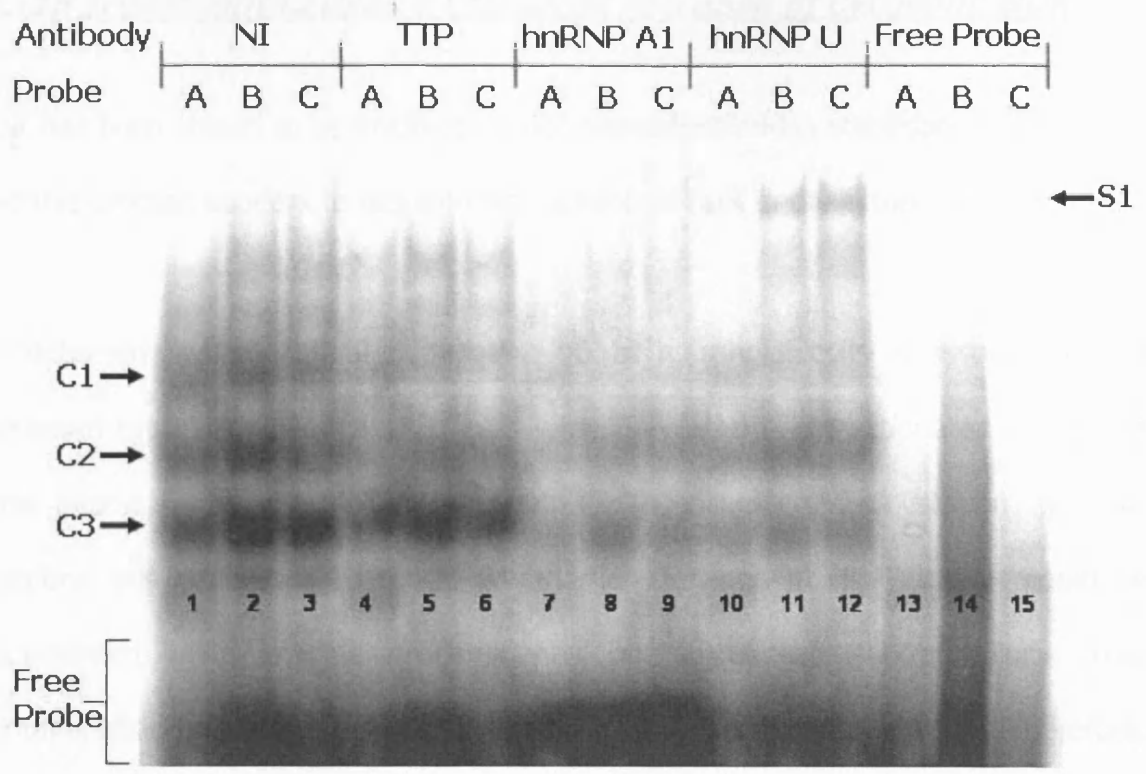

Figure 8: Antibody Supershift – TTP, hnRNP A1, hnRNP U

Antibody supershift study, using the nuclear fraction of rat mesangial cells incubated with three labelled RNA probes – probe "A" (1-60), probe "B" (20-60) and probe "C" (24-60). Non-immune serum (Lanes 1-3) was used as a control and antibodies directed against the following known RNA-binding proteins were tested - TTP (Lanes 4-6), hnRNP A1 (Lanes 7-9), and hnRNP U (Lanes10-12). Lanes 13-15 contain free probe only. Again, all three major RNA-protein complexes were present when non-immune serum was included in the binding reaction. Anti-hnRNP U produced a supershift (S1) with the truncated RNA probes only. Although, no supershift was seen with either anti-hnRNP A1 or anti-TTP, both produced a significant decrease in the intensity of RNA-protein complexes (C1, C2 and C3).

IL-1β treatment causes a transient increase in cytosolic HuR

HuR has been shown to be involved in ARE-dependent mRNA stabilisation[222,224,288-290] and this process appears to require translocation of HuR to the cytoplasm[293].

To determine whether IL1β stimulation of rat mesangial cells is associated with increased cytoplasmic HuR levels, cells were harvested and fractionated at various time intervals following IL1β stimulation. Then western analysis on cytosolic fractions was performed to reveal whether any change in HuR content could be documented. As HuR is predominantly nuclear in localisation[282], any cross contamination between fractions could significantly interfere with results. Therefore, cell fraction purity was verified using western analysis with anti- U1 snRNP 70 as a marker of nuclear fractions and an anti-GAPDH as a cytosolic protein marker (Figure 9A).

As expected, the vast majority of HuR in rat mesangial cell was nuclear in localisation and cell fraction purity was confirmed using anti-U1 snRNP 70 and anti-GADPH (Figure 9A).

HuR was only detectable in the cytosolic fractions by western analysis if increasing amounts of sample protein were tested (Figure 9B). Its cytosolic content increased within 15 minutes of IL1β stimulation, had peaked by 30 minutes and remained elevated for at least 4 hours (Figure 9C and 10). Testing for GAPDH ensured equal loading of sample protein and cytosolic levels of HuR were shown to return to baseline after 24 hours (Figure 10). To illustrate the effect of IL1β treatment on the cytosolic content of HuR, western Blots were quantitated on a densitometer using Quantity One software from PDI and the results are illustrated in figure 10.

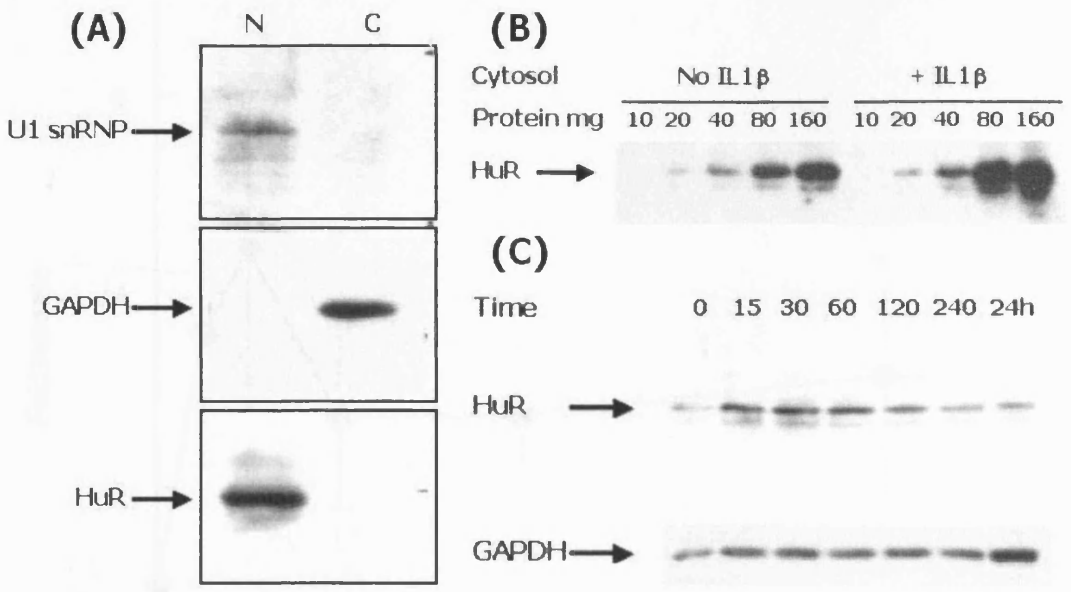

Figure 9:
Subcellular distribution of HuR following IL1β Stimulation

Western analysis of rat mesangial cell fractions, harvested at the specified times, following treatment with IL1β (100 units/ml) as indicated.

A – Nuclear (N) and cytosolic (C) fractions were tested with antibodies directed against the splicing factor, U1 SNP 70, and GAPDH to verify the purity of cell fractions. As expected, HuR is predominantly nuclear in localisation.

B – Only by using increasing amounts of cytosolic protein was HuR detectable in the cytoplasm. Cytosolic levels of HuR increased following 80 minutes of IL1β stimulation.

C – Timecourse of HuR levels in the cytoplasm of rat mesangial cells (using 60mg cytosolic protein) treated with IL1β. Testing for GAPDH was performed to ensure equal loading of sample protein.

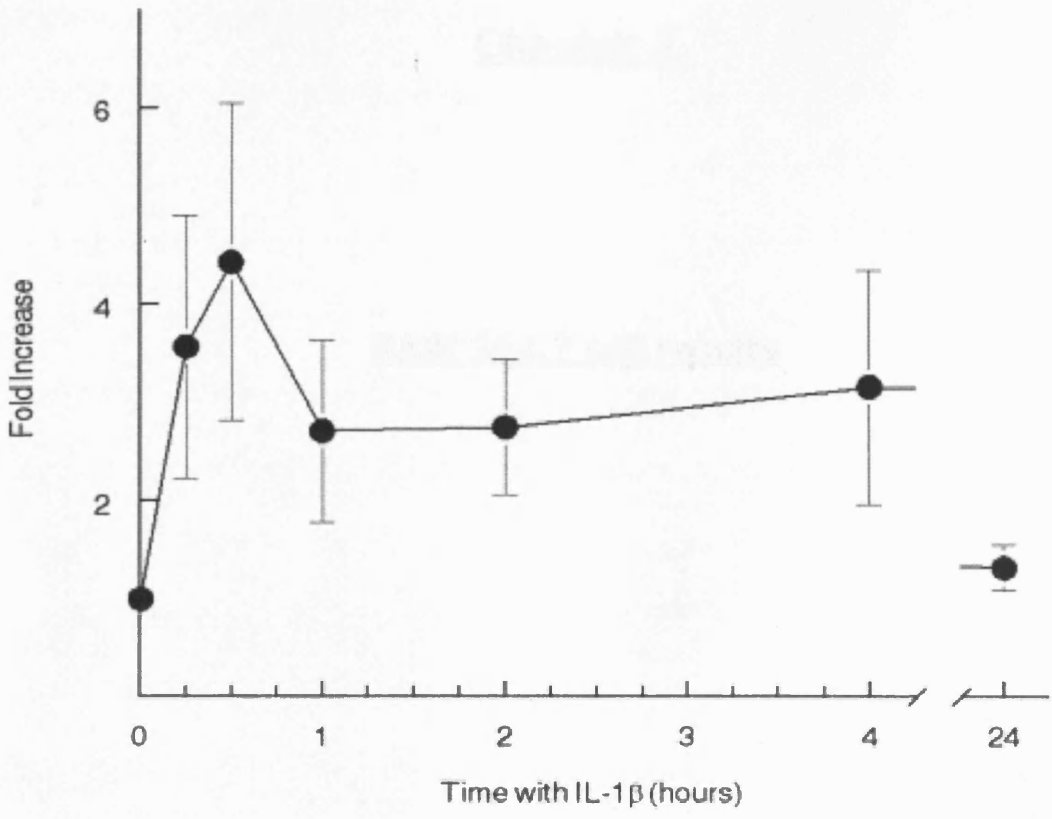

Figure 10:
Densitometry of Cytosolic Levels of HuR following IL1β

Densitometry of western analysis showing the relative change in levels HuR in the cytosol of rat mesangial cells following stimulation with IL1β 100 units/ml. Levels increase as early as 15 minutes and peak at 30 minutes. They remain elevated for at least four hours, but have returned to baseline by 24 hours.

Chapter 7

RAW 264.7 cell results

Lipopolysaccharide (LPS) induces cox-2 expression in Raw 264.7 cells, an immortalised murine macrophage cell line. LPS acts via the TLR4 receptor, with downstream activation of NFκB and one or more of the MAPK pathways being involved in the transcriptional activation of the cox-2 gene[397,411,412,415-419]. Although, it is well documented that post-transcriptional control is involved in IL1β induced cox-2 expression in rat mesangial cells, most studies in RAW cells have focused on the transcriptional events and signalling pathways involved in LPS induced cox-2 expression. However, as both these ligands signal through related receptors, with many similarities in intracellular signal transduction[420] and post-transcriptional control of LPS induced cox-2 has been documented in human macrophages[421] , it seems likely that post-transcriptional mechanisms will be active in LPS induced cox-2 expression in RAW 264.7 cells.

Expression of Cox-2 protein following LPS treatment

RAW 264.7 cells were cultured and harvested for western analysis, as described in the methods section. Samples were tested for expression of cox-2 protein, which was not detectable while cells were in their resting state. However, stimulation with LPS (10-100ng/ml) resulted in rapid and robust expression of cox-2 protein (Figure 11), with near maximal stimulation occurring with LPS 50ng/ml. Under identical conditions, little or no expression of cox-2 occurred following treatment with IL1β, TNFα or Interferon γ (Figure 12).

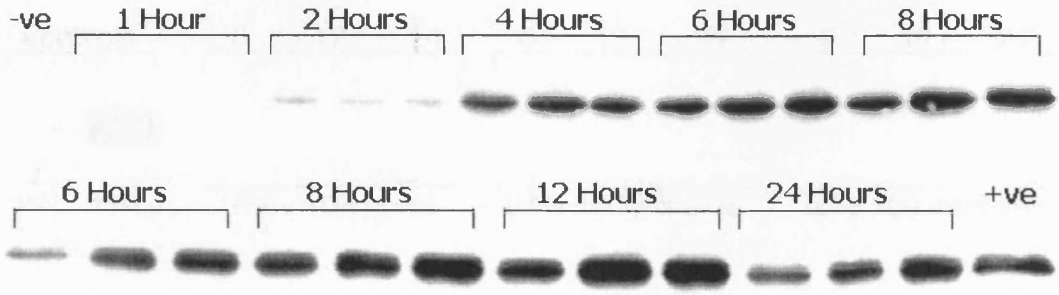

Figure 11:
Cox-2 protein expression in RAW 264.7 Cells following LPS

RAW 264.7 cells were treated with lipopolysaccharide for the specified time before harvesting. Timepoints were done in triplicates using LPS at 10, 50, 100ng/ml and 20µg of whole cell lysate was used for western analysis to detect cox-2 protein expression. Protein samples obtained from unstimulated RAW 264.7 cells and IL1β treated rat mesangial cells were used as negative and positive controls, respectively. Following treatment with LPS, cox-2 protein expression can clearly be seen after 2 hours, peaks at 8-12 hours and diminishes thereafter. Maximal response occurs at an LPS concentration of 50 to 100ng/ml. Result shown is representative of n=3 experiments.

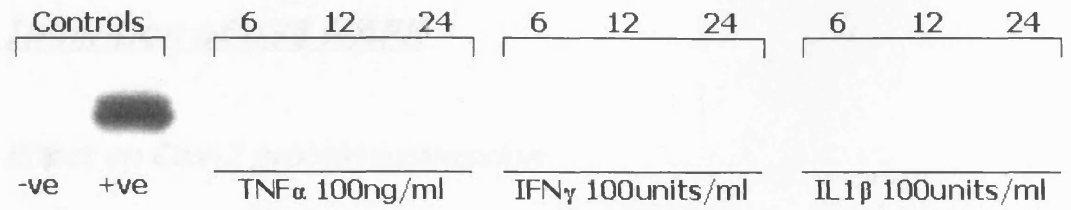

Figure 12:
Cox-2 is not induced by TNFα, IL1β or IFNγ in RAW Cells

Western analysis for cox-2 protein was performed using 20µg of protein from whole cell lysate of RAW 264.7 cells. Multiple ligands were used to induce cox-2 protein expression and cells were harvested after 6, 12 and 24 hours. Positive and negative controls were obtained using 20µg whole cell lysate harvested at 24 hours, treated with or without LPS 100ng/ml respectively. No stimulation of cox-2 was seen with TNFα, IL1β or interferonγ. The same result was obtained in two independent experiments.

Inhibition of p38 MAPK

Effect on Cox-2 protein expression

Timecourse experiments of LPS stimulation were performed over 24 hours. These showed that cox-2 protein was detectable within two hours and peaked by 8-12 hours. Expression of cox-2 protein diminished thereafter (Figure 11 and 13A).

Identical experiments involving pre-incubation of RAW 264.7 cells with 1 to 10μm of SB203580, a specific p38 MAPK inhibitor, for 30 minutes showed delayed onset of cox-2 protein expression following LPS stimulation with augmentation of expression at later time-points (Figure 13A). The effect of p38 inhibition on LPS induced cox-2 expression in this cell type was seen consistently and was more marked when 10μm of SB203580 was used. Western blots of 5 independent experiments were quantitated on a densitometer using Quantity One software from PDI and results are illustrated in figure 13B.

The significance of this effect is unclear, but may suggest that LPS activates a negative feedback loop in RAW 264.7 cells, which ultimately down-regulates cox-2 expression following sustained LPS exposure. This "dual" action of LPS, involving p38 MAPK, has previously been described related to TNFα and tristetraprolin expression[326] in RAW 264.7 cells and probably acts as a protective mechanism against sustained early response gene expression.

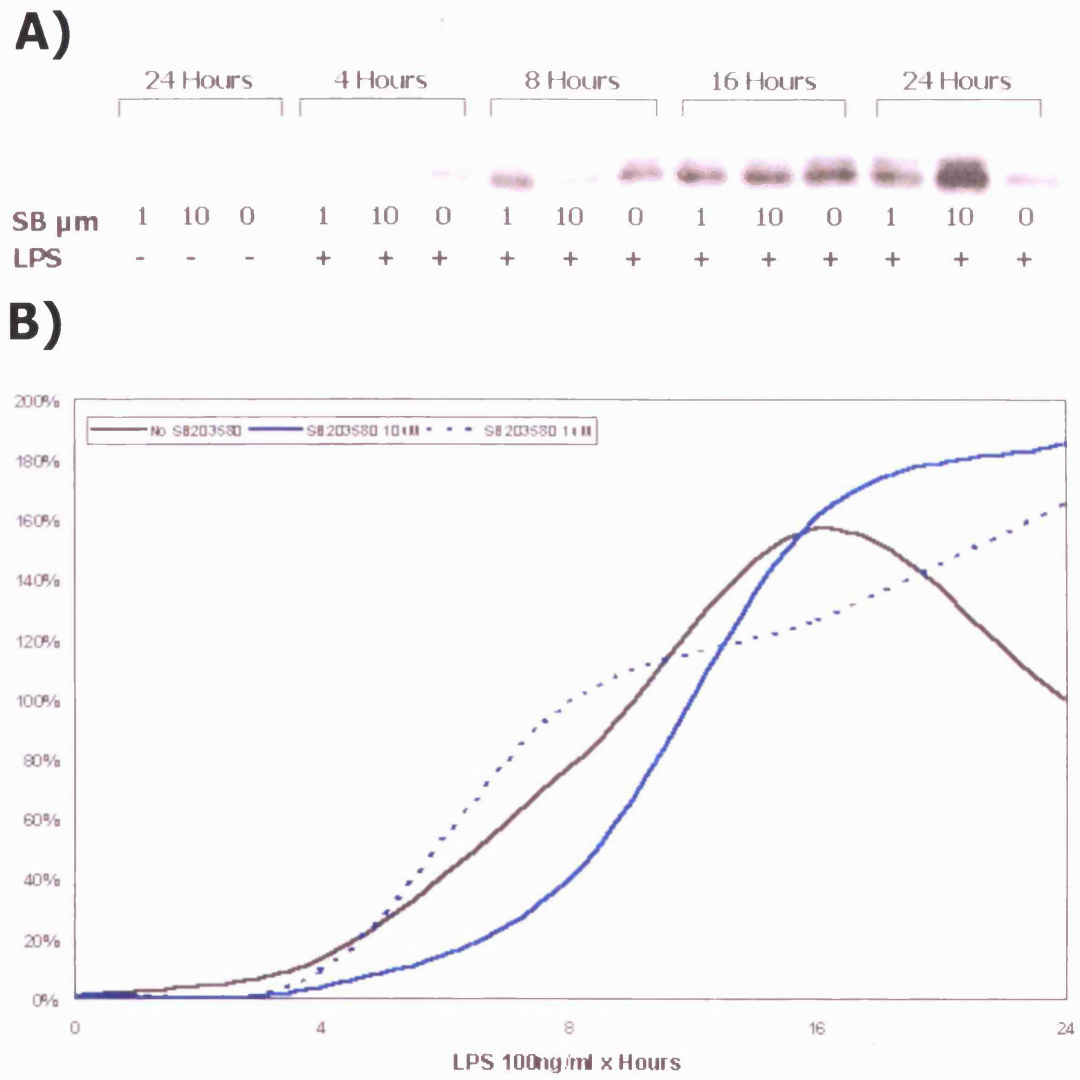

Figure 13:
Effect of p38 Inhibition with SB203580 on Cox-2 Expression

A) RAW 264.7 cells were treated with LPS 100ng/ml for the specified times before harvesting for western analysis. Where indicated, cells were pre-incubated for 30 minutes with SB203580 (1 or 10µm) or an equal volume of carrier (DMSO). 5µg of whole cell lysis was then examined for cox-2 protein expression. Negative controls showed no cox-2 expression regardless of the SB203580 concentration. Pre-treatment with the p38 inhibitor lead to a biphasic response in cox-2 protein expression; inhibition occurred at earlier timepoints, but expression of cox-2 protein was greater at later timepoints compared to treatment with LPS alone.

B) Densitometry was used to semi-quantify cox-2 expression following LPS treatment to illustrate the effect of p38 inhibition with SB203580. Measurements were expressed as a percentage of the 24-hour "LPS-only" level and the results of five independent experiments were averaged. The biphasic response with p38 inhibition was most marked when 10μm concentrations were used. This may indicate that the p38 signal transduction pathway may play multiple roles in the LPS induced activation of cox-2 in RAW cells.

Reporter Gene Transfections

Multiple Regions of the 3'UTR alter Reporter Gene Expression

Luciferase reporter gene constructs, containing the luciferase coding region followed by various sequences of the cox-2 3'-UTR, were transiently transfected into RAW 264.7 cells and incubated overnight. Cell monolayers were harvested and assayed for luciferase activity, which was expressed as a percentage of levels from cells transfected with unaltered pGL3c (control). As previously explained, any resultant change in reporter gene activity is most likely secondary to post-transcriptional mechanisms controlled by the inserted sequences.

Insertion of the full-length 3'-UTR (1-2232) reduced luciferase activity by more than 90%, when compared to control (Figure 14). Luciferase activity decreased 65% with insertion of the proximal 60 nucleotides of the 3'-UTR. Sequential deletion of the proximal portion of the 1-60 sequence resulted in first an increase in reporter-gene expression and then a further decrease in expression (Figure 14), suggesting that multiple control elements are operative within this region of the cox-2 3'UTR.

Further transient transfection studies were performed using luciferase reporter genes constructs containing multiple other regions of the cyclooxygenase-2 3'UTR. The results of luciferase activity from these transfections are illustrated in figure 15 and summarised in table 1.

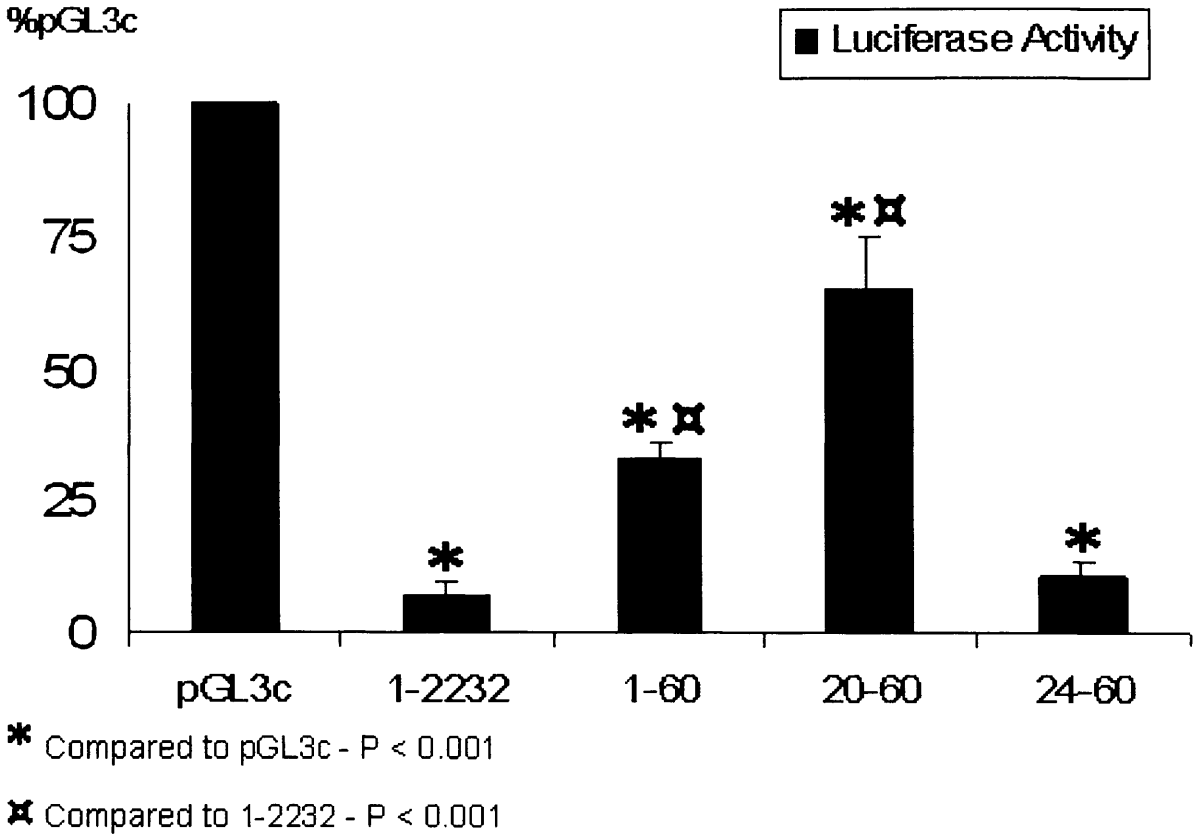

Figure 14: Transient Transfections in RAW 264.7 Cells

The graph represents the average results of N ≥ 6 independent experiments involving transient transfections of RAW 264.7 cells with the 1-60 constructs. Luciferase activity is expressed as a percentage of levels obtained using unaltered pGL3c. As in previous experiments, insertion of the full-length 3'UTR of cox-2 resulted in a significant fall in luciferase activity (>90%) and the 1-60 sequence decreased activity by approximately 65%. Disruption or deletion of the proximal three AUUUA sequence caused an increase or a further decrease in activity, respectively. This suggests that multiple "control elements" exist within this sequence and interact to regulate reporter gene expression.

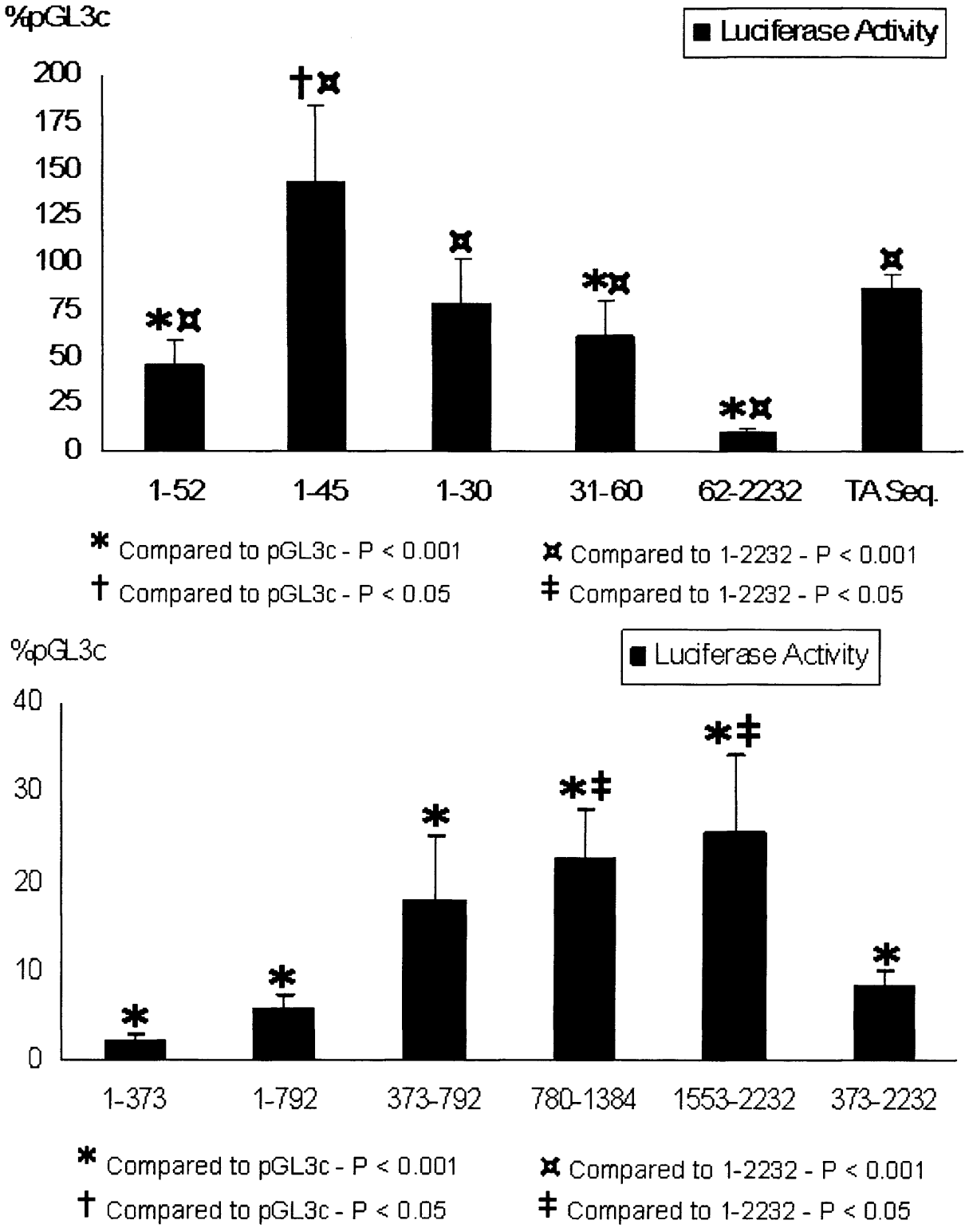

Figure 15:
Transient Transfections of Miscellaneous Constructs in RAW Cells

Luciferase activity is expressed as a percentage of levels obtained using unaltered pGL3c.

Construct	N =	%Control	SEM +/-
pGL3c	19	100	0
1-2232	17	7.34	2.12
1-60	14	32.66	3.28
20-60	9	65.35	9.34
24-60	6	10.81	2.77
1-52	5	46.25	13.16
1-45	5	143.5	40.63
1-30	6	78.29	24.51
31-60	5	61.2	19.85
1-80	11	27.92	4.84
20-80	9	3.06	0.94
24-80	10	97.9	17.8
62-2232	12	9.61	2.12
1-180	3	60.57	13.36
1-373	11	2.09	0.86
1-792	7	5.57	1.73
373-792	3	17.9	7.16
780-1384	4	22.62	5.48
1553-2232	4	25.29	8.81
373-2232	3	8.16	1.73
TA Sequence	3	87.21	6.84

Table 1:
Summary of Transient Transfections in RAW 264.7 Cells

A summary of all transient transfections performed using RAW 264.7 cells and various pGL3c constructs. Luciferase activity is expressed as a percentage of levels obtained using unaltered pGL3c (control).

Effect of LPS on Reporter Gene Expression

In previous experiments using rat mesangial cells transiently transfected with luciferase reporter genes, we were unable to demonstrate that IL1β had any affect on reporter gene expression. This lack of response could be due to numerous factors, including the possibility that sequences outside the cox-2 3'-UTR are required, or may simply be secondary to technical shortcomings related to the system examined. Demonstrating ligand responsiveness would prove very useful in determining which elements within the 3'UTR are involved in the post-transcriptional control of cox-2 and allow further examination of the mechanisms by which it is achieved. To determine whether any regions of the cox-2 3'-UTR would confer LPS responsiveness to a hybrid reporter gene, following transient transfection into RAW 264.7 cells, we stimulated the cells with LPS 100ng/ml for 6-10 hours before assaying for luciferase activity.

As before, luciferase activity was expressed as a percentage of levels from cells transfected with unaltered pGL3c (control). LPS treatment resulted in augmentation of luciferase activity from all constructs, including unaltered pGL3c, which increased by 2 – 4.5 fold with 6-10 hour of treatment (Figure 16). However, some regions of the cox-2 3'-UTR gave rise to a disproportionate increase in luciferase activity (Figure 16), probably secondary to a direct LPS effect, which became more pronounced with increasing duration of stimulation (Figure 16). Under the same treatment conditions, the activity of the construct containing the entire 3'-UTR increased 10 to 30-fold (Figure 16). Insertion of the 1-60 region caused a 6-fold increase in luciferase activity within 6 hours and a 12-fold after 10 hours of LPS stimulation (Figure 16).

The most likely explanation for the disproportionate increase in luciferase activity is LPS mediated post-transcriptional control of reporter genes, acting via cis-acting elements within the cox-2 3'UTR. However, the observed increased expression of unaltered pGL3c suggests a generalised increase in transcriptional activation also occurs following lipopolysaccharide treatment.

Further truncation of the proximal end of the 1-60 region resulted in the loss of the LPS response. Accordingly, it appears that the first 60 nucleotides of the 3'-UTR of cox-2 contains major control elements that confer decreased expression of the reporter gene under non-stimulated conditions and increased expression in response to LPS stimulation. The response to lipopolysaccharide appears dependent on a cis-acting element within the proximal 24 nucleotides of this sequence. The results of all transient transfections performed with LPS stimulation are summarised in table 2.

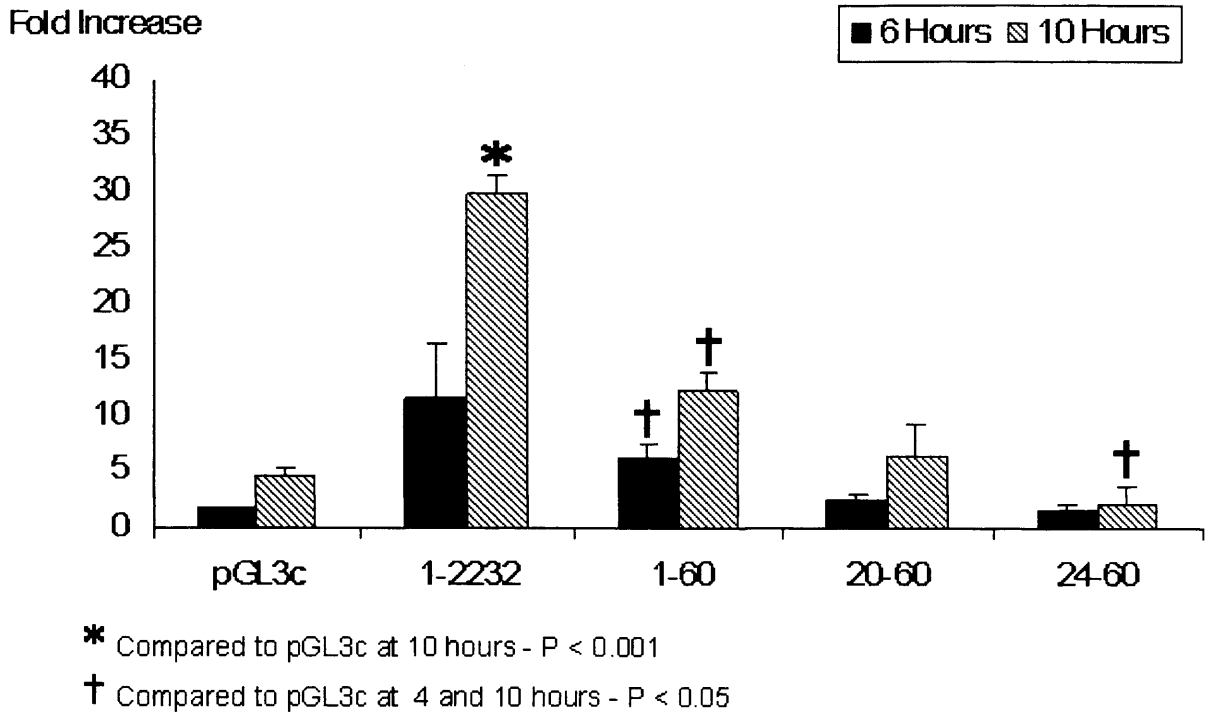

Figure 16: LPS Effect on Reporter Gene Expression in RAW 264.7 Cells

Raw 264.7 cells were transfected and stimulated with LPS (100ng/ml) for 6 and 10 hours and the results expressed as a fold increase compared with non-stimulated controls.

Construct	LPS x 6 hrs (SEM+/-)	N =	LPS x 10hrs (SEM+/-)	N =
pGL3c	1.71 (0.2)	7	4.58 (0.74)	9
1-2232	11.55 (4.79)	9	29.76 (1.67)	9
1-60	6.19 (1.28)	8	12.23 (2.74)	4
20-60	2.59 (0.5)	5	6.52 (1.64)	5
24-60	1.71 (0.39)	2	2.13 (0.45)	5
1-52	3.03 (1.99)	2	7.2 (1.39)	3
1-45	1.98 (0.7)	2	4.9 (0.72)	3
1-30	1.62 (0.53)	2	5.39 (0.89)	3
31-60	3.98	1	6.77 (0.86)	4
1-80	5.47 (1.14)	7	12.45 (2.67)	6
20-80	1.84 (0.58)	3	-	0
24-80	2.03 (0.34)	5	4.18 (1.8)	3
62-2232	4.82 (2.13)	3	11.85 (1.5)	7
1-180	-	0	7.32 (1.2)	3
1-373	2.63 (0.68)	3	15.48 (3.1)	4
1-792	-	0	15.4 (3.33)	3
373-792	-	0	6.99 (0.25)	3
373-2232	-	0	7.33 (0.41)	3

Table 2:
Summary of LPS Effect on Reporter Gene Expression in RAW 264.7 Cells

A summary of all transient transfections performed using RAW 264.7 cells and various pGL3c constructs, following treatment with LPS (100ng/ml) for 6 or 10 hours. Increased luciferase activity is expressed as a **fold increase** compared with non-stimulated controls.

Reporter Genes have no effect on Endogenous Cox-2

As shown above, many sequences within the 3'-UTR of cox-2 have a dramatic effect on luciferase activity, when inserted downstream of the coding sequence in a hybrid reporter gene. It is likely that the affects on luciferase expression are secondary to post-transcriptional mechanisms controlled by interactions between trans-acting factors and cis-elements within the 3'-UTR sequence. Transient transfection of these reporter-gene constructs may result in large volumes of these sequences being expressed within each cell and could lead to sequestration of key mRNA-binding factors and altered post-transcriptional control of the endogenous cox-2 gene.

To determine whether this is the case, we repeated the transient transfections studies using a number of reporter-genes constructs. After incubation overnight to allow reporter gene expression, cells were stimulated with LPS 100ng/ml for 10 hours, before being harvested to measure luciferase activity and perform western analysis to assess expression of endogenous cox-2.

Despite the obvious effect that LPS has on reporter gene expression (Figure 18B), dependent of the sequence of cox-2 3'-UTR present, no change in endogenous cox-2 protein expression was seen under basal conditions or following LPS stimulation in transiently transfected cells (Figure 18A).

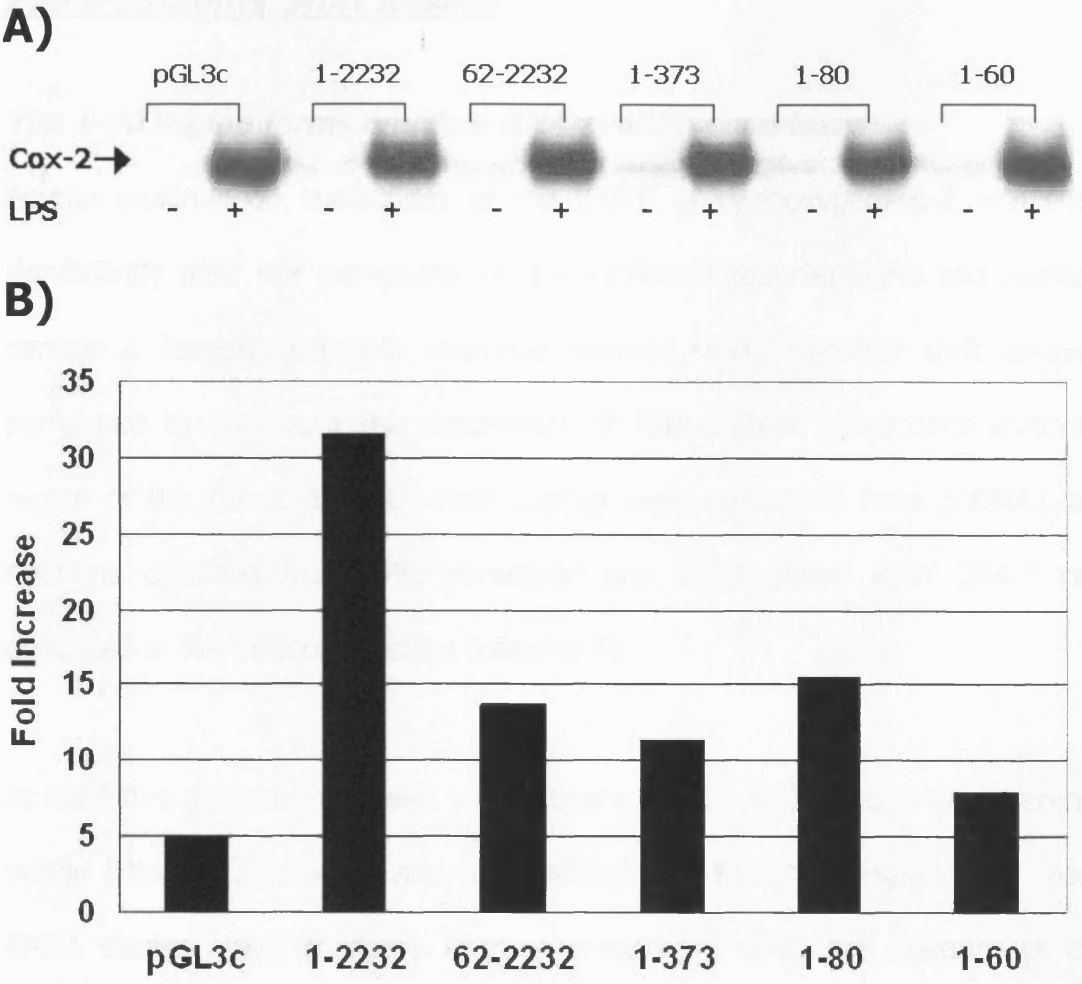

Figure 17:
Transient Transfection has no Effect on Endogenous Cox-2 Expression

Raw 264.7 cells were transiently transfected with luciferase reporter-genes and incubated overnight before treatment with LPS 100ng/ml for 10 hours. Cells were harvested and luciferase activity measured. **A)** Cox-2 protein was detected by western analysis. As shown, no change in endogenous cox-2 expression was seen related to transfection. **B)** Luciferase activity following LPS treatment for 10 hours, expressed as a fold increase compared with non-stimulated cells. Results represent the average of n=2 experiments and the fold changes expressed were not statistically different from control (pGL3c).

Electromobilty Shift Assays

The 1-60 region forms multiple RNA-protein complexes

As the proximal 60 nucleotides of the 3'UTR of cyclooxygenase-2 was shown to significantly alter the expression of the luciferase reporter gene and appeared to contain a lipopolysaccharide response element, electromobility shift assays were performed to document the occurrence of RNA-protein interactions involving this region of the Cox-2 3'-UTR. RNA probes were generated from pcDNA3 and cell fractions obtained from LPS stimulated and unstimulated RAW 264.7 cells, as described in the methods section (chapter 5).

At least five distinct complexes were observed (C1 - C5), though no difference was visible between stimulated and unstimulated cell fractions (Figure 19). As in the EMSA studies using fractions from rat mesangial cells, the quantity of complex formation is greater when using the nuclear fractions (N), despite loading equal amounts of total protein. The size and distribution of complexes are similar between cell fractions, suggesting that this difference is related to a higher concentration of RNA-binding proteins in the nucleus, which is not unexpected.

Truncating the RNA probe resulted in decreased intensity of some complexes (figure 19, C4 and C5) and increased intensity of others (figure 19, C2 and C3), which was more prominent in the nuclear fractions. Despite the altered intensity, the mobility of the complexes was similar using all three RNA probes. This implies a difference in protein binding ability between the 1-60 and the two shorter probes, with the presence of the proximal 20 nucleotides allowing more effective formation of larger RNA-protein complexes.

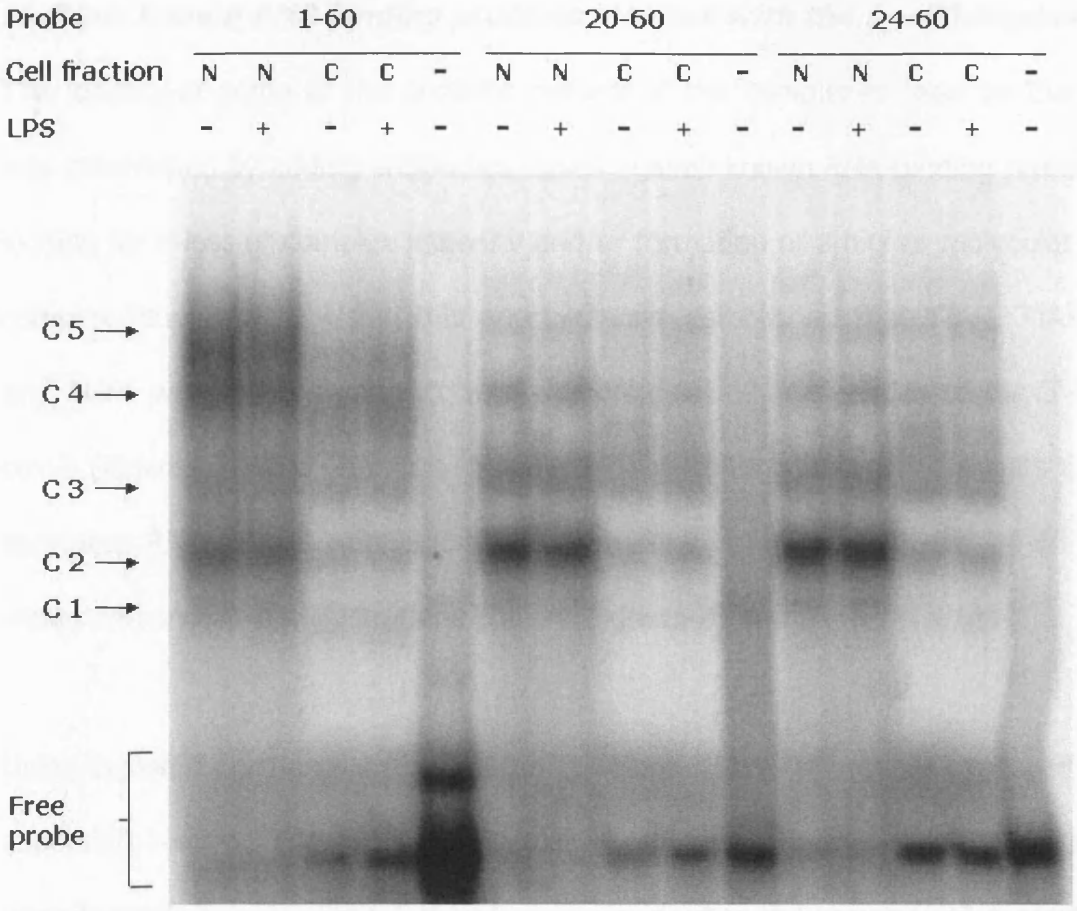

Figure 18: EMSA using cell fractions from RAW 264.7 Cells
This gel is representative of electromobility shift assays performed by incubating radiolabeled probes with protein from cell fractions of RAW 264.7 cells. Both nuclear (N) and cytosolic (C) fractions were obtained from untreated cells (-) and following stimulation (+) with lipopolysaccharide.

RNA probes corresponding to regions 1 – 60 (Lanes 1-5), 20 – 60 (Lanes 6-10) and 24 – 60 (Lanes 11-15) of the cox-2 3'UTR were used and at least 5 distinct RNA-protein complexes were observed. No difference was visible between stimulated and unstimulated cell fractions. The quantity of complex formation is greater when using the nuclear fractions. However, the size and distribution of complexes are similar between different cell fractions, suggesting that this difference is related to a higher concentration of RNA-binding proteins in the nucleus.

Antibody Supershift Studies

Multiple known RNA binding proteins interact with the 1 – 60 Region

The identity of some of the proteins present in the complexes seen on the EMSAs was determined by adding antibodies raised against known RNA-binding proteins and looking for a loss of complex intensity and/or formation of a higher molecular weight complex (supershift). Using this approach, we established that TIAR, TIA-1, HuR and AUF1 were able to interact with the proximal 60 nucleotides of the 3'-UTR of cox-2 (Figures 20 and 21). As in the previous EMSA studies, the results for both truncated RNA probes were identical. Therefore, only the 1-60 and 24-60 probes were compared in the illustrations shown (Figures 20 and 21).

Using cytosolic fractions, antibodies to TIAR and TIA-1 (figure 20) produced similar supershift results. Two higher molecular weight complexes (supershifts S2 and S3) were formed, but only the S3 complex remained when the proximal 23 nucleotides of the RNA probe were removed. Furthermore, addition of these antibodies resulted in diminished intensity of complex C3 with both probes.

Also, anti-HuR produced a single supershift (S1) and decreased intensity of complexes C1 and C2 (figure 20). The HuR supershift was more evident using the 60-nucleotide probe and decreased in intensity as the probe was truncated. Although in the gel displayed, the HuR supershift appeared far more prominent in LPS stimulated cytosolic fractions, which could be related to improved binding conditions or increased cytosolic HuR content following LPS stimulated nuclear export, this was not consistently observed. However, the loss of complexes C1 and C2 was consistently seen with all the probes.

When anti-AUF1 antibody was added to the binding reaction between RNA probes and RAW cell cytosolic fractions, no major change in complex intensity or formation was seen (figure 20).

Further supershift studies were performed using nuclear fractions of RAW cells (figure 21). Results with TIA-1, TIAR and HuR antibodies were similar to those using proteins isolated from cytosolic fractions (figure 20). The following exceptions were noted. TIA-1 and TIAR antibodies formed a single higher molecular weight complex with both RNA probes (Figure 21, S2). The HuR supershift was attenuated and showed no alteration with LPS treatment (figure 21, S1).

However, anti-AUF1 resulted in nearly a complete disappearance of all RNA gel shifts when added to RAW cell nuclear fractions (figure 21). These changes in RNA-protein complex formation were consistently present, suggesting that AUF1 is an essential component of most protein complexes interacting with this region of the Cox-2 mRNA within the nucleus. The absence of any supershift using anti-AUF1 with cytosolic fractions suggests that AUF1 doesn't associate with this sequence in the cytosol or that its antigenic determinant is masked.

Using protein from both cell fractions, no obvious change was seen in supershift studies following treatment with LPS (Figure 21).

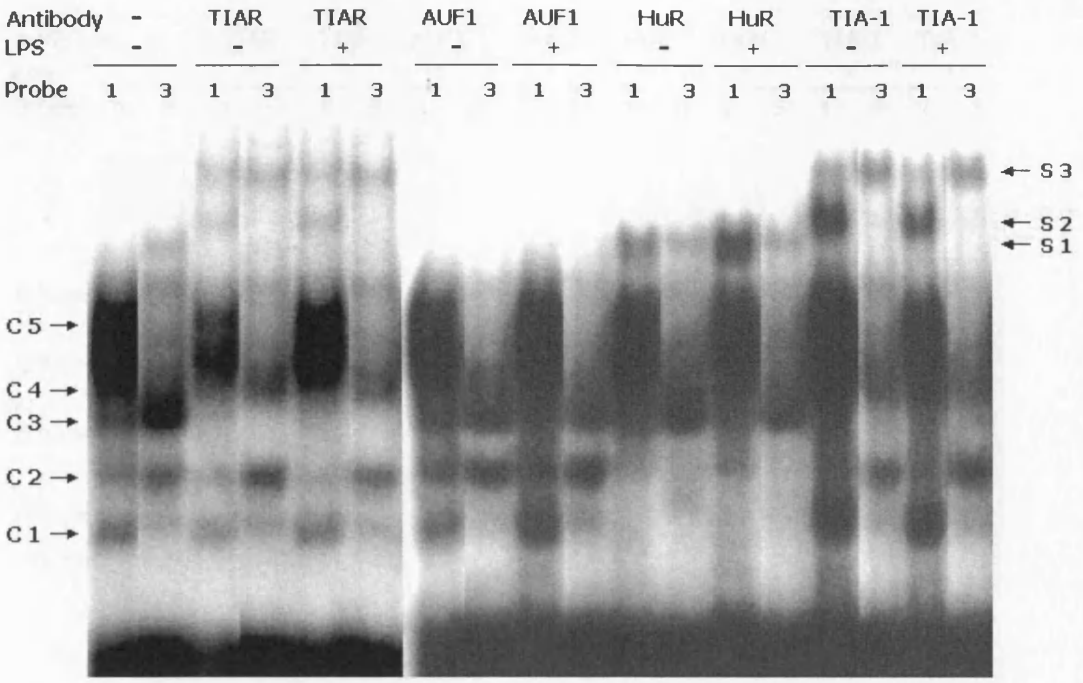

Figure 19:
Antibody Supershift – TIAR, AUF1, HuR and TIA-1 – using cytosolic protein

Antibodies to the TIAR, AUF1, HuR and TIA-1 were added to the binding reaction along with cytosolic protein from RAW 264.7 cells. Samples obtained from LPS treated cells are labelled (+) and only the 1 – 60 (probe 1) and 24 – 60 (probe 3) were used. Non-immune serum was used as control (Lanes 1 and 2). TIAR and TIA-1 both produced two higher molecular weight complexes (supershifts S2 and S3), but only the S3 complex remained when the proximal 23 nucleotides of the RNA probe were removed. Addition of these antibodies resulted in diminished intensity of complex C3 with both probes. Anti-HuR produced a single supershift (S1) and decreased intensity of complexes C1 and C2. The HuR supershift was more evident using the 60-nucleotide probe. However, the loss of complexes C1 and C2, when anti-HuR was included, occurred consistently seen with all the probes and was independent of LPS treatment. Anti-AUF1 antibody produced no change in complex formation when added to the binding reaction with the cytosolic fraction of RAW cells.

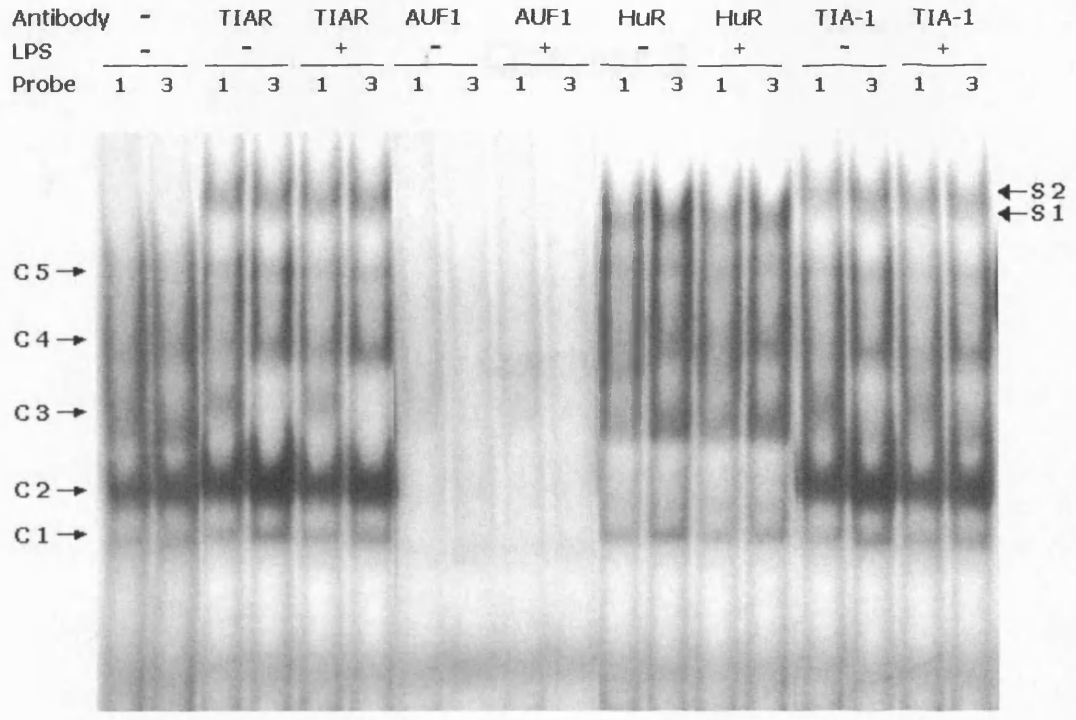

Figure 20:
Antibody Supershift – TIAR, AUF1, HuR, TIA-1 – using nuclear protein

Antibodies to the TIAR, AUF1, HuR and TIA-1 were added to the binding reaction along with nuclear protein from RAW 264.7 cells. Samples obtained from LPS treated cells are labelled (+) and only the 1 – 60 (probe 1) and 24 – 60 (probe 3) were used. Non-immune serum was used as control (Lanes 1 and 2). Results with TIA-1, TIAR and HuR antibodies were similar to those using proteins isolated from cytosolic fractions (figure 20). However, a number of differences are noteworthy. TIA-1 and TIAR antibodies formed a single higher molecular weight complex with both RNA probes, S2. The HuR supershift was attenuated and showed no alteration with LPS treatment, S1. Interestingly, anti-AUF1 resulted in nearly a complete disappearance of all RNA gel shifts when added to RAW cell nuclear fractions (Lanes 7-10). These changes in RNA-protein complex formation were consistently present, suggesting that AUF1 is an essential component of most protein complexes interacting with this region of the Cox-2 mRNA within the nucleus. Again, no obvious change was seen in supershift studies following treatment with LPS.

Chapter 8

Conclusions

Cyclooxygenase-2 plays a key role in many pathophysiological processes, such as thrombosis, carcinogenesis and reproduction. Inhibition of this enzyme has proven to be an extremely useful mode of treatment for many common medical conditions and preliminary evidence suggests that cox-2 may be a viable target in the treatment of neoplasia and Alzheimer's disease. However, the use of both non-selective and selective cox-2 inhibitors is associated with considerable side effects due to their interference with the critical physiological roles of this enzyme. An in-depth understanding of both its regulation and function will not only provide an important insight into a diverse number of pathophysiological processes but, may allow the development of novel therapies that can modulate cox-2 activity in a cell-specific and site-specific manner.

Post-transcriptional mechanisms are now well recognised as an integral part of the regulation of cyclooxygenase-2 by multiple ligands and its 3' untranslated region has significant effects on mRNA stability and translation. An increasing number of RNA binding proteins are being identified, which interact with this area of the cox-2 mRNA and are probably involved in its post-transcriptional control. The precise sequences required for these interactions and the exact mechanisms by which they alter cox-2 expression remain to be elucidated[241,301], but already this "pathway" of regulation has been implicated in abnormal expression of cox-2 in neoplastic cells[239,240,264,332].

From previous work, we knew that the conserved AREs, located in the proximal 1 - 60 region, of the 3'-UTR of COX-2 play an important role in regulating gene expression[216,422]. Therefore, we subcloned this sequence into a luciferase reporter-gene, as well as two truncations designed to disrupt and completely remove the first three overlapping AUUUA sequences. Insertion of the 1 - 60 sequence was sufficient

to cause a marked decrease in expression of the hybrid luciferase reporter-gene, in both rat mesangial and RAW 264.7 cells. Truncation of this segment by removal of the first 20 nucleotides diminished the negative effect on luciferase activity, particularly in the RAW cells. In both cell types, the complete removal of the proximal 3 AUUUAs lead to an even greater decline in luciferase activity than was seen with the 1 - 60 sequence. The decreased steady-state luciferase mRNA levels, seen in rat mesangial cells, are compatible with reduced stability being the primary mechanism underlying these results.

Furthermore, insertion of the full length 3'-UTR or its proximal 60 nucleotides resulted in increased luciferase expression following stimulation with lipopolysaccharide in RAW cells. The regulation by LPS was attenuated by removal of the first 60 nucleotides from the full length 3'-UTR and completely lost following removal of the first group of AUUUA repeats from the 1 – 60 sequence. Taken together, these results suggest that multiple interacting control elements exist within this part of the 3'UTR, which modulate the expression of cox-2 by post-transcriptional mechanisms. Some of these elements perform multiple roles depending on environmental conditions and these may vary depending on the cell type and ligand studied. For example in RAW 264.7 cells, the 1 - 60 region of the 3'UTR lead to decreased gene expression under basal conditions and was also required for full induction of gene expression following LPS treatment. The actual mechanism by which LPS stimulation leads to changes in target gene expression is not fully understood. A combination of transcriptional activation and message stabilization is known to take place [421,423]. While the changes in control plasmid activity following LPS treatment are consistent with a transcriptional, and possibly a proliferative effect, the differential increase in luciferase activity associated with

insertion of the cox-2 3' UTR strongly suggests that post-transcriptional mechanisms are operative in its control RAW 264.7 cells.

In light of observations that changes in mRNA stability and translation occur through specific interactions with trans-acting factors, proteins that bind to this region of the cox-2 message are likely to be involved in the post-transcriptional regulation of this gene. The electromobility shift assays clearly show that the proximal part of the 3'UTR associates with multiple protein complexes, which contain many known RNA binding proteins, including HuR, TIA-1 and TIAR, AUF1 and hnRNP U, though no ligand induced difference was observed using this technique.

Binding of cox-2 mRNA[239,301,359], as well as multiple other mRNA, by HuR has previously been reported. Our results show that one of the HuR binding sites is located within the first 60 nucleotides of the 3'-UTR of murine cox-2, as evidenced by the HuR antibody-dependent supershift in both rat mesangial (figure 7) and RAW 264.7 cells (figures 20 and 21). The supershift obtained with anti-HuR antibody was also accompanied by a significant decrease in intensity of one or more of the RNA-protein complexes. Truncating the RNA probes, to disrupt the proximal three overlapping AUUUAs, was still associated with the decrease in RNA-protein complexes, but the HuR supershift was greatly diminished. Possible explanations for these observations include that more than one HuR-RNA complex occurs and/or that more stable complex formation takes place when the proximal 20 nucleotides of this sequence are present.

The decreased intensity of the HuR supershift associated with disruption of the three overlapping AUUUAs is consistent with previous studies, which ascertained the

optimum mRNA sequence required for binding of two related ELAV proteins, Hel N1[424] and HuD[286,425]. Hel N1 most closely associated with the sequence UUAUUUAUU and HuD required at least three AUUU repeats for maximum affinity and complex stability. Thus, it seems plausible that disruption of the proximal AUUUA repeats not only decreased HuR's affinity for the RNA probes, but also decreased the stability of complex formation. It is also noteworthy that HuR cytosol levels increase transiently in stimulated rat mesangial cells (figure 9), given that its involvement with changes in message stability appears to be related to its translocation from the nucleus to the cytoplasm [282,289,293]. Its shuttling ability has also been linked to mRNA export from the nucleus[297-299], allowing mRNA access to ribosomes for translation.

In our experiments, we can see circumstantial evidence that HuR is implicated in the post-transcriptional control of cox-2. Firstly, HuR associates with the proximal 60 nucleotides of the 3'UTR of cyclooxygenase-2, probably involving a high-affinity binding site encompassing the first three overlapping AUUA repeats. Secondly, reporter gene assay demonstrate that removal of this site results in decreased steady-state mRNA levels in rat mesangial cells and loss of LPS induced regulation in RAW cells. Thirdly, induction of cox-2 in rat mesangial cells is associated with increased levels of HuR in the cytoplasm. Whether, this translocation of HuR is directly related to stabilisation of cox-2 mRNA or increases its export from the nucleus is not possible to determine from these experiments

Unlike the HuR supershift, TIA-1 and TIAR both appeared to form more stable complexes with the truncated RNA probes and the similarity in EMSA studies suggested that both might participate in the same protein complexes. A single supershift was observed using the rat mesangial cells and the nuclear fractions of

RAW 264.7 cells with no discernible change following IL1β or LPS treatment (figures 7 and 22). Both of these related AUBPs have been shown to bind the ARE of TNFα, resulting in its translational silencing [214,218] and over-expression of TIA-1 in COS cells decreased expression of a reporter gene containing the TNFα ARE [310]. Recently, TIA-1 has been shown to be involved in the translational silencing of cox-2, which may be relevant to the pathogenesis of neoplasia related to cox-2[241]. Therefore, it is plausible that binding of these proteins may suppress translation of cyclooxygenase-2 mRNA in rat mesangial and RAW cells. Moreover, when using the cytosolic fractions of RAW cells, these antibodies produced two supershifts, with the faster moving complex disappearing as the probe was truncated (figure 21). Though no change in supershift studies was observed following ligand stimulation, this truncation of the sequence was associated with a significant change in reporter-gene expression and loss of LPS responsiveness. It is possible that LPS treatment resulted in a functionally significant post-translational modification of TIA-1 and/or TIAR, not detectable using this method of investigation, producing increased reporter gene expression.

As other investigators had reported that AUF1 interacted with the proximal part of the cox-2 3'UTR in HeLa cells[212], it was somewhat surprising that no supershift was seen using this antibody in the rat mesangial cell fractions (figure 7). Possible explanations for the apparent "absence" of AUF1 include differences in length of RNA probe, cell-type examined or experimental conditions.

Despite the rat mesangial cell findings, there was a dramatic loss of virtually all RNA-protein complexes when AUF1 was added to the binding reaction along with the nuclear fractions of RAW cells (figure 22). Yet, there was no visible change in gel-

shift pattern using the cytosolic fractions of these cells (figure 21). The explanation for the difference between the RAW cell fractions is not readily apparent, but it does appear that AUF1 is an integral component of most RNA-protein complexes that associate with this part of the cox-2 mRNA in the nucleus. In the cytoplasm, either AUF1 doesn't bind to this sequence or the antigen epitope is sequestered, thereby preventing antibody binding. Although, AUF1 has been shown to play a role in ARE-mediated mRNA decay, no conclusion regarding the physiological consequence of its interaction with the cox-2 mRNA can be drawn from these experimental findings.

In rat mesangial cells, we also found that hnRNP U binds to 20 – 60 region of the 3'UTR of cyclooxygenase-2 (figure 8). The significance of this interaction is unclear, as little is known of hnRNP U's role in the post-transcriptional control of gene expression. This RNA binding protein [426,427] has been shown to associate with a number of proteins, including the glucocorticoid receptor [428,429], raising the possibility that hnRNP U may act as a scaffolding protein, which mediates the interaction between mRNA and proteins regulating its expression. Glucocorticoids have been shown to regulate cox-2 expression both by transcriptional and post-transcriptional mechanisms[380,430,431]. Their effect on message stability requires de novo protein synthesis, involves inhibition of the p38 pathway and the 3'UTR[382,430,432]. The involvement of the 3'UTR in this process is supported by the differential effect that dexamethasone exerts on the stability of endogenous cox-2 mRNA dependent on the length of it 3'UTR[380], with dexamethasone decreasing mRNA half-life in the presence of the conserved ARE region. Although these findings do not prove that hnRNP U binding to the 20 – 60 region is responsible for the glucocorticoid-mediated effect on cox-2 mRNA stability, it is tempting to speculate that this interaction is physiologically significant. Glucocorticoids are highly effective anti-inflammatory agents, with some

of there actions likely related to inhibition of prostaglandin production. Also, they exacerbate the "ulcerogenic" potential of cyclooxygenase inhibitors, without significantly increasing the risks when used alone. From what's known of the role of cox-1 and cox-2 in maintaining gastric mucosal integrity, this finding is in keeping with preferential inhibition of cox-2.

Using the rat mesangial cell fractions, relatively minor changes in gel-shift pattern, of questionable significance, were seen following the addition of antibodies to two other known RNA binding proteins, TTP and hnRNP A1. Following the addition of anti-TTP to EMSA studies, no supershifts were seen but there was a decrease in intensity of complexes C1 and C2 (Figure 8), suggesting that this protein interacted with the RNA probes. Tristetraprolin is known to bind the ARE of TNFα, GM-CSF[208,220,228,321] and a distal sequence within the 3'UTR of cox-2[240,332]. Lipopolysaccharide induces TTP expression in RAW 264.7 cells and results in its phosphorylation by p38, enhancing its binding to and subsequent degradation of TNFα mRNA. It is possible that the cell fractions used in our experiments were harvested before maximal induction of TTP occurred and "missed" its interaction with the probes. Alternatively, there may not be a specific TTP binding site in this region of the 3'UTR or its interaction may be indirect as part of a multi-protein complex.

Lastly, a general decrease in complex intensity was seen, with all three RNA probes, following the addition of antibody directed against hnRNP A1. This may suggest that hnRNP A1 is an integral part of RNA-protein complexes interacting with this region of the 3'UTR of cyclooxygenase-2, which may be relevant given its role in mRNA export from the nucleus[113,118].

While these experiments confirm the interaction of a number of known RNA binding proteins with the proximal portion of the cox-2 3'UTR, they do not prove that the identified proteins are involved in the post-transcriptional control of this gene. However, of the RNA binding proteins that were shown to interact with the 1 - 60 region, most are known to be involved in the post-transcriptional regulation of numerous genes and altered RNA-protein interactions with the proximal region of the cox-2 3'UTR is associated with IL1β stimulated message stabilisation[402]. Therefore, it is probable that at least some of these interactions are functionally active, especially as this region of the 3'UTR has a significant effect on the expression of our hybrid reporter gene, most likely by altered message stability. Moreover, in RAW 264.7 cells, this region conferred responsiveness to LPS resulting in enhanced expression of the luciferase reporter gene.

Further study of these RNA binding proteins, including ligand stimulated post-translational modifications, and their target sequences should provide us with a deeper understanding of the mechanisms by which they alter gene expression, as well as allowing us to ascertain the extent to which post-transcriptional control is involved in gene expression.

Chapter 9

Future Directions

Although, these methods successfully identified an interaction between a number of known RNA binding proteins and the conserved ARE of the cyclooxygenase 3'UTR, they offer little information on the exact mechanisms involved in its posttranscriptional control. Also, given the size of the cox-2 mRNA, it is difficult to predict how the 1 – 60 region would "behave" in the context of the full mRNA. However, its very size makes it virtually impossible to identify the functional elements, while working with the complete mRNA. Using reporter gene assays, as a screening tool, helps identify cis-acting elements within the 3'UTR, which may be of physiological significance. The identification of these sequences and their associated RNA binding proteins is a constructive initial step in unravelling the complex interaction of the numerous processes involved in the post-transcriptional regulation of this gene. I believe that the manageable size of the 1-60 sequence, the LPS response observed and the presence of multiple RNA-protein complexes make this region an ideal choice for further examination.

The ultimate fate of each mRNA is intimately linked to its processing history, as well as the composition of protein complexes associated with it. Many of these RNA binding proteins are expressed as multiple isoforms and undergo post-translational modifications that alter their cellular localisation, binding affinity and function. LPS is known to activate a number of intracellular kinases and iNOS, with the resultant potential for post-translational modification of RNA binding proteins. Phosphorylation of AUF-1, TTP and TIA-1 has been documented and a resultant change in function shown for both TTP and AUF-1[306,326,330,337]. Also, the involvement of iNOS in the induction of cox-2 by LPS has been described in RAW 264.7 cells[433,434], with the possibility that nitrosylation[435] may involved in regulating the function of RNA binding proteins.

Using RNA, the point at which post-transcriptional events converge, as the focus for initial study optimises the potential of isolating the trans-acting factors involved. The 1 – 60 sequence could be harnessed to isolate many of the proteins present in the RNA protein complexes detected by electromobility shift assay. A combination of 2D-gel electrophoresis, western analysis and mass spectrometry would enable their identification, whether multiple isoforms of a given protein are present and whether post-translational modifications have occurred. Any observed differences related to lipopolysaccharide treatment are likely to be functionally related to cox-2 post-transcriptional control. However, the temporal pattern of cox-2 expression in RAW 264.7 cells would suggest that multiple time-points would require examination to identify the relevant changes.

Once more of the relevant RNA binding proteins are identified, it may be possible to ascertain a direct link to the mRNA degradation/translation machinery or signal transduction pathway intermediates. Alternatively, an indirect link via protein-protein interactions could be detected using yeast two-hybrid and immunoprecipitation studies, as they may exert their effect through associated proteins. Direct visualisation of the intracellular localisation of RNA binding proteins and their relationship to cox-2 mRNA could be examined utilising GFP fusion proteins, fluorescent in-situ hybridisation and immunoprecipitation.

Further examination of the involvement of the p38 pathway is warranted given the increasing evidence linking it to post-transcriptional regulation. The biphasic response to p38 inhibition seen in RAW 264.7 cells is suggestive that it plays multiple roles in the induction of cox-2 in this cell type. Manipulation of this MAP kinase signal transduction pathway, using dominant negatives of its multiple isoforms and specific

pharmacological inhibitors, together with nuclear run-ons and tet-off vectors may determine whether it is primarily involved in mediating specific post-transcriptional events and which p38 isoforms are particularly involved.

Once these techniques are refined using the 1 – 60 sequence, the rest of the cox-2 3′ untranslated region could be screened for other potential control elements. However, it is likely that these cis-acting elements would behave differently in the context of the complete sequence. Ideally, the various species of the 3′ UTR expressed under normal physiological conditions should be compared using these methods, as there is already some evidence of differences in post-transcriptional control[380].

Lastly, a search for polymorphisms within 3′UTR of cyclooxygenase-2 of patients with various pathological conditions may uncover its clinical relevance. If an association is discovered, this region of sequence could be used to identify the pathogenesis of the process involved. Abnormalities would probably need to be gene specific (i.e. not major abnormalities of multi-function AUBPs) to lead to "low grade", cumulative environmental damage resulting in disease.

Appendix A

Solutions

Cell culture preparation

Rat mesangial cell:

RPMI-1640 medium supplemented with
10% (v/v) heat-inactivated foetal bovine serum, 0.6% (v/v) insulin 100 U/ml,
100 U/ml penicillin, 100 μg/ml streptomycin, 250 μg/ml amphotericin B, and
15mM N-2-hydroxyethylpiperazine-N'-2-ethanesulfonic acid (HEPES) pH 7.4

RAW 264.7 cells:

Dulbecco's Modified Eagle's Medium supplemented with
10% (v/v) heat-inactivated foetal calf serum, 100 U/ml penicillin,
100 μg/ml streptomycin, and 15 mM HEPES pH 7.4

Freezing media:

DMEM / RPMI media
containing 20% (v/v) foetal calf serum and 8% (v/v) DMSO

Heat Inactivation of Foetal Calf Serum:

Thaw at 37°C
Heat at 56°C for 30mins
Separate into 50ml aliquots
Store at -20°C

Cell fractionation buffers preparation

Buffer A:

10 mM HEPES pH 7.5, 10 mM KCl, 1 mM EDTA, 1 mM EGTA,
1 mM DTT, 1 mM $MgCl_2$, 5% glycerol, 0.1 mM $NaVO_4$, with protease inhibitors
(1 μg/ml leupeptin, 2 μg/ml aprotinin, and 1 μg/ml pefabloc)

Buffer B:

10 mM HEPES pH 7.5, 10 mM KCl, 1 mM DTT and 1 mM $MgCl_2$

Nuclear Lysis Buffer:

20 mM HEPES pH7.5, 0.4 M NaCl, 1 mM EDTA, 1 mM EGTA,
1 mM DTT, 1 mM $MgCl_2$, 25% glycerol with protease inhibitors

EMSA buffer preparation

Binding Buffer:

10 mM HEPES pH 7.6, 5 mM $MgCl_2$, 40 mM KCl,
1 mM DTT, 5% glycerol, 5 mg/ml Heparin

Loading buffer:

80% glycerol, 0.1% bromphenol blue in 50 mM Tris-Cl pH 7.5

Polyacrylamide Gel 4%:

44 mM Tris-Cl pH 8.3, 44 mM Boric acid, 1 mM EDTA,
4% acrylamide-bisacrylamide (29:1) and 2.5% glycerol
(prerun 1 hour at 250 V)

Protein standard preparation

BSA stock solution 10mg/ml was diluted in water to obtain five protein standards of increasing concentrations of 0.25, 0.5, 1.0, 2.0, 4.0µg/µl

Western Analysis

Whole Cell Extract (WCE) buffer:
25 mM HEPES (pH 7.4), 0.3 M NaCl, 1.5 mM $MgCl_2$, 0.2 mM EDTA, 0.1% Triton X-100, 0.5 mM dithiothreitol (DTT), 20 mMglycerophosphate, 100 µM $NaVO_4$, 1 µg/ml leupeptin, 2 µg/ml aprotinin and 0.5mg/ml pefabloc

Tris-Buffered Saline:
50 mM Tris-HCl, pH 8.0, 150 mM NaCl
with 0.05 % Tween 20 (TBS-T)

Phosphate Buffered Saline: 10X solution
80g NaCl, 2g KCl, 11.5g Na2HPO4.7H2O, 2g KH2PO4,
water to 1L pH = 7.3.

SDS Running Buffer: 10X solution
0.25M Tris, 2.5M Glycine, 1% SDS pH 8.3.

Transfer Buffer:
48mM Tris, 39mM Glycine, 20% methanol, 0.037% SDS pH 9.2.

Electrocompetent E. Coli-DH5α

DH5α were grown in 3ml of LB medium overnight at 37°C
Inoculate 1L of LB medium with pre-culture
Grow at 37°C, with vigorous shaking, until an OD_{600nm} of 0.5-0.8
Remove from the incubator and chill on ice for 30 minutes
All further steps are performed in a cold room at 4°C, with the cells on ice

Precipitate cells by centrifugation (15min x 4000g x 4°), discard supernatant and resuspend gently in 1L of chilled sterile water. Precipitate as before and discard supernatant
Repeat wash-step once more with 0.5L of water

Resuspend cells in 20ml of sterile 10% glycerol
Precipitate and discard supernatant
Resuspend in 2ml of 10% glycerol and separate into 80µl aliquots
Freeze on dry ice and store at -70°C.

SOC Medium

2% Tryptone
0.5% Yeast Extract
10mM NaCl
2.5mM KCl
10mM $MgCl_2$
10mM $MgSO_4$
20mM Glucose

Luria-Bertani Medium

1% Tryptone
0.5% Yeast Extract
1% NaCl
pH 7.0
Store at room temperature

Luria-Bertani Agar

As per LB medium but add Agar 15g/L before autoclaving
Store at room temperature

X-Gal

To make 40mg/ml stock solution
Dissolve 400mg in 10ml dimethylforamide
Protect from light
Store at -20°C

Electromobility Shift Assay

Binding Buffer: 10x solution

100 mM HEPES pH 7.6
50 mM MgCl2
400 mM KCl
10 mM DTT
50% Glycerol

Loading Buffer: 5X solution

80% Glycerol
0.1% Bromophenol Blue
50mM Tris-HCl pH 7.5

Running Buffer:

0.5X TBE

TBE: 10x solution

0.88M Tris-HCl pH 8.3
0.88M Boric Acid
0.02M EDTA

Gel Recipe: 55 ml

2.75 ml 10X TBE
1.7 ml 80% Glycerol
5.5 ml 40% Polyacrylamide-Bisacrylamide (29:1)
44.6 ml H_2O
27.5 µl TEMED
412.5 µl 10%APS

References

1. Smith, W. L., Garavito, R. M. & Dewitt, D. L. Prostaglandin endoperoxide H synthases (cyclooxygenases)-1 and -2. *Journal of Biological Chemistry* **271**, 33157-33160 (1996).

2. Vane, J. R., Bakhle, Y. S. & Botting, R. M. Cyclooxygenases 1 and 2. *Annu Rev Pharmacol Toxicol* **38**, 97-120 (1998).

3. Majerus, P. W. Prostaglandins: critical roles in pregnancy and colon cancer. *Curr Biol* **8**, R87-R89 (1998).

4. Tilley, S. L., Coffman, T. M. & Koller, B. H. Mixed messages: modulation of inflammation and immune responses by prostaglandins and thromboxanes. *Journal of Clinical Investigation* **108**, 15-23 (2001).

5. Smith, W. L. & Langenbach, R. Why there are two cyclooxygenase isozymes. *Journal of Clinical Investigation* **107**, 1491-1495 (2001).

6. Rocca, B. *et al.* - Distinct roles of prostaglandin H synthases 1 and 2 in T-cell development [In Process Citation]. - *J Clin Invest 1999 May 15;103(10):1469-77* 1469-1777.

7. Sakamoto, C. Roles of COX-1 and COX-2 in gastrointestinal pathophysiology. *J Gastroenterol* **33**, 618-624 (1998).

8. Perini, R. F., Ma, L. & Wallace, J. L. Mucosal repair and COX-2 inhibition. *Curr. Pharm. Des* **9**, 2207-2211 (2003).

9. Catella-Lawson, F. Vascular biology of thrombosis: platelet-vessel wall interactions and aspirin effects. *Neurology* **57**, S5-S7 (2001).

10. Zhang, M. Z., Wang, J. L., Cheng, H. F., Harris, R. C. & McKanna, J. A. Cyclooxygenase-2 in rat nephron development. *AJP - Renal Physiology* **273**, F994-1002 (1997).

11. Harris, R. C. Cyclooxygenase-2 and the kidney: functional and pathophysiological implications. *J. Hypertens.* **20 Suppl 6**, S3-S9 (2002).

12. Loftin, C. D. *et al.* - Failure of ductus arteriosus closure and remodeling in neonatal mice deficient in cyclooxygenase-1 and cyclooxygenase-2. - *Proc Natl Acad Sci U S A 2001 Jan 30;98(3):1059-64.* 1059-1064.

13. Cao, Y. & Prescott, S. M. Many actions of cyclooxygenase-2 in cellular dynamics and in cancer. *J Cell Physiol* **190**, 279-286 (2002).

14. Fosslien, E. Review: molecular pathology of cyclooxygenase-2 in cancer-induced angiogenesis. *Ann. Clin. Lab Sci.* **31**, 325-348 (2001).

15. Saukkonen, K. *et al.* Cyclooxygenase-2 and gastric carcinogenesis. *APMIS* **111**, 915-925 (2003).

16. Dubinett, S. M. *et al.* Cyclooxygenase-2 in lung cancer. *Prog. Exp. Tumor Res.* **37**, 138-162 (2003).

17. Furstenberger, G., Marks, F. & Muller-Decker, K. Cyclooxygenase-2 and skin carcinogenesis. *Prog. Exp. Tumor Res.* **37**, 72-89 (2003).

18. Hussain, T., Gupta, S. & Mukhtar, H. Cyclooxygenase-2 and prostate carcinogenesis. *Cancer Lett.* **191**, 125-135 (2003).

19. Eberhart, C. E. *et al.* Up-regulation of cyclooxygenase 2 gene expression in human colorectal adnenomas and adenocarcinomas. *Gastroenterology* **107**, 1183-1188 (1994).

20. Bazan, N. G., Colangelo, V. & Lukiw, W. J. Prostaglandins and other lipid mediators in Alzheimer's disease. *Prostaglandins Other Lipid Mediat.* **68-69**, 197-210 (2002).

21. Dore, S. *et al.* Neuronal overexpression of cyclooxygenase-2 increases cerebral infarction. *Ann. Neurol.* **54**, 155-162 (2003).

22. Maihofner, C. *et al.* Expression and localization of cyclooxygenase-1 and -2 in human sporadic amyotrophic lateral sclerosis. *Eur. J. Neurosci.* **18**, 1527-1534 (2003).

23. Teismann, P. *et al.* COX-2 and neurodegeneration in Parkinson's disease. *Ann. N. Y. Acad. Sci.* **991**, 272-277 (2003).

24. Green, G. A. Understanding NSAIDs: from aspirin to COX-2. *Clin. Cornerstone.* **3**, 50-60 (2001).

25. Simon, L. S. Actions and toxicity of nonsteroidal anti-inflammatory drugs. *Current Opinion in Rheumatology* **8**, 169-175 (1996).

26. Hawkey, C. J. & Langman, M. J. Non-steroidal anti-inflammatory drugs: overall risks and management. Complementary roles for COX-2 inhibitors and proton pump inhibitors. *Gut* **52**, 600-608 (2003).

27. Schwappach, D. L. & Koeck, C. M. Selective COX-2 inhibitors: a health economic perspective. *Wien. Med. Wochenschr.* **153**, 116-122 (2003).

28. Pascucci, R. A. Use of nonsteroidal anti-inflammatory drugs and cyclooxygenase-2 (COX-2) inhibitors: indications and complications. *J. Am. Osteopath. Assoc.* **102**, 487-489 (2002).

29. James, M. W. & Hawkey, C. J. Assessment of non-steroidal anti-inflammatory drug (NSAID) damage in the human gastrointestinal tract. *Br. J. Clin. Pharmacol.* **56**, 146-155 (2003).

30. Wallace, J. L. Pathogenesis of NSAID-induced gastroduodenal mucosal injury. *Best. Pract. Res. Clin. Gastroenterol.* **15**, 691-703 (2001).

31. Bleumink, G. S., Feenstra, J., Sturkenboom, M. C. & Stricker, B. H. Nonsteroidal anti-inflammatory drugs and heart failure. *Drugs* **63**, 525-534 (2003).

32. Stollberger, C. & Finsterer, J. Nonsteroidal anti-inflammatory drugs in patients with cardio- or cerebrovascular disorders. *Z. Kardiol.* **92**, 721-729 (2003).

33. Simon, R. A. Adverse respiratory reactions to aspirin and nonsteroidal anti-inflammatory drugs. *Curr. Allergy Asthma Rep.* **4**, 17-24 (2004).

34. Gambaro, G. & Perazella, M. A. Adverse renal effects of anti-inflammatory agents: evaluation of selective and nonselective cyclooxygenase inhibitors. *J. Intern. Med.* **253**, 643-652 (2003).

35. Kramer, B. K., Kammerl, M. C. & Komhoff, M. Renal cyclooxygenase-2 (COX-2). Physiological, pathophysiological, and clinical implications. *Kidney Blood Press Res.* **27**, 43-62 (2004).

36. O'Banion, M. K., Sadowski, H. B., Winn, V. & Young, D. A. A serum- and glucocorticoid-regulated 4-kilobase mRNA encodes a cyclooxygenase-related protein. *Journal of Biological Chemistry* **266**, 23261-23267 (1991).

37. Kujubu, D. A., Fletcher, B. S., Varnum, B. C., Lim, R. W. & Herschman, H. R. TIS10, a phorbol ester tumor promoter-inducible mRNA from Swiss 3T3 cells, encodes a novel prostaglandin synthase/cyclooxygenase homologue. *Journal of Biological Chemistry* **266**, 12866-12872 (1991).

38. Hla, T. & Neilson, K. Human Cyclooxygenase-2 cDNA. *PNAS* **89**, 7384-7388 (1992).

39. Fitzgerald, G. A. & Patrono, C. The coxibs, selective inhibitors of cyclooxygenase-2. *N. Engl. J. Med.* **345**, 433-442 (2001).

40. Vane, J. R. & Botting, R. M. Anti-inflammatory drugs and their mechanism of action. *Inflamm Res* **47**, Suppl-87 (1998).

41. Oviedo, J. A. & Wolfe, M. M. Gastroprotection by coxibs: what do the Celecoxib Long-Term Arthritis Safety Study and the Vioxx Gastrointestinal Outcomes Research Trial tell us? *Rheum. Dis. Clin. North Am.* **29**, 769-788 (2003).

42. DeMaria, A. N. & Weir, M. R. Coxibs--beyond the GI tract: renal and cardiovascular issues. *J. Pain Symptom. Manage.* **25**, S41-S49 (2003).

43. Weir, M. R. Renal effects of nonselective NSAIDs and coxibs. *Cleve. Clin. J. Med.* **69 Suppl 1**, SI53-SI58 (2002).

44. Fitzgerald, G. A. Cardiovascular pharmacology of nonselective nonsteroidal anti-inflammatory drugs and coxibs: clinical considerations. *Am. J. Cardiol.* **89**, 26D-32D (2002).

45. Bombardier, C. An evidence-based evaluation of the gastrointestinal safety of coxibs. *Am. J. Cardiol.* **89**, 3D-9D (2002).

46. Stiller, C. O. & Hjemdahl, P. Endothelial COX-2 inhibition: possible relevance for hypertension and cardiovascular risk? *J. Hypertens.* **21**, 1615-1618 (2003).

47. Giovanni, G. & Giovanni, P. Do non-steroidal anti-inflammatory drugs and COX-2 selective inhibitors have different renal effects? *J. Nephrol.* **15**, 480-488 (2002).

48. Fowles, R. E. Potential cardiovascular effects of COX-2 selective nonsteroidal antiinflammatory drugs. *J. Pain Palliat. Care Pharmacother.* **17**, 27-50 (2003).

49. FDA Consumer magazine May-June 2005 Issue. 2005.
Ref Type: Generic

50. Sabichi, A. L. & Lippman, S. M. COX-2 inhibitors and other NSAIDs in bladder and prostate cancer. *Prog. Exp. Tumor Res.* **37**, 163-178 (2003).

51. Nasir, A., Fernandez, P. M., Chughtai, O. R. & Kaiser, H. E. COX-2, NSAIDs and human neoplasia. Part I: Colorectal neoplasms. *In Vivo* **16**, 501-509 (2002).

52. Haller, D. G. COX-2 inhibitors in oncology. *Semin. Oncol.* **30**, 2-8 (2003).

53. Anderson, W. F., Umar, A. & Hawk, E. T. Cyclooxygenase inhibition in cancer prevention and treatment. *Expert. Opin. Pharmacother.* **4**, 2193-2204 (2003).

54. Dormond, O. & Ruegg, C. Regulation of endothelial cell integrin function and angiogenesis by COX-2, cAMP and Protein Kinase A. *Thromb. Haemost.* **90**, 577-585 (2003).

55. Ruegg, C., Dormond, O. & Mariotti, A. Endothelial cell integrins and COX-2: mediators and therapeutic targets of tumor angiogenesis. *Biochim. Biophys. Acta* **1654**, 51-67 (2004).

56. Pasinetti, G. M. Cyclooxygenase as a target for the antiamyloidogenic activities of nonsteroidal anti-inflammatory drugs in Alzheimer's disease. *Neurosignals.* **11**, 293-297 (2002).

57. Aisen, P. S. Evaluation of selective COX-2 inhibitors for the treatment of Alzheimer's disease. *J. Pain Symptom. Manage.* **23**, S35-S40 (2002).

58. McGeer, P. L. COX-2 and ALS. *Amyotroph. Lateral. Scler. Other Motor Neuron Disord.* **2**, 121-122 (2001).

59. Hoozemans, J. J., Veerhuis, R., Rozemuller, A. J. & Eikelenboom, P. Non-steroidal anti-inflammatory drugs and cyclooxygenase in Alzheimer's disease. *Curr. Drug Targets.* **4**, 461-468 (2003).

60. Harris, R. C. *et al.* Cyclooxygenase-2 is associated with the macula densa of rat kidney and increases with salt restriction. *J. Clin. Invest* **94**, 2504-2510 (1994).

61. Komhoff, M., Grone, H. J., Klein, T., Seyberth, H. W. & Nusing, R. M. Localization of cyclooxygenase-1 and -2 in adult and fetal human kidney: implication for renal function. *Am. J. Physiol* **272**, F460-F468 (1997).

62. Nantel, F. *et al.* Immunolocalization of cyclooxygenase-2 in the macula densa of human elderly. *FEBS Lett.* **457**, 475-477 (1999).

63. Breyer, M. D. & Harris, R. C. Cyclooxygenase 2 and the kidney. *Curr. Opin. Nephrol. Hypertens.* **10**, 89-98 (2001).

64. Perazella, M. A. & Tray, K. Selective cyclooxygenase-2 inhibitors: a pattern of nephrotoxicity similar to traditional nonsteroidal anti-inflammatory drugs. *Am. J. Med.* **111**, 64-67 (2001).

65. Lim, W. C., Park, J. B. & Lee, Y. J. Analysis of angiotensin II mediated COX-2 downregulation in angiotensin II- or aldosterone-infused hypertensive rat. *Biol. Pharm. Bull.* **26**, 1086-1088 (2003).

66. Harris, R. C., Zhang, M. Z. & Cheng, H. F. Cyclooxygenase-2 and the renal renin-angiotensin system. *Acta Physiol Scand.* **181**, 543-547 (2004).

67. Zhang, M. Z. *et al.* Renal cortical cyclooxygenase 2 expression is differentially regulated by angiotensin II AT(1) and AT(2) receptors. *Proc. Natl. Acad. Sci. U. S. A* **103**, 16045-16050 (2006).

68. Zhang, M. Z., Yao, B., McKanna, J. A. & Harris, R. C. Cross talk between the intrarenal dopaminergic and cyclooxygenase-2 systems. *Am. J. Physiol Renal Physiol* **288**, F840-F845 (2005).

69. Zhang, M. Z. *et al.* Regulation of renal cortical cyclooxygenase-2 in young rats. *Am. J. Physiol Renal Physiol* **285**, F881-F888 (2003).

70. Madsen, K. *et al.* Low endogenous glucocorticoid allows induction of kidney cortical cyclooxygenase-2 during postnatal rat development. *Am. J. Physiol Renal Physiol* **286**, F26-F37 (2004).

71. Zhang, M. Z., Sanchez, L. P., McKanna, J. A. & Harris, R. C. Regulation of cyclooxygenase expression by vasopressin in rat renal medulla. *Endocrinology* **145**, 1402-1409 (2004).

72. Cheng, H. F. *et al.* Genetic deletion of COX-2 prevents increased renin expression in response to ACE inhibition. *Am. J. Physiol Renal Physiol* **280**, F449-F456 (2001).

73. Qi, Z. *et al.* Opposite effects of cyclooxygenase-1 and -2 activity on the pressor response to angiotensin II. *J. Clin. Invest* **110**, 61-69 (2002).

74. Ichihara, A., Imig, J. D., Inscho, E. W. & Navar, L. G. Cyclooxygenase-2 participates in tubular flow-dependent afferent arteriolar tone: interaction with neuronal NOS. *Am. J. Physiol* **275**, F605-F612 (1998).

75. Ichihara, A., Imig, J. D. & Navar, L. G. Cyclooxygenase-2 modulates afferent arteriolar responses to increases in pressure. *Hypertension* **34**, 843-847 (1999).

76. Rodriguez, F., Llinas, M. T., Gonzalez, J. D., Rivera, J. & Salazar, F. J. Renal changes induced by a cyclooxygenase-2 inhibitor during normal and low sodium intake. *Hypertension* **36**, 276-281 (2000).

77. Roig, F., Llinas, M. T., Lopez, R. & Salazar, F. J. Role of cyclooxygenase-2 in the prolonged regulation of renal function. *Hypertension* **40**, 721-728 (2002).

78. Catella-Lawson, F. *et al.* Effects of specific inhibition of cyclooxygenase-2 on sodium balance, hemodynamics, and vasoactive eicosanoids. *J. Pharmacol. Exp. Ther.* **289**, 735-741 (1999).

79. Whelton, A. *et al.* Effects of celecoxib and naproxen on renal function in the elderly. *Arch. Intern. Med.* **160**, 1465-1470 (2000).

80. Rossat, J., Maillard, M., Nussberger, J., Brunner, H. R. & Burnier, M. Renal effects of selective cyclooxygenase-2 inhibition in normotensive salt-depleted subjects. *Clin. Pharmacol. Ther.* **66**, 76-84 (1999).

81. Swan, S. K. *et al.* Effect of cyclooxygenase-2 inhibition on renal function in elderly persons receiving a low-salt diet. A randomized, controlled trial. *Ann. Intern. Med.* **133**, 1-9 (2000).

82. Gross, J. M., Dwyer, J. E. & Knox, F. G. Natriuretic response to increased pressure is preserved with COX-2 inhibitors. *Hypertension* **34**, 1163-1167 (1999).

83. Yang, T. X. *et al.* REGULATION OF CYCLOOXYGENASE EXPRESSION IN THE KIDNEY BY DIETARY SALT INTAKE. *American Journal of Physiology - Renal Fluid & Electrolyte Physiology* **43**, F.

84. Yang, T. *et al.* MAPK Mediation of Hypertonicity-stimulated Cyclooxygenase-2 Expression in Renal Medullary Collecting Duct Cells. *Journal of Biological Chemistry* **275**, 23281-23286 (2000).

85. Hao, C. M. *et al.* Dehydration activates an NF-kappaB-driven, COX2-dependent survival mechanism in renal medullary interstitial cells. *J. Clin. Invest* **106**, 973-982 (2000).

86. Schlondorff, D. Renal complications of nonsteroidal anti-inflammatory drugs. *Kidney Int.* **44**, 643-653 (1993).

87. Bach, P. H. & Nguyen, T. K. Renal papillary necrosis--40 years on. *Toxicol. Pathol.* **26**, 73-91 (1998).

88. Norwood, V. F., Morham, S. G. & Smithies, O. Postnatal development and progression of renal dysplasia in cyclooxygenase-2 null mice. *Kidney Int.* **58**, 2291-2300 (2000).

89. Morham, S. G. *et al.* Prostaglandin synthase 2 gene disruption causes severe renal pathology in the mouse. *Cell* **83**, 473-482 (1995).

90. Dinchuk, J. E. *et al.* Renal abnormalities and an altered inflammatory response in mice lacking cyclooxygenase II. *Nature* **378**, 406-409 (1995).

91. Komhoff, M. *et al.* - Cyclooxygenase-2-selective inhibitors impair glomerulogenesis and renal cortical development. - *Kidney Int 2000 Feb;57(2):414-22.* 414-422.

92. Veersema, D., de Jong, P. A. & van Wijck, J. A. Indomethacin and the fetal renal nonfunction syndrome. *Eur. J. Obstet. Gynecol. Reprod. Biol.* **16**, 113-121 (1983).

93. Voyer, L. E., Drut, R. & Mendez, J. H. Fetal renal maldevelopment with oligohydramnios following maternal use of piroxicam. *Pediatr. Nephrol.* **8**, 592-594 (1994).

94. Peruzzi, L., Gianoglio, B., Porcellini, M. G. & Coppo, R. Neonatal end-stage renal failure associated with maternal ingestion of cyclo-oxygenase-type-1 selective inhibitor nimesulide as tocolytic. *Lancet* **354**, 1615 (1999).

95. Ali, U. S. *et al.* Renal tubular dysgenesis associated with in utero exposure to Nimuselide. *Pediatr. Nephrol.* **21**, 274-276 (2006).

96. Zatz, R. & Fujihara, C. K. Mechanisms of progressive renal disease: role of angiotensin II, cyclooxygenase products and nitric oxide. *J. Hypertens. Suppl* **20**, S37-S44 (2002).

97. Wang, J. L., Cheng, H. F., Zhang, M. Z., McKanna, J. A. & Harris, R. C. Selective increase of cyclooxygenase-2 expression in a model of renal ablation. *Am. J. Physiol* **275**, F613-F622 (1998).

98. Komers, R. *et al.* Immunohistochemical and functional correlations of renal cyclooxygenase-2 in experimental diabetes. *J. Clin. Invest* **107**, 889-898 (2001).

99. Komers, R. *et al.* Renal cyclooxygenase-2 in obese Zucker (fatty) rats. *Kidney Int.* **67**, 2151-2158 (2005).

100. Blume, C. *et al.* Effect of flosulide, a selective cyclooxygenase 2 inhibitor, on passive heymann nephritis in the rat. *Kidney Int.* **56**, 1770-1778 (1999).

101. Tomasoni, S. *et al.* Upregulation of renal and systemic cyclooxygenase-2 in patients with active lupus nephritis. *J. Am. Soc. Nephrol.* **9**, 1202-1212 (1998).

102. Schneider, A. *et al.* Cyclooxygenase metabolites mediate glomerular monocyte chemoattractant protein-1 formation and monocyte recruitment in experimental glomerulonephritis. *Kidney Int.* **55**, 430-441 (1999).

103. Waldner, C. *et al.* Selective cyclooxygenase-2 inhibition upregulates renal cortical alpha V integrin expression. *Nephron Exp. Nephrol.* **93**, e72 (2003).

104. Fujihara, C. K. *et al.* Cyclooxygenase-2 (COX-2) inhibition limits abnormal COX-2 expression and progressive injury in the remnant kidney. *Kidney Int.* **64**, 2172-2181 (2003).

105. Goncalves, A. R. *et al.* Renal expression of COX-2, ANG II, and AT1 receptor in remnant kidney: strong renoprotection by therapy with losartan and a nonsteroidal anti-inflammatory. *Am. J. Physiol Renal Physiol* **286**, F945-F954 (2004).

106. Cheng, H. F. *et al.* Cyclooxygenase-2 inhibitor blocks expression of mediators of renal injury in a model of diabetes and hypertension. *Kidney Int.* **62**, 929-939 (2002).

107. Komers, R., Lindsley, J. N., Oyama, T. T. & Anderson, S. Cyclo-oxygenase-2 inhibition attenuates the progression of nephropathy in uninephrectomized diabetic rats. *Clin. Exp. Pharmacol. Physiol* **34**, 36-41 (2007).

108. Heise, G., Grabensee, B., Schror, K. & Heering, P. Different actions of the cyclooxygenase 2 selective inhibitor flosulide in rats with passive Heymann nephritis. *Nephron* **80**, 220-226 (1998).

109. Orphanides, G. & Reinberg, D. A unified theory of gene expression. *Cell* **108**, 439-451 (2002).

110. Custodio, N. & Carmo-Fonseca, M. Quality control of gene expression in the nucleus. *J. Cell Mol. Med.* **5**, 267-275 (2001).

111. Hieronymus, H. & Silver, P. A. A systems view of mRNP biology. *Genes Dev.* **18**, 2845-2860 (2004).

112. Moore, M. J. & Rosbash, M. Cell biology. TAPping into mRNA export. *<EM>Science</EM>* **294**, 1841-1842 (2001).

113. Mili, S., Shu, H. J., Zhao, Y. & Pinol-Roma, S. Distinct RNP complexes of shuttling hnRNP proteins with pre-mRNA and mRNA: candidate intermediates in formation and export of mRNA. *Mol. Cell Biol.* **21**, 7307-7319 (2001).

114. Kress, T. L., Yoon, Y. J. & Mowry, K. L. Nuclear RNP complex assembly initiates cytoplasmic RNA localization. *J. Cell Biol.* **165**, 203-211 (2004).

115. Dreyfuss, G., Kim, V. N. & Kataoka, N. Messenger-RNA-binding proteins and the messages they carry. *Nat. Rev. Mol. Cell Biol.* **3**, 195-205 (2002).

116. Wilkinson, M. F. & Shyu, A. B. Multifunctional regulatory proteins that control gene expression in both the nucleus and the cytoplasm. *Bioessays* **23**, 775-787 (2001).

117. Singh, R. RNA-protein interactions that regulate pre-mRNA splicing. *Gene Expr.* **10**, 79-92 (2002).

118. Izaurralde, E. *et al.* A role for the M9 transport signal of hnRNP A1 in mRNA nuclear export. *J. Cell Biol.* **137**, 27-35 (1997).

119. Shyu, A. B. & Wilkinson, M. F. The double lives of shuttling mRNA binding proteins. *Cell* **102**, 135-138 (2000).

120. Le Hir, H., Moore, M. J. & Maquat, L. E. Pre-mRNA splicing alters mRNP composition: evidence for stable association of proteins at exon-exon junctions. *Genes Dev.* **14**, 1098-1108 (2000).

121. Le Hir, H., Gatfield, D., Izaurralde, E. & Moore, M. J. The exon-exon junction complex provides a binding platform for factors involved in mRNA export and nonsense-mediated mRNA decay. *EMBO J.* **20**, 4987-4997 (2001).

122. Keene, J. D. Ribonucleoprotein infrastructure regulating the flow of genetic information between the genome and the proteome. *Proc. Natl. Acad. Sci. U. S. A* **98**, 7018-7024 (2001).

123. Daneholt, B. Assembly and transport of a premessenger RNP particle. *Proc. Natl. Acad. Sci. U. S. A* **98**, 7012-7017 (2001).

124. Krecic, A. M. & Swanson, M. S. hnRNP complexes: composition, structure, and function. *Curr. Opin. Cell Biol.* **11**, 363-371 (1999).

125. Steinmetz, E. J. Pre-mRNA processing and the CTD of RNA polymerase II: the tail that wags the dog? *Cell* **89**, 491-494 (1997).

126. Fong, N. & Bentley, D. L. Capping, splicing, and 3' processing are independently stimulated by RNA polymerase II: different functions for different segments of the CTD. *Genes Dev.* **15**, 1783-1795 (2001).

127. Hirose, Y. & Manley, J. L. RNA polymerase II and the integration of nuclear events. *Genes Dev.* **14**, 1415-1429 (2000).

128. Bentley, D. The mRNA assembly line: transcription and processing machines in the same factory. *Curr. Opin. Cell Biol.* **14**, 336-342 (2002).

129. Neugebauer, K. M. On the importance of being co-transcriptional. *J. Cell Sci.* **115**, 3865-3871 (2002).

130. Schroeder, S. C., Schwer, B., Shuman, S. & Bentley, D. Dynamic association of capping enzymes with transcribing RNA polymerase II. *Genes Dev.* **14**, 2435-2440 (2000).

131. Maquat, L. E. & Carmichael, G. G. Quality control of mRNA function. *Cell* **104**, 173-176 (2001).

132. Wilusz, C. J., Wormington, M. & Peltz, S. W. The cap-to-tail guide to mRNA turnover. *Nat. Rev. Mol. Cell Biol.* **2**, 237-246 (2001).

133. Moore, M. J. Nuclear RNA turnover. *Cell* **108**, 431-434 (2002).

134. Wilkinson, M. F. & Shyu, A. B. RNA surveillance by nuclear scanning? *Nat. Cell Biol.* **4**, E144-E147 (2002).

135. Mignone, F., Gissi, C., Liuni, S. & Pesole, G. Untranslated regions of mRNAs. *Genome Biol.* **3**, REVIEWS0004 (2002).

136. Shatkin, A. J. & Manley, J. L. The ends of the affair: capping and polyadenylation. *Nat. Struct. Biol.* **7**, 838-842 (2000).

137. Proudfoot, N. & O'Sullivan, J. Polyadenylation: a tail of two complexes. *Curr. Biol.* **12**, R855-R857 (2002).

138. Hall, T. M. Poly(A) tail synthesis and regulation: recent structural insights. *Curr. Opin. Struct. Biol.* **12**, 82-88 (2002).

139. Gray, N. K. & Wickens, M. Control of translation initiation in animals. *Annu Rev Cell Dev Biol* **14**, 399-458 (1998).

140. Mangus, D. A., Evans, M. C. & Jacobson, A. Poly(A)-binding proteins: multifunctional scaffolds for the post-transcriptional control of gene expression. *Genome Biol.* **4**, 223 (2003).

141. Dreyfus, M. & Regnier, P. The poly(A) tail of mRNAs: bodyguard in eukaryotes, scavenger in bacteria. *Cell* **111**, 611-613 (2002).

142. de Sauvage, F., Kruys, V., Marinx, O., Huez, G. & Octave, J. N. Alternative polyadenylation of the amyloid protein precursor mRNA regulates translation. *EMBO J* **11**, 3099-3103 (1992).

143. Le Hir, H., Nott, A. & Moore, M. J. How introns influence and enhance eukaryotic gene expression. *Trends Biochem. Sci.* **28**, 215-220 (2003).

144. Reed, R. Mechanisms of fidelity in pre-mRNA splicing. *Curr. Opin. Cell Biol.* **12**, 340-345 (2000).

145. Kramer, A. The structure and function of proteins involved in mammalian pre-mRNA splicing. *Annu. Rev. Biochem.* **65**, 367-409 (1996).

146. Black, D. L. Mechanisms of alternative pre-messenger RNA splicing. *Annu. Rev. Biochem.* **72**, 291-336 (2003).

147. Smith, C. W. & Valcarcel, J. Alternative pre-mRNA splicing: the logic of combinatorial control. *Trends Biochem. Sci.* **25**, 381-388 (2000).

148. König, H., Ponta, H. & Herrlich, P. Coupling of signal transduction to alternative pre-mRNA splicing by a composite splice regulator. *EMBO J. 1998. May. 15.* **17**, 2904-2913 (1998).

149. Smith, H. C., Gott, J. M. & Hanson, M. R. A guide to RNA editing. *RNA.* **3**, 1105-1123 (1997).

150. Gott, J. M. & Emeson, R. B. Functions and mechanisms of RNA editing. *Annu. Rev. Genet.* **34**, 499-531 (2000).

151. Schmauss, C. & Howe, J. R. RNA editing of neurotransmitter receptors in the Mammalian brain. *Sci STKE* **2002**, E26 (2002).

152. Izaurralde, E. A novel family of nuclear transport receptors mediates the export of messenger RNA to the cytoplasm. *Eur. J. Cell Biol.* **81**, 577-584 (2002).

153. Calapez, A. *et al.* The intranuclear mobility of messenger RNA binding proteins is ATP dependent and temperature sensitive. *J. Cell Biol.* **159**, 795-805 (2002).

154. Zenklusen, D. & Stutz, F. Nuclear export of mRNA. *FEBS Lett.* **498**, 150-156 (2001).

155. Reed, R. Coupling transcription, splicing and mRNA export. *Curr. Opin. Cell Biol.* **15**, 326-331 (2003).

156. Reed, R. & Hurt, E. A conserved mRNA export machinery coupled to pre-mRNA splicing. *Cell*

108, 523-531 (2002).

157. Stutz, F. & Izaurralde, E. The interplay of nuclear mRNP assembly, mRNA surveillance and export. *Trends Cell Biol.* **13**, 319-327 (2003).

158. Kloc, M., Zearfoss, N. R. & Etkin, L. D. Mechanisms of subcellular mRNA localization. *Cell* **108**, 533-544 (2002).

159. Schell, T., Kulozik, A. E. & Hentze, M. W. Integration of splicing, transport and translation to achieve mRNA quality control by the nonsense-mediated decay pathway. *Genome Biol.* **3**, REVIEWS1006 (2002).

160. Palacios, I. M. & St Johnston, D. Getting the message across: the intracellular localization of mRNAs in higher eukaryotes. *Annu. Rev. Cell Dev. Biol.* **17**, 569-614 (2001).

161. Hentze, M. W. & Kulozik, A. E. A perfect message: RNA surveillance and nonsense-mediated decay [Review]. *Cell* **96**, 307-310 (1999).

162. Iborra, F. J., Jackson, D. A. & Cook, P. R. Coupled Transcription and Translation Within Nuclei of Mammalian Cells. *<EM>Science</EM>* **293**, 1139-1142 (2001).

163. Gray, N. K., Coller, J. M., Dickson, K. S. & Wickens, M. Multiple portions of poly(A)-binding protein stimulate translation in vivo. *EMBO J.* **19**, 4723-4733 (2000).

164. Gallie, D. R. A tale of two termini: a functional interaction between the termini of an mRNA is a prerequisite for efficient translation initiation. *Gene* **216**, 1-11 (1998).

165. van Hoof, A. & Parker, R. Messenger RNA degradation: beginning at the end. *Curr. Biol.* **12**, R285-R287 (2002).

166. Grosset, C. *et al.* A mechanism for translationally coupled mRNA turnover: interaction between the poly(A) tail and a c-fos RNA coding determinant via a protein complex. *Cell* **103**, 29-40 (2000).

167. Sachs, A. B. & Varani, G. Eukaryotic translation initiation: there are (at least) two sides to every story. *Nat. Struct. Biol.* **7**, 356-361 (2000).

168. Brewer, G. Messenger RNA decay during aging and development. *Ageing Res. Rev.* **1**, 607-625 (2002).

169. Pyronnet, S. & Sonenberg, N. Cell-cycle-dependent translational control. *Curr. Opin. Genet. Dev.* **11**, 13-18 (2001).

170. Mitchell, P. & Tollervey, D. mRNA turnover. *Curr. Opin. Cell Biol.* **13**, 320-325 (2001).

171. Liebhaber, S. A. mRNA stability and the control of gene expression. *Nucleic Acids Symp. Ser.* 29-32 (1997).

172. Dever, T. E. Gene-specific regulation by general translation factors. *Cell* **108**, 545-556 (2002).

173. Sonenberg, N. & Dever, T. E. Eukaryotic translation initiation factors and regulators. *Curr. Opin. Struct. Biol.* **13**, 56-63 (2003).

174. van der Velden, A. W. & Thomas, A. A. The role of the 5' untranslated region of an mRNA in translation regulation during development. *Int. J. Biochem. Cell Biol.* **31**, 87-106 (1999).

175. Cormier, P., Pyronnet, S., Salaun, P., Mulner-Lorillon, O. & Sonenberg, N. Cap-dependent translation and control of the cell cycle. *Prog. Cell Cycle Res.* **5**, 469-475 (2003).

176. Yaman, I. *et al.* The Zipper Model of Translational Control. A Small Upstream ORF Is the Switch that Controls Structural Remodeling of an mRNA Leader. *Cell* **113**, 519-531 (2003).

177. Svitkin, Y. V. *et al.* The requirement for eukaryotic initiation factor 4A (eIF4A) in translation is in direct proportion to the degree of mRNA 5' secondary structure. *RNA.* **7**, 382-394 (2001).

178. Narberhaus, F. mRNA-mediated detection of environmental conditions. *Arch. Microbiol.* **178**, 404-410 (2002).

179. Wilkie, G. S., Dickson, K. S. & Gray, N. K. Regulation of mRNA translation by 5'- and 3'-UTR-binding factors. *Trends Biochem. Sci.* **28**, 182-188 (2003).

180. Vagner, S., Galy, B. & Pyronnet, S. Irresistible IRES. Attracting the translation machinery to internal ribosome entry sites. *EMBO Rep.* **2**, 893-898 (2001).

181. Kozak, M. Alternative ways to think about mRNA sequences and proteins that appear to promote internal initiation of translation. *Gene* **318**, 1-23 (2003).

182. Spicher, A. *et al.* Highly Conserved RNA Sequences That Are Sensors of Environmental Stress. *Mol. Cell Biol 1998. Dec.* **18**, 7371-7382.

183. Kuersten, S. & Goodwin, E. B. The power of the 3' UTR: translational control and development. *Nat. Rev. Genet.* **4**, 626-637 (2003).

184. Grzybowska, E. A., Wilczynska, A. & Siedlecki, J. A. Regulatory functions of 3'UTRs. *Biochem. Biophys. Res. Commun.* **288**, 291-295 (2001).

185. Mazumder, B., Seshadri, V. & Fox, P. L. Translational control by the 3'-UTR: the ends specify the means. *Trends Biochem. Sci.* **28**, 91-98 (2003).

186. Wickens, M., Bernstein, D. S., Kimble, J. & Parker, R. A PUF family portrait: 3'UTR regulation as a way of life. *Trends Genet.* **18**, 150-157 (2002).

187. Wickens, M., Anderson, P. & Jackson, R. J. Life and death in the cytoplasm: messages from the 3' end. *Curr Opin Genet Dev* **7**, 220-232 (1997).

188. Wightman, B., Ha, I. & Ruvkun, G. - Posttranscriptional regulation of the heterochronic gene lin-14 by lin-4 mediates temporal pattern formation in C. elegans. - *Cell 1993 Dec 3;75(5):855-62* 855-622.

189. Eddy, S. R. Non-coding RNA genes and the modern RNA world. *Nat Rev Genet* **2**, 919-929 (2001).

190. Richter, J. D. Cytoplasmic polyadenylation in development and beyond. *Microbiol. Mol. Biol. Rev.* **63**, 446-456 (1999).

191. Macdonald, P. Diversity in translational regulation. *Curr. Opin. Cell Biol.* **13**, 326-331 (2001).

192. Mendez, R. & Richter, J. D. Translational control by CPEB: a means to the end. *Nat. Rev. Mol. Cell Biol.* **2**, 521-529 (2001).

193. Groisman, I., Huang, Y. S., Mendez, R., Cao, Q. & Richter, J. D. Translational control of embryonic cell division by CPEB and maskin. *Cold Spring Harb. Symp. Quant. Biol.* **66**, 345-351 (2001).

194. Groisman, I., Jung, M. Y., Sarkissian, M., Cao, Q. & Richter, J. D. Translational control of the embryonic cell cycle. *Cell* **109**, 473-483 (2002).

195. Sachs, A. The role of poly(A) in the translation and stability of mRNA. *Curr. Opin. Cell Biol.* **2**, 1092-1098 (1990).

196. Colgan, D. F. & Manley, J. L. Mechanism and regulation of mRNA polyadenylation. *Genes Dev.* **11**, 2755-2766 (1997).

197. Wickens, M. Forward, backward, how much, when: Mechanisms of poly(A) addition and

removal and their role in early development. *Semin. Dev. Biol.* **3**, 399-412 (1992).

198. Siomi, H. & Dreyfuss, G. RNA-binding proteins as regulators of gene expression. [Review] [70 refs]. *Current Opinion in Genetics & Development* **7**, 345-353 (1997).

199. Standart, N. & Jackson, R. J. Regulation of translation by specific protein/mRNA interactions. *Biochimie* **76**, 867-879 (1994).

200. Osman, F., Jarrous, N., Ben Asouli, Y. & Kaempfer, R. A cis-acting element in the 3'-untranslated region of human TNF-alpha mRNA renders splicing dependent on the activation of protein kinase PKR. *Genes Dev* **13**, 3280-3293 (1999).

201. Bakheet, T., Frevel, M., Williams, B. R., Greer, W. & Khabar, K. S. - ARED: human AU-rich element-containing mRNA database reveals an unexpectedly diverse functional repertoire of encoded proteins. - *Nucleic Acids Res 2001 Jan 1;29(1):246-54.* 246-254.

202. Chen, C. Y. & Shyu, A. B. AU-rich elements: characterization and importance in mRNA degradation. *Trends Biochem. Sci.* **20**, 465-470 (1995).

203. Paillard, L., Legagneux, V., Maniey, D. & Osborne, H. B. c-Jun ARE Targets mRNA Deadenylation by an EDEN-BP (Embryo Deadenylation Element-binding Protein)-dependent Pathway. *Journal of Biological Chemistry* **277**, 3232-3235 (2002).

204. Shyu, A. B., Belasco, J. G. & Greenberg, M. E. Two distinct destabilizing elements in the c-fos message trigger deadenylation as a first step in rapid mRNA decay. *Genes Dev* **5**, 221-231 (1991).

205. Voeltz, G. K. & Steitz, J. A. AUUUA sequences direct mRNA deadenylation uncoupled from decay during Xenopus early development. *Mol. Cell Biol.* **18**, 7537-7545 (1998).

206. Xu, N., Chen, C. Y. & Shyu, A. B. Versatile role for hnRNP D isoforms in the differential regulation of cytoplasmic mRNA turnover. *Mol. Cell Biol.* **21**, 6960-6971 (2001).

207. Shaw, G. & Kamen, R. A conserved AU sequence from the 3' untranslated region of GM-CSF mRNA mediates selective mRNA degradation. *Cell* **46**, 659-667 (1986).

208. Lai, W. S. & Blackshear, P. J. Interactions of CCCH zinc finger proteins with mRNA: tristetraprolin-mediated AU-rich element-dependent mRNA degradation can occur in the absence of a poly(A) tail. *J. Biol. Chem.* **276**, 23144-23154 (2001).

209. Wilson, G. M., Sutphen, K., Chuang, K. & Brewer, G. Folding of A+U-rich RNA elements modulates AUF1 binding. Potential roles in regulation of mRNA turnover. *J. Biol. Chem.* **276**, 8695-8704 (2001).

210. Winzen, R. *et al.* The p38 MAP kinase pathway signals for cytokine-induced mRNA stabilization via MAP kinase-activated protein kinase 2 and an AU-rich region-targeted mechanism. *EMBO J.* **18**, 4969-4980 (1999).

211. Neininger, A. *et al.* MK2 Targets AU-rich Elements and Regulates Biosynthesis of Tumor Necrosis Factor and Interleukin-6 Independently at Different Post-transcriptional Levels. *Journal of Biological Chemistry* **277**, 3065-3068 (2002).

212. Lasa, M. *et al.* Regulation of cyclooxygenase 2 mRNA stability by the mitogen-activated protein kinase p38 signaling cascade. *Mol Cell Biol* **20**, 4265-4274 (2000).

213. Zhang, T., Kruys, V., Huez, G. & Gueydan, C. AU-rich element-mediated translational control: complexity and multiple activities of trans-activating factors. *Biochem. Soc. Trans.* **30**, 952-958 (2002).

214. Piecyk, M. *et al.* TIA-1 is a translational silencer that selectively regulates the expression of TNF-alpha. *EMBO J.* **19**, 4154-4163 (2000).

215. Kontoyiannis, D. *et al.* Interleukin-10 targets p38 MAPK to modulate ARE-dependent TNF mRNA translation and limit intestinal pathology. *EMBO J.* **20**, 3760-3770 (2001).

216. Cok, S. J. & Morrison, A. R. The 3'-Untranslated Region of Murine Cyclooxygenase-2 Contains Multiple Regulatory Elements That Alter Message Stability and Translational Efficiency. *Journal of Biological Chemistry* **276**, 23179-23185 (2001).

217. Zhang, T., Kruys, V., Huez, G. & Gueydan, C. AU-rich element-mediated translational control: complexity and multiple activities of trans-activating factors. *Biochem. Soc. Trans.* **30**, 952-958 (2002).

218. Gueydan, C. *et al.* Identification of TIAR as a protein binding to the translational regulatory AU-rich element of tumor necrosis factor alpha mRNA. *J. Biol. Chem.* **274**, 2322-2326 (1999).

219. Loflin, P., Chen, C. Y. & Shyu, A. B. Unraveling a cytoplasmic role for hnRNP D in the in vivo mRNA destabilization directed by the AU-rich element. *Genes Dev* **13**, 1884-1897 (1999).

220. Lai, W. S. *et al.* Evidence that tristetraprolin binds to AU-rich elements and promotes the deadenylation and destabilization of tumor necrosis factor alpha mRNA. *Mol. Cell Biol.* **19**, 4311-4323 (1999).

221. Wang, W., Caldwell, M. C., Lin, S., Furneaux, H. & Gorospe, M. HuR regulates cyclin A and cyclin B1 mRNA stability during cell proliferation. *EMBO J.* **19**, 2340-2350 (2000).

222. Dean, J. L. E. *et al.* The 3' Untranslated Region of Tumor Necrosis Factor Alpha mRNA Is a Target of the mRNA-Stabilizing Factor HuR. *Molecular and Cellular Biology* **21**, 721-730 (2001).

223. Yaman, I. *et al.* Nutritional control of mRNA stability is mediated by a conserved AU-rich element that binds the cytoplasmic shuttling protein HuR. *J. Biol. Chem.* **277**, 41539-41546 (2002).

224. Chen, C. Y., Xu, N. & Shyu, A. B. Highly selective actions of HuR in antagonizing AU-rich element-mediated mRNA destabilization. *Mol. Cell Biol.* **22**, 7268-7278 (2002).

225. Blaxall, B. C., Pende, A., Wu, S. C. & Port, J. D. Correlation between intrinsic mRNA stability and the affinity of AUF1 (hnRNP D) and HuR for A+U-rich mRNAs. *Mol. Cell Biochem.* **232**, 1-11 (2002).

226. Katz, D. A., Theodorakis, N., Cleveland, D. W., Lindsten, T. & Thompson, C. B. AU-A, an RNA-binding activity distinct from hnRNP A1, is selective for AUUUA repeats and shuttles between the nucleus and the cytoplasm. *Nucleic. Acids. Res.* **22**, 238-246 (1994).

227. Hamilton, B. J., Burns, C. M., Nichols, R. C. & Rigby, W. F. Modulation of AUUUA response element binding by heterogeneous nuclear ribonucleoprotein A1 in human T lymphocytes. The roles of cytoplasmic location, transcription, and phosphorylation. *J. Biol. Chem.* **272**, 28732-28741 (1997).

228. Lai, W. S., Carballo, E., Thorn, J. M., Kennington, E. A. & Blackshear, P. J. Interactions of CCCH zinc finger proteins with mRNA. Binding of tristetraprolin-related zinc finger proteins to Au-rich elements and destabilization of mRNA. *J. Biol. Chem.* **275**, 17827-17837 (2000).

229. Brooks, S. A. & Rigby, W. F. Characterization of the mRNA ligands bound by the RNA binding protein hnRNP A2 utilizing a novel in vivo technique. *Nucleic Acids Res* **28**, E49 (2000).

230. Rousseau, S. *et al.* Inhibition of SAPK2a/p38 prevents hnRNP A0 phosphorylation by MAPKAP-K2 and its interaction with cytokine mRNAs. *EMBO J.* **21**, 6505-6514 (2002).

231. Pioli, P. A., Hamilton, B. J., Connolly, J. E., Brewer, G. & Rigby, W. F. Lactate dehydrogenase is an AU-rich element-binding protein that directly interacts with AUF1. *J. Biol. Chem.* **277**, 35738-35745 (2002).

232. Dean, J. L. *et al.* Identification of a novel AU-rich-element-binding protein which is related to AUF1. *Biochem. J.* **366**, 709-719 (2002).

233. Mukhopadhyay, D., Houchen, C. W., Kennedy, S., Dieckgraefe, B. K. & Anant, S. Coupled mRNA stabilization and translational silencing of cyclooxygenase-2 by a novel RNA binding protein, CUGBP2. *Mol. Cell* **11**, 113-126 (2003).

234. Lu, J. Y. & Schneider, R. J. Tissue distribution of AU-rich mRNA binding proteins involved in regulation of mRNA decay. *J. Biol. Chem.* (2004).

235. Donnini, M. *et al.* Identification of Tino: A new evolutionarily conserved bcl-2 AU-rich element RNA binding protein. *J. Biol. Chem.* (2004).

236. Giles, K. M. *et al.* The 3'-untranslated region of p21WAF1 mRNA is a composite cis-acting sequence bound by RNA-binding proteins from breast cancer cells, including HuR and poly(C)-binding protein. *J. Biol. Chem.* **278**, 2937-2946 (2003).

237. Nichols, R. C. *et al.* The RGG domain in hnRNP A2 affects subcellular localization. *Exp Cell Res* **256**, 522-532 (2000).

238. Bevilacqua, A., Ceriani, M. C., Capaccioli, S. & Nicolin, A. Post-transcriptional regulation of gene expression by degradation of messenger RNAs. *J. Cell Physiol* **195**, 356-372 (2003).

239. Dixon, D. A. *et al.* Altered expression of the mRNA stability factor HuR promotes cyclooxygenase-2 expression in colon cancer cells. *Journal of Clinical Investigation* **108**, 1657-1665 (2001).

240. Boutaud, O., Dixon, D. A., Oates, J. A. & Sawaoka, H. Tristetraprolin binds to the COX-2 mRNA 3' untranslated region in cancer cells. *Adv. Exp. Med. Biol.* **525**, 157-160 (2003).

241. Dixon, D. A. *et al.* Regulation of cyclooxygenase-2 expression by the translational silencer TIA-1. *J. Exp. Med.* **198**, 475-481 (2003).

242. van Hoof, A. & Parker, R. The exosome: a proteasome for RNA? *Cell* **99**, 347-350 (1999).

243. Chen, C. Y. *et al.* AU binding proteins recruit the exosome to degrade ARE-containing mRNAs. *Cell* **107**, 451-464 (2001).

244. Tran, H., Schilling, M., Wirbelauer, C., Hess, D. & Nagamine, Y. Facilitation of mRNA deadenylation and decay by the exosome-bound, DExH protein RHAU. *Mol. Cell* **13**, 101-111 (2004).

245. Laroia, G., Sarkar, B. & Schneider, R. J. Ubiquitin-dependent mechanism regulates rapid turnover of AU-rich cytokine mRNAs. *PNAS* **99**, 1842-1846 (2002).

246. Moraes, K. C., Quaresma, A. J., Maehnss, K. & Kobarg, J. Identification and characterization of proteins that selectively interact with isoforms of the mRNA binding protein AUF1 (hnRNP D). *Biol. Chem.* **384**, 25-37 (2003).

247. Mukherjee, D. *et al.* The mammalian exosome mediates the efficient degradation of mRNAs that contain AU-rich elements. *EMBO J.* **21**, 165-174 (2002).

248. Wilson, G. M., Sutphen, K., Moutafis, M., Sinha, S. & Brewer, G. Structural remodeling of an A + U-rich RNA element by cation or AUF1 binding. *J. Biol. Chem.* **276**, 38400-38409 (2001).

249. Wilson, G. M., Sun, Y., Lu, H. & Brewer, G. Assembly of AUF1 oligomers on U-rich RNA targets by sequential dimer association. *J. Biol. Chem.* **274**, 33374-33381 (1999).

250. Sully, G. *et al.* Structural and functional dissection of a conserved destabilizing element of cyclo-oxygenase-2 mRNA: evidence against the involvement of AUF-1 [AU-rich

element/poly(U)-binding/degradation factor-1], AUF-2, tristetraprolin, HuR (Hu antigen R) or FBP1 (far-upstream-sequence-element-binding protein 1). *Biochem. J.* **377**, 629-639 (2004).

251. Phillips, K., Kedersha, N., Shen, L., Blackshear, P. J. & Anderson, P. Arthritis suppressor genes TIA-1 and TTP dampen the expression of tumor necrosis factor alpha, cyclooxygenase 2, and inflammatory arthritis. *Proc. Natl. Acad. Sci. U. S. A* **101**, 2011-2016 (2004).

252. Carballo, E. & Blackshear, P. J. Roles of tumor necrosis factor-alpha receptor subtypes in the pathogenesis of the tristetraprolin-deficiency syndrome. *Blood* **98**, 2389-2395 (2001).

253. Taylor, G. A. *et al.* A pathogenetic role for TNF alpha in the syndrome of cachexia, arthritis, and autoimmunity resulting from tristetraprolin (TTP) deficiency. *Immunity.* **4**, 445-454 (1996).

254. Kaytor, M. D. & Orr, H. T. RNA targets of the fragile X protein. *Cell* **107**, 555-557 (2001).

255. Darnell, J. C. *et al.* Fragile X mental retardation protein targets G quartet mRNAs important for neuronal function. *Cell* **107**, 489-499 (2001).

256. Levadoux-Martin, M. *et al.* Impaired gametogenesis in mice that overexpress the RNA-binding protein HuR. *EMBO Rep.* **4**, 394-399 (2003).

257. Gouble, A. & Morello, D. Synchronous and regulated expression of two AU-binding proteins, AUF1 and HuR, throughout murine development. *Oncogene* **19**, 5377-5384 (2000).

258. van der, G. K., Di Marco, S., Clair, E. & Gallouzi, I. E. RNAi-mediated HuR depletion leads to the inhibition of muscle cell differentiation. *J. Biol. Chem.* **278**, 47119-47128 (2003).

259. Brewer, G. Misregulated Posttranscriptional Checkpoints: Inflammation and Tumorigenesis. *The Journal of Experimental Medicine* **193**, 1F-4 (2001).

260. Gouble, A. *et al.* A New Player in Oncogenesis: AUF1/hnRNPD Overexpression Leads to Tumorigenesis in Transgenic Mice. *Cancer Research* **62**, 1489-1495 (2002).

261. Denkert, C. *et al.* Overexpression of the embryonic-lethal abnormal vision-like protein HuR in ovarian carcinoma is a prognostic factor and is associated with increased cyclooxygenase 2 expression. *Cancer Res.* **64**, 189-195 (2004).

262. Erkinheimo, T. L. *et al.* Cytoplasmic HuR expression correlates with poor outcome and with cyclooxygenase 2 expression in serous ovarian carcinoma. *Cancer Res.* **63**, 7591-7594 (2003).

263. Lopez, d. S., I *et al.* Role of the RNA-binding protein HuR in colon carcinogenesis. *Oncogene* **22**, 7146-7154 (2003).

264. Dixon, D. A. Dysregulated post-transcriptional control of COX-2 gene expression in cancer. *Curr. Pharm. Des* **10**, 635-646 (2004).

265. Perrotti, D. & Calabretta, B. Post-transcriptional mechanisms in BCR/ABL leukemogenesis: role of shuttling RNA-binding proteins. *Oncogene* **21**, 8577-8583 (2002).

266. Galban, S. *et al.* Influence of the RNA-binding protein HuR in pVHL-regulated p53 expression in renal carcinoma cells. *Mol. Cell Biol.* **23**, 7083-7095 (2003).

267. Nabors, L. B. *et al.* Tumor necrosis factor alpha induces angiogenic factor up-regulation in malignant glioma cells: a role for RNA stabilization and HuR. *Cancer Res.* **63**, 4181-4187 (2003).

268. Zhang, W. *et al.* Purification, characterization, and cDNA cloning of an AU-rich element RNA-binding protein, AUF1. *Molec. Cell. Biol.* **13**, 7652-7665 (1993).

269. Wagner, B. J., DeMaria, C. T., Sun, Y., Wilson, G. M. & Brewer, G. Structure and genomic organization of the human AUF1 gene: alternative pre-mRNA splicing generates four protein

isoforms. *Genomics* **48**, 195-202 (1998).

270. Inoue, A. *et al.* Identification of S1 proteins B2, C1 and D1 as AUF1 isoforms and their major role as heterogeneous nuclear ribonucleoprotein proteins. *Biochem. J.* **372**, 775-785 (2003).

271. Wilson, G. M. *et al.* Regulation of AUF1 expression via conserved alternatively spliced elements in the 3' untranslated region. *Mol. Cell Biol.* **19**, 4056-4064 (1999).

272. Sarkar, B., Lu, J. Y. & Schneider, R. J. Nuclear import and export functions in the different isoforms of the AUF1/heterogeneous nuclear ribonucleoprotein protein family. *J. Biol. Chem.* **278**, 20700-20707 (2003).

273. Kiledjian, M., DeMaria, C. T., Brewer, G. & Novick, K. Identification of AUF1 (heterogeneous nuclear ribonucleoprotein D) as a component of the alpha-globin mRNA stability complex. *Mol. Cell Biol.* **17**, 4870-4876 (1997).

274. Raineri, I., Wegmueller, D., Gross, B., Certa, U. & Moroni, C. Roles of AUF1 isoforms, HuR and BRF1 in ARE-dependent mRNA turnover studied by RNA interference. *Nucleic Acids Res.* **32**, 1279-1288 (2004).

275. DeMaria, C. T., Sun, Y., Long, L., Wagner, B. J. & Brewer, G. Structural determinants in AUF1 required for high affinity binding to A + U-rich elements. *J. Biol. Chem.* **272**, 27635-27643 (1997).

276. DeMaria, C. T. & Brewer, G. AUF1 binding affinity to A+U-rich elements correlates with rapid mRNA degradation. *J. Biol. Chem.* **271**, 12179-12184 (1996).

277. Lapucci, A. *et al.* AUF1 Is a bcl-2 A + U-rich element-binding protein involved in bcl-2 mRNA destabilization during apoptosis. *J. Biol. Chem.* **277**, 16139-16146 (2002).

278. Sarkar, B., Xi, Q., He, C. & Schneider, R. J. Selective degradation of AU-rich mRNAs promoted by the p37 AUF1 protein isoform. *Mol. Cell Biol.* **23**, 6685-6693 (2003).

279. Buzby, J. S., Brewer, G. & Nugent, D. J. Developmental regulation of RNA transcript destabilization by A + U-rich elements is AUF1-dependent. *J. Biol. Chem.* **274**, 33973-33978 (1999).

280. Lafon, I., Carballes, F., Brewer, G., Poiret, M. & Morello, D. Developmental expression of AUF1 and HuR, two c-myc mRNA binding proteins. *Oncogene* **16**, 3413-3421 (1998).

281. Brewer, G., Saccani, S., Sarkar, S., Lewis, A. & Pestka, S. Increased interleukin-10 mRNA stability in melanoma cells is associated with decreased levels of A + U-rich element binding factor AUF1. *J. Interferon Cytokine Res.* **23**, 553-564 (2003).

282. Fan, X. C. & Steitz, J. A. HNS, a nuclear-cytoplasmic shuttling sequence in HuR. *Proc. Natl. Acad. Sci. U. S. A* **95**, 15293-15298 (1998).

283. Atasoy, U., Watson, J., Patel, D. & Keene, J. D. ELAV protein HuA (HuR) can redistribute between nucleus and cytoplasm and is upregulated during serum stimulation and T cell activation. *J Cell Sci* **111**, 3145-3156 (1998).

284. Guttinger, S., Muhlhausser, P., Koller-Eichhorn, R., Brennecke, J. & Kutay, U. From The Cover: Transportin2 functions as importin and mediates nuclear import of HuR. *Proc. Natl. Acad. Sci. U. S. A* **101**, 2918-2923 (2004).

285. Yao, K. M., Samson, M. L., Reeves, R. & White, K. Gene elav of Drosophila melanogaster: a prototype for neuronal-specific RNA binding protein gene family that is conserved in flies and humans. *J. Neurobiol.* **24**, 723-739 (1993).

286. Park-Lee, S., Kim, S. & Laird-Offringa, I. A. Characterization of the interaction between neuronal RNA-binding protein HuD and AU-rich RNA. *J. Biol. Chem.* **278**, 39801-39808 (2003).

287. De Silanes, I. L., Zhan, M., Lal, A., Yang, X. & Gorospe, M. Identification of a target RNA motif for RNA-binding protein HuR. *Proc. Natl. Acad. Sci. U. S. A* **101**, 2987-2992 (2004).

288. Myer, V. E., Fan, X. C. & Steitz, J. A. Identification of HuR as a protein implicated in AUUUA-mediated mRNA decay. *EMBO J.* **16**, 2130-2139 (1997).

289. Peng, S. S., Chen, C. Y., Xu, N. & Shyu, A. B. - RNA stabilization by the AU-rich element binding protein, HuR, an ELAV protein. - *EMBO J 1998 Jun 15;17(12):3461-70* 3461-3700.

290. Fan, X. C. & Steitz, J. A. Overexpression of HuR, a nuclear-cytoplasmic shuttling protein, increases the in vivo stability of ARE-containing mRNAs. *EMBO J.* **17**, 3448-3460 (1998).

291. Wang, W., Yang, X., Cristofalo, V. J., Holbrook, N. J. & Gorospe, M. Loss of HuR is linked to reduced expression of proliferative genes during replicative senescence. *Mol. Cell Biol.* **21**, 5889-5898 (2001).

292. Wein, G., Rossler, M., Klug, R. & Herget, T. The 3'-UTR of the mRNA coding for the major protein kinase C substrate MARCKS contains a novel CU-rich element interacting with the mRNA stabilizing factors HuD and HuR. *Eur. J. Biochem.* **270**, 350-365 (2003).

293. Wang, W. *et al.* AMP-Activated Kinase Regulates Cytoplasmic HuR. *Molecular and Cellular Biology* **22**, 3425-3436 (2002).

294. Tran, H., Maurer, F. & Nagamine, Y. Stabilization of urokinase and urokinase receptor mRNAs by HuR is linked to its cytoplasmic accumulation induced by activated mitogen-activated protein kinase-activated protein kinase 2. *Mol. Cell Biol.* **23**, 7177-7188 (2003).

295. Mazan-Mamczarz, K. *et al.* RNA-binding protein HuR enhances p53 translation in response to ultraviolet light irradiation. *Proc. Natl. Acad. Sci. U. S. A* **100**, 8354-8359 (2003).

296. Gorospe, M. HuR in the mammalian genotoxic response: post-transcriptional multitasking. *Cell Cycle* **2**, 412-414 (2003).

297. Gallouzi, I. E., Brennan, C. M. & Steitz, J. A. Protein ligands mediate the CRM1-dependent export of HuR in response to heat shock. *RNA.* **7**, 1348-1361 (2001).

298. Brennan, C. M. & Steitz, J. A. HuR and mRNA stability. *Cell Mol. Life Sci.* **58**, 266-277 (2001).

299. Brennan, C. M., Gallouzi, I. E. & Steitz, J. A. Protein ligands to HuR modulate its interaction with target mRNAs in vivo. *J. Cell Biol.* **151**, 1-14 (2000).

300. Gallouzi, I. E. *et al.* HuR binding to cytoplasmic mRNA is perturbed by heat shock. *Proc. Natl. Acad. Sci. U. S. A* **97**, 3073-3078 (2000).

301. Sengupta, S. *et al.* The RNA-binding protein HuR regulates the expression of cyclooxygenase-2. *J. Biol. Chem.* **278**, 25227-25233 (2003).

302. Dember, L. M., Kim, N. D., Liu, K. Q. & Anderson, P. Individual RNA Recognition Motifs of TIA-1 and TIAR Have Different RNA Binding Specificities. *Journal of Biological Chemistry* **271**, 2783-2788 (1996).

303. Beck, A. R., Medley, Q. G., O'Brien, S., Anderson, P. & Streuli, M. - Structure, tissue distribution and genomic organization of the murine RRM-type RNA binding proteins TIA-1 and TIAR. - *Nucleic Acids Res 1996 Oct 1;24(19):3829-35.* 3829-3835.

304. Yu, Q., Cok, S. J., Zeng, C. & Morrison, A. R. Translational repression of human matrix metalloproteinases-13 by an alternatively spliced form of T-cell-restricted intracellular antigen-

related protein (TIAR). *J. Biol. Chem.* **278**, 1579-1584 (2003).

305. Le Guiner, C., Gesnel, M. C. & Breathnach, R. TIA-1 or TIAR is required for DT40 cell viability. *J. Biol. Chem.* **278**, 10465-10476 (2003).

306. Tian, Q., Taupin, J., Elledge, S., Robertson, M. & Anderson, P. Fas-activated serine/threonine kinase (FAST) phosphorylates TIA-1 during Fas-mediated apoptosis. *J Exp Med* **182**, 865-874 (1995).

307. Anderson, P. & Kedersha, N. Visibly stressed: the role of eIF2, TIA-1, and stress granules in protein translation. *Cell Stress. Chaperones.* **7**, 213-221 (2002).

308. Anderson, P. & Kedersha, N. Stressful initiations. *J. Cell Sci.* **115**, 3227-3234 (2002).

309. Kedersha, N. & Anderson, P. Stress granules: sites of mRNA triage that regulate mRNA stability and translatability. *Biochem. Soc. Trans.* **30**, 963-969 (2001).

310. Kedersha, N. *et al.* Dynamic shuttling of TIA-1 accompanies the recruitment of mRNA to mammalian stress granules. *J. Cell Biol.* **151**, 1257-1268 (2000).

311. Kedersha, N. L., Gupta, M., Li, W., Miller, I. & Anderson, P. RNA-binding proteins TIA-1 and TIAR link the phosphorylation of eIF-2 alpha to the assembly of mammalian stress granules. *J. Cell Biol.* **147**, 1431-1442 (1999).

312. Saito, K., Chen, S., Piecyk, M. & Anderson, P. TIA-1 regulates the production of tumor necrosis factor alpha in macrophages, but not in lymphocytes. *Arthritis Rheum.* **44**, 2879-2887 (2001).

313. Gatto-Konczak, F. *et al.* The RNA-Binding Protein TIA-1 Is a Novel Mammalian Splicing Regulator Acting through Intron Sequences Adjacent to a 5' Splice Site. *Molecular and Cellular Biology* **20**, 6287-6299 (2000).

314. Zhu, H., Hasman, R. A., Young, K. M., Kedersha, N. L. & Lou, H. U1 snRNP-dependent function of TIAR in the regulation of alternative RNA processing of the human calcitonin/CGRP pre-mRNA. *Mol. Cell Biol.* **23**, 5959-5971 (2003).

315. Forch, P. *et al.* The apoptosis-promoting factor TIA-1 is a regulator of alternative pre-mRNA splicing. *Mol. Cell* **6**, 1089-1098 (2000).

316. Le Guiner, C. *et al.* TIA-1 and TIAR activate splicing of alternative exons with weak 5' splice sites followed by a U-rich stretch on their own pre-mRNAs. *J. Biol. Chem.* **276**, 40638-40646 (2001).

317. Iseni, F. *et al.* Sendai virus trailer RNA binds TIAR, a cellular protein involved in virus-induced apoptosis. *EMBO J.* **21**, 5141-5150 (2002).

318. Forch, P. & Valcarcel, J. Molecular mechanisms of gene expression regulation by the apoptosis-promoting protein TIA-1. *Apoptosis.* **6**, 463-468 (2001).

319. Taylor, G. A. *et al.* The human TTP protein: sequence, alignment with related proteins, and chromosomal localization of the mouse and human genes. *Nucleic Acids Res.* **19**, 3454 (1991).

320. Fairhurst, A. M. *et al.* Regulation and localization of endogenous human tristetraprolin. *Arthritis Res. Ther.* **5**, R214-R225 (2003).

321. Carballo, E., Lai, W. S. & Blackshear, P. J. Evidence that tristetraprolin is a physiological regulator of granulocyte-macrophage colony-stimulating factor messenger RNA deadenylation and stability. *Blood* **95**, 1891-1899 (2000).

322. Phillips, R. S., Ramos, S. B. & Blackshear, P. J. Members of the tristetraprolin family of tandem CCCH zinc finger proteins exhibit CRM1-dependent nucleocytoplasmic shuttling. *J. Biol. Chem.* **277**, 11606-11613 (2002).

323. Cao, H., Tuttle, J. S. & Blackshear, P. J. Immunological characterization of tristetraprolin as a low abundance, inducible, stable cytosolic protein. *J. Biol. Chem.* (2004).

324. Raghavan, A. *et al.* HuA and tristetraprolin are induced following T cell activation and display distinct but overlapping RNA binding specificities. *J. Biol. Chem.* **276**, 47958-47965 (2001).

325. Carballo, E., Lai, W. S. & Blackshear, P. J. Feedback inhibition of macrophage tumor necrosis factor-alpha production by tristetraprolin. *<EM>Science</EM>* **281**, 1001-1005 (1998).

326. Mahtani, K. R. *et al.* Mitogen-Activated Protein Kinase p38 Controls the Expression and Posttranslational Modification of Tristetraprolin, a Regulator of Tumor Necrosis Factor Alpha mRNA Stability. *Molecular and Cellular Biology* **21**, 6461-6469 (2001).

327. Zhu, W. *et al.* Gene suppression by tristetraprolin and release by the p38 pathway. *Am J Physiol Lung Cell Mol Physiol* **281**, L499-L508 (2001).

328. Carballo, E. *et al.* Decreased sensitivity of tristetraprolin-deficient cells to p38 inhibitors suggests the involvement of tristetraprolin in the p38 signaling pathway. *J. Biol. Chem.* **276**, 42580-42587 (2001).

329. Stoecklin, G. *et al.* MK2-induced tristetraprolin:14-3-3 complexes prevent stress granule association and ARE-mRNA decay. *EMBO J.* (2004).

330. Chrestensen, C. A. *et al.* MAPKAP Kinase 2 Phosphorylates Tristetraprolin on in Vivo Sites Including Ser178, a Site Required for 14-3-3 Binding. *J. Biol. Chem.* **279**, 10176-10184 (2004).

331. Taylor, G. A., Thompson, M. J., Lai, W. S. & Blackshear, P. J. Phosphorylation of tristetraprolin, a potential zinc finger transcription factor, by mitogen stimulation in intact cells and by mitogen-activated protein kinase in vitro. *J. Biol. Chem.* **270**, 13341-13347 (1995).

332. Sawaoka, H., Dixon, D. A., Oates, J. A. & Boutaud, O. Tristetraprolin binds to the 3'-untranslated region of cyclooxygenase-2 mRNA. A polyadenylation variant in a cancer cell line lacks the binding site. *J. Biol. Chem.* **278**, 13928-13935 (2003).

333. Frevel, M. A. *et al.* p38 Mitogen-activated protein kinase-dependent and -independent signaling of mRNA stability of AU-rich element-containing transcripts. *Mol. Cell Biol.* **23**, 425-436 (2003).

334. Clark, A. R., Dean, J. L. & Saklatvala, J. Post-transcriptional regulation of gene expression by mitogen-activated protein kinase p38. *FEBS Lett.* **546**, 37-44 (2003).

335. Kotlyarov, A. *et al.* Distinct cellular functions of MK2. *Mol. Cell Biol.* **22**, 4827-4835 (2002).

336. Wilson, G. M. *et al.* Regulation of A + U-rich Element-directed mRNA Turnover Involving Reversible Phosphorylation of AUF1. *J. Biol. Chem.* **278**, 33029-33038 (2003).

337. Wilson, G. M. *et al.* Phosphorylation of p40AUF1 Regulates Binding to A + U-rich mRNA-destabilizing Elements and Protein-induced Changes in Ribonucleoprotein Structure. *J. Biol. Chem.* **278**, 33039-33048 (2003).

338. Lasko, P. Gene regulation at the RNA layer: RNA binding proteins in intercellular signaling networks. *Sci. STKE.* **2003**, RE6 (2003).

339. Soret, J. & Tazi, J. Phosphorylation-dependent control of the pre-mRNA splicing machinery. *Prog. Mol. Subcell. Biol.* **31**, 89-126 (2003).

340. Dodson, R. E. & Shapiro, D. J. Regulation of pathways of mRNA destabilization and

stabilization. *Prog. Nucleic Acid Res. Mol. Biol.* **72**, 129-164 (2002).

341. Guhaniyogi, J. & Brewer, G. Regulation of mRNA stability in mammalian cells. *Gene* **265**, 11-23 (2001).

342. Reynolds, P. R. In sickness and in health: the importance of translational regulation. *Arch Dis Child* **86**, 322-324 (2002).

343. Matter, N. *et al.* Heterogeneous ribonucleoprotein A1 is part of an exon-specific splice-silencing complex controlled by oncogenic signaling pathways. *J. Biol. Chem.* **275**, 35353-35360 (2000).

344. Akker, S. A., Smith, P. J. & Chew, S. L. Nuclear post-transcriptional control of gene expression. *J. Mol. Endocrinol.* **27**, 123-131 (2001).

345. Wilson, K. F. & Cerione, R. A. Signal transduction and post-transcriptional gene expression. *Biol. Chem.* **381**, 357-365 (2000).

346. Saklatvala, J., Dean, J. & Clark, A. Control of the expression of inflammatory response genes. *Biochem. Soc. Symp.* 95-106 (2003).

347. Burton, T. R., Kashour, T., Wright, J. A. & Amara, F. M. Cellular signaling pathways affect the function of ribonucleotide reductase mRNA binding proteins: mRNA stabilization, drug resistance, and malignancy (Review). *Int. J. Oncol.* **22**, 21-31 (2003).

348. Pende, A. *et al.* Characterization of the binding of the RNA-binding protein AUF1 to the human AT(1) receptor mRNA. *Biochem. Biophys. Res. Commun.* **266**, 609-614 (1999).

349. Sela-Brown, A., Silver, J., Brewer, G. & Naveh-Many, T. Identification of AUF1 as a parathyroid hormone mRNA 3'-untranslated region-binding protein that determines parathyroid hormone mRNA stability. *J. Biol. Chem.* **275**, 7424-7429 (2000).

350. Pende, A. *et al.* Regulation of the mRNA-binding protein AUF1 by activation of the beta-adrenergic receptor signal transduction pathway. *J. Biol. Chem.* **271**, 8493-8501 (1996).

351. Adams, D. J. *et al.* HADHB, HuR, and CP1 bind to the distal 3'-untranslated region of human renin mRNA and differentially modulate renin expression. *J. Biol. Chem.* **278**, 44894-44903 (2003).

352. Akool, e. *et al.* Nitric oxide increases the decay of matrix metalloproteinase 9 mRNA by inhibiting the expression of mRNA-stabilizing factor HuR. *Mol. Cell Biol.* **23**, 4901-4916 (2003).

353. Culbertson, M. R. RNA surveillance. Unforeseen consequences for gene expression, inherited genetic disorders and cancer. *Trends Genet.* **15**, 74-80 (1999).

354. Ryu, S. *et al.* 3'UTR polymorphisms in the NRAMP1 gene are associated with susceptibility to tuberculosis in Koreans. *Int. J. Tuberc. Lung Dis.* **4**, 577-580 (2000).

355. Timchenko, L. T. *et al.* Identification of a (CUG)n triplet repeat RNA-binding protein and its expression in myotonic dystrophy. *Nucleic. Acids. Research. 1996. Nov. 15.* **24**, 4407-4414 (1997).

356. McMullen, M. R., Cocuzzi, E., Hatzoglou, M. & Nagy, L. E. Chronic ethanol exposure increases the binding of HuR to the TNFalpha 3'-untranslated region in macrophages. *J. Biol. Chem.* **278**, 38333-38341 (2003).

357. Perrone-Bizzozero, N. & Bolognani, F. Role of HuD and other RNA-binding proteins in neural development and plasticity. *J. Neurosci. Res.* **68**, 121-126 (2002).

358. Brook, J. D. *et al.* Molecular basis of myotonic dystrophy: Expansion of a trinucleotide (CTG) repeat at the 3' end of a transcript encoding a protein kinase family member. *Cell* **66**, 799-808 (1992).

359. Subbaramaiah, K., Marmo, T. P., Dixon, D. A. & Dannenberg, A. J. Regulation of cyclooxgenase-2 mRNA stability by taxanes: evidence for involvement of p38, MAPKAPK-2, and HuR. *J. Biol. Chem.* **278**, 37637-37647 (2003).

360. Zaman, G. J., Michiels, P. J. & van Boeckel, C. A. Targeting RNA: new opportunities to address drugless targets. *Drug Discov. Today* **8**, 297-306 (2003).

361. Garavito, R. M., Malkowski, M. G. & Dewitt, D. L. The structures of prostaglandin endoperoxide H synthases-1 and -2. *Prostaglandins Other Lipid Mediat.* **68-69**, 129-152 (2002).

362. Smith, W. L., DeWitt, D. L. & Garavito, R. M. CYCLOOXYGENASES: Structural, Cellular, and Molecular Biology. *Annu. Rev. Biochem.* **69**, 145-182 (2000).

363. Tanabe, T. & Tohnai, N. Cyclooxygenase isozymes and their gene structures and expression. *Prostaglandins Other Lipid Mediat.* **68-69**, 95-114 (2002).

364. Hla, T., Bishop-Bailey, D., Liu, C. H., Schaefers, H. J. & Trifan, O. C. Cyclooxygenase-1 and -2 isoenzymes. *Int. J. Biochem. Cell Biol.* **31**, 551-557 (1999).

365. Spencer, A. *et al.* - The Membrane Binding Domains of Prostaglandin Endoperoxide H Synthases 1 and 2. PEPTIDE MAPPING AND MUTATIONAL ANALYSIS. - *J* **Biol. Chem. 1999 Nov 12;274**, 32936-32942.

366. Parfenova, H. *et al.* Dynamics of nuclear localization sites for COX-2 in vascular endothelial cells. *Am. J. Physiol.* **281**, C166-C178 (2001).

367. Lim, H. & Dey, S. K. A novel pathway of prostacyclin signaling-hanging out with nuclear receptors. *Endocrinology* **143**, 3207-3210 (2002).

368. Dussault, I. & Forman, B. M. Prostaglandins and fatty acids regulate transcriptional signaling via the peroxisome proliferator activated receptor nuclear receptors. *Prostaglandins & Other Lipid Mediators* **62**, 1-13 (2000).

369. Funk, C. D., Funk, L. B., Kennedy, M. E., Pong, A. S. & Fitzgerald, G. A. Human platelet/erythroleukemia cell prostaglandin G/H synthase: cDNA cloning, expression, and gene chromosomal assignment. *FASEB Journal* **5**, 2304-2312 (1991).

370. Taniura, S., Kamitani, H., Watanabe, T. & Eling, T. E. Transcriptional Regulation of Cyclooxygenase-1 by Histone Deacetylase Inhibitors in Normal Human Astrocyte Cells. *Journal of Biological Chemistry* **277**, 16823-16830 (2002).

371. Olson, D. M. The role of prostaglandins in the initiation of parturition. *Best. Pract. Res. Clin. Obstet. Gynaecol.* **17**, 717-730 (2003).

372. Reese, J. *et al.* - Coordinated regulation of fetal and maternal prostaglandins directs successful birth and postnatal adaptation in the mouse. - *Proc Natl Acad Sci U S A 2000 Aug 15;97(17):9759-9764* 9759-97644.

373. Cohn, S. M., Schloemann, S., Tessner, T., Seibert, K. & Stenson, W. F. Crypt stem cell survival in the mouse intestinal epithelium is regulated by prostaglandins synthesized through cyclooxygenase-1. *Journal of Clinical Investigation* **99**, 1367-1379 (1997).

374. Morita, I. Distinct functions of COX-1 and COX-2. *Prostaglandins Other Lipid Mediat.* **68-69**, 165-175 (2002).

375. Chandrasekharan, N. V. *et al.* COX-3, a cyclooxygenase-1 variant inhibited by acetaminophen

and other analgesic/antipyretic drugs: cloning, structure, and expression. *Proc. Natl. Acad. Sci. U. S. A* **99**, 13926-13931 (2002).

376. Schwab, J. M., Schluesener, H. J., Meyermann, R. & Serhan, C. N. COX-3 the enzyme and the concept: steps towards highly specialized pathways and precision therapeutics? *Prostaglandins Leukot. Essent. Fatty Acids* **69**, 339-343 (2003).

377. Herschman, H. R. Prostaglandin synthase 2. *Biochim Biophys Acta* **1299**, 125-140 (1996).

378. Maier, J. A., Hla, T. & Maciag, T. Cyclooxygenase is an immediate-early gene induced by interleukin- 1 in human endothelial cells. *Journal of Biological Chemistry* **265**, 10805-10808 (1990).

379. Newton, R., Seybold, J., Liu, S. F. & Barnes, P. J. Alternate COX-2 Transcripts Are Differentially Regulated: Implications for Post-Transcriptional Control. *Biochemical and Biophysical Research Communications* **234**, 85-89 (1997).

380. Ristimaki, A., Narko, K. & Hla, T. Down-regulation of cytokine-induced cyclo-oxygenase-2 transcript isoforms by dexamethasone: evidence for post-transcriptional regulation. *Biochem J* **318**, 325-331 (1996).

381. Stack, E. & DuBois, R. N. Regulation of cyclo-oxygenase-2. *Best. Pract. Res. Clin. Gastroenterol.* **15**, 787-800 (2001).

382. Lasa, M., Brook, M., Saklatvala, J. & Clark, A. R. Dexamethasone Destabilizes Cyclooxygenase 2 mRNA by Inhibiting Mitogen-Activated Protein Kinase p38. *Molecular and Cellular Biology* **21**, 771-780 (2001).

383. Evett, G. E., Xie, W., Chipman, J. G., Robertson, D. L. & Simmons, D. L. Prostaglandin G/H synthase isoenzyme 2 expression in fibroblasts: regulation by dexamethasone, mitogens, and oncogenes. *Archives of Biochemistry & Biophysics* **306**, 169-177 (1993).

384. Prescott, S. M. & Fitzpatrick, F. A. Cyclooxygenase-2 and carcinogenesis. *Biochim Biophys Acta* **1470**, M69-M78 (2000).

385. Williams, C. S., Mann, M. & DuBois, R. N. The role of cyclooxygenases in inflammation, cancer, and development. *Oncogene* **18**, 7908-7916 (1999).

386. Cheng, H. F., Wang, J. L., Zhang, M. Z., McKanna, J. & Harris, R. C. Nitric oxide regulates renal cortical cyclooxygenase-2 expression. *AJP - Renal Physiology* **279**, F122-F129 (2000).

387. Zhang, M. Z., Harris, R. C. & McKanna, J. A. Regulation of cyclooxygenase-2 (COX-2) in rat renal cortex by adrenal glucocorticoids and mineralocorticoids. *PNAS* **96**, 15280-15285 (1999).

388. Persaud, S. J., Burns, C. J., Belin, V. D. & Jones, P. M. Glucose-induced regulation of COX-2 expression in human islets of Langerhans. *Diabetes* **53 Suppl 1**, S190-S192 (2004).

389. Hedin, L. *et al.* Prostaglandin endoperoxide synthetase in rat ovarian follicles: Content, cellular distribution and evidence for hormonal induction preceding ovulation. *Endocrinology* **121**, 722-731 (1987).

390. Garavito, R. M. & Mulichak, A. M. The structure of mammalian cyclooxygenases. *Annu. Rev. Biophys. Biomol. Struct.* **32**, 183-206 (2003).

391. Ejima, K. *et al.* Cyclooxygenase-2-deficient mice are resistant to endotoxin-induced inflammation and death. *FASEB J.* **17**, 1325-1327 (2003).

392. Liu, C. H. *et al.* Overexpression of Cyclooxygenase-2 Is Sufficient to Induce Tumorigenesis in Transgenic Mice. *Journal of Biological Chemistry* **276**, 18563-18569 (2001).

393. Neufang, G., Furstenberger, G., Heidt, M., Marks, F. & Muller-Decker, K. Abnormal differentiation of epidermis in transgenic mice constitutively expressing cyclooxygenase-2 in skin. *PNAS* **98**, 7629-7634 (2001).

394. Singer, C. A. *et al.* p38 MAPK and NF-kappaB mediate COX-2 expression in human airway myocytes. *Am. J. Physiol Lung Cell Mol. Physiol* **285**, L1087-L1098 (2003).

395. Gorgoni, B., Caivano, M., Arizmendi, C. & Poli, V. The Transcription Factor C/EBPbeta Is Essential for Inducible Expression of the cox-2 Gene in Macrophages but Not in Fibroblasts. *Journal of Biological Chemistry* **276**, 40769-40777 (2001).

396. Reddy, S. T., Wadleigh, D. J. & Herschman, H. R. Transcriptional Regulation of the Cyclooxygenase-2 Gene in Activated Mast Cells. *Journal of Biological Chemistry* **275**, 3107-3113 (2000).

397. Wadleigh, D. J., Reddy, S. T., Kopp, E., Ghosh, S. & Herschman, H. R. Transcriptional Activation of the Cyclooxygenase-2 Gene in Endotoxin-treated RAW 264.7 Macrophages. *Journal of Biological Chemistry* **275**, 6259-6266 (2000).

398. Wadleigh, D. J. & Herschman, H. R. Transcriptional regulation of the cyclooxygenase-2 gene by diverse ligands in murine osteoblasts. *Biochem. Biophys. Res. Commun.* **264**, 865-870 (1999).

399. Xie, W. & Herschman, H. R. Transcriptional regulation of prostaglandin synthase 2 gene expression by platelet-derived growth factor and serum. *Journal of Biological Chemistry* **271**, 31742-31748 (1996).

400. Crofford, L. J., Tan, B., McCarthy, C. J. & Hla, T. Involvement of nuclear factor kappa B in the regulation of cyclooxygenase-2 expression by interleukin-1 in rheumatoid synoviocytes. *Arthritis Rheum* **40**, 226-236 (1997).

401. Okada, Y., Voznesensky, O., Herschman, H., Harrison, J. & Pilbeam, C. Identification of multiple cis-acting elements mediating the induction of prostaglandin G/H synthase-2 by phorbol ester in murine osteoblastic cells. *J Cell Biochem* **78**, 197-209 (2000).

402. Srivastava, S. K., Tetsuka, T., Daphna-Iken, D. & Morrison, A. R. IL-1 beta stabilizes COX II mRNA in renal mesangial cells: role of 3'-untranslated region. *American Journal of Physiology* **267**, F504-F508 (1994).

403. Dixon, D. A., Kaplan, C. D., McIntyre, T. M., Zimmerman, G. A. & Prescott, S. M. Post-transcriptional Control of Cyclooxygenase-2 Gene Expression. THE ROLE OF THE 3'-UNTRANSLATED REGION. *Journal of Biological Chemistry* **275**, 11750-11757 (2000).

404. Ristimaki, A., Garfinkel, S., Wessendorf, J., Maciag, T. & Hla, T. Induction of cyclooxygenase-2 by interleukin-1 alpha. Evidence for post-transcriptional regulation. *J Biol Chem* **269**, 11769-755 (1994).

405. Gou, Q., Liu, C. H., Ben Av, P. & Hla, T. Dissociation of basal turnover and cytokine-induced transcript stabilization of the human cyclooxygenase-2 mRNA by mutagenesis of the 3'-untranslated region. *Biochem Biophys Res Commun* **242**, 508-512 (1998).

406. Jang, B. C. *et al.* Serum Withdrawal-induced Post-transcriptional Stabilization of Cyclooxygenase-2 mRNA in MDA-MB-231 Mammary Carcinoma Cells Requires the Activity of the p38 Stress-activated Protein Kinase. *Journal of Biological Chemistry* **275**, 39507-39515 (2000).

407. Dormond, O., Foletti, A., Paroz, C. & Ruegg, C. NSAIDs inhibit alpha V beta 3 integrin-mediated and Cdc42/Rac-dependent endothelial-cell spreading, migration and angiogenesis. *Nat. Med.* **7**, 1041-1047 (2001).

408. Guan, Z., Buckman, S. Y., Springer, L. D. & Morrison, A. R. Regulation of cyclooxygenase-2 by

the activated p38 MAPK signaling pathway. *Adv Exp Med Biol* **469**, 9-15 (1999).

409. Guan, Z., Buckman, S. Y., Miller, B. W., Springer, L. D. & Morrison, A. R. Interleukin-1beta-induced cyclooxygenase-2 expression requires activation of both c-Jun NH2-terminal kinase and p38 MAPK signal pathways in rat renal mesangial cells. *J. Biol. Chem.* **273**, 28670-28676 (1998).

410. Guan, Z., Buckman, S. Y., Pentland, A. P., Templeton, D. J. & Morrison, A. R. Induction of cyclooxygenase-2 by the activated MEKK1 --> SEK1/MKK4 --> p38 mitogen-activated protein kinase pathway. *J Biol Chem* **273**, 12901-12908 (1998).

411. Hwang, D., Jang, B. C., Yu, G. & Boudreau, M. Expression of Mitogen-Inducible Cyclooxygenase Induced by Lipopolysaccharide; Mediation through both mitogen-activated protein kinase and NF-[kappa]B signaling pathways in macrophages. *Biochemical Pharmacology* **54**, 87-96 (1997).

412. Chanmugam, P. *et al.* Radicicol, a Protein Tyrosine Kinase Inhibitor, Suppresses the Expression of Mitogen-inducible Cyclooxygenase in Macrophages Stimulated with Lipopolysaccharide and in Experimental Glomerulonephritis. *Journal of Biological Chemistry* **270**, 5418-5426 (1995).

413. Gilroy, D. W. *et al.* Inducible cyclooxygenase may have anti-inflammatory properties. *Nat. Med.* **5**, 698-701 (1999).

414. Guan, Z., Tetsuka, T., Baier, L. D. & Morrison, A. R. Interleukin-1 beta activates c-jun NH2-terminal kinase subgroup of mitogen-activated protein kinases in mesangial cells. *American Journal of Physiology* **270**, F634-F641 (1996).

415. Hwang, D. Modulation of the expression of cyclooxygenase-2 by fatty acids mediated through toll-like receptor 4-derived signaling pathways. *FASEB J.* **15**, 2556-2564 (2001).

416. Rhee, S. H. & Hwang, D. Murine TOLL-like Receptor 4 Confers Lipopolysaccharide Responsiveness as Determined by Activation of NFkappa B and Expression of the Inducible Cyclooxygenase. *Journal of Biological Chemistry* **275**, 34035-34040 (2000).

417. Paul, A. *et al.* Involvement of Mitogen-Activated Protein Kinase Homologues in the Regulation of Lipopolysaccharide-Mediated Induction of Cyclo-oxygenase-2 but not Nitric Oxide Synthase in RAW 264.7 Macrophages. *Cellular Signalling* **11**, 491-497 (1999).

418. Lee, S. H. *et al.* Selective expression of mitogen-inducible cyclooxygenase in macrophages stimulated by lipopolysaccharide. *Journal of Biological Chemistry* **267**, 25934-25938 (1992).

419. Jones, B. W. *et al.* Different Toll-like receptor agonists induce distinct macrophage responses. *J Leukoc Biol* **69**, 1036-1044 (2001).

420. O'Neill, L. A. The interleukin-1 receptor/Toll-like receptor superfamily: signal transduction during inflammation and host defense. *Sci STKE* **2000**, RE1 (2000).

421. Barrios-Rodiles, M., Tiraloche, G. & Chadee, K. Lipopolysaccharide modulates cyclooxygenase-2 transcriptionally and posttranscriptionally in human macrophages independently from endogenous IL-1 beta and TNF-alpha. *J. Immunol.* **163**, 963-969 (1999).

422. Dean, J. L., Sarsfield, S. J., Tsounakou, E. & Saklatvala, J. p38 mitogen-activated protein kinase stabilises mRNAs that contain cyclooxygenase-2 and tumour necrosis factor AU-rich elements by inhibiting deadenylation. *J. Biol. Chem.* (2003).

423. Eliopoulos, A. G., Dumitru, C. D., Wang, C. C., Cho, J. & Tsichlis, P. N. Induction of COX-2 by LPS in macrophages is regulated by Tpl2-dependent CREB activation signals. *EMBO J.* **21**, 4831-4840 (2002).

424. Levine, T. D., Gao, F., King, P. H., Andrews, L. G. & Keene, J. D. - Hel-N1: an autoimmune RNA-binding protein with specificity for 3' uridylate-rich untranslated regions of growth factor mRNAs. - *Mol Cell Biol 1993 Jun;13(6):3494-504* 3494-5044.

425. Park, S., Myszka, D. G., Yu, M., Littler, S. J. & Laird-Offringa, I. A. HuD RNA recognition motifs play distinct roles in the formation of a stable complex with AU-rich RNA. *Mol. Cell Biol.* **20**, 4765-4772 (2000).

426. Dreyfuss, G., Matunis, M. J., Pinol-Roma, S. & Burd, C. G. hnRNP proteins and the biogenesis of mRNA. *Annu. Rev. Biochem.* **62**, 289-321 (1993).

427. Kiledjian, M. & Dreyfuss, G. Primary structure and binding activity of the hnRNP U protein: binding RNA through RGG box. *EMBO J.* **11**, 2655-2664 (1992).

428. Eggert, M. *et al.* The glucocorticoid receptor is associated with the RNA-binding nuclear matrix protein hnRNP U. *J. Biol. Chem.* **272**, 28471-28478 (1997).

429. Eggert, H., Schulz, M., Fackelmayer, F. O., Renkawitz, R. & Eggert, M. Effects of the heterogeneous nuclear ribonucleoprotein U (hnRNP U/SAF-A) on glucocorticoid-dependent transcription in vivo. *J. Steroid Biochem. Mol. Biol.* **78**, 59-65 (2001).

430. Nishimori, T., Inoue, H. & Hirata, Y. Involvement of the 3'-untranslated region of cyclooxygenase-2 gene in its post-transcriptional regulation through the glucocorticoid receptor. *Life Sci.* **74**, 2505-2513 (2004).

431. Brewer, J. A. *et al.* T-cell glucocorticoid receptor is required to suppress COX-2-mediated lethal immune activation. *Nat. Med.* **9**, 1318-1322 (2003).

432. Newton, R., Seybold, J., Kuitert, L. M. E., Bergmann, M. & Barnes, P. J. Repression of Cyclooxygenase-2 and Prostaglandin E2 Release by Dexamethasone Occurs by Transcriptional and Post-transcriptional Mechanisms Involving Loss of Polyadenylated mRNA. *Journal of Biological Chemistry* **273**, 32312-32321 (1998).

433. Tanaka, Y., Igimi, S. & Amano, F. Inhibition of prostaglandin synthesis by nitric oxide in RAW 264.7 macrophages. *Arch Biochem Biophys* **391**, 207-217 (2001).

434. Guastadisegni, C. *et al.* Prostaglandin E2 synthesis is differentially affected by reactive nitrogen intermediates in cultured rat microglia and RAW 264.7 cells. *FEBS Lett* **413**, 314-318 (1997).

435. Lane, P., Hao, G. & Gross, S. S. S-nitrosylation is emerging as a specific and fundamental posttranslational protein modification: head-to-head comparison with O-phosphorylation. *Sci STKE* **2001**, RE1 (2001).

Reprints

THE JOURNAL OF BIOLOGICAL CHEMISTRY
© 2004 by The American Society for Biochemistry and Molecular Biology, Inc.

Vol. 279, No. 9, Issue of February 27, pp. 8196–8205, 2004
Printed in U.S.A.

Identification of RNA-binding Proteins in RAW 264.7 Cells That Recognize a Lipopolysaccharide-responsive Element in the 3-Untranslated Region of the Murine Cyclooxygenase-2 mRNA*

Received for publication, August 1, 2003, and in revised form, December 5, 2003
Published, JBC Papers in Press, December 8, 2003, DOI 10.1074/jbc.M308475200

Steven J. Cok, Stephen J. Acton‡, Alison E. Sexton, and Aubrey R. Morrison§

From the Departments of Medicine and Molecular Biology and Pharmacology, Washington University School of Medicine, St. Louis, Missouri 63110

RAW 264.7 cells rapidly induce cyclooxygenase-2 (COX-2) in response to lipopolysaccharide treatment. Part of the increased COX-2 expression occurred through post-transcriptional mechanisms mediated through specific regions of the 3′-untranslated region (UTR) of the message. The proximal region of the 3′-UTR of COX-2 contains a highly conserved AU-rich element that was able to confer lipopolysaccharide regulation of a chimeric reporter-gene. Electrophoretic mobility shift assays demonstrated that the RNA-binding proteins TIAR, AUF1, HuR, and TIA-1 all form an RNA-protein complex with the first 60 nucleotides of the 3′-UTR of COX-2. Biotinylated RNA probes were used to isolate additional proteins that bind the 3′-UTR of COX-2. We identified several RNA-binding proteins including TIAR, AUF1, CBF-A, RBM3, heterogeneous nuclear ribonucleoprotein (hnRNP) A3, and hnRNP A2/B1. We identified four alternatively spliced isoforms of AUF1 which migrated at multiple isoelectric points. Likewise, we identified alternatively spliced isoforms of CBF-A, hnRNP A3, and hnRNP A2/B1. Western analysis of two-dimensional gels identified multiple isoforms of TIA-1, TIAR, and AUF1 at pI values that spanned nearly 3 pH units. Thus, through a combination of alternative splicing and post-translational modification cells are able to increase greatly the repertoire of protein species expressed at a given time or in response to extracellular stimuli.

Macrophages play a pivotal role in potentiating the proinflammatory response. Activation of macrophages with bacterial lipopolysaccharides (LPS)[1] leads to production and secretion of various cytokines and prostaglandins. Prostaglandin production requires induction of cyclooxygenase-2 (COX-2), which catalyzes the conversion of arachidonic acid to prostaglandin H_2, the common precursor to all prostaglandins, thromboxanes, and prostacyclins (for review, see Ref. 1). The LPS-dependent induction of COX-2 occurs transcriptionally and post-transcriptionally (2–4). Specifically, LPS has been shown to regulate COX-2 message stability through mitogen-activated protein kinase p38 (5, 6).

The stability of mRNA is determined in many cases by interactions between specific RNA-binding proteins and cis-acting sequences located in the 3′-untranslated region (3′-UTR) of the message (7, 8). One of the best characterized cis-acting sequences is the adenylate/uridylate-rich element (ARE). AREs have been identified in numerous mRNAs (6, 9, 10), including COX-2. AREs can range in size and generally contain one or more copies of the pentameric sequence AUUUA. The COX-2 message contains up to 22 copies of AUUUA in the 3′-UTR, many of which are clustered in the proximal 10% of the 3′-UTR. Murine COX-2 mRNA contains 7 AUUUA repeats within the first 60 nucleotides of the 3′-UTR. We have shown previously that this region plays an important role in regulating message stability and translational efficacy in rat mesangial cells stimulated with interleukin-1β (11).

Several RNA-binding proteins have been identified which recognize ARE-containing sequences. Binding of some proteins can lead to increased message expression, as seen for ELAV family proteins (HuR, HuB/Hel-N1, HuC, and HuD) (12, 13). Binding of other proteins, such as TIA-1, TIAR, and tristetraprolin, promotes decreased message expression (14–18). Still other proteins like AUF1 (also known as hnRNP D) may play a role in both degradation and stabilization of target messages (7, 19). Adding to the complexity of these interactions is the fact that many of these proteins exist as multiple isoforms that arise because of alternative splicing events, all of which may be subject to post-translational modifications.

As a first approach to understanding the mechanism whereby LPS regulates COX-2 expression, we used the proximal region of the 3′-UTR of COX-2 as a target to identify sequences required for LPS stimulation and proteins that bind this region of the 3′-UTR. The proximal 60 nucleotides of the 3-UTR of COX-2 contained a LPS response element that bound a large number of RNA-binding proteins. Many of these proteins were present as alternatively spliced isoforms and appear to be post-translationally modified.

EXPERIMENTAL PROCEDURES

Cell Culture—The RAW 264.7 macrophage cell line was maintained in a 95% air, 5% CO_2 atmosphere in Dulbecco's modified Eagle's medium plus 10% (v/v) heat-inactivated fetal calf serum, 100 units/ml penicillin, 100 μg/ml streptomycin, and 15 mM HEPES. Cell were stimulated with LPS (*Escherichia coli* 0111:B4, Sigma) at 100 ng/ml for the indicated times.

* This work was supported by United States Public Health Service Award DK 59932 (to A. R. M.) and Barnes-Jewish Hospital Foundation Grant 5680–02 (to S. J. C.). The costs of publication of this article were defrayed in part by the payment of page charges. This article must therefore be hereby marked "*advertisement*" in accordance with 18 U.S.C. Section 1734 solely to indicate this fact.

‡ Present address: Dept. of Nephrology, Leicester General Hospital, Gwendolen Rd., Leicester LE5 4PW, United Kingdom.

§ To whom correspondence should be addressed: Washington University School of Medicine, 4940 Parkview Place, Wohl Clinic, Rm. 8843, St. Louis, MO 63110. Tel.: 314-454-8464; Fax: 314-454-8430; E-mail: Morrison@pcg.wustl.edu.

[1] The abbreviations used are: LPS, lipopolysaccharide(s); ARE, adenylate/uridylate-rich element; CHAPS, 3-[(3-cholamidopropyl)dimethylammonio]-1-propanesulfonic acid; COX-2, cyclooxygenase-2; DTT, dithiothreitol; EMSA, electrophoretic mobility shift assay; hnRNP, heterogeneous nuclear ribonucleoprotein; MALDI, matrix-assisted laser desorption/ionization; UTR, untranslated region.

This paper is available on line at http://www.jbc.org

Downloaded from www.jbc.org by on January 31, 2007

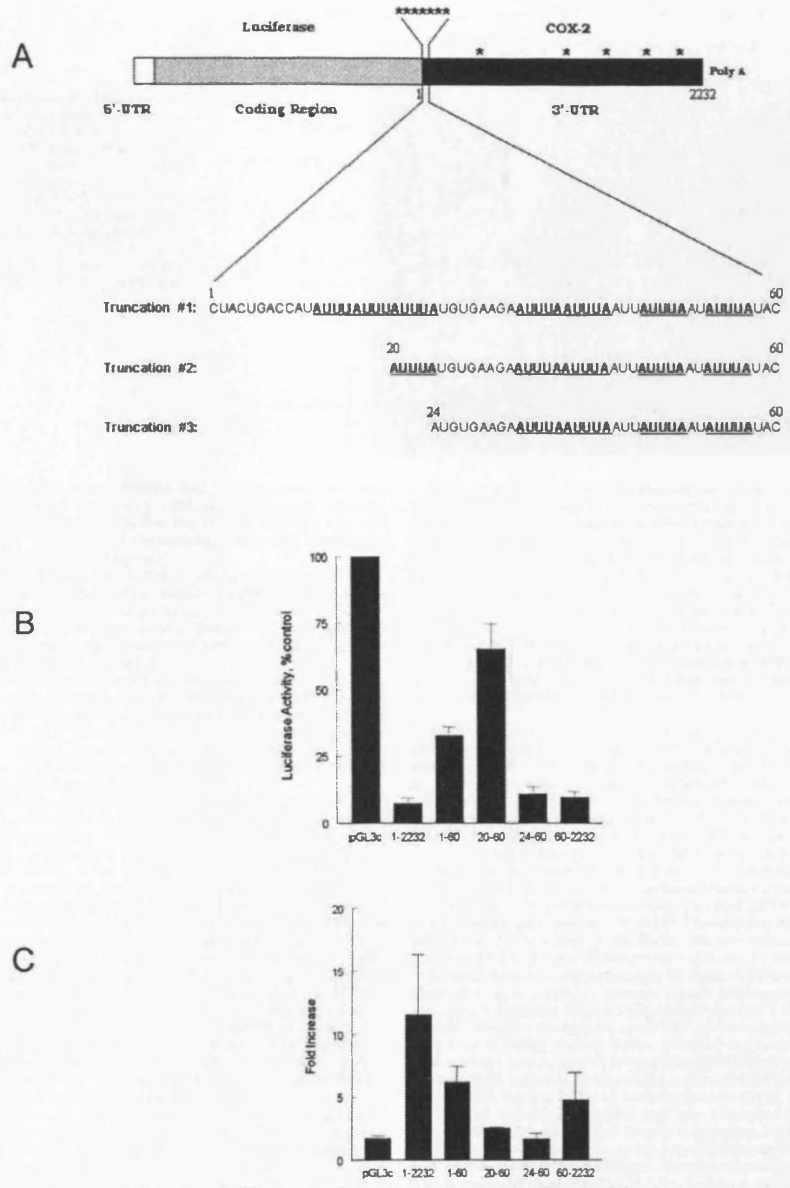

FIG. 1. **Reporter-gene assay identifies a LPS response element in the 3'-UTR of COX-2.** RAW 264.7 cells were transiently transfected with plasmids encoding luciferase alone, pGL3c, or containing the indicated region of the 3'-UTR of COX-2. Luciferase activity was measured in cell lysates and normalized to cellular protein. *A*, sequence of the first 60 nucleotides of the 3'-UTR of COX-2 and indicated truncations. *B*, luciferase activity in lysates from nonstimulated cells. *C*, -fold increase in luciferase activity in lysates from cell stimulated with LPS for 6 h. Luciferase results represent the mean ± S.E. for three to seven independent experiments.

Plasmids—Reporter-gene constructs were generated as described previously (11). Briefly, various regions of the 3'-UTR of COX-2 were amplified by PCR using primers terminating in XbaI recognition sequences. PCR products were ligated in the unique XbaI site of the pGL3 control vector (Promega Corp.), located in the 3'-UTR of the firefly luciferase gene. Vectors used for synthesis of RNA probes for electro-

Downloaded from www.jbc.org by on January 31, 2007

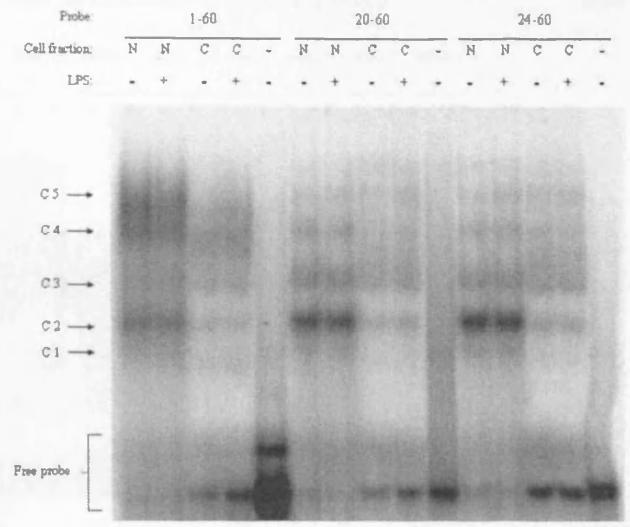

FIG. 2. **Formation of RNA-protein complexes with the proximal region of the 3′-UTR of COX-2 and cellular fractions of RAW 264.7 cells.** Radiolabeled RNA probes were incubated with either cytosolic or nuclear fractions isolated from RAW 264.7 cells treated with or without LPS for 1 h. Complexes were separated on nondenaturing gels and visualized by autoradiography. Complexes were identified by changes in electrophoretic mobility compared with free probe.

phoretic mobility shift assays (EMSAs) and binding assays were constructed by amplifying the same 3′-UTR sequences except that the primers encoded a HindIII recognition site at the 5′-end and a BamHI site at the 3′-end. The PCR products were ligated into the HindIII and BamHI sites of pcDNA3 (Stratagene).

Transient Transfections—RAW 264.7 cells were transiently transfected using SuperFect Transfection Reagent (Qiagen Corp.). Cells were plated into 6-well cluster dishes, grown to 75% confluence, and transfected with 1 μg of reporter-gene plasmid DNA at a 4:1 SuperFect:DNA ratio. After transfection, cells were incubated overnight and subsequently analyzed for gene expression.

Luciferase Assay—Luciferase activity was determined using a luciferase assay system, following the manufacturer's protocol (Promega Corp.). Briefly, cell monolayers in 6-well cluster dishes were removed by scraping into 100 μl of reporter lysis buffer. Cells were vortexed and cellular debris removed by centrifugation (30 s at 12,000 × *g*). Luciferase activity was measured using a Lumat LB 9507 luminometer (E G & G Wallac) as described previously (11).

Cell Fractionation—All fractionation buffers were kept on ice and contained 0.25 mM Pefabloc, 2 μM leupeptin, 0.3 μM aprotinin, and 0.1 mM sodium orthovanadate. Cells were washed in ice-cold phosphate-buffered saline, scraped off the flasks into buffer A (10 mM HEPES, 10 mM KCl, 1 mM EDTA, 1 mM EGTA, 1 mM DTT, 1 mM $MgCl_2$, 5% glycerol), and incubated on ice for 10 min. After incubation, Nonidet P-40 was added (final concentration 0.25%), and the cells were vortexed for 10 s. Nuclei were isolated by centrifugation (1,500 × *g* for 10 min at 4 °C). The supernatant was further centrifuged for 5 min at 16,000 × *g* and saved as the cytosolic fraction. Nuclei were washed twice in buffer B (10 mM HEPES, 1 mM $MgCl_2$, 1 mM DTT, 10 mM KCl_2), resuspended in buffer C (20 mM HEPES, 400 mM $NaCl_2$, 1 mM EDTA, 1 mM EGTA, 1 mM $MgCl_2$, 1 mM DTT, 25% glycerol), and allowed to swell on ice for 15 min with frequent vortexing. Lysed nuclei were centrifuged at 5,000 × *g* for 5 min at 4 °C. The supernatant (nuclear protein) was removed and used immediately or frozen at −20 °C. For each 225-cm^2 flask, ~1 mg of nuclear protein and 7 mg of cytosolic protein were obtained. Protein concentrations were determined using the BCA protein assay.

In Vitro Transcription—Radiolabeled RNA probes were generated by *in vitro* transcription using T7 RNA polymerase plus (Ambion, Inc.) and COX-2 3′-UTR plasmids (described above) as template. Transcription reactions contained 100 units of T7 polymerase; 500 μM each ATP, CTP, GTP; 12.5 μM UTP; 200 μCi of [^{32}P]UTP (6,000 Ci/mmol, PerkinElmer Life Sciences); 10 mM DTT; 10 μg of plasmid template linearized by digestion with BamHI for the COX-2 gene or EcoRI for TA vector control, in a total volume of 50 μl of 1× transcription buffer (Ambion, Inc.). Transcription reactions were incubated for 1 h at 37 °C. Unincorporated nucleotides were removed using Sephadex G-25 mini Quick Spin RNA Columns (Roche Applied Science).

Biotinylated RNA oligonucleotides corresponding to either the 3′-UTR of the COX-2 gene or a 63-nucleotide region of the TA cloning vector (Invitrogen) were made by *in vitro* transcription using a modified protocol of the T7-MEGAshortscript high yield kit (Ambion). A final reaction volume of 20 μl contained the following: 2 μl of 10× transcription buffer; 2 μl each of 75 mM ATP, GTP, UTP; 1 μl of 75 mM CTP; 7.5 μl of 10 mM biotinylated CTP (Invitrogen); 10 μg of COX-2 DNA template, and 2 μl of T7 MEGAshortscript enzyme mix. Transcription was carried out overnight at 37 °C and the reaction stopped by adding 2 μl of RNase-free DNase and incubating for 15 min at 37 °C. Unincorporated nucleotides were removed with mini Quick Spin RNA columns centrifuged at 1500 × *g* for 4 min. The final concentration of RNA was determined spectrophotometrically by measuring absorbance at 260 nm.

EMSA and Antibody Supershifts—Typically, 5–10 μg of cell fraction protein was incubated for 30 min at 37 °C in EMSA binding buffer (10 mM HEPES pH 7.6, 5 mM $MgCl_2$, 40 mM KCl, 1 mM DTT, 5% glycerol, 5 mg/ml heparin) with 1–5 pmol of ^{32}P-labeled RNA probe in a final volume of 20 μl. For supershift experiments, binding mixtures included 0.2 μg of affinity-purified IgG for anti-HuR, -TIA-1 and -TIAR (Santa Cruz Biotechnology); or 1 μl of anti-AUF1 (20); or 1 μl of normal goat serum (Sigma). RNase T1 (10 units) was added to EMSA or supershift samples and incubated for 15 min at 37 °C. Loading buffer (5 μl) containing 80% glycerol, 0.1% bromphenol blue in 50 mM Tris-HCl, pH 7.5 was added, and samples were electrophoresed (250 V for 3 h) on 4% polyacrylamide gels (pre-run 1 h at 200 V) containing 44 mM Tris-HCl, pH 8.3, 44 mM boric acid, 1 mM EDTA, 4% acrylamide:bisacrylamide (29:1), and 2.5% glycerol. EMSAs were visualized by autoradiography.

Binding Reaction—Approximately 20 units of RNase inhibitor was added to 5 mg of nuclear or cytosolic protein and incubated with 120–150 μg of biotinylated RNA at room temperature for 2 h with constant rotation. Streptavidin-agarose beads (600 μl) were washed three times with 1 ml of EMSA binding buffer, added to the protein/biotinylated RNA mixture, and incubated for an additional 2 h at room temperature with constant agitation. The beads were then washed four times with 1 ml of EMSA binding buffer at room temperature, and bound proteins were eluted from the RNA with a high ionic strength salt solution (1 M NaCl in EMSA binding buffer) or with rehydration buffer.

Sample Preparation—For protein identification experiments, samples were desalted using a Millipore Centricon centrifugal filter device with a molecular mass cutoff of 10 kDa. Protein samples were brought up to a volume of 2 ml in a 4% CHAPS solution, applied to the Centricon membrane, and centrifuged at 1,500 × *g* for 4 h. The concentrated sample was again diluted to 2 ml in 4% CHAPS, applied to the membrane, and centrifuged at 1,500 × *g* for 8 h to a final volume of ~30 μl. Protein concentrations were measured using the RC DC protein assay (Bio-Rad).

Downloaded from www.jbc.org by on January 31, 2007

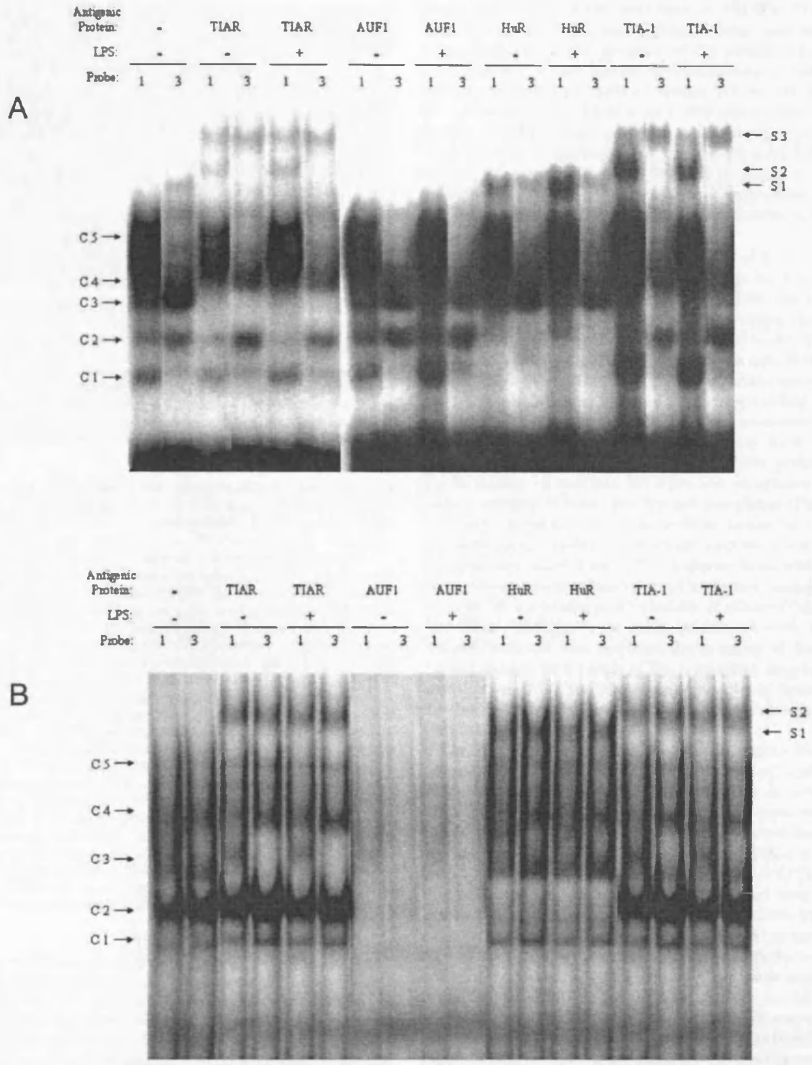

FIG. 3. **Identification of RNA-binding proteins present in several RNA-protein complexes.** Radiolabeled RNA probes corresponding to the first 60 nucleotides (probe 1) or nucleotides 24–60 (probe 3) of the 3′-UTR of COX-2 were incubated with cellular fraction from RAW 264.7 cells in the presence of nonimmune serum (*NI*) or antibodies raised against the indicated protein. RNA-protein complexes (C1–C5) and supershifted complexes (S1–S3) are indicated. Incubations were conducted with either cytosolic fractions (*A*) or nuclear fractions (*B*).

For Western analysis, samples were desalted and concentrated by acetone precipitation. Acetone, stored at −80 °C, was added at a ratio of 5:1 (v/v), vortexed briefly, and incubated for 30 min at −80 °C. The precipitate was collected by centrifugation for 5 min at 16,000 × *g*. The supernatant was removed, and the protein pellet was air dried for 5 min. Protein was resuspended in 250 μl of rehydration buffer prior to isoelectric focusing.

Isoelectric Focusing—Samples were added to the rehydration solution (8 M urea, 0.15 mg/ml DeStreak reagent (Amersham Biosciences), 4% CHAPS, 0.2% carrier ampholytes, pH 7–10, 0.0002% bromphenol blue) in a ratio of 9:1 of rehydration solution to sample. Samples were applied to 11-cm immobilized pH gradient strips, pH 7–10 (Bio-Rad) and incubated at room temperature for 1 h. Strips were passively rehydrated overnight (16 h) while covered in mineral oil. After rehydration, the strips were transferred to a focusing tray with prewetted wicks and covered with fresh mineral oil. The strips were focused for a total of 17,000 volt-hours with rapid ramping on the Bio-Rad Protean IEF Cell.

Second Dimension—After focusing the strips were equilibrated in equilibration buffer I (6 M urea, 2% SDS, 0.05 M Tris-HCl, 20% glycerol, and 2% DTT) for 10 min and equilibration buffer II (6 M urea, 2% SDS, 0.05 M Tris-HCl, 20% glycerol, and 2.5% iodoacetamide) for 10 min, both

Downloaded from www.jbc.org by on January 31, 2007

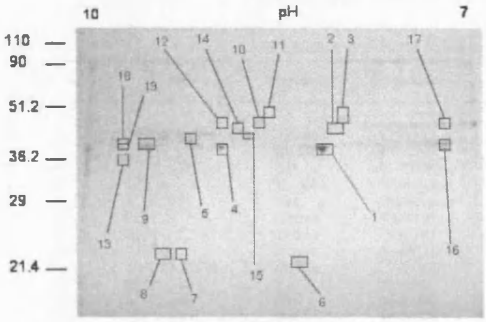

FIG. 4. **Identification of proteins bound to the proximal region of the 3′-UTR of COX-2.** Nuclear protein fraction isolated from non-stimulated RAW 264.7 cells was incubated with biotinylated RNA corresponding to the first 60 nucleotides of the 3′-UTR of COX-2. Bound proteins were isolated with streptavidin-coated agarose beads and eluted in a 1 M NaCl-containing buffer. Proteins were resolved by two-dimensional gel electrophoresis spanning a pH range of 7–10. Proteins were visualized with Coomassie Blue and identified by mass fingerprint analysis and electrospray mass spectrometry sequencing (see Table I).

with gentle agitation. The strips were rinsed in SDS running buffer (25 mM Tris-HCl, 250 mM glycine, and 0.1% SDS) and applied to the well of an 8–16% acrylamide Criterion precast gel (Bio-Rad) for protein identification and 10.5–14% acrylamide for Western analysis. The strips were covered with an overlay of agarose and run for 1 h at 200 V.

Protein Identification—Gels were transferred to the Protein and Nucleic Acid Chemistry Laboratory (PNACL) at Washington University, where spots were picked by an automated gel cutter and transferred to an automated sample digestion robot. Samples were analyzed by a PE-Biosystems Voyager DE-PRO MALDI-time of flight mass spectrometer and a Finnigan liquid chromatography quadrupole ion trap electrospray mass spectrometer. Data base searching utilized Mascot software and MM-Fit from Protein Prospector version 4.05 (UCSF).

Western Blot Analysis—Nuclear and cytosolic fractions were isolated from RAW 264.7 cells treated with and without LPS for 1 h. Proteins that bound to biotinylated RNA were eluted with rehydration buffer and subjected to two-dimensional electrophoresis as described above. Proteins were transferred to Immobilon-P membranes (Millipore Corp.) for 1 h at 20 V, blocked with 5% nonfat milk, and probed with monoclonal anti-HuR antibody, polyclonal anti-TIA-1 (Santa Cruz Biotechnology); polyclonal anti-TIAR (BD Biosciences); or polyclonal anti-AUF1 (Upstate Biotechnology) all at a 1:1,000 dilution. Horseradish peroxidase-linked secondary antibodies (Amersham Biosciences) were used at a 1:10,000 dilution. Signal detection was carried out using enhanced chemiluminescence system (ECL, Amersham Biosciences).

RESULTS

The First 60 Nucleotides of the 3′-UTR of COX-2 Contain a Negative Control Element That Is Regulated by LPS—Various regions of the 3′-UTR of COX-2 were inserted into the 3′-UTR of the luciferase reporter-gene (Fig. 1*A*) and transiently expressed in RAW 264.7 cells. When the full-length 3′-UTR (1–2232) was placed in the reporter message, luciferase activity decreased more than 90% compared with luciferase alone (Fig. 1*B*). Luciferase activity decreased 60% with insertion of only the first 60 nucleotide of the 3′-UTR of murine COX-2. This region of the 3′-UTR contains multiple copies of the AUUUA consensus sequence reported to confer decreased stability and/or translational efficiency of COX-2 mRNA (11). Sequential deletion of the proximal portion of this region of the 3′-UTR resulted in first an increase in reporter-gene expression and then a further decrease in expression (Fig. 1*B*), suggesting that multiple control elements were operative. When RAW cells were exposed to LPS, reporter-gene activity from a message-containing luciferase control without any COX-2 sequence increased less than 2-fold within a 6-h treatment time (Fig. 1*C*). However, the activity of the reporter-gene containing the full-length 3′-UTR increased more than 10-fold (Fig. 1*C*) under the same treatment conditions. Again, a large portion of the increase occurred in the presence of the proximal region of the 3′-UTR alone, where the 60-nucleotide insert caused a 6-fold increase in luciferase activity within 6 h of stimulation (Fig. 1*C*) and more than 10-fold over a 10-h stimulation (results not shown). The LPS responsiveness of the reporter-gene was lost when the first 23 nucleotides of the 3′-UTR were deleted. Thus, the first 60 nucleotides of the 3′-UTR of COX-2 contain major control elements that confer decreased expression under non-stimulated conditions and increased expression in response to LPS stimulation.

The First 60 Nucleotides of the 3′-UTR of COX-2 Form Multiple RNA-Protein Complexes That Contain Known RNA-binding Proteins—To understand more fully how the proximal region of the 3′-UTR of COX-2 regulates message expression, we set out to identify protein factors that bind to this region of the message. In the first set of experiments we used EMSAs to look for known RNA-binding proteins that regulate message expression. When *in vitro* transcribed RNA representing the first 60 nucleotides of the 3′-UTR of COX-2 was incubated with either nuclear fractions or cytosolic fractions from RAW 264.7 cells, there were shifts in the mobility of the RNA probe indicating the formation of multiple RNA-protein complexes. EMSA results identified at least five distinct complexes (Fig. 2). These complexes formed using both nuclear (*lanes* labeled *N*) and cytosolic (*lanes* labeled *C*) fractions and were not grossly altered by treatment with LPS. However, truncating the RNA probe resulted in decreased intensity of some complexes (Fig. 2, C4 and C5) and increased intensity of others (Fig. 2, C2 and C3). These changes were more prominent with the nuclear protein fractions. The fact that the mobility of the complexes did not change as a result of the truncation suggests that the composition of the complexes was not altered drastically, and the change in intensity occurred because of a change in complex stability.

The identity of some of the proteins present in the complexes was determined by adding antibodies raised against known RNA-binding proteins and looking for a loss in complex intensity and/or formation of a higher molecular mass complex (supershift). Using this approach we demonstrated that the RNA-binding proteins TIAR, AUF1, HuR and TIA-1 were able to bind to the proximal 60 nucleotides of the 3′-UTR of COX-2. When antibodies against either TIAR or TIA-1 were included in the binding reaction containing cytosolic protein fractions and RNA probes (Fig. 3*A*), two higher molecular mass complexes formed (supershifts S2 and S3). Both supershifts were present with the 1–60 probe, whereas only the higher supershift (S3) remained when the probe was truncated. In all cases, the supershift was accompanied with a severely decreased intensity in complex C3. Likewise, addition of anti-HuR antibody resulted in formation of a supershift (S1) and decreased intensity of complexes C1 and C2 formed with cytosolic proteins (Fig. 3*A*). The supershift was more apparent in the 60-nucleotide probe and decreased as the probe was truncated, whereas the loss of complexes C1 and C2 occurred with both probes. Addition of antibody directed against AUF1 caused no major change in the intensity of the RNA-protein complexes nor caused the appearance of a supershift when used in conjunction with cytosolic protein fractions (Fig. 3*A*).

When using nuclear fractions (Fig. 3*B*), supershift results with TIA-1, TIAR, and HuR antibodies were similar to those using proteins isolated from cytosolic fractions (Fig. 3*A*). The exceptions were that the TIA-1 and TIAR antibodies formed a single higher molecular mass complex (Fig. 3*B*, S2), and the

Downloaded from www.jbc.org by on January 31, 2007

TABLE I
Identification of proteins bound to the conserved ARE of COX-2 message

Spot no.	Protein	Organism	Accession no.	Mass	% Sequence covered	MALDI % Peptides matched	ES-MS[a] Mascot score
				kDa			
1	CBF-A	Mouse	6754222	30.9	48	48	513
2	CBF-A	Mouse	6754222	30.9	20		229
3	AUF1 p45	Rat	9588096	38.1	30	40	218
4	CBF-A	Mouse	6754222	30.9	46	58	393
5	AUF1 p37	Rat	9588101	30.4	39	52	219
6	RBM 3	Mouse	7949121	16.6	11		93
7	RBM 3	Mouse	7949121	16.6	11		92
8	RBM 3	Mouse	7949121	16.6	18		106
9	hnRNP A2/B1	Mouse	7949053	36	50	66	71
10	AUF1 p42	Rat	9588098	36	26	32	282
11	AUF1 p45	Rat	9588096	38.1	21	32	135
12	AUF1 p42	Rat	9588098	36	7		110
13	hnRNP A2/B1	Mouse	21071091	36	17		318
14	AUF1 p40	Rat	9588100	32.6	13		112
15	TIA 1	Mouse	14714709	41.9	16		209
16	CBF-A	Mouse	6754222	30.9	22		339
17	CBF-A	Mouse	6754222	30.9	24		148
18	hnRNP A3	Mouse	30316201	39.7	38	33	
19	hnRNP A3	Mouse	25991929	37.1	27	55	

[a] ES-MS, electrospray-mass spectrometry.

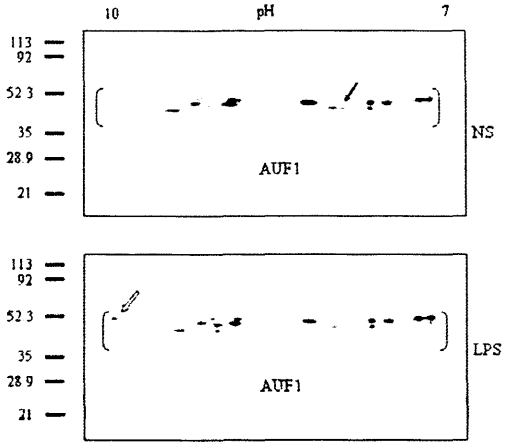

FIG. 5. **Two-dimensional Western analysis of AUF1.** Nuclear protein fractions isolated from RAW 264.7 cells that bound the proximal 60 nucleotides of the 3′-UTR of COX-2 were resolved on two-dimensional gels ranging from pH 7 to 10. Blots using proteins from nonstimulated cells (*NS*) or cells treated with LPS for 1 h (*LPS*) were probed with anti-AUF1 antibody.

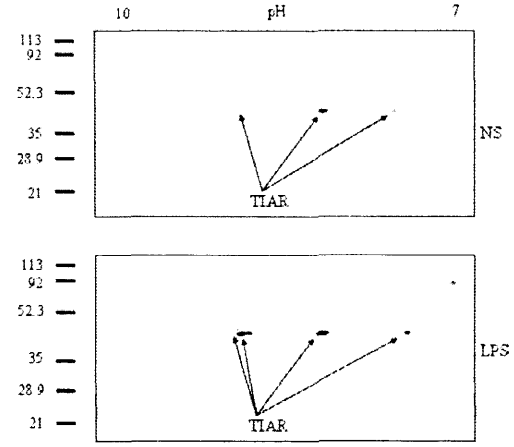

FIG. 6. **Two-dimensional Western analysis of TIAR.** Nuclear protein fractions isolated from RAW 264.7 cells that bound the proximal 60 nucleotides of the 3′-UTR of COX-2 were resolved on two-dimensional gels ranging from pH 7 to 10. Blots using proteins from nonstimulated cells (*NS*) or cells treated with LPS for 1 h (*LPS*) were probed with anti-TIAR antibody.

HuR-dependent supershift was greatly diminished (Fig. 3*B*, S1). In contrast, addition of anti-AUF1 antibody to binding reactions containing nuclear protein fractions resulted in nearly a complete disappearance of all RNA gel shifts (Fig. 3*B*). These results were reproducible and dependent on the concentration of antibody added, suggesting that AUF1 was present in all the nuclear RNA-protein complexes. In all cases, the appearance of a supershift and disappearance of complex(es) was not affected by treating cells with LPS prior to cellular fractionations.

Additional Proteins That Bind the 3′-UTR of COX-2—As a second approach to identify proteins that bind to the 3′-UTR of COX-2, biotinylated RNA probes were incubated with nuclear protein fractions, and bound proteins were isolated with streptavidin-coated agarose beads. Proteins were eluted from the RNA with a high ionic strength buffer (1 M NaCl), separated on two-dimensional gels, and stained with Coomassie Blue. The indicated spots (Fig. 4) were excised, digested with trypsin, and subjected to peptide mass fingerprinting by MALDI and confirmed by liquid chromatography coupled to electrospray mass spectrometry. The identification of the spots is summarized in Table I. The 19 spots we identified were represented by six different proteins. Two of these proteins were identified previously in the EMSA experiments described above; namely, TIAR and AUF1. The additional proteins were CPF-A (hnRNP A/B), RBM3, hnRNP A2/B1, and hnRNP A3.

CPF-A was identified as an ARE-binding protein that exists as two isoforms, p37 and p42, which arise because of alternative splicing (21). We identified five spots that matched the sequence of CBF-A, three migrated at the lower molecular mass (p37), and two at the higher molecular mass (p42). The liquid chromatography electrospray mass spectrometry data from spots 1 and 4 contained sequences that span the alternatively spliced exon junction confirming that these proteins were

Downloaded from www.jbc.org by on January 31, 2007

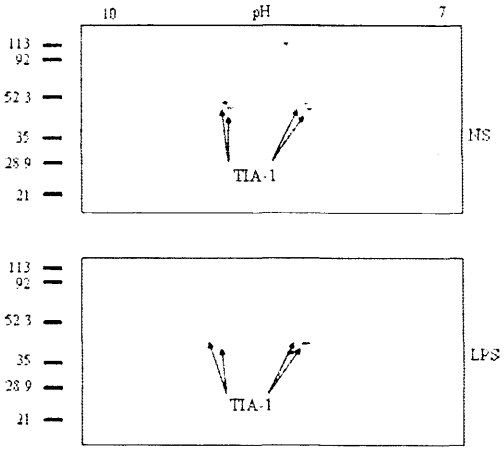

FIG. 7. **Two-dimensional Western analysis of TIA-1.** Nuclear protein fractions isolated from RAW 264.7 cells that bound the proximal 60 nucleotides of the 3′-UTR of COX-2 were resolved on two-dimensional gels ranging from pH 7 to 10. Blots using proteins from nonstimulated cells (*NS*) or cells treated with LPS for 1 h (*LPS*) were probed with anti-TIA-1 antibody.

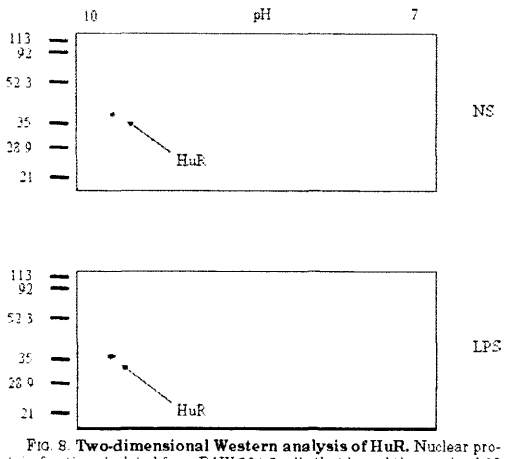

FIG. 8. **Two-dimensional Western analysis of HuR.** Nuclear protein fractions isolated from RAW 264.7 cells that bound the proximal 60 nucleotides of the 3′-UTR of COX-2 were resolved on two-dimensional gels ranging from pH 7 to 10. Blots using proteins from nonstimulated cells (*NS*) or cells treated with LPS for 1 h (*LPS*) were probed with anti-HuR antibody.

the p37 isoform. Spot 16 lacked sequence data at the splice junction; however, this protein migrated at the same apparent molecular mass as spots 1 and 4 and was also designated as the p37 isoform. Peptide sequence data for spots 2 and 17 did not confirm the presence of the alternatively spliced exon; however, the migration of these proteins in the second dimension suggests that they were the p42 isoform.

Similarly, AUF1 exists as multiple alternatively spliced isoforms (22). In this case there two exons, 2 and 7, which are alternatively spliced giving rise to four different isoforms, p37, p40, p42, and p45. Both exons 2 and 7 are present in p45, isoform p42 lacks exon 2, p40 lacks exon 7, and p37 is missing both exons 2 and 7. We have identified six different spots migrating at four different molecular masses as AUF1. Unfortunately, no peptide sequence data confirmed whether exon 7 was present or absent in any of the AUF1 spots. Peptide sequence data for spots 3 and 11 confirm the presence of exon 2, and because these proteins migrated at the highest molecular mass they were assigned to isoform p45. Spot 10 migrated at a slightly lower molecular mass, and sequence data confirmed that exon 2 was absent in this protein suggesting that this was isoform p42. Spot 12 migrated at the same apparent molecular mass and was also designated as isoform p42. AUF1 spot 5 migrated at the lowest molecular mass, and sequence data confirmed that exon 2 was absent. Accordingly, this spot was assigned to isoform p37. Finally, spot 14 migrated at a molecular mass between isoforms p37 (spot 5) and p42 (spots 10 and 12), suggesting that it was isoform p40. Thus, all four isoforms of AUF1 were able to bind to the proximal region of the 3′-UTR of COX-2.

Protein spots 9 and 13 were identified as hnRNP A2/B1. Like CBF-A and AUF1, the spots migrated at different molecular masses. Spot 13 migrates at the reported molecular mass, 36 kDa, whereas spot 9 migrated at a higher molecular mass, raising the possibility that hnRNP A2/B1 may have alternatively spliced isoforms. Likewise, hnRNP A3 was identified at two molecular masses (spots 18 and 19) but with similar isoelectric points.

RNA-binding Proteins Exist in a Wide Range of Isoelectric Points—In addition to different molecular masses, proteins present in multiple spots migrated at different isoelectric points. Some of these differences may occur because of changes in primary sequences as a consequence of alternative splicing. In other cases, isoforms of a protein of the same apparent molecular mass and most likely the same primary sequence were present at multiple isoelectric points. The range of isoelectric points for an individual protein varied from approximately half a pH unit for AUF1 isoforms p45 (spots 3 and 11) and p42 (spots 10 and 12), to 1–2 pH units for CBF-A isoforms p37 (spots 16, 1, and 4) and p42 (spots 2 and 17) and RBM3 (spots 6, 7, and 8). These changes in isoelectric points are believed to be the result of post-translational modifications.

To determine whether additional isoforms of RNA-binding proteins were bound to the 3′-UTR of COX-2, we performed Western analysis using a series of two-dimensional gels with proteins eluted from RNA affinity probes. Western blots were probed with antibodies raised against RNA-binding proteins AUF1, TIAR, TIA-1, and HuR. AUF1 antibody recognized multiple isoforms that span the entire pH range of 7–10 (Fig. 5). Several different molecular mass species appeared which migrated between the 35- and 50-kDa standards. AUF1 and CBF-A have a high degree of homology, and it has been reported that AUF1 antibodies cross-react with CBF-A (21), thus it is likely that the reactive proteins were a combination of AUF1 and CBF-A isoforms.

In contrast to the AUF1 result, antibodies directed against TIAR and TIA reacted with a limited number of protein species (Figs. 6 and 7). TIAR antibodies reacted with isoforms migrating at three different pI values and two different molecular masses. TIA-1-specific antibodies recognized two molecular mass species migrating at two different pI values. The two different molecular mass proteins for TIAR and TIA-1 were consistent with the two known alternatively spliced isoforms (23). The change in isoelectric points may represent post-translational modifications of the proteins. Finally, HuR was detected as a single spot that migrated at an isoelectric point nearly equal to 10 (Fig. 8).

RNA affinity probes were also made using an unrelated DNA template derived from the TA cloning vector that contained no

Downloaded from www.jbc.org by on January 31, 2007

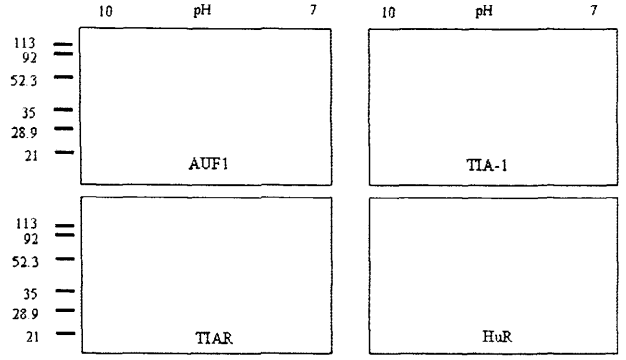

FIG. 9. **Two-dimensional Western analysis of proteins bound to control RNA probe.** Nuclear protein fractions isolated from RAW 264.7 cells that bound RNA transcribed from a 63-nucleotide region of the TA cloning vector were resolved on two-dimensional gels ranging from pH 7 to 10. Blots were probed with anti-AUF1, anti-TIAR, anti-TIA-1, and anti-HuR antibodies.

AREs. Protein eluted from this RNA migrated as multiple spots on two-dimensional gels stained with Coomassie Blue (results not shown). However, Western analysis of these gels failed to detect any of the proteins that were identified when using COX-2 RNA (Fig. 9). These results indicate that binding of proteins to COX-2 RNA was sequence-specific.

Western analysis of protein fractions from cells treated with LPS indicated subtle changes in the molecular species of the RNA-binding proteins that recognize the 3′-UTR of COX-2. Probing blots with anti-TIAR antibodies demonstrated that three isoforms of the protein, differing in their isoelectric point, were bound to the RNA probe (Fig. 6). The two isoforms of lower pI reacted with the antibody at a similar intensity when using protein from nonstimulated and LPS-treated cells. However, the reactive species present at the highest pI was present at a much higher level in the LPS treatment group. Also, the higher molecular mass isoform was identified only with the LPS-treated protein fraction. AUF1 also showed a difference in reactive protein species bound to RNA probes when using nuclear fractions from nonstimulated and LPS treatment groups (Fig. 5). Reactive proteins in the acidic half of the gel produced a pattern that was relatively the same across treatment groups, whereas the basic half of the gel had a pattern that was clearly altered by LPS treatment. In general the proteins present in this portion of the gel reacted more intensely with the antibody. Also, some of the protein species were present only in the nonstimulated group (Fig. 5, *filled arrow*), and others were present only in the LPS-treated sample (Fig. 5, *open arrow*). These results suggest that LPS treatment caused a change in the specific isoforms of various RNA-binding proteins that recognize the 3′-UTR of COX-2.

DISCUSSION

The proximal region of the 3′-UTR of the COX-2 message plays a pivotal role in regulating protein expression. The first 60 nucleotides of the message contain a highly conserved ARE composed of multiple iterations of the sequence AUUUA. This region of the COX-2 message was sufficient to cause decreased expression of a heterologous reporter-gene. When expressed in a murine macrophage cell line (RAW 264.7), reporter-gene activity increased after treatment with LPS. This response was dependent on the 3′-UTR sequences from COX-2 message which were present in the reporter-gene message. Inclusion of the full-length 3′-UTR or the proximal 60 nucleotides alone caused the reporter-gene to be regulated by LPS. Furthermore, removal of the first 60 nucleotides from the full-length 3′-UTR attenuated the LPS response and truncation of the 60 nucleotide region such that the first group of AUUUA repeats was removed caused a complete loss of LPS induction. The results suggest that the proximal region of the 3′-UTR of COX-2 plays two roles in regulating gene expression. First, this region was required for decreased gene expression under basal conditions, and second, it was required for full induction of gene expression after exposure to LPS.

The mechanism whereby LPS stimulation leads to changes in target gene expression is not fully understood. LPS induces gene expression through a combination of transcriptional activation and message stabilization (2, 3, 24). Changes in message stabilization occur through specific interactions of RNA-binding proteins. Because the proximal region of the 3′-UTR of COX-2 contained a LPS response element, identification of the proteins that bind to this region of the COX-2 message may help identify key proteins required for LPS regulation of COX-2.

Several RNA-binding proteins have been reported to bind the 3′-UTR of COX-2: AUF1 (25), HuR (26, 27), CPF-A (21), CUGBP2 (28), TTP (17), and hnRNP A0 (29). Most of these were reported to bind to the proximal region of the 3′-UTR equivalent to the region used in our study, except for TTP which bound a more distal site (the report on hnRNP A0 did not identify the specific binding site). Using a combination of EMSAs, proteomics, and Western analysis we identified many of these proteins as well as others that bind to the proximal 60 nucleotides of the 3′-UTR of COX-2. The function of many of the proteins we identified is known. Some have been reported to regulate message stability, HuR (26, 27), AUF1 (25), and CPF-A (21) and others such as TIAR and TIA-1 are believed to regulate message translation (14, 15). Many of the heterogeneous nuclear ribonucleoproteins, including hnRNP A3 and A2/B1, are implicated in cytoplasmic trafficking of RNAs (30, 31). Additionally, we identified RBM3 as a COX-2 ARE-binding protein. The exact function of this protein is not yet known, but RBM3 contains a RNA binding motif and has been reported to be up-regulated during cold-shock (32, 33) and identified as a cytokine-induced gene in human premyeloid cells (34).

The complexity of proteins that bind to the 3′-UTR of COX-2 was further exemplified by the proteomic results. Our proteomic analysis demonstrated that multiple isoforms of AUF1, CPF-A, RBM3, hnRNP A2/B1, and hnRNP A3 bind to this region of the 3′-UTR of COX-2. The different isoforms of a given protein were identified by shifts in isoelectric point and/or apparent molecular mass. Changes in molecular mass can arise because of alternative splicing events. In fact, electrospray mass spectrometric data confirmed the presence of alternative splice forms for AUF1 and CBF-A. HnRNP A2/B1 and hnRNP A3 were identified at two spots that migrated at different molecular masses, suggesting that alternatively spliced iso-

Downloaded from www.jbc.org by on January 31, 2007

forms of these proteins also exist. Alternative splice variants of TIAR and TIA-1 have been reported previously (23). Thus, the synthesis of alternatively spliced isoforms appears to be a common theme for RNA-binding proteins.

Changes in a proteins pI may be caused by post-translational modifications, such as phosphorylation, sulfation, and acetylation. We have shown that the majority of the proteins identified in this study migrate to multiple isoelectric points. AUF-1, CPF-A, and RMB3 all were identified by MALDI and electrospray mass spectrometry at different isoelectric points and the same apparent molecular mass. The range of pI values represented by each protein varied but extended from 0.5 to 2 pH units. Western analysis of two-dimensional gels demonstrated that TIA-1 and TIAR migrated at a wide range of isoelectric points. Western results with AUF-1 antibodies showed reactive proteins across the entire gel (pH 7–10). In this case it is likely that the reactive proteins were a composite of AUF-1 and CBF-A because it was reported that AUF-1 antibodies can cross-react with CBF-A because of their high degree of homology (21).

EMSA experiments demonstrated that RNA-binding proteins HuR, TIA-1, TIAR, and AUF1 could bind to the first 60 nucleotides of the 3′-UTR of COX-2. The results of these experiments differed using proteins isolated from nuclear fractions compared with cytosolic fractions. When using nuclear protein fractions, the addition of antibodies directed toward HuR, TIA-1, or TIAR resulted in a single supershift in mobility of the RNA probe which was accompanied by decreased intensity of specific RNA-protein complexes. In contrast, when using cytosolic protein fractions, the supershift formed with antibodies raised against TIA-1 and TIAR was present as a doublet. When the RNA probe was truncated, the faster migrating complex was lost. The single supershift using nuclear proteins appeared to migrate at the position of the lower band of the doublet seen with the cytosolic protein fractions. One explanation for these results is that TIA-1 and TIAR were modified prior to exiting the nucleus. This modification could affect the affinity of these proteins with other protein partners and thereby change the molecular mass of the supershifted complex. Truncation of the probe promoted the formation of the slower moving complex.

The most striking difference between nuclear and cytosolic proteins was seen with AUF1 EMSA experiments. There was no discernible change in the gel shift pattern when AUF1 antibody was added to cytosolic protein-binding reactions. However, there was nearly complete disruption of all RNA-protein complexes when AUF1 antibody was included in the nuclear protein reactions. The reason for the difference is not clear. Either AUF1 in cytosolic fractions did not bind to the RNA probe, or cytosolic protein complexes had a different composition or conformation such that the anti-AUF1 antibody no longer recognized the reactive epitope. Two-dimensional Western experiments showed that AUF-1 antibodies detected proteins from cytosolic fractions that were bound to the proximal region of the 3′-UTR of COX-2 (results not shown), suggesting that the inability to detect supershifts or disrupt RNA-protein complexes with cytosolic protein fraction was caused by sequestration of the antigenic determinant of AUF1.

In addition to altered binding properties dependent on the cellular location of proteins, we measured subtle changes in protein migration in two-dimensional gels as a result of stimulation with LPS. Western analysis indicated a change in reactivity of some isoforms of RNA-binding proteins and the appearance and disappearance of others. LPS is known to activate multiple protein kinase cascades and may lead to the phosphorylation of many of the RNA-binding proteins and alter their functional properties. Indeed, it has been shown that phosphorylation of various hnRNP proteins resulted in altered affinity of the proteins for either RNA targets and/or other proteins (29, 35, 36). Recently, it has been reported that dephosphorylation of the p40 isoform of AUF1 coincided with rapid induction and increased stability of ARE-containing messages (37). Furthermore, the phosphorylation status of p40AUF1 altered its affinity for ARE-containing messages and altered the RNA conformation (38). The changes in protein migration we have found for AUF1, as well as the other proteins, may be the result of altered phosphorylation states. Changes in pI are not limited to phosphorylation events and may arise because of other post-translational events such as sulfation and acetylation, which would lead to a change in protein charge. The cause of the differences in protein migration after stimulation with LPS is not yet known. Furthermore, it is difficult to determine the exact nature of post-translational modifications using immunological methods and requires the use of more sensitive and quantitative techniques.

The results presented in this report demonstrate a wide range of isoforms of RNA-binding proteins that were present in RAW cells which were able to bind to a specific sequence of the 3′-UTR of COX-2. EMSA results suggest that many of these proteins form stable multimeric complexes that are able to bind to RNA. Results using control RNA affinity probes suggest that binding of these proteins was sequence-specific and increases the number of members that belong to the family of ARE-binding proteins. Further work remains to be done to determine whether the same RNA-protein interactions shown in this report also occur *in vivo* and to characterize the biological significance of such interactions.

Activation of cells with LPS results in modification of the RNA-protein complexes. The precise nature of the modifications is not yet known but represents potential post-translational alterations that may regulate RNA-protein and/or protein-protein interactions. It is these interactions that ultimately determine whether the message is transported out of the nucleus and directed toward the translational machinery or targeted for degradation.

Acknowledgment—We are grateful to Gary Brewer for providing the anti-AUF1 antibody.

REFERENCES

1. Smith, W. L., DeWitt, D. L., and Garavito, R. M. (2000) *Annu. Rev. Biochem.* **69**, 145–182
2. Barrios-Rodiles, M., Tiraloche, G., and Chadee, K. (1999) *J. Immunol.* **163**, 963–969
3. Eliopoulos, A. G., Dumitru, C. D., Wang, C. C., Cho, J., and Tsichlis, P. N. (2002) *EMBO J.* **21**, 4831–4840
4. Wadleigh, D. J., Reddy, S. T., Kopp, E., Ghosh, S., and Herschman, H. R. (2000) *J. Biol. Chem.* **275**, 6259–6266
5. Dean, J. L. E., Brook, M., Clark, A. R., and Saklatvala, J. (1999) *J. Biol. Chem.* **274**, 264–269
6. Frevel, M. A. E., Bakheet, T., Silva, A. M., Hissong, J. G., Khabar, K. S. A., and Williams, B. R. G. (2003) *Mol. Cell. Biol.* **23**, 425–436
7. Guhaniyogi, J., and Brewer, G. (2001) *Gene (Amst.)* **265**, 11–23
8. Grzybowska, E. A., Wilczynska, A., and Siedlecki, J. A. (2001) *Biochem. Biophys. Res. Commun.* **288**, 291–295
9. Bakheet, T., Frevel, M., Williams, B. R., Greer, W., and Khabar, K. S. (2001) *Nucleic Acids Res.* **29**, 246–254
10. Tebo, J., Der, S., Frevel, M., Khabar, K. S. A., Williams, B. R. G., and Hamilton, T. A. (2003) *J. Biol. Chem.* **278**, 12085–12093
11. Cok, S. J., and Morrison, A. R. (2001) *J. Biol. Chem.* **276**, 23179–23185
12. Fan, X. C., and Steitz, J. A. (1998) *EMBO J.* **17**, 3448–3460
13. Peng, S. S.-Y., Chen, C.-Y. A., Xu, N., and Shyu, A.-B. (1998) *EMBO J.* **17**, 3461–3470
14. Piecyk, M., Wax, S., Beck, A. R. P., Kedersha, N., Gupta, M., Maritim, B., Chen, S., Gueydan, C., Kruys, V., Streuli, M., and Anderson, P. (2000) *EMBO J.* **19**, 4154–4163
15. Gueydan, C., Droogmans, L., Chalon, P., Huez, G., Caput, D., and Kruys, V. (1999) *J. Biol. Chem.* **274**, 2322–2326
16. Mahtani, K. R., Brook, M., Dean, J. L. E., Sully, G., Saklatvala, J., and Clark, A. R. (2001) *Mol. Cell. Biol.* **21**, 6461–6469
17. Sawaoka, H., Dixon, D. A., Oates, J. A., and Boutaud, O. (2003) *J. Biol. Chem.* **278**, 13928–13935
18. Lai, W. S., Kennington, E. A., and Blackshear, P. J. (2003) *Mol. Cell. Biol.* **23**, 3798–3812
19. DeMaria, C. T., and Brewer, G. (1996) *J. Biol. Chem.* **271**, 12179–12184
20. Zhang, W., Wagner, B. J., Ehrenman, K., Schaefer, A. W., DeMaria, C. T.,

Downloaded from www.jbc.org by on January 31, 2007

Crater, D., DeHaven, K., Long, L., and Brewer, G. (1993) *Mol. Cell Biol.* **13**, 7652–7665
21. Dean, J. L., Sully, G., Wait, R., Rawlinson, L., Clark, A. R., and Saklatvala, J. (2002) *Biochem. J.* **366**, 709–719
22. Wagner, B. J., DeMaria, C. T., Sun, Y., Wilson, G. M., and Brewer, G. (1998) *Genomics* **48**, 195–202
23. Beck, A. R., Medley, Q. G., O'Brien, S., Anderson, P., and Streuli, M. (1996) *Nucleic Acids Res.* **24**, 3829–3835
24. Kotlyarov, A., Neininger, A., Schubert, C., Eckert, R., Birchmeier, C., Volk, H. D., and Gaestel, M. (1999) *Nat. Cell Biol.* **1**, 94–97
25. Lasa, M., Mahtani, K. R., Finch, A., Brewer, G., Saklatvala, J., and Clark, A. R. (2000) *Mol. Cell. Biol.* **20**, 4265–4274
26. Dixon, D. A., Tolley, N. D., King, P. H., Nabors, L. B., McIntyre, T. M., Zimmerman, G. A., and Prescott, S. M. (2001) *J. Clin. Invest.* **108**, 1657–1665
27. Sengupta, S., Jang, B. C., Wu, M. T., Paik, J. H., Furneaux, H., and Hla, T. (2003) *J. Biol. Chem.* **278**, 25227–25233
28. Mukhopadhyay, D., Houchen, C. W., Kennedy, S., Dieckgraefe, B. K., and Anant, S. (2003) *Mol. Cell* **11**, 113–126
29. Rousseau, S., Morrice, N., Peggie, M., Campbell, D. G., Gaestel, M., and Cohen, P. (2002) *EMBO J.* **21**, 6505–6514
30. Ma, A. S. W., Moran-Jones, K., Shan, J., Munro, T. P., Snee, M. J., Hoek, K. S., and Smith, R. (2002) *J. Biol. Chem.* **277**, 18010–18020
31. Nichols, R. C., Wang, X. W., Tang, J., Hamilton, B. J., High, F. A., Herschman, H. R., and Rigby, W. F. (2000) *Exp. Cell Res.* **256**, 522–532
32. Danno, S., Nishiyama, H., Higashitsuji, H., Yokoi, H., Xue, J. H., Itoh, K., Matsuda, T., and Fujita, J. (1997) *Biochem. Biophys. Res. Commun.* **236**, 804–807
33. Danno, S., Itoh, K., Matsuda, T., and Fujita, J. (2000) *Am. J. Pathol.* **156**, 1685–1692
34. Baghdoyan, S., Dubreuil, P., Eberle, F., and Gomez, S. (2000) *Blood* **95**, 3750–3757
35. Pype, S., Slegers, H., Moens, L., Merlevede, W., and Goris, J. (1994) *J. Biol. Chem.* **269**, 31457–31465
36. Ostrowski, J., Schullery, D. S., Denisenko, O. N., Higaki, Y., Watts, J., Aebersold, R., Stempka, L., Gschwendt, M., and Bomsztyk, K. (2000) *J. Biol. Chem.* **275**, 3619–3628
37. Wilson, G. M., Lu, J., Sutphen, K., Sun, Y., Huynh, Y., and Brewer, G. (2003) *J. Biol. Chem.* **278**, 33029–33038
38. Wilson, G. M., Lu, J., Sutphen, K., Suarez, Y., Sinha, S., Brewer, B., Villanueva Felciano, E. C., Ysla, R. M., Charles, S., and Brewer, G. (2003) *J. Biol. Chem.* **278**, 33039–33048

Downloaded from www.jbc.org by on January 31, 2007

THE JOURNAL OF BIOLOGICAL CHEMISTRY
© 2003 by The American Society for Biochemistry and Molecular Biology, Inc.

Vol. 278, No. 38, Issue of September 19, pp. 36157–36162, 2003
Printed in U.S.A.

The Proximal Region of the 3′-Untranslated Region of Cyclooxygenase-2 is Recognized by a Multimeric Protein Complex Containing HuR, TIA-1, TIAR, and the Heterogeneous Nuclear Ribonucleoprotein U*

Received for publication, March 12, 2003, and in revised form, June 20, 2003
Published, JBC Papers in Press, July 9, 2003, DOI 10.1074/jbc.M302547200

Steven J. Cok, Stephen J. Acton, and Aubrey R. Morrison‡

From the Departments of Medicine and Molecular Biology and Pharmacology, Washington University School of Medicine, St. Louis, Missouri 63110

Cyclooxygenase-2 (COX-2) is an early response gene induced in renal mesangial cells by interleukin-1β (IL-1β). The 3′-untranslated region (3′-UTR) of COX-2 mRNA plays an important role in IL-1β induction by regulating message stability and translational efficiency. The first 60 nucleotides of the 3′-UTR of COX-2 are highly conserved and contain multiple copies of the regulatory sequence AUUUA. Introduction of the 60-nucleotide sequence into the 3′-UTR of a heterologous reporter gene resulted in a 70% decrease in reporter gene expression. Electrophoretic mobility shift assays (EMSAs) demonstrated that mesangial cell nuclear fractions contain a multimeric protein complex that bound this region of COX-2 mRNA in a sequence-specific manner. We identified four members of the protein-RNA complex as HuR, TIA-1, TIAR, and the heterogeneous nuclear ribonucleoprotein U (hnRNP U). Treatment of mesangial cells with IL-1β caused an increase in cytosolic HuR, which was accompanied by an increase in COX-2 mRNA that co-immunoprecipitated with cytosolic HuR. Therefore, we propose that HuR binds to the proximal region of the 3′-UTR of COX-2 following stimulation by IL-1β and increases the expression of COX-2 mRNA by facilitating its transport out of the nucleus.

Many early response genes encoding cytokines, lymphokines, and proto-oncogenes are transiently expressed in response to extra cellular stimuli. Although the gene can be transcriptionally regulated, the level of expression is determined in large part by changes in the half-life and/or translational efficiency of the mRNA. These changes are regulated through interactions between specific RNA sequences and trans-acting RNA-binding proteins that influence nuclear export, targeting to the ribosome, and translation of the mRNA into protein.

Among the best studied regulatory sequences are the adenosine- and uridine-rich elements (AREs),[1] found in the 3′-untranslated region (3′-UTR) of many short lived mRNAs (1–5). Most AREs contain multiple copies of the sequence AUUUA, which are sufficient to confer message instability when placed in the 3′-UTR of a normally stable reporter message. Additionally, AREs can play a role in regulating translational efficiency of target mRNAs (6–8). Once cells are activated by specific extracellular signals, these same ARE sequences are required for message stabilization and/or increased translational efficiency.

Several RNA-binding proteins have been isolated based on their ability to regulate mRNA expression through ARE sequences. Some of these proteins promote message expression, *e.g.* hnRNP A1 (9) and HuR (10, 11), whereas others primarily decrease message expression, *e.g.* AUF1 (hnRNP D) (12–14), tristetraprolin (TTP) (15–17), TIAR and TIA-1, (6, 8) and CUGBP2 (18). All of these proteins are believed to function in the cytoplasm but appear to be regulated by shuttling in and out of the nucleus. The mechanism whereby AREs regulate message expression in the presence of multiple and sometimes diametrically opposed signals is not fully understood.

Cyclooxygenase (COX) catalyzes the rate-limiting step in the biosynthesis of prostaglandins (19). Three isoforms of COX have been identified as follows: 1) COX-1, a constitutively expressed isoform; 2) COX-2, an early response gene that can be induced by a variety of mitogenic and pro-inflammatory stimuli; and 3) COX-3, an alternatively spliced variant of COX-1 (20). In rat mesangial cells, interleukin-1β (IL-1β) caused a significant increase in COX-2 expression due, in part, to altered mRNA stability and translational efficiency (21–23).

The 3′-UTR of COX-2 is greater than 2 kilobases in length and, depending on the species, contains 11–22 copies of the ARE core sequence AUUUA. It has been shown previously that the 3′-UTR of COX-2 contains multiple regulatory elements, some of which co-localized with several of the AREs (18, 21, 24–26). One such element identified in the first 60 nucleotides of the 3′-UTR of murine COX-2 contained seven AUUUA repeats and was able to decrease message stability and translational efficiency of a heterologous reporter gene (21). This region of the murine 3′-UTR is highly conserved across species and aligns within the region of human COX-2 mRNA that was shown to bind HuR (27), AUF1 (25), and CUGBP2 (18). Furthermore, dysregulated expression of HuR promoted increased COX-2 expression in colon cancer cells (27). Thus, the binding of HuR and other yet to be determined proteins to the 3′-UTR

* This work was supported by United States Public Health Service Award Grant DK 59932 (to A. R. M.) and Barnes-Jewish Hospital Foundation Grant 5680-02 (to S. J. C). The costs of publication of this article were defrayed in part by the payment of page charges. This article must therefore be hereby marked "*advertisement*" in accordance with 18 U.S.C. Section 1734 solely to indicate this fact.

‡ To whom correspondence should be addressed: Washington University School of Medicine, 4940 Parkview Place, Wohl Clinic, Rm. 8843, St. Louis, MO 63110. Tel.: 314-454-8464; Fax: 314-454-8430; E-mail: Morrison@pcg.wustl.edu.

[1] The abbreviations used are: ARE, adenosine- and uridine-rich element; COX, cyclooxygenase; DTT, dithiothreitol; EMSA, electrophoretic mobility shift assay; 6-FAM, 6-carboxyfluorescein; GAPDH, glyceraldehyde-3-phosphate dehydrogenase; hnRNP, heterogeneous nuclear ribonucleoprotein; IL-1β, interleukin-1β; RT, reverse transcription; snRNP, small nuclear ribonucleoprotein; TAMRA, 6-carboxytetramethylrhodamine; TTP, tristetraprolin; 3′-UTR, 3′-untranslated region.

Downloaded from www.jbc.org by on January 31, 2007

of COX-2 is likely to play an important role in regulating COX-2 expression.

In this report we show that HuR, TIA-1, TIAR, and hnRNP U bind the first 60 nucleotides of the 3′-UTR of murine COX-2. Stimulation of mesangial cells with IL-1β resulted in a transient increase in cytosolic HuR and associated COX-2 mRNA, suggesting that HuR plays a regulatory role by facilitating the transport of COX-2 mRNA out of the nucleus.

EXPERIMENTAL PROCEDURES

Mesangial Cell Culture—Primary rat mesangial cell cultures were prepared from male Sprague-Dawley rats as described previously (28). Cells were grown in RPMI 1640 medium supplemented with 10% (v/v) heat-inactivated fetal bovine serum, 0.6% (v/v) insulin, 100 units/ml penicillin, 100 μg/ml streptomycin, 250 μg/ml amphotericin B, and 15 mM HEPES. Where indicated, mesangial cells were stimulated with IL-1β (100 units/ml) for 60 min.

Plasmids—Reporter gene constructs were generated as described previously (21). Briefly, various regions of the 3′-UTR of COX-2 were amplified by PCR using primers terminating in *Xba*I recognition sequences. PCR products were ligated in the unique *Xba*I site of the pGL3 control vector (Promega) located in the 3′-UTR of the firefly luciferase gene. Vectors used for synthesis of RNA probes for electrophoretic mobility shift assays (EMSAs) were constructed by amplifying the same 3′-UTR sequences, except that the primers encoded a *Hin*dIII recognition site at the 5′ end and a *Bam*HI site at the 3′ end. The PCR products were ligated into the *Hin*dIII and *Bam*HI sites of pcDNA3 (Stratagene).

Transient Transfections—Mesangial cells were transiently transfected using SuperFect Transfection Reagent (Qiagen). Cells were plated into 60-mm dishes, grown to 50–75% confluency, and transfected with 5 μg of reporter gene plasmid DNA at a 2:1 SuperFect-to-DNA ratio. Following transfection, cells were incubated overnight for gene expression.

Luciferase Assay—Luciferase activity was determined using a luciferase assay system following the manufacturer's protocol (Promega). Briefly, cell monolayers in 60-mm dishes were removed by scraping into 200 μl of reporter lysis buffer. Cells were vortexed, and cellular debris was removed by centrifugation (30 s at 12,000 × *g*). Luciferase activity was measured using a Lumat LB 9507 luminometer (EG & G Wallac) as described previously (21).

Quantitative RT-PCR—Total RNA was isolated from cells using RNA STAT-60 reagent (Tel-Test, Inc.). Luciferase RNA was quantified by RT-PCR using TaqMan real-time PCR. Luciferase amplification primers were 5′-GCGCGGAGGAGTTGTGTT-3′ for the forward primer, 5′-TCTGATTTTTCTTGCGTCGAGTT-3′ for the reverse primer, and 6-FAM-TGGACGAAGTACCGAAAGGTCTTACCGG-TAMRA as the TaqMan probe. Luciferase expression was normalized to ribosomal RNA as measured using TaqMan ribosomal RNA control reagents (Applied Biosystems). Relative amounts of luciferase cDNA were calculated by the comparative C_T method (Applied Biosystems user bulletin number 2) and expressed as a percentage of luciferase cDNA measured in cells transfected with pGL3-control. COX-2 RNA was quantified by RT-PCR using primers and probes purchased from Applied Biosystems (Assays-on-Demand number MM-00478374).

RNA Probe Synthesis—Labeled RNA probes were generated by *in vitro* transcription using T7 RNA polymerase plus (Ambion) and RNA probe plasmids (described above) as template. A sequence-nonspecific probe was generated using EcoR1 linearized TOPO TA cloning vector pCR 2.1-TOPO (Invitrogen) as template. Transcription reactions contained 100 units of T7 polymerase, 500 μM each ATP, CTP, and GTP, 12.5 μM UTP, 200 μCi of [^{32}P]UTP (6000 Ci/mmol, PerkinElmer Life Sciences), 10 mM DTT, and 10 μg of plasmid template linearized by *Bam*HI digestion in a total volume of 50 μl of 1× transcription buffer (Ambion). Transcription reactions were incubated for 1 h at 37 °C. For cold probes, [^{32}P]UTP was substituted with 500 μM UTP. Unincorporated nucleotides were removed using Sephadex G-25 mini Quick Spin RNA columns (Roche Applied Science).

Cell Fractionation—Rat mesangial cells were harvested by scraping into hypotonic buffer containing 10 mM HEPES, pH 7.5, 10 mM KCl, 1 mM EDTA, 1 mM EGTA, 1 mM DTT, 1 mM $MgCl_2$, 5% glycerol, and 0.1 mM $NaVO_4$ with protease inhibitors (1 μg/ml leupeptin, 2 μg/ml aprotinin, and 1 μg/ml Pefabloc) and allowed to swell for 15 min. Cells were lysed by adding 10% Nonidet P-40 (final concentration, 0.25%), and nuclei were pelleted by centrifugation (30 s at 15,000 × *g*). Supernatant was centrifuged for 5 min at 15,000 × *g* and stored as the cytoplasmic fraction at −70 °C. The nuclei were washed two times by centrifugation (1500 × *g* for 10 min) in 10 mM HEPES, pH 7.5, 10 mM KCl, 1 mM DTT, and 1 mM $MgCl_2$. The final pellet was resuspended in nuclear lysis buffer (20 mM HEPES, pH7.5, 0.4 M NaCl, 1 mM EDTA, 1 mM EGTA, 1 mM DTT, 1 mM $MgCl_2$, and 25% glycerol with protease inhibitors). Nuclei were incubated on ice for 15 min with vortexing every 2–3 min and centrifuged for 5 min at 15,000 × *g*. Supernatant was saved as the nuclear fraction and stored at −70 °C.

EMSAs and Antibody Supershifts—Typically, 5–10 μg of cell fraction protein was incubated for 30 min at 37 °C in binding buffer (10 mM HEPES, pH 7.6, 5 mM $MgCl_2$, 40 mM KCl, 1 mM DTT, 5% glycerol, and 5 mg/ml heparin) with 1–5 pmol of labeled RNA probe in a final volume of 20 μl. For supershift experiments, binding mixtures included 0.2 μg of affinity-purified IgG raised against HuR, TIA-1, TIAR, or TTP (Santa Cruz Biotechnology), 1 μg of affinity-purified anti-AUF1 (Upstate Biotechnology), 1 μl of anti-hnRNP A1 and anti-hnRNP U (generous gift of Gideon Dreyfuss), or 1 μl of normal goat serum (Sigma). RNase T1 (10 units) was added to EMSA or supershift samples and incubated for 15 min at 37 °C. Loading buffer (5 μl) containing 80% glycerol and 0.1% bromphenol blue in 50 mM Tris-Cl, pH 7.5, was added, and samples were electrophoresed (250 V for 2.5 h) on 4% polyacrylamide gels (pre-run for 1 h at 250 V) containing 44 mM Tris-Cl, pH 8.3, 44 mM boric acid, 1 mM EDTA, 4% acrylamide-bisacrylamide (29:1), and 2.5% glycerol. EMSAs were visualized by autoradiography.

Immunoprecipitation—Antibodies were immobilized onto an agarose gel using a Seize Primary immunoprecipitation kit (Pierce Biotechnology). An equivalent of 3 μg of immobilized antibody was added to 5 mg of nuclear protein and incubated at room temperature for 2 h. Immunoprecipitates were isolated by centrifugation (1 min at 12,000 × *g*) and washed two times with immunoprecipitation buffer (25 mM Tris, 150 mM NaCl, pH 7.2). Total RNA was extracted from immunoprecipitates using an RNeasy RNA isolation kit (Qiagen).

Western Analysis—Cytosolic and nuclear proteins were separated by PAGE-SDS and transferred to Immobilon-P transfer membranes (Millipore). Western blots were probed with monoclonal anti-HuR antibody (Santa Cruz Biotechnology) at a 1:1000 dilution. Signal detection was carried out using an enhanced chemiluminescence system (ECL, Amersham Biosciences). Western analysis of cell fractionations was carried out using a polyclonal anti-U1 snRNP 70 antibody (Santa Cruz Biotechnology) at a 1:1000 dilution and a monoclonal anti-GAPDH antibody (Ambion) at a 1:4000 dilution. Cytosolic HuR was quantitated on the Discovery Series densitometer, and the band intensities were measured using Quantity One software (Bio-Rad).

RESULTS

AREs from the 3′-UTR of COX 2 Regulate Message Stability—The first 60 nucleotides of the 3′-UTR of COX-2 message contains multiple copies of the sequence AUUUA (Fig. 1, *Truncation #1*). We have reported previously that this region of the 3′-UTR of COX-2 had a significant effect on post-transcriptional regulation of COX-2 expression (21). These 60 nucleotides contain a major translational control element and caused a decrease in message stability when placed in a chimeric reporter gene expressed in an immortalized mouse mesangial cell system. In this study, we used primary rat mesangial cells to further define key regulatory sequences and trans-acting protein factors that may play important roles in regulating the expression of COX-2 in response to stimulation with IL-1β.

Insertion of the first 60 nucleotides of the 3′-UTR of COX-2 into the 3′-UTR of a luciferase reporter message resulted in a 70% decrease in luciferase activity and a similar decrease in steady-state mRNA levels when expressed in primary rat mesangial cells (Fig. 2). This region contains seven copies of the sequence AUUUA, *i.e.* three that are overlapping and located within the proximal 25 nucleotides and four copies clustered within the distal 28 nucleotide region (Fig. 1, *Truncation #1*). Removal of the first 19 nucleotides (Fig. 1, *Truncation #2*) disrupted the proximal overlapping AUUUA repeats but had no effect on luciferase reporter gene activity or mRNA levels (Fig. 2). Truncation from the proximal 5′-end to nucleotide 24 (Fig. 1, *Truncation #3*) resulted in an additional 75% decrease (93% overall) in luciferase activity and mRNA levels (Fig. 2). This deletion coincides with the removal of all of the first three AUUUA consensus sequences (Fig. 1, *Truncation #3*), suggest-

Downloaded from www.jbc.org by on January 31, 2007

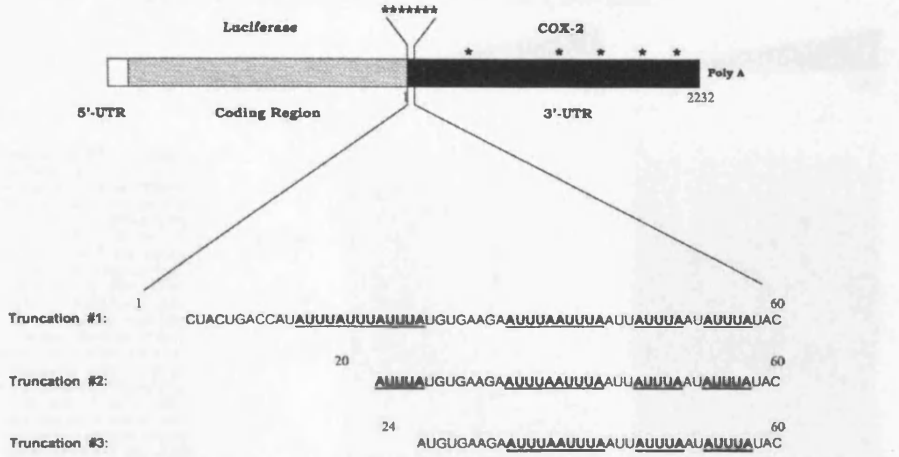

FIG. 1. **Features of the 3′-UTR of COX-2 mRNA and the sequence of truncations used for RNA probes and reporter gene assays.** The 3′-UTR of murine COX-2 contains several copies of the consensus sequence, AUUUA, as indicated by the *asterisks* (*). Primary sequences of the truncated RNA affinity probes with AUUUA elements are *underlined* and in *boldface*. Numbering begins with the first nucleotide of the 3′-UTR of COX-2.

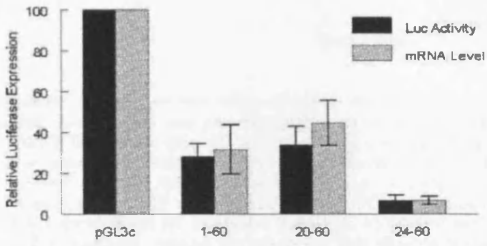

FIG. 2. **Relative expression of chimeric reporter-gene constructs in rat mesangial cells.** Primary rat mesangial cells were transiently transfected with plasmids encoding luciferase alone, pGL3c, or containing the indicated portion of the first 60 nucleotides of the 3′-UTR of COX-2. Luciferase enzyme activities were measured in cell lysates and normalized to cell protein. Luciferase mRNA levels were measured in total RNA extracts and normalized to ribosomal RNA. Results were expressed as a percentage of measurements using cells transfected with pGL3c. Values are the means ± S.E. for $n = 10$ (activity) or $n = 3$ (mRNA) independent experiments.

ing that the first 24 nucleotides contain a positive control element and that the distal 17 nucleotides contained a negative control element.

Nuclear Protein Complexes Bind to COX-2 AREs—To determine whether changes in luciferase activity following truncation of the 3′-UTR of COX-2 were reflected by altered binding of protein(s) to this region of the message, we performed EMSAs using radiolabeled RNA probes corresponding to the regions of the three truncations shown in Fig. 1 and protein fractions isolated from rat mesangial cells. Incubation of the RNA probe encoded by the first 60 nucleotides of the 3′-UTR of COX-2 with mesangial cell nuclear protein fractions resulted in the formation of three prominent RNA-protein complexes (Fig. 3). The RNA-protein interaction was sequence-specific, because the addition of increasing concentrations of non-labeled RNA of the same nucleotide sequence effectively competed for all three complexes, whereas there was no effect when including equal amounts of a non-related RNA of the same size derived from the TOPO TA cloning vector. All of the three complexes were present at similar levels using each of the various truncated RNA probes (Fig. 4; non-immune controls), suggesting that removal of the proximal portion of the RNA had no significant effect on the formation of the RNA-protein complexes. Incubating probes with cytosolic fractions also resulted in formation of three RNA-protein complexes that had a similar electrophoretic mobility but at a consistently lower intensity compared with complexes formed using an equal mass of nuclear proteins (results not shown). Stimulation of rat mesangial cells with IL-1β for 30–120 min had no effect on the pattern of shift and little or no change in the intensity of the shifted RNA probe (results not shown).

TIA-1, TIAR, HuR, and hnRNP U Bind the ARE Region of the 3′-UTR of COX-2—As a first step toward identifying which proteins were present in the protein-RNA complexes, we included in the binding incubation antibodies to known RNA-binding proteins, as well as non-immune serum as a control, and assessed either the formation of a higher molecular weight RNA-protein complex (supershift) or disruption of one or more of the RNA-protein complexes. Both results would suggest that the epitope recognized by the antibody was present in the complex. The three major RNA-protein complexes were still present when non-immune serum was included in the binding reaction (Fig. 4, *lanes* labeled *NI*). In contrast, inclusion of both anti-TIA-1 and anti-TIAR antibodies produced a supershift (Fig. 4*A*, *S1*) that was accompanied by a significant reduction in RNA-protein complex C2. The intensity of the supershift increased as the RNA probe was truncated, suggesting that a more stable complex forms between TIA-1 and TIAR and the shortened RNA probes.

Addition of HuR antibody also resulted in a supershift (Fig. 4*A*, S2) and a loss of the C3 complex. The supershift was most prominent with the 60-nucleotide probe and decreased as the probes were truncated. However, the disappearance of the C3 complex occurred to the same extent for all three RNA probes. A less prominent complex migrating below complex C3 also disappeared from the 1–60 probe when HuR antibodies were added, suggesting that HuR may form more than one complex with COX-2 RNA. Thus, it appears that HuR binds all the RNA probes, but only in the presence of the 1–60 probe was a

Downloaded from www.jbc.org by on January 31, 2007

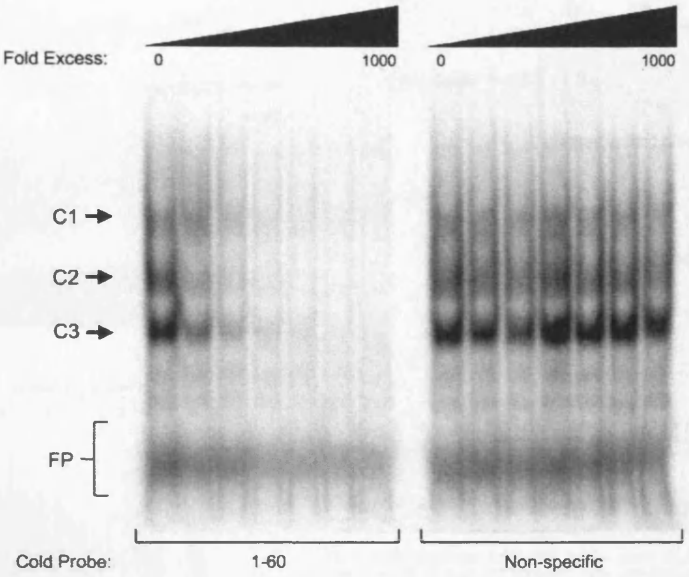

FIG. 3. **Detection of RNA protein complexes that form with the first 60 nucleotides of the 3′-UTR of COX-2.** Radiolabeled RNA probes corresponding to nucleotides 1–60 were incubated with nuclear protein fractions for 30 min at 37 °C, digested with RNase T1 (10 units), and subjected to electrophoresis on non-denaturing polyacrylamide gels. Complexes were detected by a change in electrophoretic mobility compared with free probes (*FP*). Increasing amounts of non-labeled RNA probes were added to radiolabeled RNA prior to the addition of cellular fractions. Radiolabeled RNA-protein complexes (*C1*, *C2*, and *C3*) were inhibited by increasing concentrations of non-labeled RNA of the same sequence but not by non-related RNA species of the same nucleotide length.

complex formed that was stable enough to result in a supershift. A supershift was also observed when using the anti-hnRNP U antibody (Fig. 4*B*, *S1*). In this case, the supershift was only seen in the presence of the truncated probes and failed to occur with the full-length probe. Inclusion of antibodies directed against TTP or hnRNP A1 failed to show any observable supershift but did result in a decreased intensity of some of the complexes, raising the possibility that these proteins may also be directly or indirectly associated with the RNA probes. In our hands, EMSA experiments using mesangial cellular fractions failed to detect formation of a protein-RNA complex between AUF1 and this region of the 3′-UTR of murine COX-2.

Stimulation of Rat Mesangial Cells with IL-1β Caused a Transient Increase in Cytosolic HuR—It has been reported that HuR is shuttled from the nucleus to the cytoplasm in response to various cellular stresses (29–34). To determine whether cytoplasmic HuR increased in response to IL-1β stimulation, we isolated cytoplasmic protein fractions from mesangial cells at various times after treatment with IL-1β and determined the HuR protein content. The purity of the cell fractions was assessed by Western analysis using an antibody directed against the splicing factor U1 snRNP 70 as a marker of nuclear fractions and an antibody against GAPDH as a cytosolic protein marker. The Western results indicate that we have isolated nuclear and cytoplasmic cell fractions that are free of any detectable cross-contamination and that the vast majority of HuR resides in the nuclear fraction (Fig. 5*A*). When we probed for cytosolic HuR using increasing amounts of protein, we found that HuR was detectable in the cytosol and that cells treated with IL-1β for 60 min had appreciably more cytosolic HuR than non-stimulated control cells (Fig. 5*B*). Time course experiments indicate that cytosolic HuR increased as early as 15 min following administration of IL-1β and peaked at 30 min (Fig. 6*A*). Cytosolic levels of HuR remained elevated for at least 4 h and returned to control levels within 24 h. There was no appreciable decrease in nuclear HuR levels, presumably due to the fact that only a small portion of total HuR exited the nucleus. Cytosolic GAPDH remained constant over this time period (Fig. 6*A*).

Because HuR binds the 3′-UTR of COX-2 in the EMSA experiments and IL-1β stimulation increased cytosolic HuR, we next tested whether there were corresponding changes in cytosolic HuR-COX-2 mRNA complexes. Cytosolic fractions were immunoprecipitated with anti-HuR antibodies, and the amount of co-immunoprecipitated COX-2 mRNA was measured by quantitative RT-PCR. The DNA transcribed by reverse transcriptase was quantitated using a cDNA clone of COX-2 as standard. The amount of COX-2 mRNA present in immunoprecipitates of cytosolic fraction from non-stimulated cells was below the detectable limit of the assay. Cells treated with IL-1β contained detectable amounts of cytosolic HuR-COX-2 mRNA complexes that increased from 30 to 60 min (Fig. 6*B*), suggesting that increased transport of HuR into the cytosol facilitated the export of COX-2 mRNA.

DISCUSSION

Post-transcriptional regulation of gene expression is tightly orchestrated through complex interactions of various RNA-binding proteins with target mRNAs. The best characterized target sequence is the ARE. Identification of different ARE-binding proteins and the elucidation of their functions has been the subject of many recent investigations. The AREs located in the proximal region of the 3′-UTR of COX-2 play an important role in regulating gene expression (21, 24–26). This region also has been shown to be recognized by the RNA-binding proteins HuR (27), AUF1 (25), and CUBP2 (18). Here we report that the first 60 nucleotides of the 3′-UTR of murine COX-2 were recognized by TIA-1, TIAR, and hnRNP U, in addition to HuR.

Based on EMSAs using truncated RNA probes we have shown that TIA-1 and TIAR both bind to a 37-nucleotide region of the 3′-UTR of COX-2 mRNA. This corresponds to the region reported to affect message translation (21). Both TIAR and TIA-1 have been shown to bind an ARE-containing region of

THE JOURNAL OF BIOLOGICAL CHEMISTRY VOL.

Downloaded from www.jbc.org by on January 31, 2007

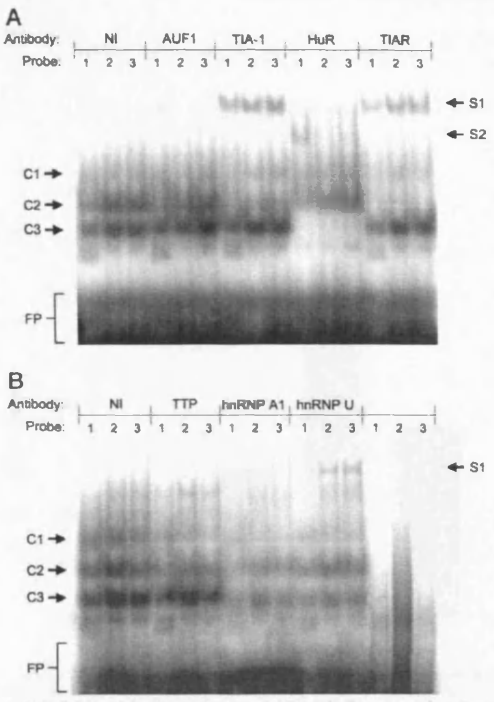

FIG. 4. **Identification of several RNA-binding proteins that recognize the first 60 nucleotides of the 3′-UTR of COX-2.** Radiolabeled RNA probes corresponding to nucleotides 1–60 (*probe 1*), 20–60 (*probe 2*), or 24–60 (*probe 3*) of the 3′-UTR of COX-2 were incubated with proteins from nuclear cellular fractions in the presence of nonimmune serum (*NI*) or antibodies raised against the AUF1, TIA-1, HuR, and TIAR (*A*) or TTP, hnRNP A1, hnRNP U, and probe alone (*B*). Protein-RNA complexes (*C1*, *C2*, and *C3*), free probe (*FP*), and supershifted complexes (*S1* and *S2*) are indicated.

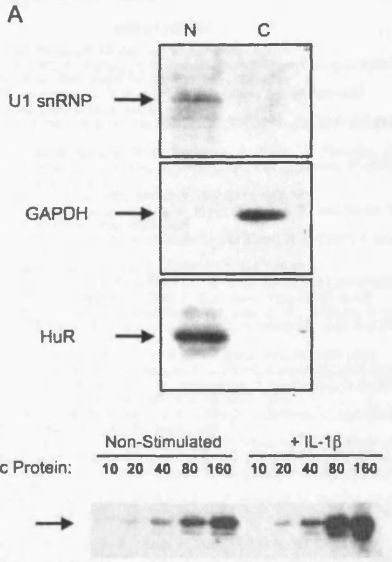

FIG. 5. **HuR localized primarily to the nucleus.** *A*, nuclear (*N*) and cytosolic (*C*) proteins (10 mg each) were separated by PAGE-SDS and analyzed for U1 snRNP 70, GAPDH, and HuR by Western blotting. Nuclear and cytosolic fractions were free of any detectable cross-contamination. HuR was detected only in the nuclear fraction at this protein concentration. *B*, increasing protein concentration was required for detection of cytosolic HuR. Cytosol from cells treated with IL-1β for 6 min contained elevated levels of HuR protein.

the 3′-UTR of tumor necrosis factor α (TNF-α), resulting in translational silencing of the TNF-α message (6, 8). Furthermore, overexpression of TIA-1 in COS cells resulted in decreased expression of a reporter gene harboring the ARE region of TNF-α (35). Thus, it seems probable that binding of TIA-1 and/or TIAR to the 3′-UTR of COX-2 promotes translational silencing of the message. We also found that hnRNP U binds to this region of the 3′-UTR of COX-2. It is not clear at this moment what the functional significance of this binding is; however, hnRNP U has been shown to bind RNA (36, 37) as well as other proteins such as the glucocorticoid receptor (38). The ability to bind both RNA and proteins raises the possibility that hnRNP U may act as a scaffolding protein and mediate interactions between target mRNAs and proteins regulating mRNA expression. Based on the report by Lasa *et al.* (25), we predicted that AUF1 and the 3′-UTR of COX-2 could form a protein-RNA complex stable to EMSA and supershift assays. The inability to detect a stable complex may represent differences in cell-type and/or species-specific interactions or be due to differences in experimental conditions.

Another well characterized ARE-binding protein is HuR. Binding of mRNA by HuR is associated with increased message stability (10, 11, 39). A number of HuR target mRNAs have been reported, including the message encoding COX-2 protein (27). We have determined that one of the HuR binding sites is within the first 60 nucleotides of the 3′-UTR of murine COX-2, as evidenced by the HuR antibody-dependent supershift (Fig. 4*A*, *S2*). The supershift was accompanied by a significant decrease of a major RNA-protein complex, C3, and a minor lower molecular weight complex. When truncated RNA probes were incubated with the anti-HuR antibody, the decrease in C3 was still evident, but there was no supershift (Fig. 4*A*), suggesting that more than one HuR-RNA complex was present and that the more stable supershifted complex required the full 60-nucleotide probe.

Translocation of HuR from the nucleus to the cytoplasm has been shown in response to a variety of stimuli, including heat shock (29–31), serum stimulation (32), UV light (33), and nutrient limitation (34). In response to heat shock, HuR binds the proteins pp32 and APRIL, which modulates the ability to transport HuR out of the nucleus through interactions with nuclear export factor CRM1 (31). The CRM1-dependent transport can be inhibited by leptomycin B. Recently, it has been reported that leptomycin B inhibited COX-2 mRNA stabilization by blocking nuclear export of the COX-2 message (40). Although it was not determined whether HuR played a direct role in the transport of COX-2 mRNA, it does represent a reasonable conclusion. Here, we show that IL-1β stimulation caused an increase in cytosolic HuR protein levels and HuR-COX-2 mRNA complexes. Thus, we propose that in response to IL-1β stimulation there was increased binding of HuR to COX-2 mRNA, which facilitates export of the message out of the nucleus.

Taken together, our results suggest that multiple proteins can bind to a relatively short portion of the 3′-UTR of COX-2.

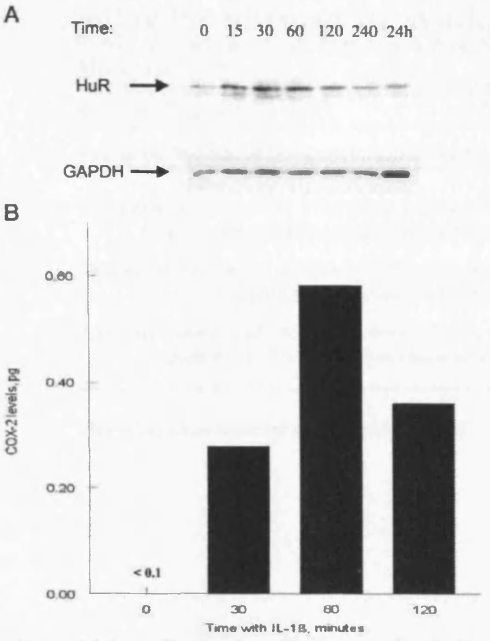

FIG. 6. **IL-1β caused a time-dependent increase in cytosolic HuR and HuR-COX-2 mRNA complexes.** *A*, representative Western blot of cytosolic proteins (60 mg) separated by PAGE-SDS and analyzed for GAPDH and HuR. Cytosol was isolated from mesangial cells treated with IL-1β for the indicated number of minutes or treated for 24 h. *B*, cytosolic fractions were immunoprecipitated with anti-HuR antibodies. Total RNA was extracted from precipitates, and COX-2 mRNA was quantified by RT-PCR using TaqMan real-time PCR and a COX-2 cDNA clone as standard. Results represent the average of two independent experiments each measured in triplicate.

The types of proteins we have identified have profound effects on message expression by regulating mRNA export from the nucleus and influencing the ability of the message to be either transported to polysomes for translation or targeted for degradation. Some of these proteins, such as HuR and TIA-1, apparently have contradictory effects on the fate of the target message. Therefore, the challenge still remains to determine the mechanism whereby cells decide whether to increase or decrease gene expression when presented with RNA-protein complexes containing potentially opposing regulatory proteins.

REFERENCES

1. Shaw, G., and Kamen, R. (1986) *Cell* **46**, 659–667
2. Caput, D., Beutler, B., Hartog, K., Thayer, R., Brown-Shimer, S., and Cerami, A. (1986) *Proc. Natl. Acad. Sci. U. S. A.* **83**, 1670–1674
3. Chen, C. Y., and Shyu, A. B. (1995) *Trends Biochem. Sci.* **20**, 465–470
4. Ross, J. (1996) *Trends Genet.* **12**, 171–175
5. Wilusz, C. J., Wormington, M., and Peltz, S. W. (2001) *Nat. Rev. Mol. Cell Biol.* **2**, 237–246
6. Piecyk, M., Wax, S., Beck, A. R. P., Kedersha, N., Gupta, M., Maritim, B., Chen, S., Gueydan, C., Kruys, V., Streuli, M., and Anderson, P. (2000) *EMBO J.* **19**, 4154–4163
7. Kruys, V., and Huez, G. (1994) *Biochimie (Paris)* **76**, 862–866
8. Gueydan, C., Droogmans, L., Chalon, P., Huez, G., Caput, D., and Kruys, V. (1999) *J. Biol. Chem.* **274**, 2822–2826
9. Hamilton, B. J., Burns, C. M., Nichols, R. C., and Rigby, W. F. (1997) *J. Biol. Chem.* **272**, 28732–28741
10. Fan, X. C., and Steitz, J. A. (1998) *EMBO J.* **17**, 3448–3460
11. Peng, S. S., Chen, C. Y., Xu, N., and Shyu, A. B. (1998) *EMBO J.* **17**, 3461–3470
12. DeMaria, C. T., and Brewer, G. (1996) *J. Biol. Chem.* **271**, 12179–12184
13. Zhang, W., Wagner, B. J., Ehrenman, K., Schaefer, A. W., DeMaria, C. T., Crater, D., DeHaven, K., Long, L., and Brewer, G. (1998) *Mol. Cell. Biol.* **13**, 7652–7665
14. Loflin, P., Chen, C. Y., and Shyu, A. B. (1999) *Genes Dev.* **12**, 1884–1897
15. Carballo, E., Lai, W. S., and Blackshear, P. J. (1998) *Science* **281**, 1001–1005
16. Lai, W. S., Carballo, E., Strum, J. R., Kennington, E. A., Phillips, R. S., and Blackshear, P. J. (1999) *Mol. Cell. Biol.* **19**, 4311–4323
17. Mahtani, K. R., Brook, M., Dean, J. L. E., Sully, G., Saklatvala, J., and Clark, A. R. (2001) *Mol. Cell. Biol.* **21**, 6461–6469
18. Anant, S., Henderson, J. O., Mukhopadhyay, D., Navaratnam, N., Kennedy, S., Min, J., and Davidson, N. O. (2001) *J. Biol. Chem.* **276**, 47338–47351
19. Smith, W. L., DeWitt, D. L., and Garavito, R. M. (2000) *Annu. Rev. Biochem.* **69**, 145–182
20. Chandrasekharan, N. V., Dai, H., Roos, K. L. T., Evanson, N. K., Tomsik, J., Elton, T. S., and Simmons, D. L. (2002) *Proc. Natl. Acad. Sci. U. S. A.* **99**, 13926–13931
21. Cok, S. J., and Morrison, A. R. (2001) *J. Biol. Chem.* **276**, 23179–23185
22. Rzymkiewicz, D., Leingang, K., Baird, N., and Morrison, A. R. (1994) *Amer. J. Physiol.* **266**, F39–F45
23. Srivastava, S. K., Tetsuka, T., Daphna-Iken, D., and Morrison, A. R. (1994) *Amer. J. Physiol.* **267**, F504–F508
24. Dixon, D. A., Kaplan, C. D., McIntyre, T. M., Zimmerman, G. A., and Prescott, S. M. (2000) *J. Biol. Chem.* **275**, 11750–11757
25. Lasa, M., Mahtani, K. R., Finch, A., Brewer, G., Saklatvala, J., and Clark, A. R. (2000) *Mol. Cell. Biol.* **20**, 4265–4274
26. Gou, Q., Liu, C. H., Ben Av, P., and Hla, T. (1998) *Biochem. Biophys. Res. Commun.* **242**, 508–512
27. Dixon, D. A., Tolley, N. D., King, P. H., Nabors, L. B., McIntyre, T. M., Zimmerman, G. A., and Prescott, S. M. (2001) *J. Clin. Invest.* **108**, 1657–1665
28. Guan, Z., Tetsuka, T., Baier, L. D., and Morrison, A. R. (1996) *Amer. J. Physiol.* **270**, F634–F641
29. Fan, X. C., and Steitz, J. A. (1998) *Proc. Natl. Acad. Sci. U. S. A.* **95**, 15293–15298
30. Gallouzi, I. E., Brennan, C. M., and Steitz, J. A. (2001) *RNA* **7**, 1348–1361
31. Brennan, C. M., Gallouzi, I. E., and Steitz, J. A. (2000) *J. Cell Biol.* **151**, 1–14
32. Atasoy, U., Watson, J., Patel, D., and Keene, J. D. (1998) *J. Cell Sci.* **111**, 3145–3156
33. Wang, W., Furneaux, H., Cheng, H., Caldwell, M. C., Hutter, D., Liu, Y., Holbrook, N., and Gorospe, M. (2000) *Mol. Cell. Biol.* **20**, 760–769
34. Yaman, I., Fernandez, J., Sarkar, B., Schneider, R. J., Snider, M. D., Nagy, L. E., and Hatzoglou, M. (2002) *J. Biol. Chem.* **277**, 41539–41546
35. Kedersha, N., Cho, M. R., Li, W., Yacono, P. W., Chen, S., Gilks, N., Golan, D. E., and Anderson, P. (2000) *J. Cell Biol.* **151**, 1257–1268
36. Dreyfuss, G., Matunis, M. J., Pinol-Roma, S., and Burd, C. G. (1993) *Annu. Rev. Biochem.* **62**, 289–321
37. Kiledjian, M., and Dreyfuss, G. (1992) *EMBO J.* **11**, 2655–2664
38. Eggert, M., Michel, J., Schneider, S., Bornfleth, H., Baniahmad, A., Fackelmayer, F. O., Schmidt, S., and Renkawitz, R. (1997) *J. Biol. Chem.* **272**, 28471–28478
39. Dean, J. L. E., Wait, R., Mahtani, K. R., Sully, G., Clark, A. R., and Saklatvala, J. (2001) *Mol. Cell. Biol.* **21**, 721–730
40. Jang, B. C., Munoz-Najar, U., Paik, J. H., Claffey, K., Yoshida, M., and Hla, T. (2003) *J. Biol. Chem.* **278**, 2773–2776

American Journal of Physiology – Cell Physiology

Effects of p38MAPK isoforms on renal mesangial cell inducible nitric oxide synthase expression

Paul Lui, Chenbo Zeng, Stephen Acton, Steven Cok, Alison Sexton and Aubrey R. Morrison

Am J Physiol Cell Physiol 286:145-152, 2004. First published Oct 1, 2003;
doi:10.1152/ajpcell.00233.2003

You might find this additional information useful...

This article cites 37 articles, 27 of which you can access free at:
http://ajpcell.physiology.org/cgi/content/full/286/1/C145#BIBL

Updated information and services including high-resolution figures, can be found at:
http://ajpcell.physiology.org/cgi/content/full/286/1/C145

Additional material and information about ***AJP - Cell Physiology*** can be found at:
http://www.the-aps.org/publications/ajpcell

This information is current as of January 31, 2007 .

AJP - Cell Physiology is dedicated to innovative approaches to the study of cell and molecular physiology. It is published 12 times a year (monthly) by the American Physiological Society, 9650 Rockville Pike, Bethesda MD 20814-3991. Copyright © 2005 by the American Physiological Society. ISSN: 0363-6143, ESSN: 1522-1563. Visit our website at http://www.the-aps.org/.

Downloaded from ajpcell.physiology.org on January 31, 2007

Am J Physiol Cell Physiol 286: C145–C152, 2004.
First published September 24, 2003; 10.1152/ajpcell.00233.2003.

Effects of p38^{MAPK} isoforms on renal mesangial cell inducible nitric oxide synthase expression

Paul Lui, Chenbo Zeng, Stephen Acton, Steven Cok, Alison Sexton, and Aubrey R. Morrison
Department of Medicine, Washington University School of Medicine, St. Louis, Missouri 63110

Submitted 3 June 2003; accepted in final form 2 September 2003

Lui, Paul, Chenbo Zeng, Stephen Acton, Steven Cok, Alison Sexton, and Aubrey R. Morrison. Effects of p38^{mapk} isoforms on renal mesangial cell inducible nitric oxide synthase expression. *Am J Physiol Cell Physiol* 286: C145–C152, 2004. First published September 24, 2003; 10.1152/ajpcell.00233.2003.—Several related isoforms of p38^{MAPK} have been identified and cloned in many species. Although they all contain the dual phosphorylation motif TGY, the expression of these isoforms is not ubiquitous. p38α and -β2 are ubiquitously expressed, whereas p38γ and -δ appear to have more restricted expression. Because there is evidence for selective activation by upstream kinases and selective preference for downstream substrates, the functions of these conserved proteins is still incompletely understood. We have demonstrated that the renal mesangial cell expresses the mRNA for all the isoforms of p38^{MAPK}, with p38α mRNA expressed at the highest level, followed by p38γ and the lowest levels of expression by p38β2 and -δ. To determine the functional effects of these proteins on interleukin (IL)-1β-induced inducible nitric oxide synthase (iNOS) expression, we transduced TAT-p38 chimeric proteins into renal mesangial cells and assessed the effects of wild-type and mutant p38 isoforms on ligand induced iNOS expression. We show that whereas p38γ and -δ had minimal effects on iNOS expression, p38α and -β2 significantly altered its expression. p38α mutant and p38β2 wild-type dose dependently inhibited IL-1β-induced iNOS expression. These data suggest that p38α and β2 have reciprocal effects on iNOS expression in the mesangial cell, and these observations may have important consequences for the development of selective inhibitors targeting the p38^{MAPK} family of proteins.

TAT proteins; p38 MAPK; inducible nitric oxide synthase; mesangial cell; interleukin-1

THE INDUCIBLE NOS (iNOS), found in several cell types including macrophages, vascular smooth muscle cells, and renal mesangial cells, is highly regulated by cytokines, which can facilitate or inhibit the induction of this enzyme. Stimulatory cytokines such as interleukin (IL)-1 and tumor necrosis factor (TNF) increase iNOS mRNA by transcriptional activation. Once iNOS protein is induced, it can produce tremendous amounts of NO that can contribute to cell and tissue regulation and damage. However, iNOS gene expression, mRNA stability, protein synthesis, and degradation are all amenable to modification by cytokines and other agents such as growth factors. Transforming growth factor-β, for example, reduces cytokine-induced iNOS activity by inhibiting mRNA translation and increases iNOS protein degradation, whereas interleukin-4 interferes with iNOS transcription. Previous data demonstrated that IL-1β increases p38^{MAPK} phosphorylation and activation, suggesting that the p38^{MAPK} signaling cascade is involved in IL-1 signaling. However, by using a pharmacological strategy, inhibition of p38^{MAPK} shows disparate results on iNOS expression and NO release in various cell types. For example, we previously found that SC68376, a p38^{MAPK} inhibitor, increases iNOS expression induced by IL-1β in mesangial cells(10). In contrast, SB-203580, another p38^{MAPK} inhibitor, was found to either inhibit iNOS expression and NO production stimulated by LPS in glial cells or have no influence on iNOS expression in human DLD-1 cells (4). In addition, p38^{MAPK} inhibited iNOS expression in RAW 264.7 cells stimulated with interferon-γ plus lipoarabinomannan (2). A possible explanation for this inconsistency is the specificity of the p38^{MAPK} inhibitors used in the studies. Because at least four different isoforms of p38^{MAPK} have been identified(35), as well as splice variants (8, 27), one would expect that different isoforms of p38^{MAPK} may have different biological functions. The p38^{MAPK} inhibitors used in previous studies may not be selective enough to inhibit one particular isoform of p38^{MAPK}. Indeed, SC-68376 was only tested as a p38^{MAPK} inhibitor on p38α^{MAPK}. Second, there clearly is cell-specific expression of the various isoforms and this needs to be added to the equation. In an earlier study, overexpression of the kinase inactive mutant of p38α^{MAPK} was found to inhibit IL-1β-induced iNOS expression and NO production, thus confirming that activation of p38α^{MAPK} is required for iNOS expression and NO production in renal mesangial cells (11). Similarly, IL-1β-induced rat pancreatic islet NOS requires p38^{MAPK} (19). Indeed, p38α^{MAPK} has been implicated to play a role in apoptosis in several cell types (15, 30); however, p38β has been shown to be antiapoptotic in Jurkat cells (22). To gain further insight into the possible roles of the different isoforms of p38^{MAPK} in rat renal mesangial cells, we transduced chimeric TAT-proteins of wild type and kinase-dead mutants of the α, β, γ, and δ isoforms into renal mesangial cells and assessed the concentration-dependent effects on IL-1β-induced iNOS protein expression.

METHODS

Materials. Human recombinant Il-1β was purchased from Roche Pharmaceuticals. Fetal bovine serum was purchased from Invitrogen (Carlsbad, CA). Polyclonal IgG against iNOS was purchased from Cayman Chemical (Ann Arbor, MI). Phospho-p38^{MAPK} antibody was from Cell Signaling (Beverly, MA). SB-203580, [4-(4-fluorophenyl)-2-(4-methylsulfinylphenyl)-5-(4-pyridinyl)-1*H*-imidazole] was purchased from Calbiochem (La Jolla, CA). SC-68376 was a generous gift from the late Dr. J. Portnova (G. D. Searle, St Louis, MO).

Cell culture. Rat primary mesangial cell cultures were prepared from male Harlan Sprague-Dawley rats as previously described (12). Cells were grown in RPMI 1640 medium supplemented with 10% (vol/vol) heat-inactivated fetal bovine serum, 0.6% (vol/vol) insulin,

Address for reprint requests and other correspondence: A. R. Morrison, Washington Univ., Renal Division, Box 8126, 660 South Euclid, St Louis, MO 63110 (E-mail: morrison@pcg.wustl.edu).

The costs of publication of this article were defrayed in part by the payment of page charges. The article must therefore be hereby marked "*advertisement*" in accordance with 18 U.S.C. Section 1734 solely to indicate this fact.

0363-6143/04 $5.00 Copyright © 2004 the American Physiological Society

American Journal of Physiology – Cell Physiology

Downloaded from ajpcell.physiology.org on January 31, 2007

American Journal of Physiology – Cell Physiology

100 U/ml penicillin, 100 μg/ml streptomycin, 250 μg/ml amphotericin B, and 15 mM HEPES. Where indicated, mesangial cells were stimulated with IL-1β (100 U/ml). RAW 264.7 cells were obtained from ATCC (American Type Culture Collection) and cultured in 15 mM HEPES, pH 7.4, in DMEM and 10% FCS with added penicillin and streptomycin.

Mutagenesis of p38MAPK isoforms. The cDNA for each of the $p38^{MAPK}$ isoforms was obtained from Roche Pharmaceuticals (generous gift from Dr. Phyllis Whitely). The coding region of each p38 isoform was amplified by PCR and subcloned into the mammalian expression vector pcDNA3 (Invitrogen). Dominant negative mutants for these isoforms were made by mutating the Thr-Gly-Tyr dual phosphorylation motif to Ala-Gly-Phe by site-directed mutagenesis. Mutagenesis was performed with the Transformer Site-Directed Mutagenesis Kit (second version) from Clontech according to the instructions provided by the manufacturer. The oligonucleotides used for mutagenesis are as follows: 5′-GATGATGAAATGGCAGGCTTCGTGGCCACTAG-3′ for p38α, 5′-GACGAGGA-GATGGCCGGCTTTGTGGCCACG-3′ for p38β2, and 5′-GACAGTGAG-ATGGCTGGGTTCGTGGTGACC-3′ for p38γ, where the mutated bases are underlined. p38β2 wild type and p38δ wild type, as well as a p38δ kinase-dead mutant, in which Lys^{54} is mutated to Met^{54}, were obtained from Dr. J. Han from the Scripps Research Institute (La Jolla, CA). The cDNA was mutated in the ATP-binding site, thus making it catalytically inactive. The DNA sequence of the mutated genes was verified by DNA sequencing.

Transient transfections. Mesangial cells were transiently transfected using SuperFect transfection reagent (Qiagen Corp, Valencia, CA). Cells were plated into six-well cluster plates at a density of 2×10^5 cells per well and incubated overnight. Mixtures of 2.5 μg of plasmid DNA in 75 μl of serum-free medium and 15 μl of SuperFect reagent were incubated 5–10 min at room temperature, followed by dilution to 0.5 ml with complete medium. The DNA-SuperFect complex was layered onto mesangial cells (2.5 μg DNA per well), and after a 2- to 3-h incubation, the medium was changed and cells were incubated overnight for gene expression.

Preparation of TAT-p38 isoforms. The vector pTAT-HA was a generous gift from Dr. Steven Dowdy (Howard Hughes Medical Institute, Washington University, St. Louis, MO). The vector shown in Fig. 3*A* carries an NH_2-terminal 6-histidine leader followed by the 11-amino acid TAT protein transduction domain flanked by glycine residues, a hemaglutinin tag (HA) followed by a polylinker (21, 29). We ligated the cDNA for human α, β, δ, and γ isoforms of $p38^{MAPK}$, both wild type (wt) and mutants (mt), into the polylinker for the expression of full-length TAT chimeric proteins. Recombinant proteins were then expressed in *Escherichia coli*, strain DH5α, denatured, and solubilized in 8 M urea and isolated on a Ni^{2+} affinity column. Rapid dialysis was then carried out using a Slide-A-Lyser dialysis cassette with a 10,000 MW cutoff (Pierce, Rockford, IL) against 20 mM HEPES, pH 7.4. The protein concentration was determined and recombinant proteins stored in 10% glycerol at −80°C until required for experiments. The TAT chimeric proteins were added to the media at the appropriate concentrations and incubated for 60 min to allow for equilibration with cytosolic concentration. Once inside the cells, transduced denatured proteins may be correctly refolded by chaperones such as HSP90 (21, 28). Transduction across the cell membrane occurred through an unidentified mechanism that is independent of receptors, transporters, and endocytosis(34) and transduced proteins are found in the cytoplasm and nucleus. The internalization occurred at 4°C, and it is therefore unlikely that uptake requires any cell-mediated process or physical arrangement (14).

Western blot analysis. At the time of harvest, cells were washed with ice-cold phosphate buffer and lysed in whole cell extract (WCE) buffer [25 mM HEPES-NaOH (pH 7.7), 0.3 M NaCl, 1.5 mM $MgCl_2$, 0.2 mM EDTA, 0.1% Triton X-100, 0.5 mM dithiothreitol, 20 mM β-glycerophosphate, 100 μM $NaVO_4$, 2 μg/ml leupeptin, and 100 μg/ml phenylmethylsulfonyl fluoride] to which ×6 sample buffer was added before heating. After boiling for 5 min, equal amounts of protein were run on 10% SDS-PAGE. Proteins were then transferred to polyvinylidene difluoride membranes (Immobilon BP; Millipore, Bedford, MA). The membranes were saturated with 5% fat-free dry milk in Tris-buffered saline (50 mM Tris·HCl, pH 8.0, 150 mM NaCl) with 0.05% Tween 20 (TBS-T) for 1 h at room temperature. Blots were then incubated overnight with primary antibodies at 1:1,000 dilution in 5% BSA TBS-T. After being washed with 5% milk TBS-T solution, blots were further incubated for 1 h at room temperature with goat anti-rabbit or mouse IgG antibody coupled to horseradish peroxidase (Amersham, Arlington Heights, IL) at 1:3,000 dilution in TBS-T. Blots were then washed five times in TBS-T before visualization. Enhanced chemiluminescence kit (ECL; Amersham) was used for detection. Blots were quantitated on a densitometer using Quantity One software from PDI. The densitometer was calibrated to an external standard.

RT-PCR and TaqMan real-time PCR. To determine the expression of the message for the p38 isoforms in rat renal mesangial cells, total RNA was isolated from cells using RNA STAT-60 reagent, DNase treated twice, and reverse-transcribed by Omniscript reverse transcriptase (Qiagen) using oligo $(dT)_{15}$ primers. The PCR amplifications were carried out using rat $p38^{MAPK}$ amplification primers unique for each isoform. For p38α, the primers were 5′-AACCTGTCCCCGGTGGGCTCG-3′ and 5′-CGATGTCCCGT-CTTTGTATGA-3′; for p38β, primers were 5′-CGCCCAGTCCTGAGGTTCT-3′ and 5′-AGACACTGCTGAGGTCCTTCT-3′; for p38γ, the primers were 5′-CGCCCCCTCCT-GAGTTT-3′ and 5′-GCTTGCGTTGGTCAGGACAGA-3′; and for p38δ, the primers were 5′-TGCTCGGCCATCGACAA-3′ and 5′-TGGCAAAGATCTCCGACTGG-3′. To quantify p38 isoform mRNA levels, TaqMan real-time PCR was performed using the gene-specific primers above and the double-stranded DNA-binding dye SYBR green I. Fluorescence was detected with an ABI Prism 5700 sequence detection system (PE Biosystems). Amplification primers for GAPDH were 5′-GAAGGTGAAGGTCGGAGTC-3′ and 5′-GAAGATGGTGATGGGATTTC-3′. Primer pairs were tested to ensure a robust amplification signal of the expected size with no additional bands. The amount of $p38^{MAPK}$ message in each RNA sample was quantified and normalized to GAPDH content. Relative amounts of $p38^{MAPK}$ cDNA were calculated by the comparative C_T method.

RESULTS

Effects of inhibition of $p38^{MAPK}$ on IL-1 and LPS-induced iNOS expression in renal mesangial and RAW 264.7 cells. Previous studied by us have shown that inhibition of $p38^{MAPK}$ with the pyridinyl oxazole SC-68376 inhibited IL-1β-induced cyclooxygenase-2 expression while enhancing iNOS expression in renal mesangial cells (10). Figure 1*A* shows that IL-1β induces the phosphorylation of p38 in renal mesangial cells at 15 min (*lane 2*), which returns to control (*lane 1*) levels by 2 h as shown in *lane 3*. Phosphorylation was detected by Western blotting using a phosphospecific anti-p38 antibody. Figure 1*B* shows the enhanced iNOS protein expression after 24 h of IL-1β at two concentrations, 10 μM (*lane 2*) and 100 μM (*lane 3*) of SC-68378. To determine whether a similar phenomenon was present in another cell type, we stimulated RAW 264.7 cells with LPS (100 ng/ml) in the presence and absence of a $p38^{MAPK}$ inhibitor, SB-203580 (pyridinyl imidazole), at a concentration of 10 μM and followed the time course of iNOS protein expression by Western blotting. At this concentration, SB-203580 inhibits p38α and -β but not p38δ and -γ (3, 5, 6).

Downloaded from ajpcell.physiology.org on January 31, 2007

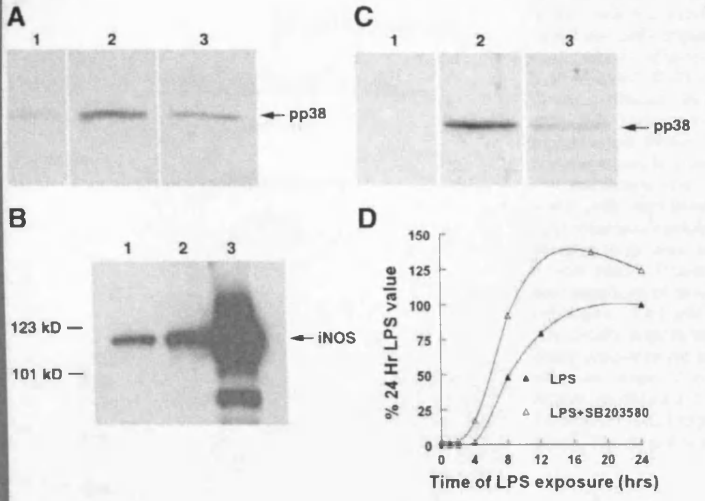

Fig. 1. *A*: phosphorylation of p38 in mesangial cells stimulated by IL-1β. *Lane 1*, control; *lane 2*, 15 min; *lane 3*, 2 h after IL-1β. *B*: effect of SC-683376 on IL-1β-induced inducible nitric oxide synthase (iNOS) expression. *Lane 1*, IL-1β; *lane 2*, IL-1β plus SC68376, 10 μM; *lane 3*, IL-1β plus 100 μM. *C*: phosphorylation of p38 by LPS in RAW 254.7 cells. *Lane 1*, control; *lane 2*, 15 min; *lane 3*, 2 h after lipopolysaccharide (LPS). *D*: effect of 10 μM SB-203580 on LPS-induced iNOS expression.

We could not use IL-1β for similar experiments because IL-1β did not stimulate iNOS protein expression in RAW 264.7 cells in our hands. Figure 1*C* shows that LPS activates and phosphorylates p38 by 15 min (*lane 2*), which returns toward control (*lane 1*) at 2 h (*lane 3*). Figure 1*D* shows the mean of two experiments in duplicate and illustrates that at virtually all time points, SB-203580 enhances iNOS protein expression in response to LPS in RAW 264.7 cells. A potential explanation for this observation is that inhibition of the inhibitory p38β2 allowed for enhanced expression of iNOS.

Effect of transfection of p38α and -β2 into mesangial cells. For these experiments, p38α (wt and mt) and p38β2 (wt and mt) were transiently transfected into rat mesangial cells and the effects on the expression of Il-1β-induced iNOS expression were assessed. The mammalian expression vector pcDNA3 was used and carried a FLAG epitope tag, which enabled determination of expressed protein in mesangial cells by Western blotting. Figure 2 shows an example of one of our more striking experiments that illustrates what we expected for p38α based on previous published data (11). It shows that transfection of p38α wt had virtually no effect on IL-1β-induced iNOS expression, whereas the mutant p38α inhibited IL-1β-induced iNOS expression. However, the results seen for p38β2 were unexpected. In this instance, the p38β2 mt was without effect, whereas the wt p38β2 inhibited IL-1β-induced iNOS expression. Because the transfection efficiency for mesangial cells was variable, the results obtained with this approach were not statistically significant, although qualitatively and consistently similar to the results as seen in Fig. 2. We therefore chose the alternative strategy of transduction of TAT chimeric proteins to assess the function of the p38 isoforms on IL-1β-induced iNOS expression in renal mesangial cells.

Concentration-dependent transduction into cells. The cDNA for wild-type and mutant p38 isoforms were ligated in the correct orientation into the prokaryotic expression vector pTAT-HA (Fig. 3*A*). Bacterial expressed TAT-proteins were purified and isolated as described in METHODS. A Coomassie blue-stained gel (Fig. 3*B*) shows the p38 wt and mt isoforms eluted from the Ni^{2+} affinity column with 0.1 M imidazole. This fraction was rapidly dialyzed, and protein concentrations were determined and stored at −70°C in 10% glycerol. TAT-p38 proteins (wt or mt) were added to 25-cm^2 flasks with 5 ml of medium to achieve increasing concentrations up to a maximum of 100 μg/ml. The mesangial cells were then allowed to incubate at 37°C for 60 min. The medium was then harvested

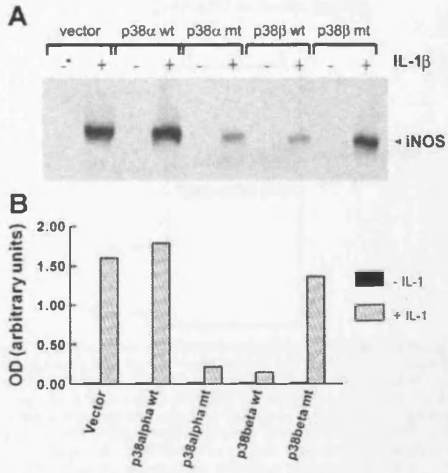

Fig. 2. Representative experiment of mesangial cells transfected with p38α and -β2 and stimulated with IL-1β. *A*: Western blot for iNOS. *B*: the densitometric quantitation of the blots. wt, wild type; mt, mutant.

American Journal of Physiology – Cell Physiology

Downloaded from ajpcell.physiology.org on January 31, 2007

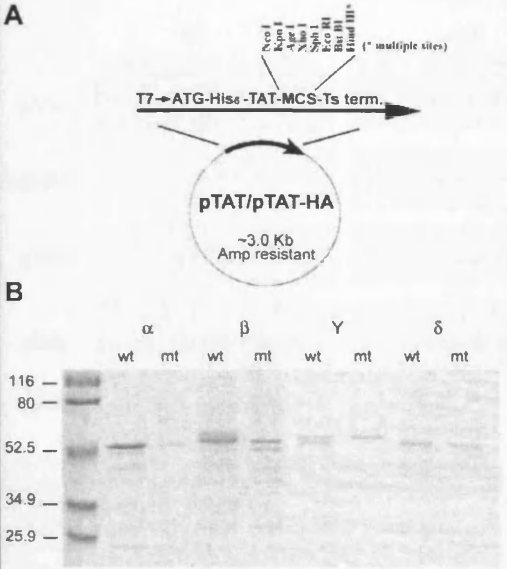

Fig. 3. *A*: the prokaryotic expression vector pTAT/pTAT-HA (without or with the HA epitope tag). *B*: Coomassie blue-stained SDS-gel illustrating the isolation of TAT-p38 isoforms.

for Western blotting; the cells were washed twice with ice-cold medium (without TAT proteins), and cell lysates were prepared with WCE buffer. Equal volumes of medium and equivalent amounts of cell lysate were then analyzed by Western blotting using anti-HA antibodies. Densitometric quantitation of the blots was carried out. Figure 4*A* shows that increasing concentrations of TAT p38 proteins in the medium was associated with a linear increase in protein transduction, which appeared to reach a plateau intracellularly at concentrations of protein that exceeded 25 μg/ml in the medium. Figure 4*A*, *inset*, shows the linear relationship of increasing the concentration of TAT protein in the medium over a range of 0.1–100 μg/ml of protein. Because of this, we did not exceed 25 μg/ml of TAT protein in our transduction experiments. Figure 4*B* shows a Western blot of cell lysates from control mesangial cells (*lane 1*) and cells transduced with 10 (*lane 2*) and 25 (*lane 3*) μg/ml of TAT-p38α. It can be seen that increasing transduction of TAT proteins had no effect on endogenous p38α protein expression. In data not shown, it was also demonstrated that the efficiency of transduction of a TAT-β-Gal protein was 95–100%. Hence, we believe transduction of TAT-p38 was also 95–100%.

Effects of p38 wild-type and mutant isoforms on IL-1β-induced iNOS expression. Each of the isoforms of p38MAPK (wt and mt) was transduced into renal mesangial cells in a concentration-dependent manner. Two hours after the addition of p38MAPK to the medium, cells were stimulated with IL-1β at 100 units/ml for 24 h. Mesangial cell lysates were harvested and analyzed by Western blotting for iNOS protein expression. Control lysates from cell cultures transduced with similar concentrations of TAT p38 proteins but not stimulated with IL-1β were harvested over the same time course as IL-1β-stimulated cells. Figure 5 shows a representative Western blot of the effects of increasing concentrations of p38 isoforms on Il-1β-induced iNOS expression. The cumulative results of these experiments are shown in Fig. 6. TAT-p38 α wt produced a 35–40% increase in IL-1β-induced iNOS expression at the highest concentration of 20 μg/ml of TAT protein but at lower concentrations had no effect. TAT-p38δ wt and mt was virtually ineffective over the full concentration range used (not statistically significant). In contrast, p38β2 wt produced a concentration-dependent inhibition of IL-1β-induced iNOS expression in rat renal mesangial cells with an IC_{50} of 20 μg/ml (~400 nmol). Figure 6 also shows the effect of increasing concentrations of mutant p38 isoforms on IL-1β-induced iNOS expression. TAT-p38-γ and -δ mutant isoforms produced no statistically significant change in iNOS expression over the entire concentration range used. p38β2 mutant was ineffective over the range of concentrations used. As expected, p38α mutant produced a concentration-dependent inhibition of IL-1β-induced iNOS expression with an IC_{50} of 10 μg/ml (~200 nmol). The data obtained for the p38α and β2 isoforms (wt and

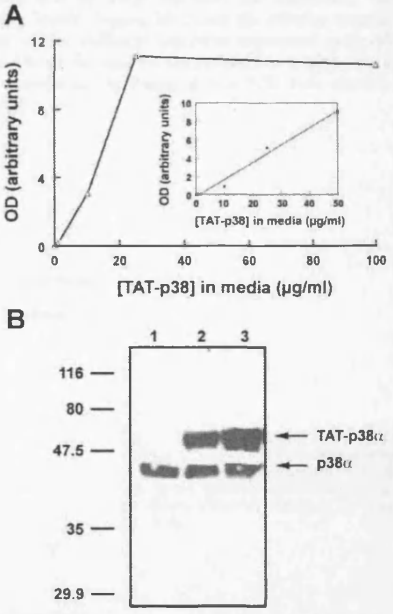

Fig. 4. *A*: concentration-dependent transduction of TAT-p38 proteins into rat mesangial cells. This appears to plateau at 25 μg/ml of protein in the medium. The amount of protein transduced intracellularly was determined by Western blotting for epitope-tagged TAT-p38 in cell lysates. The *inset* shows the relationship between the amount of TAT-p38 proteins added to the medium and the amount of HA epitope detected by Western blotting and demonstrates a linear relationship. *B*: Western blot of p38α illustrating that transduction of TAT-p38α does not influence the expression of endogenous p38α. *Lane 1*, control cells; *lanes 2* and *3*, 10 and 25 μg/ml of transduced proteins, respectively.

American Journal of Physiology – Cell Physiology

Downloaded from ajpcell.physiology.org on January 31, 2007

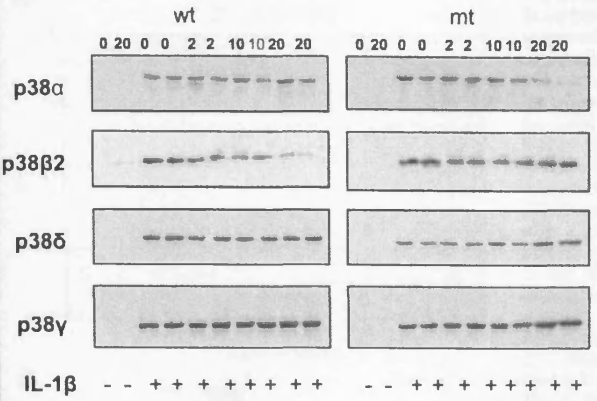

Fig. 5. Representative Western blots of mesangial cell lysates from cells transduced with TAT proteins, probed for iNOS. Cells were stimulated with IL-1β where indicated.

mt), shown in Fig. 6, represent means ± SE from five experiments. For the p38-γ and -δ, the data presented are means ±SE of three experiments in duplicate.

Expression of endogenous p38 isoforms by rat renal mesangial cell. To determine the expression patterns of the various isoforms of $p38^{MAPK}$ in the rat renal mesangial cell, we assessed the mRNA expression by real-time PCR. Amplimers were designed as indicated in METHODS, and GAPDH was used to standardize mRNA expression. Figure 7*A* shows a representative tracing of the amplification plot obtained. The plot suggests that all four isoforms are expressed, albeit at differing levels. Figure 7*B* shows the relative abundance of mRNA of the different isoforms expressed using p38α as 100%. The scale used on the ordinate is a log scale, and the figure represents the mean of two PCR runs carried out in triplicate.

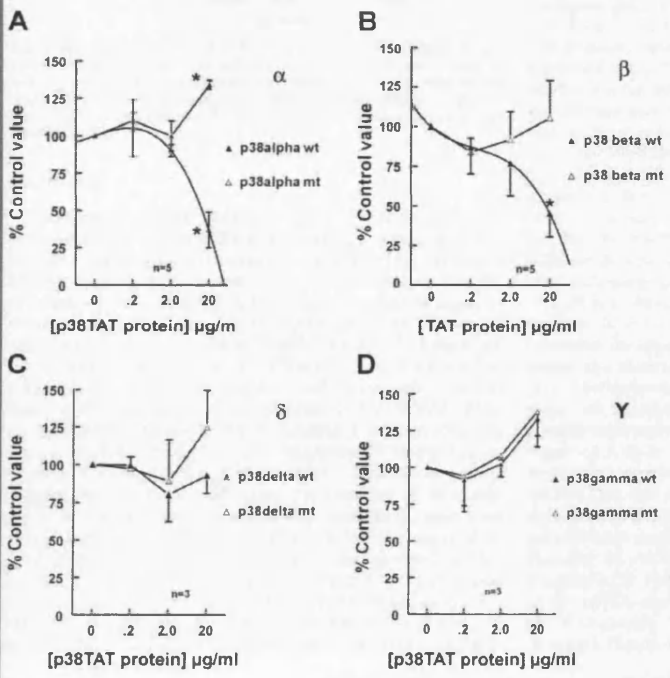

Fig. 6. Results of transduction of increasing amounts of TAT-p38 isoforms into mesangial cells on IL-β-induced iNOS expression. Wild-type p38α, -β2, -γ, and -δ isoforms and corresponding mutants are shown. Values are means ± SE. *Significant $P < 0.05$.

American Journal of Physiology – Cell Physiology

Downloaded from ajpcell.physiology.org on January 31, 2007

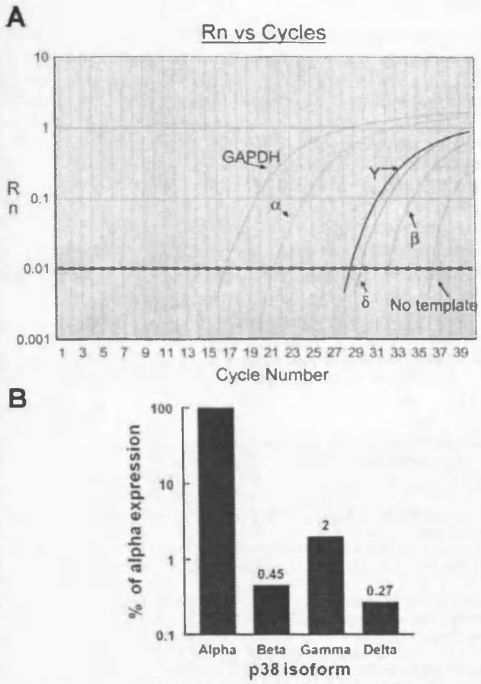

Fig. 7. Real-time quantitative PCR to assess the levels of expressed endogenous levels of mRNA for four isoforms of p38MAPK in rat renal mesangial cells. *A*: representative amplification plot obtained for the 4 isoforms and GAPDH. *B*: relative levels of expression of the mRNA levels of the 4 isoforms. The ordinate is a log scale and the data represent the means of 2 experiments done in triplicate.

DISCUSSION

There are five known isoforms of p38MAPK (α, β, β2, γ, and δ) in mammals, which differ in expression patterns, upstream activators, inhibitors, and substrate specificity (13). The major finding of this study is that p38α wt transduced into and expressed in rat mesangial cells produced a minimal augmentation of IL-1β-induced iNOS expression in rat mesangial cells. In addition, the dominant negative mutant p38α produced a dose-dependent inhibition of LPS-induced iNOS expression. Although this result was consistent with previously observed function of p38α (12), it was a surprise to observe that p38β2 wt transduced and expressed in mesangial cells produced a dose-dependent inhibition of IL-1β-induced iNOS expression, whereas the mutant was without effect. This result further suggests that in certain cell types, the presence of these two isoforms, thought to be ubiquitously expressed, may have differing functional consequences for the cellular response to extracellular ligands. In earlier experiments, we observed that pyridinyl oxazole, SC-68376 inhibitor of p38MAPK, enhanced IL-1β-induced iNOS expression in renal mesangial cells (10); however, overexpression of the kinase-dead form of p38α in renal mesangial cells inhibited IL-1β-induced iNOS expression in primary cultures of renal mesangial cells (11). This conundrum has puzzled us because experiments with the inhibitor suggested p38 was inhibiting iNOS expression, whereas the expression of the phosphorylation-defective mutant suggested p38α was facilitating iNOS expression. Similar observations have been made, albeit in different cell types, suggesting, on the basis of inhibitor studies, that in chondrocytes the p38 inhibitor SB-203580 inhibited LPS-mediated iNOS expression, whereas in RAW 264.7 cells it potentated LPS-induced iNOS expression (23). More recently, it was demonstrated that SB-203580 augmented iNOS and nitrite production in RAW 264.7 cells stimulated with IFNγ and lipoarabinomannan (2). One potential explanation for these apparent confusing observations is that different cell types are under dominant control of differing p38 isoforms, and certain isoforms may have opposite functions in the cell. Support for such a notion is suggested by several observations. First, there is the suggestion that p38β2 is 180 times more active on certain substrates, such as ATF-2, than p38α in vitro assays (33). Second, the upstream activator kinases MKK3 and MKK6 differ in their abilities to phosphorylate and activate p38MAPK, suggesting different functions within the cell (25). Indeed, MKK6 can phosphorylate p38α, p38β2, and p38γ, whereas MKK3 can only phosphorylate p38α and p38γ (7). Finally, in Jurkat cells, expression of p38β2 attenuated the apoptotic effect of SB-202190 and the cell death induced by Fas ligation and ultraviolet irradiation (22). In contrast, expression of p38α induced cell death (22). In our current study, we tested the function of all the isoforms of p38MAPK on IL-1β-induced iNOS expression by transducing both wt and mt isoforms of TAT-protein chimeras into renal mesangial cells. The results suggest opposing effects of p38α and -β on iNOS expression.

The quantitative PCR also suggest that all the isoforms are expressed at the mRNA level, however, at markedly different levels. Of some surprise was the observation that p38γ was the second most abundant isoform expressed and suggests that this isoform is not restricted in expression to skeletal muscle as was originally suggested (16). What is not known is whether the four isoforms are expressed in unique subcellular compartments that allow unique functions within the cells. Thus, even though p38 and -β may be inhibited equally well by SB-203580, the functional consequences to inhibition could be different depending on where the proteins are expressed and what their respective downstream targets are. Indeed, p38β and -γ appear to have opposing effects on AP-1-dependent transcription in two breast cancer cell lines (24). Thus there is a precedent for opposing biology exhibited by certain p38 isoforms, and there is some evidence to support this possibility (31). Another possibility is that the two p38 isoforms (α and β) exert their functions at different sites in the transcriptional and posttrancriptional machinery of the cell. The iNOS gene can be regulated both at a transcriptional (18, 20) and posttranscriptional level, exhibiting both 3′ instability determinants in the mRNA (26) and regulation of RNA-binding proteins, which could influence mRNA stability and translation (32). p38MAPK has also been implicated in kinase-dependent and -independent signaling of mRNA stability of AU-rich element-containing transcripts (9). Furthermore, tristetraprolin has been recognized as an mRNA-interacting protein that can be phosphorylated and functionally regulated by p38MAPK (1). Which of the relevant isoforms is capable of carrying out this cellular func-

American Journal of Physiology – Cell Physiology

Downloaded from ajpcell.physiology.org on January 31, 2007

tion remains to be determined. Recently, it has been suggested that p38δ can phosphorylate eEF2 kinase and inhibit its activity, thus having an effect on protein translation (17). The evidence would support, therefore, unique functions for differing isoforms of $p38^{MAPK}$.

We have demonstrated that p38α and -β appear to have opposing function in the rat renal mesangial cell. The subcellular localization where these functions occur and the sites (transcriptional and/or posttranscriptional) within the protein synthetic machinery where these interactions occur remain to be determined. We believe these observations have important implications for drug design, targeting the inhibition of $p38^{MAPK}$.

GRANTS

This work is supported by National Institute of Diabetes and Digestive and Kidney Diseases Grants DK-09976 and DK-59932 (to A. R. Morrison).

REFERENCES

1. **Carballo E, Cao H, Lai WS, Kennington EA, Campbell D, and Blackshear PJ.** Decreased sensitivity of tristetraprolin-deficient cells to p38 inhibitors suggests the involvement ofTristetraprolin in the p38 signaling pathway. *J Biol Chem* 276: 42580–42587, 2001.
2. **Chan ED, Morris KR, Belisle JT, Hill P, Remigio LK, Brennan PJ, and Riches DWH.** Induction of inducible nitric oxide synthase-NO by lipoarabinomannan of mycobacterium tuberculosis is mediated by MEK1-ERK, MKK7-JNK, and NF-κB signaling pathways. *Infect Immun* 69: 2001–2010, 2001.
3. **Cuenda A, Cohen P, Buee-Scherrer V, and Goedert M.** Activation of stress-activated protein kinase-3 (SAPK3) by cytokines and cellular stresses is mediated via SAPKK3 (MKK6); comparison of the specificities of SAPK3 and SAPK2 (RK/p38). *EMBO J* 16: 295–305, 1997.
4. **Da Silva J, Pierrat B, Mary JL, and Lesslauer W.** Blockade of p38 mitogen-activated protein kinase pathway inhibits inducible nitric-oxide synthase expression in mouse astrocytes. *J Biol Chem* 272: 28373–28380, 1997.
5. **Dashti SR, Efimova T, and Eckert RL.** MEK6 regulates human involucrin gene expression via a p38α- and p38δ-dependent mechanism. *J Biol Chem* 276: 27214–27220, 2001.
6. **Enslen H, Brancho DM, and Davis RJ.** Molecular determinants that mediate selective activation of p38 MAP kinase isoforms. *EMBO J* 19: 1301–13111, 2000.
7. **Enslen H, Raingeaud J, and Davis RJ.** Selective activation of p38 mitogen-activated protein (MAP) kinase isoforms by the MAP kinase kinases MKK3 and MKK6. *J Biol Chem* 273: 1741–1748, 1998.
8. **Faccio L, Chen A, Fusco C, Martinotti S, Bonventre JV, and Zervos AS.** Mxi2, a splice variant of p38 stress-activated kinase, is a distal nephron protein regulated with kidney ischemia. *Am J Physiol Cell Physiol* 278: C781–C790, 2000.
9. **Frevel MAE, Bakheet T, Silva AM, Hissong JG, Khabar KSA, and Williams BRG.** p38 mitogen-activated protein kinase-dependent and -independent signaling of mRNA stability of AU-rich element-containing transcripts. *Mol Cell Biol* 23: 425–436, 2003.
10. **Guan Z, Baier LD, and Morrison AR.** p38 mitogen-activated protein kinase down-regulates nitric oxide and up-regulates prostaglandin E2 biosynthesis stimulated by interleukin-1beta. *J Biol Chem* 272: 8083–8089, 1997.
11. **Guan Z, Buckman SY, Springer LD, and Morrison AR.** Both p38alpha MAPK and JNK/SAPK pathways are important for induction of nitric-oxide synthase by interleukin-1beta in rat glomerular mesangial cells. *J Biol Chem* 274: 36200–36206, 1999.
12. **Guan Z, Tetsuka T, Baier LD, and Morrison AR.** Interleukin-1 beta activates c-jun NH2-terminal kinase subgroup of mitogen-activated protein kinases in mesangial cells. *Am J Physiol Renal Fluid Electrolyte Physiol* 270: F634–F641, 1996.
13. **Herlaar E and Brown Z.** p38 MAPK signalling cascades in inflammatory disease. *Mol Med Today* 5: 439–447, 1999.
14. **Ho A, Schwarze SR, Mermelstein SJ, Waksman G, and Dowdy SF.** Synthetic protein transduction domains: enhanced transduction potential in vitro and in vivo. *Cancer Res* 61: 474–477, 2001.
15. **Ichijo H, Nishida E, Irie K, ten Dijke P, Saitoh M, Moriguchi T, Takagi M, Matsumoto K, Miyazono K, and Gotoh Y.** Induction of apoptosis by ASK1, a mammalian MAPKKK that activates SAPK/JNK and p38 signaling pathways. *Science* 275: 90–94, 1997.
16. **Jiang Y, Gram H, Zhao M, New L, Gu J, Feng L, Di Padova F, Ulevitch RJ, and Han J.** Characterization of the structure and function of the fourth member of p38 group mitogen-activated protein kinases, p38delta. *J Biol Chem* 272: 30122–30188, 1997.
17. **Knebel A, Morrice N, and Cohen P.** A novel method to identify protein kinase substrates: eEF2 kinase is phosphorylated and inhibited by SAPK4/p38δ. *EMBO J* 20: 4360–4369, 2001.
18. **Kunz D, Walker G, Eberhardt W, and Pfeilschifter J.** Molecular mechanisms of dexamethasone inhibition of nitric oxide synthase expression in IL-1β-stimulated mesangial cells: evidence for the involvement of transcriptional and posttranscriptional regulation. *Proc Natl Acad Sci USA* 92: 255–259, 1996.
19. **Larsen CM, Wadt KAW, Juhl LF, Andersen HU, Karlsen AE, Su MSS, Seedorf K, Shapiro L, Dinarello CA, and Mandrup-Poulsen T.** Interleukin-1β-induced rat pancreatic islet nitric oxide synthesis requires both the p38 and extracellular signal-regulated kinase 1/2 mitogen-activated protein kinases. *J Biol Chem* 273: 15294–15300, 1998.
20. **Marks-Konczalik J, Chu SC, and Moss J.** Cytokine-mediated transcriptional induction of the human inducible nitric oxide synthase gene requires both activator protein 1 and nuclear factor kappaB-binding sites. *J Biol Chem* 273: 22201–22208, 1998.
21. **Nagahara H, Vocero-Akbani AM, Snyder EL, Ho A, Latham DG, Lissy NA, Becker-Hapak M, Ezhevsky SA, and Dowdy SF.** Transduction of full-length TAT fusion proteins into mammalian cells: TAT-p27Kip1 induces cell migration. *Nat Med* 4: 1449–1522, 1998.
22. **Nemoto S, Xiang J, Huang S, and Lin A.** Induction of apoptosis by SB202190 through inhibition of p38β mitogen-activated protein kinase. *J Biol Chem* 273: 16415–16420, 1998.
23. **Patel R, Attur MG, Dave MN, Kumar S, Lee JC, Abramson SB, and Amin AR.** Regulation of nitric oxide and prostaglandin E2 production by CSAIDS (SB203580) in murine macrophages and bovine chondrocytes stimulated with LPS. *Inflamm Res* 48: 337–343, 1999.
24. **Pramanik R, Qi X, Borowicz S, Choubey D, Schultz RM, Han J, and Chen G.** p38 isoforms have opposite effects on AP-1-dependent transcription through regulation of c-Jun. The determinant role of the isoforms in the p38 MAPK signal specificity. *J Biol Chem* 278: 4831–4839, 2003.
25. **Raingeaud J, Whitmarsh AJ, Barrett T, Derijard B, and Davis RJ.** MKK3- and MKK6-regulated gene expression is mediated by the p38 mitogen-activated protein kinase signal transduction pathway. *Mol Cell Biol* 16: 1247–1255, 1996.
26. **Rodriguez-Pascual F, Hausding M, Ihrig-Biedert I, Furneaux H, Levy AP, Forstermann U, and Kleinert H.** Complex contribution of the 3′-untranslated region to the expressional regulation of the human inducible nitric-oxide synthase gene. Involvement of the RNA-binding protein HuR. *J Biol Chem* 275: 26040–26049, 2000.
27. **Sanz-Moreno V, Casar B, and Crespo P.** p38α isoform Mxi2 binds to extracellular signal-regulated kinase 1 and 2 mitogen-activated protein kinase and regulates its nuclear activity by sustaining its phosphorylation levels. *Mol Cell Biol* 23: 3079–3090, 2003.
28. **Schneider C, Sepp-Lorenzino L, Nimmesgern E, Ouerfelli O, Danishefsky S, Rosen N, and Hartl FU.** Pharmacologic shifting of a balance between protein refolding and degradation mediated by Hsp90. *Proc Natl Acad Sci USA* 93: 14536–14541, 1996.
29. **Schwarze SR, Ho A, Vocero-Akbani A, and Dowdy SF.** In vivo protein transduction: delivery of a biologically active protein into the mouse [see comments]. *Science* 285: 1569–1572, 1999.
30. **Schwenger P, Bellosta P, Vietor I, Basilico C, Skolnik EY, and Vilcek J.** Sodium salicylate induces apoptosis via p38 mitogen-activated protein kinase but inhibits tumor necrosis factor-induced c-Jun N-terminal kinase/stress-activated protein kinase activation. *Proc Natl Acad Sci USA* 94: 2869–2873, 1997.
31. **Seternes OM, Johansen B, Hegge B, Johannessen M, Keyse SM, and Muens U.** Both binding and activation of p38 mitogen-activated protein kinase (MAPK) play essential roles in regulation of the nucleocytoplasmic distribution of MAPK-activated protein kinase 5 by cellular stress. *Mol Cell Biol* 22: 6931–6945, 2002.
32. **Soderberg M, Raffalli-Mathieu F, and Lang MA.** Inflammation modulates the interaction of heterogeneous nuclear ribonucleoprotein (hnRNP) I/polypyrimidine tract binding protein and hnRNP L with the 3′untrans-

American Journal of Physiology – Cell Physiology

Downloaded from ajpcell.physiology.org on January 31, 2007

lated region of the murine inducible nitric-oxide synthase mRNA. *Mol Pharmacol* 62: 423–431, 2002.
33. **Stein B, Yang MX, Young DB, Janknecht R, Hunter T, Murray BW, and Barbosa MS.** p38–2, a novel mitogen-activated protein kinase with distinct properties. *J Biol Chem* 272: 19509–19517, 1997.
34. **Wadia JS and Dowdy SF.** Protein transduction technology. *Curr Opin Biotechnol* 13: 52–56, 2002.
35. **Widmann C, Gibson S, Jarpe MB, and Johnson GL.** Mitogen-activated protein kinase: conservation of a three-kinase module from yeast to human. *Physiol Rev* 79: 143–180, 1999.

American Journal of Physiology – Cell Physiology

Downloaded from ajpcell.physiology.org on January 31, 2007